doi : 10.17596/0003314

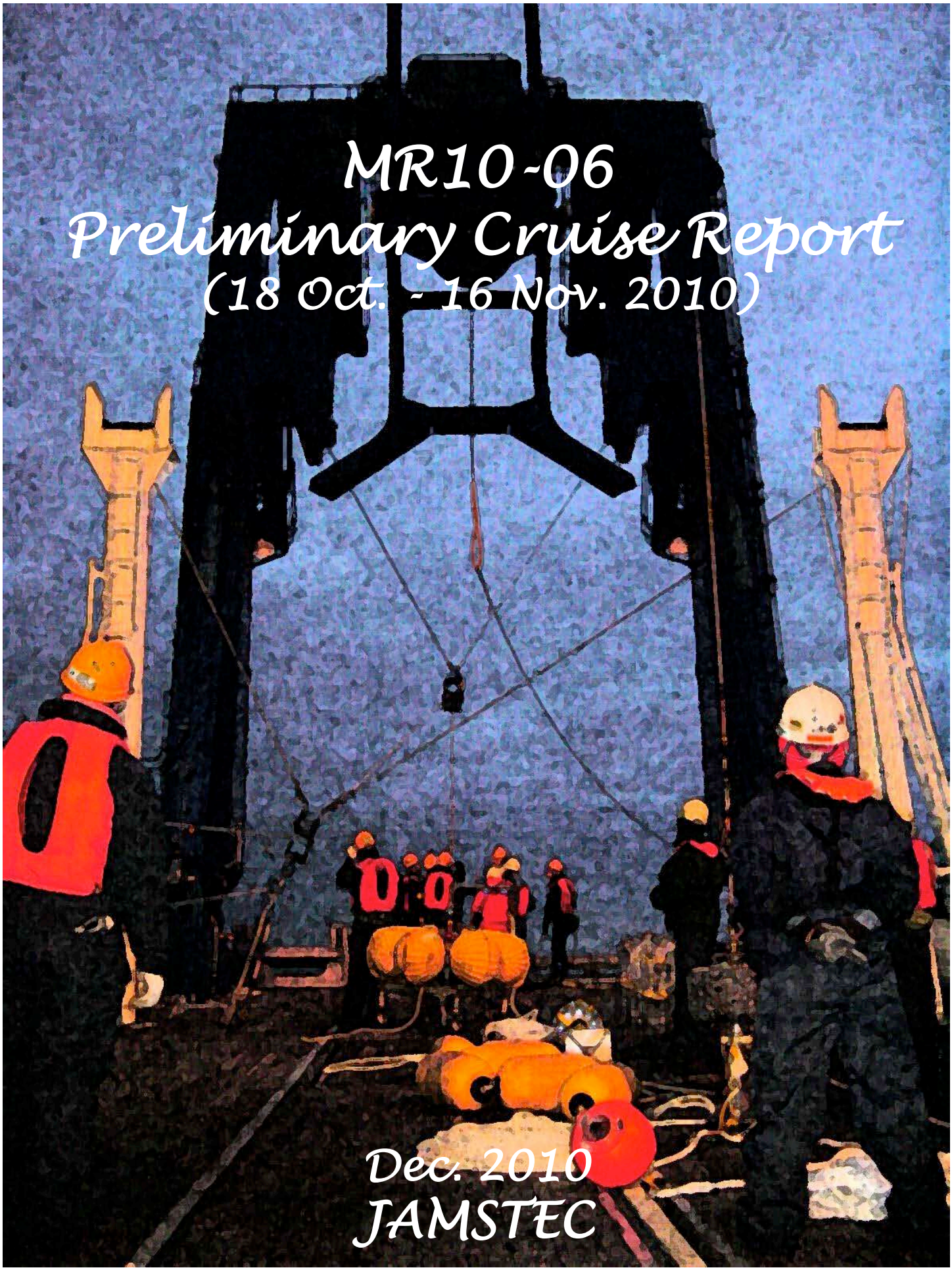

MR10-06
Preliminary Cruise Report
(18 Oct. - 16 Nov. 2010)

Dec. 2010

JAMSTEC

Note

This cruise report is a preliminary documentation published in approximately a month after the end of this cruise. It may not be corrected even if changes on contents are found after publication. It may also be changed without notice. Data on the cruise report may be raw or not processed. Please ask the principal investigator and parsons in charge of respective observations for the latest information and permission before using. Users of data are requested to submit their results to JAMSTEC Data Integration and Analysis Group (DIAG).

12 December 2010

Principal Investigator of MR10-06

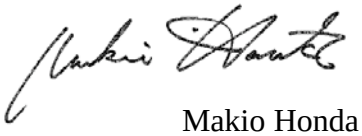

Makio Honda
JAMSTEC

Cruise Report ERRATA of the Nutrients part

page	Error	Correction
77	potassium nitrate CAS No. 7757-91-1	potassium nitrate CAS No. 7757-79-1
75	1N H_2SO_4	1M H_2SO_4

Cruise Report ERRATA of the Photosynthetic Pigments part

page	Error	Correction
131	Ethyl-apo-8'-carotenoate	trans-β-Apo-8'-carotenal
*132	DHI Co. SIGMA Co. WACO Ltd.	Sigma-Aldrich Co. Sigma-Aldrich Co. WAKO Ltd.

*: in Table 1

Contents of MR10-06 Preliminary Cruise Report

Cover sheet: the first prize of “MR10-06 CRUISE REPORT COVER SHEET CONTEST” by M. Honda

A. Cruise summary

1. Cruise information

(1) Cruise designation (research vessel)
MR10-06 (R/V MIRAI)

(2) Cruise title (principal science proposal) and introduction
Change in material cycles and ecosystem by the climate change and its feedback
Introduction

Some disturbing effects are progressively coming to the fore in the ocean by climate change, such as rising water temperature, intensification of upper ocean stratification and ocean acidification. It is supposed that these effects result in serious damage to the ocean ecosystems. Disturbed ocean ecosystems will change a material cycle through the change of biological pump efficiency, and it will be fed back into the climate. We are aimed at clarifying the mechanisms of changes in the ocean structure in ocean ecosystems derived from the climate change,

We arranged the time-series observation stations in the subarctic gyre (K2: 47°N 160°E) and the subtropical gyre (S1: 30°N, 145°E) in the western North Pacific. In general, biological pump is more efficient in the subarctic gyre than the subtropical gyre because large size phytoplankton (diatom) is abundant in the subarctic gyre by its eutrophic oceanic condition. It is suspected that the responses against climate change are different for respective gyres. To elucidate the oceanic structures in ocean ecosystems and material cycles at both gyres is important to understand the relationship between ecosystem, material cycle and climate change in the global ocean.

There are significant seasonal variations in the ocean environments in both gyres. The seasonal variability of oceanic structures will be estimated by the mooring systems and by the seasonally repetitive ship observations scheduled for next several years.

(3) Principal Investigator (PI)
Makio Honda
Research Institute for Global Change (RIGC)
Japan Agency for Marine-Earth Science and Technology (JAMSTEC)

(4) Science proposals of cruise

Affiliation	PI	Proposal titles
AORI / The Univ. Tokyo	Koji HAMASAKI	Studies on the microbial-geochemical processes that regulate the operation of the biological pump in the subarctic and subtropical regions of the western North Pacific
Kagoshima Univ.	Toru KOBARI	Effects of meso-zooplankton on food web and vertical flux
Nagoya Univ.	Osamu ABE	An evaluation of past change of primary productivity at the region of NPIW formation using oxygen triple isotopes, O_2, N_2 and noble gases.
Nagoya Univ.	Ippei NAGAO	Measurement of sea-to-air flux of marine biogenic gas (dimethyl sulfide) by eddy covariance method
JAMSTEC	Makio HONDA	Research and development of optical measurement of marine snow
Okayama	Osamu	Onboard continuous air-sea eddy flux measurement

Univ.	TSUKAMOTO	
Nagoya Univ,	Yoshihisa MINO	Settling velocity of particles in the twilight zone
JAMSTEC	Hisanori TAKASHIMA	Tropospheric aerosol and gas profile observations by MAX-DOAS on a research vessel
MRI	Michio AOYAMA	Long-term study on nutrients in global ocean
Toyama Univ.	Kazuma AOKI	Maritime aerosol optical properties from measurements of Ship-borne sky radiometer
JAMSTEC	Toshio SUGA	Study of ocean circulation and heat and freshwater transport and their variability, and experimental comprehensive study of physical, chemical, and biochemical processes in the western North Pacific by the deployment of Argo floats and using Argo data
NIES	Nobuo SUGIMOTO	Study of distribution and optical characteristics of ice/water clouds and marine aerosols
Chiba Univ.	Masao NAKANISHI	Tectonics of the mid-Cretaceous Pacific Plate
Ryukyu Univ.	Takeshi MATSUMOTO	Standardization of marine geophysical data and its application to the ocean floor geodynamics studies
JAMSTEC	Yoshimi KAWAI	Observational research on air-sea interaction in the Kuroshio-Oyashio Extension region
JAMSTEC	Naoyuki KURITA	Rain and seawater sampling for stable isotopes

(4) Cruise period (port call)
18 October 2010 (Dutch Harbor) – 16 November 2010 (Sekinehama)

(5) Cruise region (geographical boundary)
The western North Pacific (60°N – 30°N, 140°E – 165°W)

(6) Cruise truck and stations

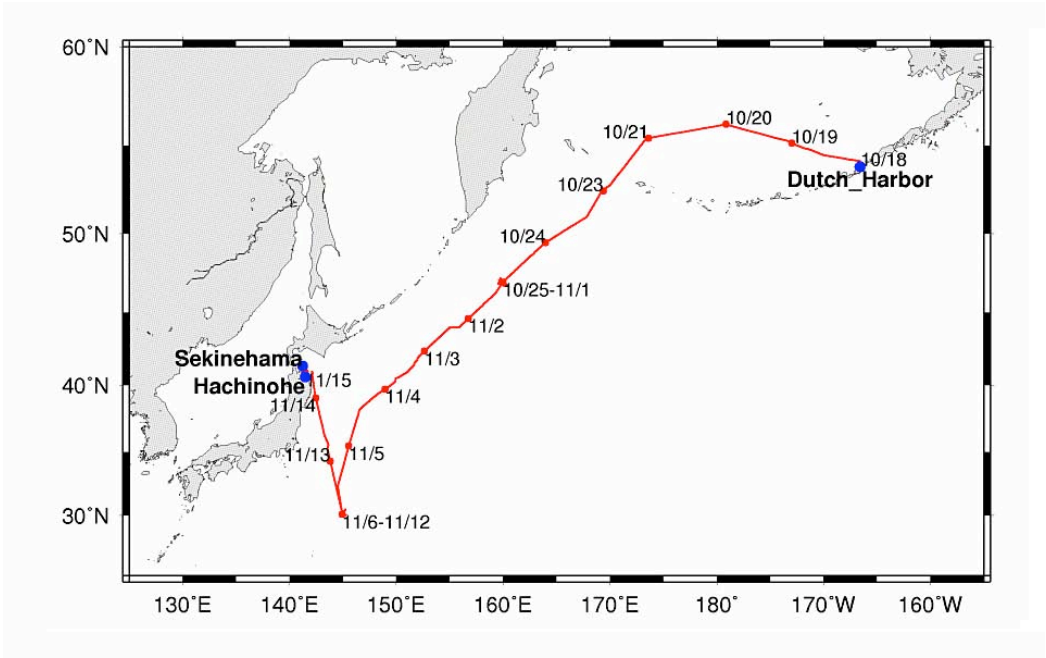

2. Overview of MR10-06

(1) Objective

Objective of this cruise is to collect biogeochemical and physical data in late autumn at our western Pacific time-series stations K2 (subarctic gyre) and S1 (subtropical data).

(2) Overview of MR10-06

Scientific cruises for the time-series observational study of biogeochemical oceanography in the western North Pacific has been conducted since late 1990's. These cruises have been in trouble for bad weather and rough sea condition very often. We expected that we would be also forced to suffer from bad condition and would give up many observations during coming cruise. Actually a fright (Anchorage - Dutch Harbor) for several participants was cancelled and their arrival was delayed. In addition, approach of R/V MIRAI to Dutch Harbor was very tough because of rough sea condition. However unlike we expected, MR10-06 cruise was generally plain sailing. We were sometimes forced to cancel some observations and to wait the good sea condition for observation, and but that was only a tiny part. We were able to conducted comprehensive observations including water sampling, plankton sampling, meteorological observation, recovery and deployment of mooring systems and so on at stations K2 and S1 on schedule. The followings are a part of preliminary results of our observation.

1) Ocean structure

Surface seawater temperature (SST) at station K2 was approximately 8°C (Fig. 1a). Intermediate cold water (dichothermal layer) of 1°C was observed at around 100 m. SST at station S1 was 26°C. These temperatures were approximately 5°C warmer than those in winter (January and February) observed during previous cruise (MR10-01). Surface mixed layer depth (MLD: 0.125 criteria) at station K2 and S1 was approximately 42 m and 35 m, respectively (Fig. 1b). These MLD were approximately 50 m shallower than winter MLD.

Euphotic layer (depth with 0.5% of surface photosynthetic available radiation (PAR)) at station K2 was approximately 50 m (no data shown). On the other hand, euphotic layer at station S1 was approximately 100 m. It is easily suspected that this is attributed to the difference in abundance of particulate materials in the water column.

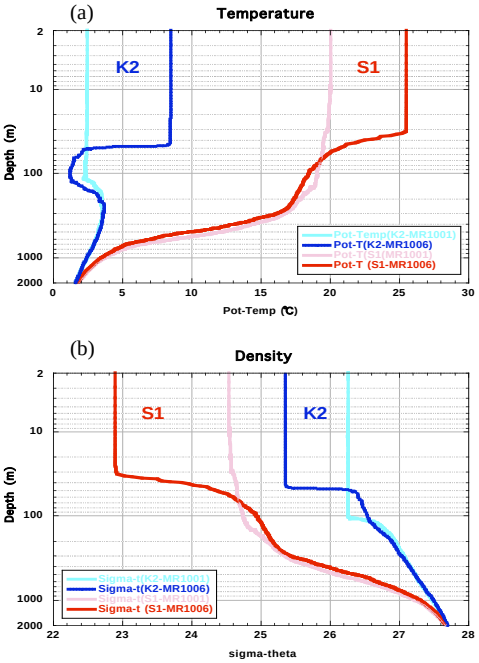

Fig.1 SST (a) and density in sigma-theta (b)

2) pCO_2

During cruise, underway pCO_2 observation was conducted. Surface pCO_2 (xCO_2) at station K2 (47°N) was approximately 340 ppm against approximately 390 ppm of atmospheric pCO_2 (Fig. 2 a). It is indicative of that station K2 during this cruise was potentially the sink of atmospheric CO_2 unlike winter (source of CO_2). Surface pCO_2 at station S1 (30°N) was 375 ppm and slightly smaller than atmospheric pCO_2. Station S1 was also the sink of atmospheric CO_2 during

MR10-06. Compared to winter pCO_2 (Fig. 2 b) observed previous cruise (MR10-06), surface pCO_2 at station K2 in autumn decreased by approximately 80 ppm (from 420 to 340 ppm). This is attributed to uptake of CO_2 by biological activity. On the other hand, pCO_2 at station S1 increased by approximately 50 pm (from 325 to 375 ppm). This is attributed to increase of SST.

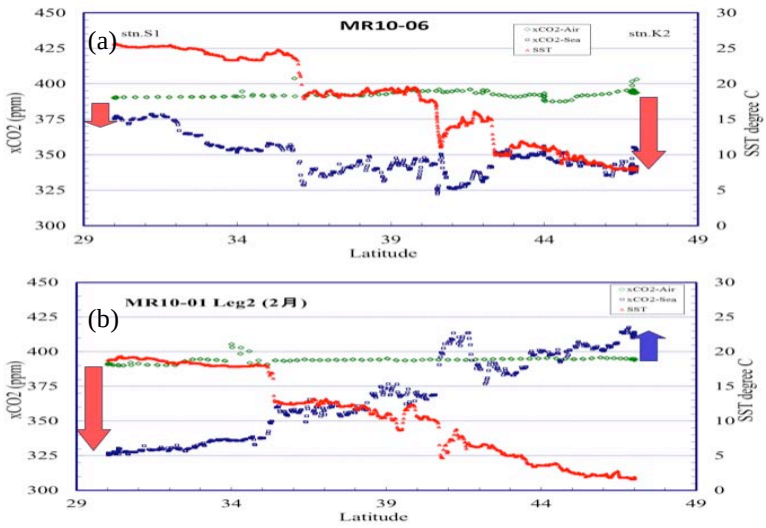

Fig.2 Surface pCO_2 (blue), atmospheric pCO_2 (green) and SST (red) during this MR10-06 cruise (a) and previous MR10-01 cruise (b).

3) Phytoplankton and Primary productivity

Concentration of Chlorophyll *a* (Chl-*a*) in the upper 40 m was approximately 0.6 mg m^{-3} at station K2 (Fig. 3 a). Below 40m, Chl-*a* decreased largely. Based on measurement of accesary pigments by HPLC, it was suspected that a half of phytoplankton was *haptophytes*, and *diatom*, that is representative phytoplankton of Western Pacific subarctic gyre, was small fraction during this cruise. At station S1, concentration of Chl-a was smaller than that at station K2. Subsurface Chl-*a* maximum was observed at around 90 m (Fig. 3 b). Subsurface Chl-*a* maximum is generally observed in the area where surface light intensity is too strong for phytoplankton growth and nutrient is depleted near surface. Oceanographic condition of Station

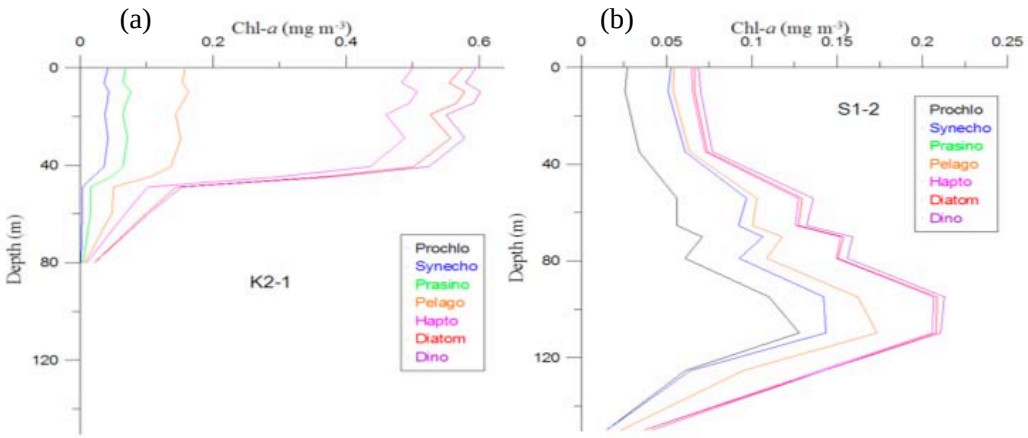

Fig. 3 Chl-*a* concentration at station K2 (a) and S1 (b). Composition of phytoplankton is also shown.

S1 might correspond to this condition. *Prochlorococcus* was pre-dominant and it is noted that diatom was very little.

Primary productivity (PP) was measured twice by simulated in situ incubation (SIS) at station K2 (Fig. 4). PP decreased with depth and nearly zero at the bottom of euphotic layer (~ 50 m). Integrated PP were 284 and 401 mg-C m^{-2} day^{-1}. Compared to winter PP (~ 100 mg-C m^{-2} day^{-1}), PP was high. PP at station S1 also decrease with depth. PP was observed to the deeper depth because euphotic layer was approximately 100 m. Integrated PP at station S1 was 131 mg m^{-2} day^{-1} and one fourth of PP observed during MR10-01 cruise (~ 500 mg-C m^{-2} day^{-1}). It is noted that weather during the above incubation was cloudy or rainy and surface PAR was very low (~ 7 mol quanta m^{-2} day^{-1}).

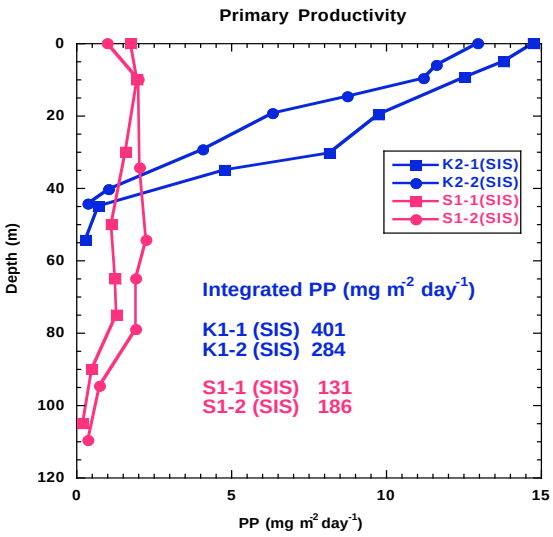

Fig.4 Primary productivity

4) Sinking particles collected by sediment traps

Seasonal sinking particle fluxes were collected at approximately 200 m, 500 m and 5000 m at stations K2 and S1 between February and October 2010. In order to know seasonal variability of sinking particle flux qualitatively onboard, heights of collected particles in collecting cups were measured with a scale. Particles collected at 200 m mainly consist of creature larger than 1 mm such as small fish, shrimp and large zooplankton. Thus these materials might not be sinking particles, but “swimmer”.

(Station K2)

Sinking particle flux at 200 m started to increase from 22 February (start date of sample collection) and peaked at around middle May (Fig. 5a). Sinking particle flux at 200 m also increased in autumn centering early September. Sinking particle flux at 500 m show similar seasonal variability to that at 200 m with some differences: period of flux peak was delayed by one cup period (12 days), and peak in autumn was smaller than that observed at 200 m (Fig. 5b). The first peak also appeared at 5000 m with time lag (12 days) from 500 m flux peak (Fig. 5c). If sinking particle flux at 500 m arrived at 5000 m after 12 days, sinking velocity can be estimated to be approximately 375 m day^{-1}. After high flux was observed, little sinking particles were collected by 5000 m sediment trap. It is likely attributed not to that sinking particle fluxes were very small, but to “the clogging” of 5000 m sediment trap after high flux.

(Station S1)

Sinking particle flux at 200 m increased in late April 2010 (Fig. 5d). Small flux peak was also observed in late February and early March. Small flux peak was observed in March at 500 m (Fig. 5e). On the other hand, clear flux increase at 5000 m was not observed (Fig. 5f). Compared to fluxes at station K2, seasonal variability and flux of sinking particles was very small at station S1.

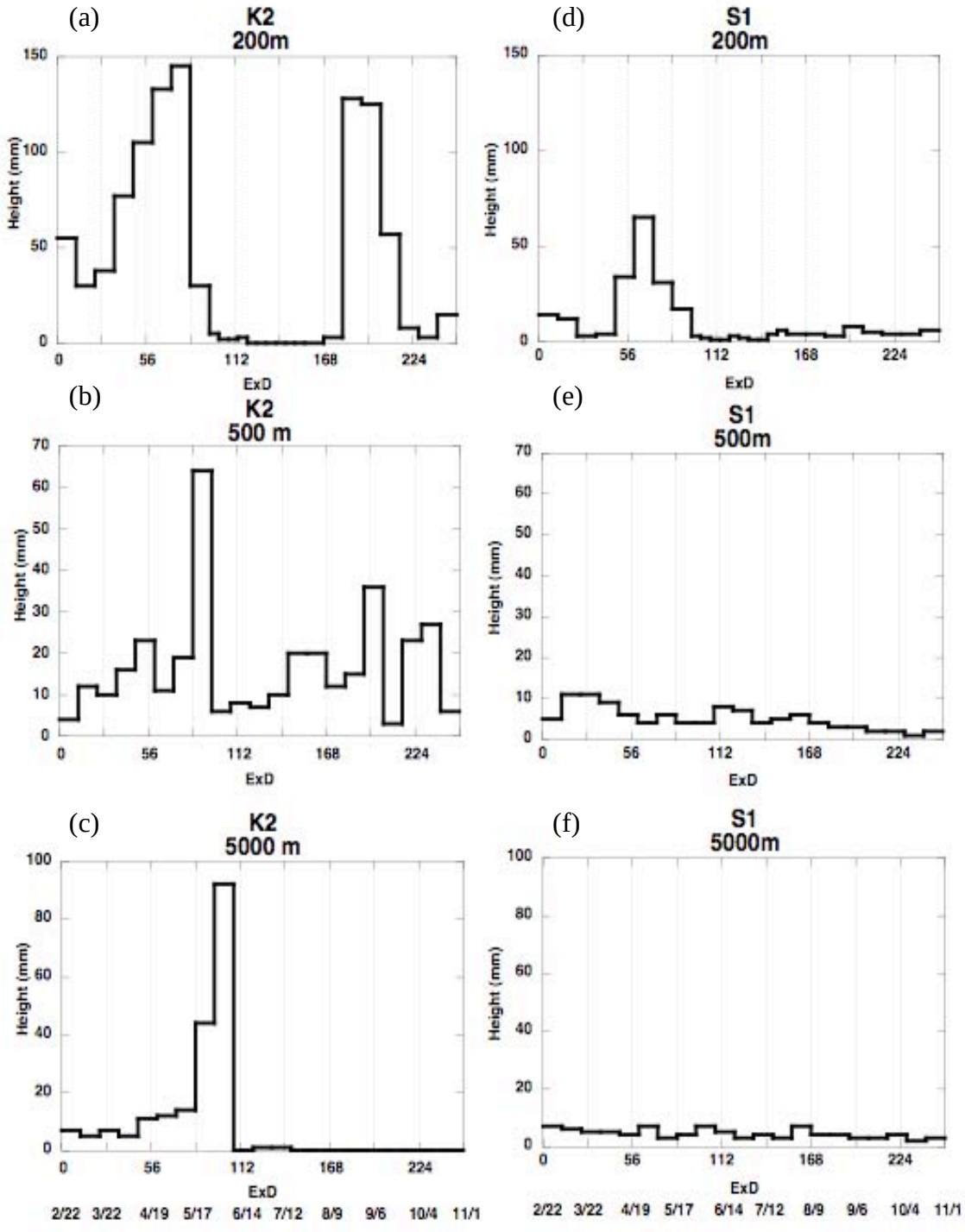

Fig. 5 Visual estimation of total mass flux at respective depths at station K2 (left side figures) and S1 (right side figures)

B. Text

1. Outline of MR10-06

Makio HONDA (JAMSTEC RIGC)
Principal Investigator of MR10-06

1.1 Cruise summary

(1) Introduction of principal science proposal

Some disturbing effects are progressively coming to the fore in the ocean by climate change, such as rising water temperature, intensification of upper ocean stratification and oceanic acidification. It is supposed that these effects result in serious damage to the ocean ecosystems. Disturbed ocean ecosystems will change a material cycle through the change of biological pump efficiency, and it will be fed back into the climate. We are aimed at clarifying the mechanisms of changes in the oceanic structure in ocean ecosystems derived from the climate change,

We arranged the time-series observation stations in the subarctic gyre (K2: 47°N 160°E) and the subtropical gyre (S1: 30°N, 145°E) in the western North Pacific. In general, biological pump is more efficient in the subarctic gyre than the subtropical gyre because large size phytoplankton (diatom) is abundant in the subarctic gyre by its eutrophic oceanic condition. It is suspected that the responses against climate change are different for respective gyres. To elucidate the oceanic structures in ocean ecosystems and material cycles at both gyres is important to understand the relationship between ecosystem, material cycle and climate change in the global ocean.

There are significant seasonal variations in the ocean environments in both gyres. The seasonal variability of oceanic structures will be estimated by the mooring systems and by the seasonally repetitive ship observations scheduled for next several years.

(2) Objective of this cruise

Objective of this cruise is to collect biogeochemical and physical data in late autumn at our western Pacific time-series stations K2 (subarctic gyre) and S1 (subtropical data).

(3) Overview of MR08-05

Scientific cruises for the time-series observational study of biogeochemical oceanography in the western North Pacific has been conducted since late 1990's. These cruises have been in trouble for bad weather and rough sea condition very often. We expected that we would be also forced to suffer from bad condition and would give up many observations during coming cruise. Actually a fright (Anchorage - Dutch Harbor) for several participants was cancelled and their arrival was delayed. In addition, approach of R/V MIRAI to Dutch Harbor was very tough because of rough sea condition. However unlike we expected, MR10-06 cruise was generally plain sailing. We were sometimes forced to cancel some observations and to wait the good sea condition for observation, and but that was only a tiny part. We were able to conducted comprehensive observations including water sampling, plankton sampling, meteorological observation, recovery and deployment of mooring systems and so on at stations K2 and S1 on schedule. The followings are a part of preliminary results of our observation.

1) Ocean structure

Surface seawater temperature (SST) at station K2 was approximately 8°C (Fig. 1a). Intermediate cold water (dichothermal layer) of 1°C was observed at around 100 m. SST at station S1 was 26°C. These temperatures were approximately 5°C warmer than those in winter (January and February) observed during previous cruise (MR10-01). Surface mixed layer depth (MLD: 0.125 criteria) at station K2 and S1 was approximately 42 m and 35 m, respectively (Fig. 1b). These MLD were approximately 50 m shallower than winter MLD.

Euphotic layer (depth with 0.5% of surface photosynthetic available radiation (PAR)) at station K2 was approximately 50 m (no data shown). On the other hand, euphotic layer at station S1 was approximately 100 m. It is easily suspected that this is attributed to the difference in abundance of particulate materials in the water column.

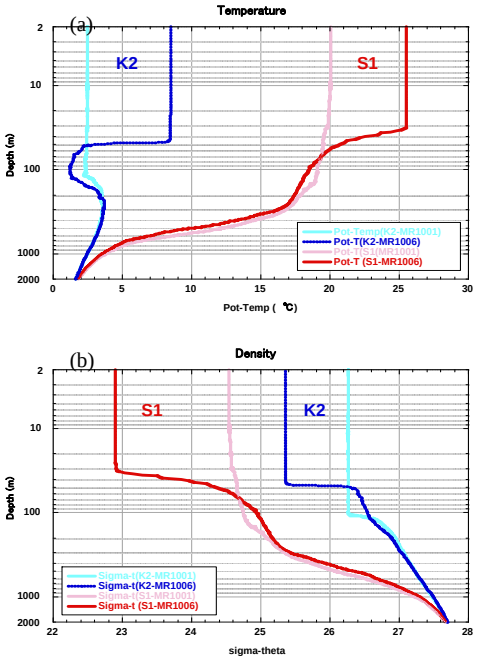

Fig.1 SST (a) and density in sigma-theta (b)

2) pCO_2

During cruise, underway pCO_2 observation was conducted. Surface pCO_2 (xCO_2) at station K2 (47°N) was approximately 340 ppm against approximately 390 ppm of atmospheric pCO_2 (Fig. 2 a). It is indicative of that station K2 during this cruise was potentially the sink of atmospheric CO_2 unlike winter (source of CO_2). Surface pCO_2 at station S1 (30°N) was 375 ppm and slightly smaller than atmospheric pCO_2. Station S1 was also the sink of atmospheric CO_2 during MR10-06. Compared to winter pCO_2 (Fig. 2 b) observed previous cruise (MR10-06), surface pCO_2 at station K2 in autumn decreased by approximately 80

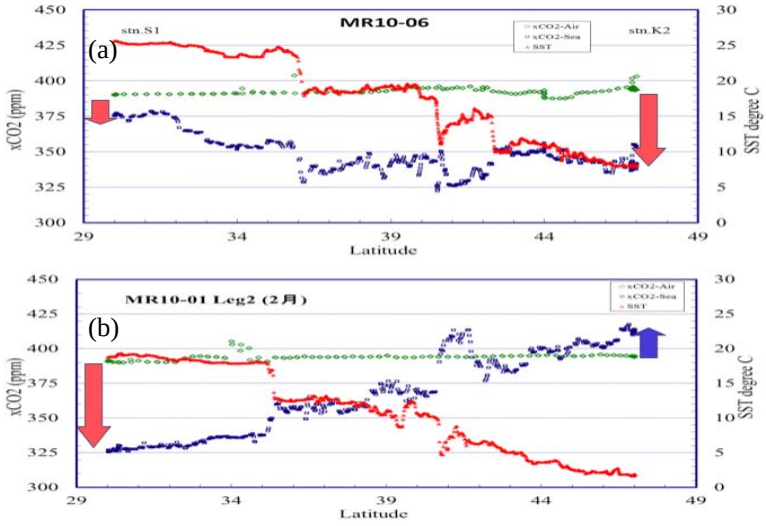

Fig.2 Surface pCO_2 (blue), atmospheric pCO_2 (green) and SST (red) during this MR10-06 cruise (a) and previous

ppm (from 420 to 340 ppm). This is attributed to uptake of CO_2 by biological activity. On the other hand, pCO_2 at station S1 increased by approximately 50 pm (from 325 to 375 ppm). This is attributed to increase of SST.

3) Phytoplankton and Primary productivity

Concentration of Chlorophyll *a* (Chl-*a*) in the upper 40 m was approximately 0.6 mg m^{-3} at station K2 (Fig. 3 a). Below 40m, Chl-*a* decreased largely. Based on measurement of accesary pigments by HPLC, it was suspected that a half of phytoplankton was *haptophytes*, and *diatom*, that is representative phytoplankton of Western Pacific subarctic gyre, was small fraction during this cruise. At station S1, concentration of Chl-a was smaller than that at station K2. Subsurface Chl-*a* maximum was observed at around 90 m (Fig. 3 b). Subsurface Chl-*a* maximum is generally observed in the area where surface light intensity is too strong for

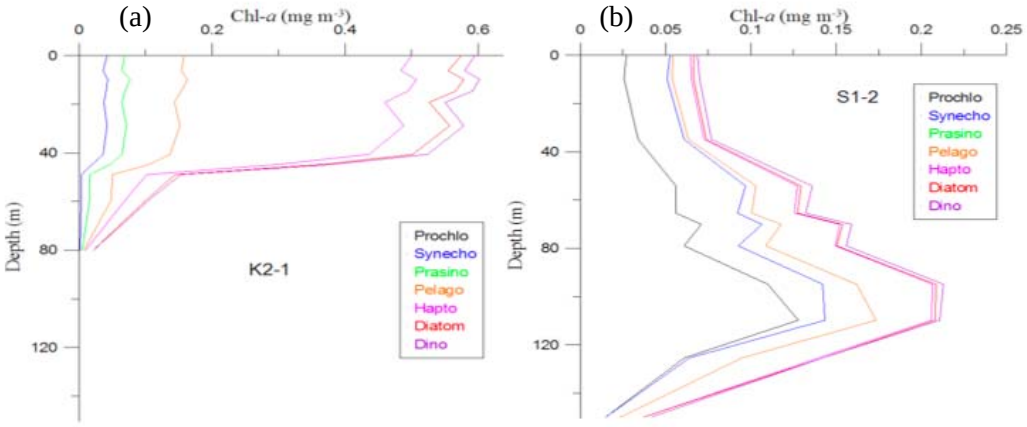

Fig. 3 Chl-*a* concentration at station K2 (a) and S1 (b). Composition of

phytoplankton growth and nutrient is depleted near surface. Oceanographic condition of Station S1 might correspond to this condition. *Prochlorococcus* was pre-dominant and it is noted that diatom was very little.

Primary productivity (PP) was measured twice by simulated in situ incubation (SIS) at station K2 (Fig. 4). PP decreased with depth and nearly zero at the bottom of euphotic layer (~ 50 m). Integrated PP were 284 and 401 mg-C m^{-2} day^{-1}. Compared to winter PP (~ 100 mg-C m^{-2} day^{-1}), PP was high. PP at station S1 also decrease with depth. PP was observed to the deeper depth because euphotic layer was approximately 100 m. Integrated PP at station S1 was 131 mg m^{-2} day^{-1} and one fourth of PP observed during MR10-01 cruise (~ 500 mg-C

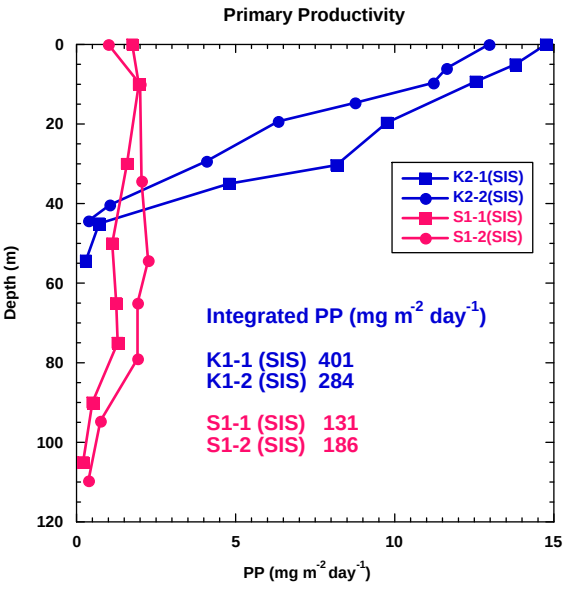

Fig.4 Primary productivity

m^{-2} day^{-1}). It is noted that weather during the above incubation was cloudy or rainy and surface PAR was very low (~ 7 mol quanta m^{-2} day^{-1}).

4) Sinking particles collected by sediment traps

Seasonal sinking particle fluxes were collected at approximately 200 m, 500 m and 5000 m at stations K2 and S1 between February and October 2010. In order to know seasonal variability of sinking particle flux qualitatively onboard, heights of collected particles in collecting cups were measured with a scale. Particles collected at 200 m mainly consist of creature larger than 1 mm such as small fish, shrimp and large zooplankton. Thus these materials might not be sinking particles, but “swimmer”.

(Station K2)

Sinking particle flux at 200 m started to increase from 22 February (start date of sample collection) and peaked at around middle May (Fig. 5a). Sinking particle flux at 200 m also increased in autumn centering early September. Sinking particle flux at 500 m show similar seasonal variability to that at 200 m with some differences: period of flux peak was delayed by one cup period (12 days), and peak in autumn was smaller than that observed at 200 m (Fig. 5b). The first peak also appeared at 5000 m with time lag (12 days) from 500 m flux peak (Fig. 5c). If sinking particle flux at 500 m arrived at 5000 m after 12 days, sinking velocity can be estimated to be approximately 375 m day^{-1}. After high flux was observed, little sinking particles were collected by 5000 m sediment trap. It is likely attributed not to that sinking particle fluxes were very small, but to “the clogging” of 5000 m sediment trap after high flux.

(Station S1)

Sinking particle flux at 200 m increased in late April 2010 (Fig. 5d). Small flux peak was also observed in late February and early March. Small flux peak was observed in March at 500 m (Fig. 5e). On the other hand, clear flux increase at 5000 m was not observed (Fig. 5f). Compared to fluxes at station K2, seasonal variability and flux of sinking particles was very small at station S1.

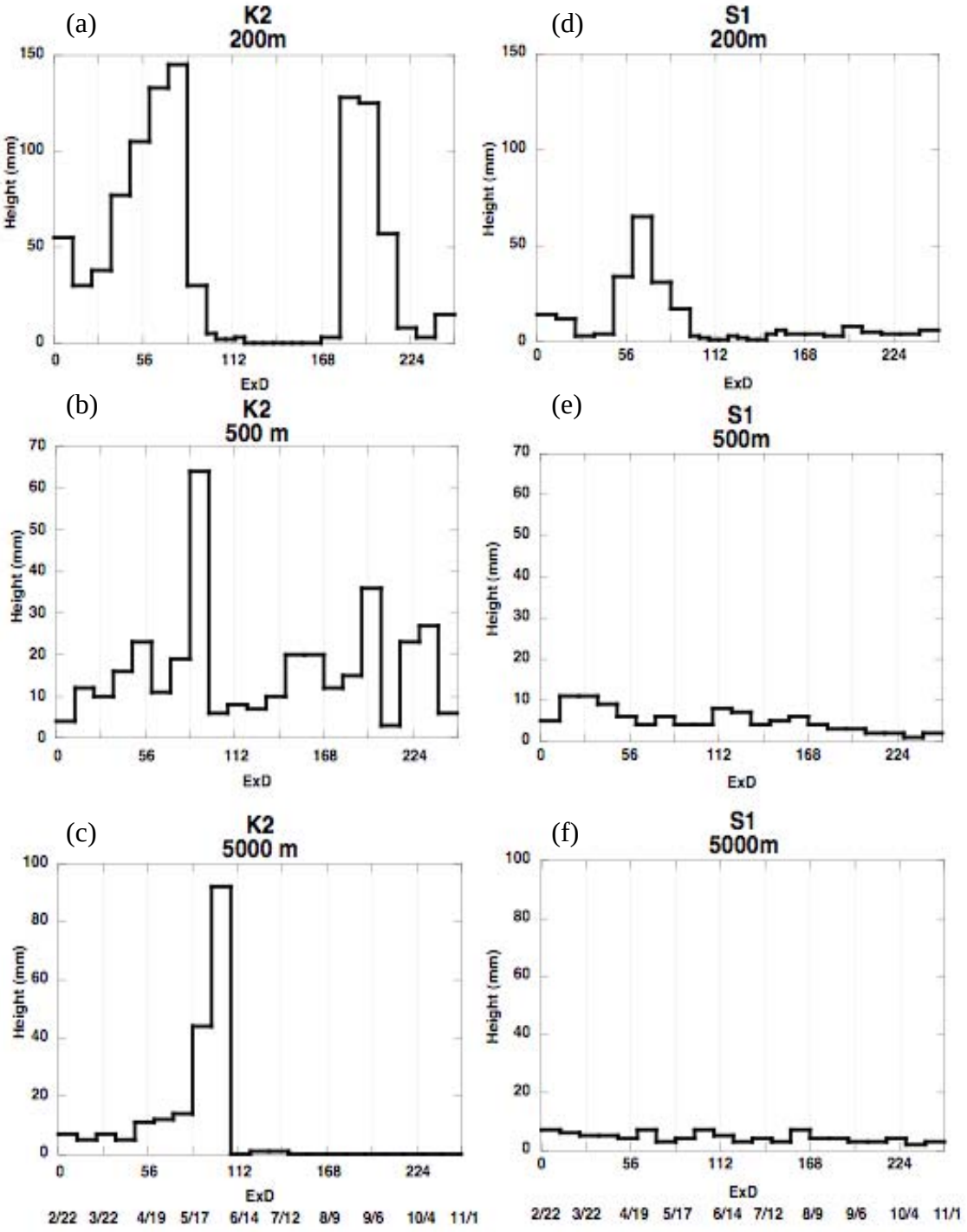

Fig. 5 Visual estimation of total mass flux at respective depths at station K2 (left side figures) and S1 (right side figures)

(4) Scientific gears

All hydrocasts were conducted using 36-position 12 liter Niskin bottles carousel system with SBE CTD-DO system, fluorescence and transmission sensors. JAMSTEC scientists and MWJ (Marine Work Japan Co. Ltd.) technician group were responsible for analyzing water sample for salinity, dissolved oxygen, nutrients, CFCs, total carbon contents, alkalinity and pH. Cruise participants from JAMSTEC, Nagoya University, Tokyo University, Kagoshima University and Okayama University helped to divide seawater from Niskin bottles to sample bottles for analysis. Surface water was collected with bucket.

Optical measurement in air and underwater was conducted with PAR sensor (RAMSES-ACC) and SPMR/SMSR called “Free Fall”.

For collecting suspended particles at stationK2, Large Volume Pump (LVP) was deployed.

For observing in situ particles, optical sensor called LISST (Laser In Situ Scattering and Transmissometer) was deployed by University of Tokyo.

GODI technicians group undertook responsibility for underway current direction and velocity measurements using an Acoustic Current Profiler (ADCP), geological measurements (topography, geo-magnetic field and gravity), and collecting meteorological data. In addition, approximately eighty XCTD were deployed in the Kuroshio-Oyashio mixture zone.

For collection of zooplankton, NORPAC plankton net, and IONESS were deployed.

For conducting in situ incubation for measurement of primary productivity and collecting sinking particles at station K2, drifter was deployed at station K2.

For observing vertical profile of primary productivity optically, FRRF was deployed.

In order to conduct time-series observation in biogeochemical cycle, JAMSTEC BGC and POPPS mooring was recovered and re-deployed at station K2 (only BGC) and S1. The BGC consisted of 3 sediment traps at 200, 500, and 5000 m.

For observation of atmospheric chemistry (aerosol and gas), various instruments including “sky-radiometer” and “MAX-DOAS” were onboard and automatic measurement was conducted.

Please read text for more detail information and other instruments used for oceanographic and meteorological or atmospheric observation.

1.2 Track and log

1.2.1 Research Area

The western North Pacific (60°N – 30°N, 140°E – 165°W)

1.2.2 Cruise track

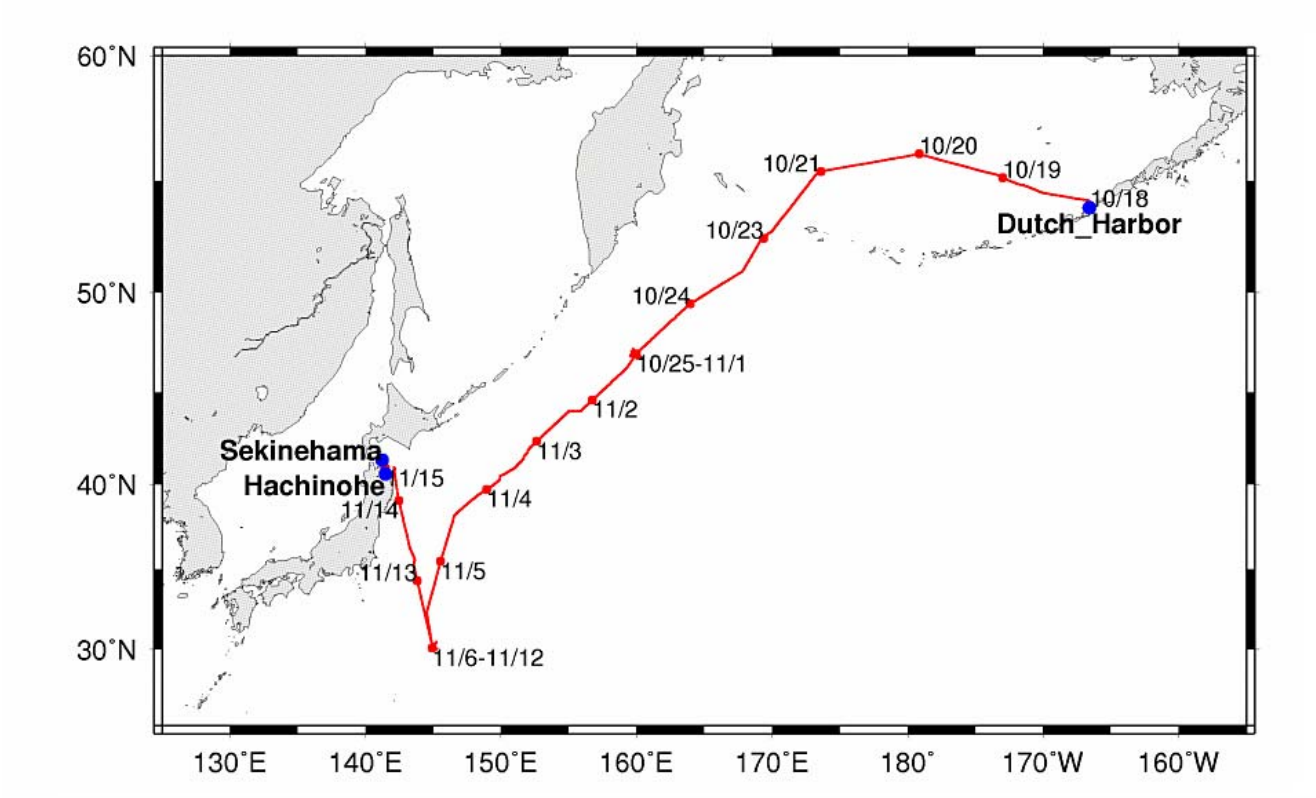

1.2.3 Cruise log

U.T.C.		S.M.T.		Position		Event logs
Date	Time	Date	Time	Lat.	Lon.	
10.18	19:00	10.18	11:00	53-54N	166-32W	Departure from Dutch Harbor
10.19	0:00		16:00	-	-	Continuously observations start
	6:00		22:00	-	-	Time adjustment -1 hour (SMT=UTC-9h)
	21:54	10.19	12:54	55-14N	173-14W	Arrival at Station 01
	22:10		13:10	55-14.06N	173-13.92W	FRRF #01 (150 m)
	22:47		13:47	55-14.26N	173-13.56W	CTD cast #01 (1,000 m)
	23:48		14:48	-	-	Departure from Station 01
10.20	7:00		22:00	-	-	Time adjustment -1 hour (SMT=UTC-10h)
	19:42	10.20	9:42	56-08N	179-08W	Arrival at Station 02
	19:58		9:58	56-08.47N	179-07.50W	CTD cast #02 (3,773 m)
	23:03		13:03	56-09.21N	179-07.73W	FRRF #02 (150 m)
	23:36		13:36	-	-	Departure from Station 02
10.21	8:00		22:00	-	-	Time adjustment -1 hour (SMT=UTC-11h)
	23:48	10.21	12:48	-	-	Station 03 - cancel
10.22	9:00		22:00	-	-	Time adjustment -1 hour (SMT=UTC-12h)
		10.22	-	-	-	Skip for passing International Date Line (SMT=UTC+12h)
	18:48	10.23	06:48	52-45N	169-50E	Arrival at CTD cable test point
	18:57		06:57	52-45.42N	169-50.09E	CTD cable test (6,000 m)
	22:12		10:12	-	-	Departure from CTD cable test point
10.23	0:54		12:54	52-24N	169-10E	Arrival at Station 04
	0:56		12:56	52-24.01N	169-09.85E	FRRF #03 (100 m)
	1:22		13:22	52-24.02N	169-09.58E	CTD cast #03 (1,000 m)
	2:30		14:30	-	-	Departure from Station 04
	10:00		22:00	-	-	Time adjustment -1 hour (SMT=UTC+11h)
10.24	1:48	10.24	12:48	49-24N	163-50E	Arrival at Station 05
	1:59		12:59	49-23.88N	163-50.23E	FRRF #04 (100 m)
	2:26		13:26	49-23.70N	163-50.37E	CTD cast #04 (1,000 m)
	3:30		14:30	-	-	Departure from Station 05

	19:06	10.25	06:06	47-00N	160-00E	Arrival at Station 06 (K2)
	20:57		07:57	46-59.32N	159-58.50E	CTD cast #05 (5,195 m)
10.25	0:28		11:28	46-59.20N	159-58.72E	FRRF #05 (100 m)
	0:55		11:55	46-59.38N	159-58.71E	Free fall optical measruements #01
	2:29		13:29	47-00.82N	159-58.66E	BGC mooring recovery
	5:43		16:43	46-59.48N	160-03.27E	CTD cast #06 (300 m)
	6:27		17:27	46-59.38N	160-03.27E	Plankton net #01 (20 m)
	6:40		17:40	46-59N	160-04E	Flux mesurements start
	15:00	10.26	02:00	46-48N	160-17E	Flux mesurements finish
	16:59		03:59	46-53.21N	160-00.07E	CTD cast #07 (300 m)
	17:57		04:57	46-53.27N	160-01.20E	FRRF #06 (100 m)
	19:59		06:59	46-52.95N	160-01.12E	LISST #01 (200 m)
	20:55		07:55	46-52.69N	160-01.96E	CTD cast #08 (2,000 m)
	22:32		09:32	46-52.11N	160-02.51E	FRRF #07 (100 m)
	22:59		09:59	49-51.93N	160-02.50E	Plankton net #02-1 (20 m)
	23:08		10:08	49-51.80N	160-02.53E	Plankton net #02-2 (50 m)
	23:20		10:20	49-51.68N	160-02.63E	Plankton net #02-3 (100 m)
	23:33		10:33	49-51.56N	160-02.64E	Plankton net #02-4 (150 m)
	23:49		10:49	49-51.42N	160-02.65E	Plankton net #02-5 (200 m)
10.26	0:06		11:06	49-51.33N	160-02.58E	Plankton net #02-6 (5 m)
	0:12		11:12	49-51.23N	160-02.49E	Plankton net #02-7 (300 m)
	2:58		13:58	46-52.11N	160-02.51E	FRRF #08 (100 m)
	3:22		14:22	46-50.85N	160-02.66E	Plankton net #03 (NORPAC: 200 m)
	3:48		14:48	46-50.77N	160-02.82E	CTD cast #09 (1,000 m)
	20:56	10.27	07:56	46-51.78N	159-56.10E	CTD cast #10 (1,000 m)
	22:04		09:04	46-51.80N	159-56.11E	Plankton net #04 (Twin-NORPAC: 200 m)
	23:28		10:28	46-51.67N	159-56.90E	CTD cast #11 (5,000 m)
10.27	2:49		13:49	46-51.22N	159-57.27E	Plankton net #05-1 (1,000 m)
	3:55		14:55	46-51.20N	159-57.21E	Plankton net #05-2 (700 m)
	4:43		15:43	46-51.01N	159-57.17E	Plankton net #05-3 (500 m)
	5:17		16:17	46-50.95N	159-57.17E	Plankton net #05-4 (50 m)
	5:30		16:30	46-50.93N	159-57.16E	Plankton net #05-5 (50 m)
	5:39		16:39	46-50.90N	159-57.18E	Plankton net #05-6 (100 m)
	7:56		18:56	46-49.65N	160-00.34E	Plankton net #06 (Twin-NORPAC: 200 m)
	8:54		19:54	46-49.31N	160-00.65E	Plankton net #07-1 (Twin-NORPAC: 50 m)
	9:06		20:06	46-49.21N	160-00.72E	Plankton net #07-2 (Twin-NORPAC: 150 m)
	10:30		21:30	46-49N	160-00E	Flux mesurements start
	17:00	10.28	04:00	46-55N	159-38E	Flux mesurements finish

10.28	0:14		11:14	46-51.85N	160-00.61E	Free fall optical measruements #02
	2:05		13:05	46-51.68N	159-59.78E	POPPS mooring recovery
	7:29		18:29	46-52.48N	159-55.52E	CTD cast #12 (100 m)
	7:55		18:55	46-52.54N	159-55.77E	Plankton net #08 (NORPAC: 40 m)
	16:59	10.29	03:59	46-51.79N	159-59.42E	CTD cast #13 (300 m)
	17:50		04:50	46-51.56N	159-59.40E	FRRF #09 (100 m)
	19:35		06:35	46-52.43N	159-59.77E	Surface drifting float buoy deployment
	20:56		07:56	46-54.80N	159-56.29E	FRRF #10 (100 m)
	21:20		08:20	46-54.80N	159-58.36E	LVP #01 (200 m)
10.29	0:04		11:04	46-54.22N	159-55.79E	IONESS #01 (1,000 m)
	3:06		14:06	46-50.13N	159-51.82E	FRRF #11 (100 m)
	3:55		14:55	46-49.76N	159-51.67E	Free fall optical measruements #03
	10:06		21:06	46-55.71N	159-54.38E	IONESS #02 (1,000 m)
	13:00	10.30	0:00	46-58N	159-49E	Flux mesurements start
	19:00		6:00	47-07N	159-37E	Flux mesurements finish
10.31	1:55	10.31	12:55	46-57.22N	160-06.47E	BGC mooring deployment
				47-00.37N	159-58.24E	BGC mooring fixed position
	8:00		19:00	47-00.11N	160-03.52E	Calibration for magnetometer #01
	19:04	11.1	6:04	46-50.09N	160-17.60E	Surface drifting float buoy recovery
	21:59		8:59	46-49.04N	160-01.36E	Water sampling for buckets #01
	23:53		10:53	46-49.40N	159-54.22E	IONESS #03 (1,000 m)
11.1	4:36		15:36	46-52.52N	159-53.91E	LVP #02 (1,000 m)
	10:06		21:06	-	-	Departure from Station 06 (K2)
11.2	7:36	11.2	18:36	44-00N	155-00E	Arrival at Station 07 (KNOT)
	7:41		18:41	44-00.05N	155-00.36E	CTD cast #14 (5,294 m)
	11:00		22:00	-	-	Departure from Station 07 (KNOT)
11.3	4:18	11.3	15:18	42-00N	152-07E	Arrival at Station 08
	4:24		15:24	42-00.01N	152-06.41E	FRRF #12 (100 m)
	4:49		15:49	41-59.92N	152-07.16E	CTD cast #15 (1,000 m)
	5:54		16:54	-	-	Departure from Station 08
11.4	11:54	11.4	22:54	38-00N	146-29E	Arrival at Station 09
	11:55		22:55	37-59.88N	146-29.41E	CTD cast #16 (1,000 m)
	12:11		23:11	37-59.93N	146-29.40E	XCTD #01 (JKEO)

	13:01	11.5	0:01	37-59.54N	146-29.66E	FRRF #13 (100 m)
	13:24		0:24	-	-	Departure from Station 09
	14:13		1:13	37-49.99N	146-27.99E	XCTD #02 (E01)
	15:05		2:05	37-40.00N	146-23.88E	XCTD #03 (E02)
	15:57		2:57	37-29.99N	146-19.46E	XCTD #04 (E03)
	16:47		3:47	37-19.99N	146-15.14E	XCTD #05 (E04)
	17:47		4:47	37-07.76N	146-10.49E	XCTD #06 (E05)
	18:25		5:25	37-00.01N	146-07.67E	XCTD #07 (E06)
	19:14		6:14	36-49.99N	146-04.00E	XCTD #08 (E07)
	20:03		7:03	36-39.99N	146-00.12E	XCTD #09 (E08)
	20:45		7:45	36-29.99N	145-56.31E	XCTD #10 (E09)
	21:27		8:27	36-19.99N	145-52.73E	XCTD #11 (E10)
	22:07		9:07	36-10.00N	145-49.21E	XCTD #12 (E11)
	22:46		9:46	36-00.00N	145-45.37E	XCTD #13 (E12)
	23:28		10:28	35-50.01N	145-41.65E	XCTD #14 (E13)
11.5	0:09		11:09	35-40.00N	145-38.00E	XCTD #15 (E14)
	0:52		11:52	35-30.00N	145-34.29E	XCTD #16 (E15)
	1:36		12:36	35-19.99N	145-30.91E	XCTD #17 (E16)
	2:19		13:19	35-10.00N	145-27.47E	XCTD #18 (E17)
	3:02		14:02	35-00.00N	145-24.15E	XCTD #19 (E18)
	3:44		14:44	34-49.99N	145-20.79E	XCTD #20 (E19)
	4:28		15:28	34-39.99N	145-17.85E	XCTD #21 (E20)
	5:12		16:12	34-29.99N	145-14.68E	XCTD #22 (E21)
	5:56		16:56	34-19.99N	145-11.45E	XCTD #23 (E22)
	6:40		17:40	34-10.00N	145-08.25E	XCTD #24 (E23)
	7:30		18:30	34-00N	145-05E	Arrival at Station 10
	7:32		18:32	33-59.97N	145-04.97E	FRRF #14 (150 m)
	8:07		19:07	34-00.03N	145-04.91E	CTD cast #17 (1,000 m)
	8:25		19:25	34-00.01N	145-04.92E	XCTD #25 (E24)
	9:12		20:12	-	-	Departure from Station 10
	9:58		20:58	22-49.99N	145-01.77E	XCTD #26 (E25)
	10:41		21:41	33-39.99N	144-58.22E	XCTD #27 (E26)
	11:00		22:00	-	-	Time adjustment -1 hours (SMT=UTC+10h)
	11:24		21:24	33-29.98N	144-54.96E	XCTD #28 (E27)
	12:07		22:07	33-19.95N	144-51.70E	XCTD #29 (E28)
	12:49		22:49	33-09.99N	144-48.27E	XCTD #30 (E29)
	13:31		23:31	33-00.00N	144-45.05E	XCTD #31 (E30)

	14:14	11.6	0:14	32-50.00N	144-41.80E	XCTD #32 (E31)
	14:57		0:57	32-40.01N	144-38.68E	XCTD #33 (E32)
	15:38		1:38	32-29.98E	144-35.36E	XCTD #34 (E33)
	16:05		2:05	32-23.68E	144-33.37E	XCTD #35 (KEO)
11.6	1:30		11:30	30-00N	145-00E	Arrival at Station 11 (S1)
	3:05		13:05	30-04.30N	144-57.74E	BGC mooring recovery
	6:48		16:48	30-00.08N	145-00.03E	CTD cast #18 (2,000 m)
	8:17		18:17	30-00.11N	144-59.94E	Plankton net #09-1 (NORPAC: 20 m)
	8:23		18:23	30-00.11N	144-59.94E	Plankton net #09-2 (NORPAC: 50 m)
	8:34		18:34	30-00.14N	144-59.92E	Plankton net #09-3 (NORPAC: 100 m)
	8:46		18:46	30-00.15N	144-59.92E	Plankton net #09-4 (NORPAC: 150 m)
	9:01		19:01	30-00.19N	144-59.90E	Plankton net #09-5 (NORPAC: 200 m)
	9:20		19:20	30-00.32N	144-59.85E	Plankton net #09-6 (NORPAC: 300 m)
	9:44		19:44	30-00.26N	144-59.86E	Plankton net #09-7 (NORPAC: 100 m)
	10:10		20:10	30-00N	145-00E	Flux mesurements start
	17:30	11.7	3:30	30-03N	145-18E	Flux mesurements finish
	20:28		6:28	30-00.17N	145-00.07E	CTD cast #19 (5,948 m)
11.7	2:21		12:21	30-00.80N	144-51.23E	Free fall optical measruements #04
	2:58		12:58	30-00.39N	144-56.42E	POPPS mooring deployment
	14:00			29-56.45N	144-57.91E	POPPS mooring fixed position
	8:53		18:53	30-00.00N	144-59.96E	Plankton net #10 (NORPAC: 100 m)
	9:08		19:08	30-00.10N	145-00.04E	CTD cast #20 (200 m)
	17:46	11.8	3:46	30-00.19N	144-59.81E	CTD cast #21 (300 m)
	18:38		4:38	30-00.49N	144-59.60E	FRRF #15 (150 m)
	20:02		6:02	29-59.97N	145-06.45E	Surface drifting float buoy deployment
	21:54		7:54	30-00.42N	145-02.79E	FRRF #16 (150 m)
	22:25		8:25	30-00.58N	145-02.72E	Plankton net #11 (Twin-NORPAC: 200 m)
	22:50		8:50	30-00.74N	145-02.69E	CTD cast #22 (1,000 m)
	23:54		9:54	30-01.10N	145-02.79E	Free fall optical measruements #05
11.8	0:20		10:20	30-01.35N	145-02.80E	FRRF #17 (150 m)
	1:09		11:09	30-01.60N	145-03.04E	IONESS #04 (1,000 m)
	4:25		14:25	30-05.23N	145-08.71E	FRRF #18 (150 m)
	5:53		15:53	29-59.99N	145-00.00E	CTD cast #23 (5,000 m)
	9:03		19:03	30-00.21N	144-59.91E	LISST #02 (200 m)
	9:55		19:55	30-00.37N	144-59.93E	Plankton net #12 (NORPAC: 200 m)
	10:30		20:30	30-00N	145-01E	Flux mesurements start
	17:00	11.9	3:00	29-56N	145-14E	Flux mesurements finish

	19:40		5:40	30-09.03N	145-06.70E	Surface drifting float buoy recovery
	20:59		6:59	30-08.90N	145-06.70E	Surface drifting float buoy deployment
	22:25		8:25	30-00.01N	144-59.97E	LVP #03 (1,000 m)
	23:28		9:28	30-00.02N	144-59.97E	Water sampling for buckets #02
11.9	4:01		14:01	29-59.98N	145-00.00E	CTD cast #24 (100 m)
	4:35		14:35	30-00.04N	144-59.98E	Free fall optical measruements #06
	5:08		15:08	30-00.08N	145-00.08E	Plankton net #13-1 (NORPAC: 500 m)
	5:47		15:47	30-00.16N	145-00.37E	Plankton net #13-2 (NORPAC: 700 m)
	8:28		18:28	29.59.99N	145-00.05E	CTD cast #25 (2,000 m)
	9:07		19:07	29-59.99N	144-59.97E	Plankton net #14-1 (Twin-NORPAC: 50 m)
	9:15		19:15	30-00.00N	145-00.02E	Plankton net #14-2 (Twin-NORPAC: 150 m)
	9:31		19:31	29.59.99N	145-00.04E	Plankton net #15-1 (NORPAC: 100 m)
	9:41		19:41	29-59.98N	145-00.06E	Plankton net #15-2 (NORPAC: 100 m)
	9:52		19:52	29-59.96N	145-00.08E	Plankton net #15-3 (NORPAC: 100 m)
	10:07		20:07	29-59.96N	145-00.00E	CTD cast #26 (80 m)
	17:56	11.10	3:56	30-00.04N	145-00.09E	CTD cast #27 (300 m)
	18:47		4:47	30-00.05N	145-00.38E	FRRF #19 (150 m)
	21:55		7:55	29-59.97N	145-00.02E	FRRF #20 (200 m)
	22:33		8:33	29-59.77N	144-59.95E	LVP #04 (200 m)
11.10	0:38		10:38	29-59.72N	144-59.94E	FRRF #21 (200 m)
	1:22		11:22	29-59.83N	145-00.02E	Free fall optical measruements #07
	2:56		12:56	30-00.07N	144-59.99E	CTD cast #28 (1,000 m)
	4:56		14:56	29-59.72N	145-00.15E	FRRF #22 (200 m)
	5:36		15:36	29-59.60N	145-00.36E	Plankton net #16 (200 m)
	7:57		17:57	30-00.02N	145-00.02E	Plankton net #17-1 (NORPAC: 20 m)
	8:04		18:04	29-59.99N	145-00.05E	Plankton net #17-2 (NORPAC: 50 m)
	8:14		18:14	29-59.96N	145-00.11E	Plankton net #17-3 (NORPAC: 100 m)
	8:28		18:28	29-59.92N	145-00.23E	Plankton net #17-4 (NORPAC: 150 m)
	8:52		18:52	29-59.83N	145-00.42E	Plankton net #17-5 (NORPAC: 200 m)
	9:09		19:09	29-59.78N	145-00.55E	Plankton net #17-6 (NORPAC: 300 m)
	10:59		20:59	29-59.84N	145-01.38E	IONESS #05 (1,000 m)
	14:10	11.11	0:10	30-02N	144-56E	Flux mesurements start
	18:00		4:00	30-05N	144-46E	Flux mesurements finish
	21:58		7:58	30-00.58N	145-04.08E	CTD cast #29 (200 m)
	22:32		8:32	30-00.64N	145-03.88E	BGC mooring deployment
	14:00			30-09.92N	144-57.98E	BGC mooring fixed position
11.11	4:30		14:30	30-00.24N	144-59.92E	Plankton net #18-1 (1,000 m)
	5:26		15:26	30-00.38N	144-59.85E	Plankton net #18-2 (300 m)

	5:51		15:51	30-00.49N	144-59.89E	Calibration fot Plankton net flow meter (50 m)
	9:00		19:00	29-59.33N	145-01.68E	Calibration for magnetometer #02
	9:55		19:55	29-59-97N	145-00.13E	Plankton net #19 (Twin-NORPAC: 200 m)
	11:02		21:02	29-59.79N	144-59.04E	IONESS #06 (1,000 m)
	21:44		7:44	30-27.99N	145-14.75E	Surface drifting float buoy recovery
11.12	1:03	11.12	11:03	30-07.93N	145-04.51E	IONESS #07 (1,000 m)
	4:25		14:25	30-02.27N	145-03.09E	ARGO float deployment
	4:33		14:33	30-02.87N	145-02.38E	XCTD #36 (S1)
	4:36		14:36	-	-	Departure from Station 11 (S1)
	5:09		15:09	30-10.01N	144-59.78E	XCTD #37 (W01)
	6:01		16:01	30-20.01N	144-55.97E	XCTD #38 (W02)
	6:52		16:52	30-30.01N	144-52.61E	XCTD #39 (W03)
	7:42		17:42	30-40.01N	144-49.61E	XCTD #40 (W04)
	8:33		18:33	30-50.18N	144-46.88E	XCTD #41 (W05)
	9:23		19:23	31-00.02N	144-44.07E	XCTD #42 (W06)
	10:15		20:15	31-10.06N	144-41.39E	XCTD #43 (W07)
	11:07		21:07	31-20.01N	144-39.15E	XCTD #44 (W08)
	11:58		21:58	31-30.01N	144-36.10E	XCTD #45 (W09)
	12:48		22:48	31-40.02N	144-33.34E	XCTD #46 (W10)
	13:38		23:38	31-50.00N	144-30.59E	XCTD #47 (W11)
	14:29	11.13	0:29	32-00.01N	144-27.90E	XCTD #48 (W12)
	15:19		1:19	32-09.99N	144-25.16E	XCTD #49 (W13)
	16:09		2:09	32-20.00N	14422.36E	XCTD #50 (W14)
	16:58		2:58	32-29.99N	144-19.65E	XCTD #51 (W15)
	17:47		3:47	32-39.99N	144-17.08E	XCTD #52 (W16)
	18:37		4:37	32-50.00N	144-14.30E	XCTD #53 (W17)
	19:26		5:26	33-00.01N	144-11.68E	XCTD #54 (W18)
	20:15		6:15	33-10.01N	144-09.03E	XCTD #55 (W19)
	21:04		7:04	33-20.00N	144-06.30E	XCTD #56 (W20)
	21:53		7:53	33-30.00N	144-03.50E	XCTD #57 (W21)
	22:43		8:43	33-40.01N	144-00.82E	XCTD #58 (W22)
	23:32		9:32	33-50.00N	143-58.12E	XCTD #59 (W23)
11.13	0:22		10:22	34-00.03N	143-55.38E	XCTD #60 (W24)
	1:13		11:13	34-10.00N	143-52.49E	XCTD #61 (W25)
	2:04		12:04	34-20.01N	143-49.48E	XCTD #62 (W26)
	2:55		12:55	34-30.00N	143-46.96E	XCTD #63 (W27)
	3:46		13:46	34-40.00N	143-44.30E	XCTD #64 (W28)
	4:36		14:36	34-50.02N	143-41.38E	XCTD #65 (W29)
	5:25		15:25	35-00.02N	143-38.52E	XCTD #66 (W30)

	6:15		16:15	35-10.01N	143-35.72E	XCTD #67 (W31)
	7:13		17:13	35-20.01N	143-35.23E	XCTD #68 (W32)
	8:26		18:26	35-30.00N	143-38.39E	XCTD #69 (W33)
	9:30		19:30	35-40.01N	143-37.88E	XCTD #70 (W34)
	10:23		20:23	35-50.01N	143-32.10E	XCTD #71 (W35)
	11:16		21:16	36-00.02N	143-26.56E	XCTD #72 (W36)
	12:00		22:00	-	-	Time adjustment -1 hours (SMT=UTC-9h)
	12:02		21:02	36-10.02N	143-21.28E	XCTD #73 (W37)
	12:58		21:58	36-20.02N	143-16.39E	XCTD #74 (W38)
	13:46		22:46	36-30.02N	143-13.31E	XCTD #75 (W39)
	14:34		23:34	36-39.99N	143-10.60E	XCTD #76 (W40)
	15:22	11.14	0:22	36-50.00N	143-08.10E	XCTD #77 (W41)
	16:11		1:11	36-59.99N	143-06.19E	XCTD #78 (W42)
	17:01		2:01	37-10.00N	143-02.96E	XCTD #79 (W43)
	17:50		2:50	37-20.00N	142-59.20E	XCTD #80 (W44)
	18:39		3:39	37-30.00N	142-55.90E	XCTD #81 (W45)
	19:28		4:28	37-40.10N	142-53.11E	XCTD #82 (W46)
11.14	21:28	11.15	6:28	-	-	Continuously observations finish
11.15	0:00	11.15	9:00	40-34N	141-29E	Arrival at Hachinohe
	7:00		16:00	-	-	Departure from Hachinohe
11.16	0:10	11.16	09:10	41-22N	141-14E	Arrival at Sekinehama

1.3 Cruise Participants

	Name	Affiliation	Appointment
1	Makio HONDA (Principal Investigator)	Research Institute for Global Change (RIGC), Japan Agency for Marine-Earth Science and Technology (JAMSTEC)	Principal research scientist (II)
2	Kazuhiko MATSUMOTO (Deputy PI)	RIGC, JAMSTEC	Research scientist
3	Minoru KITAMURA	Institute of Biogeoscience (BIOGEOS) , JAMSTEC	Scientist
4	Hajime KAWAKAMI	Mutsu Institute for Oceanography (MIO), JAMSTEC	Research scientist
5	Masahide WAKITA	Same as above	Scientist
6	Tetsuichi FUJIKI	RIGC, JAMSTEC	Scientist
7	Katsunori KIMOTO	RIGC, JAMSTEC	Scientist
8	Atsushi KURASAWA	BOGEOS, JAMSTEC	Postdoctoral fellow
9	Koji HAMASAKI	Atmosphere and Ocean Research Institute (AORI), The University of Tokyo	Associate professor
10	Hideki FUKUDA	Same as above	Assistant professor
11	Mario UCHIMIYA	Same as above	Graduate student
12	Yuya TADA	Same as above	Postdoctoral fellow
13	Ippei NAGAO	Graduate school of Environmental Studies, Nagoya University	Assistant professor
14	Osamu ABE	Same as above	Same as above
15	Yoshihisa MINO	Hydrospheric Atmospheric Research Center (HyARC), Nagoya University	Same as above
16	Chiho SUKIGARA	Same as above	Postdoctoral fellow
17	Keisuke UNNO	Kagoshima University	Graduate student
18	Kei ISAMI	Same as above	Undergraduate student
19	Yasuo KAMEI	Okayama University	Graduate student
20	Toru IDAI （Principal Marine Tech.）	Marine Works Japan Inc. (MWJ)	Marin Technician
21	Kenichi KATAYAMA	Same as above	Same as above
22	Naoko TAKAHASHI	Same as above	Same as above
23	Yasumi YAMADA	Same as above	Same as above
24	Tamami UENO	Same as above	Same as above
25	Hiroki USHIROMURA	Same as above	Same as above
26	Hiroyasu SATO	Same as above	Same as above
27	Ai TAKANO	Same as above	Same as above
28	Junji MATSUSHITA	Same as above	Same as above

29	Yoshiko ISHIKAWA	Same as above	Same as above
30	Minoru KAMATA	Same as above	Same as above
31	Hatsumi AOYAMA	Same as above	Same as above
32	Shoko TATAMISASHI	Same as above	Same as above
33	Masahiro ORUI	Same as above	Same as above
34	Miyo IKEDA	Same as above	Same as above
35	Ai YASUDA	Same as above	Same as above
36	Kanako YOSHIDA	Same as above	Same as above
37	Katsunori MAENO (Principal Marine Tech.)	Global Ocean Development Inc. (GODI)	Same as above
38	Kazuho YOSHIDA	Same as above	Same as above

2 General observation

2.1 Meteorological observations

2.1.1 Surface Meteorological Observation

Katsuhisa MAENO (Global Ocean Development Inc., GODI)
Kazuho YOSHIDA (GODI)
Wataru TOKUNAGA (Mirai Crew)

(1) Objectives

Surface meteorological parameters are observed as a basic dataset of the meteorology. These parameters bring us the information about the temporal variation of the meteorological condition surrounding the ship.

(2) Methods

Surface meteorological parameters were observed throughout the MR10-06 cruise. During this cruise, we used three systems for the observation.

i. MIRAI Surface Meteorological observation (SMet) system
ii. Shipboard Oceanographic and Atmospheric Radiation (SOAR) system

i. MIRAI Surface Meteorological observation (SMet) system

Instruments of SMet system are listed in Table.2.1.1-1 and measured parameters are listed in Table.2.1.1-2. Data were collected and processed by KOAC-7800 weather data processor made by Koshin-Denki, Japan. The data set consists of 6-second averaged data.

ii. Shipboard Oceanographic and Atmospheric Radiation (SOAR) measurement system

SOAR system designed by BNL (Brookhaven National Laboratory, USA) consists of major three parts.

a) Portable Radiation Package (PRP) designed by BNL – short and long wave downward radiation.
b) Zeno Meteorological (Zeno/Met) system designed by BNL – wind, air temperature, relative humidity, pressure, and rainfall measurement.
c) Scientific Computer System (SCS) developed by NOAA (National Oceanic and Atmospheric Administration, USA) – centralized data acquisition and logging of all data sets.

SCS recorded PRP data every 6 seconds, while Zeno/Met data every 10 seconds. Instruments and their locations are listed in Table.2.1.1-3 and measured parameters are listed in Table.2.1.1-4.

For the quality control as post processing, we checked the following sensors, before and after the cruise.

i. Young Rain gauge (SMet and SOAR)

Inspect of the linearity of output value from the rain gauge sensor to change Input value by adding fixed quantity of test water.

ii. Barometer (SMet and SOAR)

Comparison with the portable barometer value, PTB220CASE, VAISALA.

iii.Thermometer (air temperature and relative humidity) (SMet and SOAR)

Comparison with the portable thermometer value, HMP41/45, VAISALA.

(3) Preliminary results

Figure 2.1.1-1 shows the time series of the following parameters;

Wind (SMet)
Air temperature (SMet)
Relative humidity (SMet)
Precipitation (SOAR, Capacitive rain gauge)
Short/long wave radiation (SMet)
Pressure (SMet)
Sea surface temperature (SMet)
Significant wave height (SMet)

(4) Data archives

These data obtained in this cruise will be submitted to the Data Management Group (DMG) of JAMSTEC, and will be opened to the public via "R/V MIRAI Data Web Page" in JAMSTEC home page.

(5) Remarks

i. We did not collect data in the territorial waters of U.S.A in the following periods.
19:00UTC 18 Oct. - 00:00UTC19 Oct.2010

ii. SST (Sea Surface Temperature) data were available in the following period.
00:15UTC 19 Oct. - 21:30UTC 14 Nov. 2010

iii. The following time, increasing of SMet capacitive rain gauge data were invalid.
23:50, 23:55UTC, 23 Oct. 2010
01:17UTC, 27 Oct. 2010
01:19UTC, 29 Oct. 2010
10:11, 10:15UTC, 31 Oct. 2010
10:18, 10:34UTC, 12 Nov. 2010

iv. Air temperature, dew point temperature and relative humidity of SMet portside were invalid in the following period
23:51 - 23:52UTC, 08 Nov. 2010

Table.2.1.1-1 Instruments and installations of MIRAI Surface Meteorological observation system

Sensors	Type	Manufacturer	Location (altitude from surface)
Anemometer	KE-500	Koshin Denki, Japan	foremast (24 m)
Tair/RH	HMP45A	Vaisala, Finland	
with 43408 Gill aspirated radiation shield		R.M. Young, USA	compass deck (21 m)
			starboard side and port side
Thermometer: SST	RFN1-0	Koshin Denki, Japan	4th deck (-1m, inlet -5m)
Barometer	Model-370	Setra System, USA	captain deck (13 m)
			weather observation room
Rain gauge	50202	R. M. Young, USA	compass deck (19 m)
Optical rain gauge	ORG-815DR	Osi, USA	compass deck (19 m)
Radiometer (short wave)	MS-801	Eiko Seiki, Japan	radar mast (28 m)
Radiometer (long wave)	MS-200	Eiko Seiki, Japan	radar mast (28 m)
Wave height meter	MW-2	Tsurumi-seiki, Japan	bow (10 m)

Table.2.1.1-2 Parameters of MIRAI Surface Meteorological observation system

Parameter	Units	Remarks
1 Latitude	degree	
2 Longitude	degree	
3 Ship's speed	knot	Mirai log, DS-30 Furuno
4 Ship's heading	degree	Mirai gyro, TG-6000, Tokimec
5 Relative wind speed	m/s	6sec./10min. averaged
6 Relative wind direction	degree	6sec./10min. averaged
7 True wind speed	m/s	6sec./10min. averaged
8 True wind direction	degree	6sec./10min. averaged
9 Barometric pressure	hPa	adjusted to sea surface level
		6sec. averaged
10 Air temperature (starboard side)	degC	6sec. averaged
11 Air temperature (port side)	degC	6sec. averaged
12 Dewpoint temperature (starboard side)	degC	6sec. averaged
13 Dewpoint temperature (port side)	degC	6sec. averaged
14 Relative humidity (starboard side)	%	6sec. averaged
15 Relative humidity (port side)	%	6sec. averaged
16 Sea surface temperature	degC	6sec. averaged
17 Rain rate (optical rain gauge)	mm/hr	hourly accumulation
18 Rain rate (capacitive rain gauge)	mm/hr	hourly accumulation
19 Down welling shortwave radiation	W/m2	6sec. averaged
20 Down welling infra-red radiation	W/m2	6sec. averaged
21 Significant wave height (bow)	m	hourly
22 Significant wave height (aft)	m	hourly
23 Significant wave period (bow)	second	hourly
24 Significant wave period (aft)	second	hourly

Table.2.1.1-3 Instruments and installation locations of SOAR system

Sensors (Zeno/Met)	Type	Manufacturer	Location (altitude from surface)
Anemometer	05106	R.M. Young, USA	foremast (26 m)
Tair/RH	HMP45A	Vaisala, Finland	
with 43408 Gill aspirated radiation shield		R.M. Young, USA	foremast (23 m)
Barometer	61202V	R.M. Young, USA	
with 61002 Gill pressure port		R.M. Young, USA	foremast (23 m)
Rain gauge	50202	R.M. Young, USA	foremast (25 m)
Optical rain gauge	ORG-815DA	Osi, USA	foremast (25 m)

Sensors (PRP)	Type	Manufacturer	Location (altitude from surface)
Radiometer (short wave)	PSP	Epply Labs, USA	foremast (25 m)
Radiometer (long wave)	PIR	Epply Labs, USA	foremast (25 m)
Fast rotating shadowband radiometer		Yankee, USA	foremast (25 m)

Table.2.1.1-4 Parameters of SOAR system

Parameter	Units	Remarks
1 Latitude	degree	
2 Longitude	degree	
3 SOG	knot	
4 COG	degree	
5 Relative wind speed	m/s	
6 Relative wind direction	degree	
7 Barometric pressure	hPa	
8 Air temperature	degC	
9 Relative humidity	%	
10 Rain rate (optical rain gauge)	mm/hr	
11 Precipitation (capacitive rain gauge)	mm	reset at 50 mm
12 Down welling shortwave radiation	W/m2	
13 Down welling infra-red radiation	W/m2	
14 Defuse irradiance	W/m2	

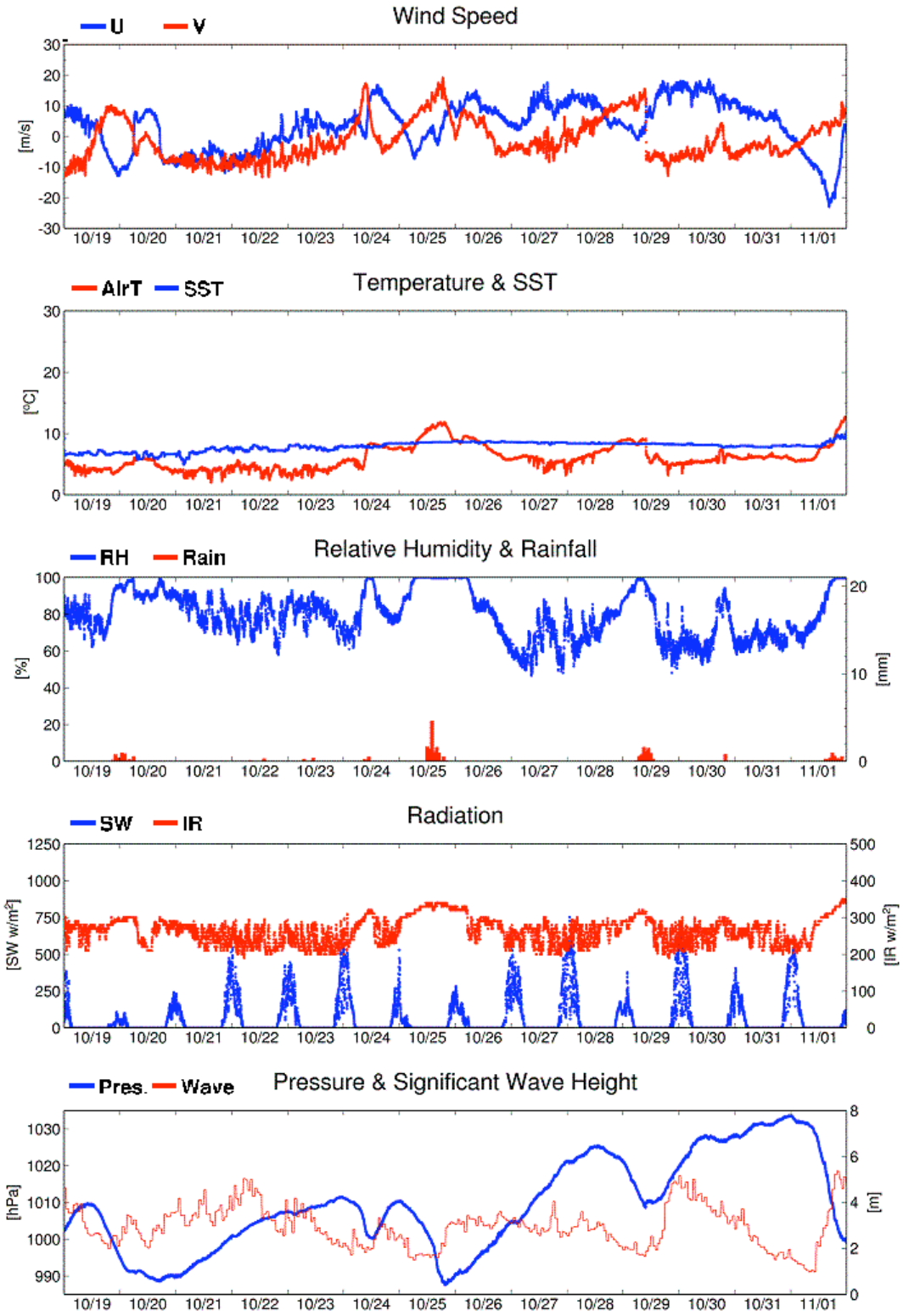

Fig.2.1.1-1 Time series of surface meteorological parameters during the MR10-06 cruise

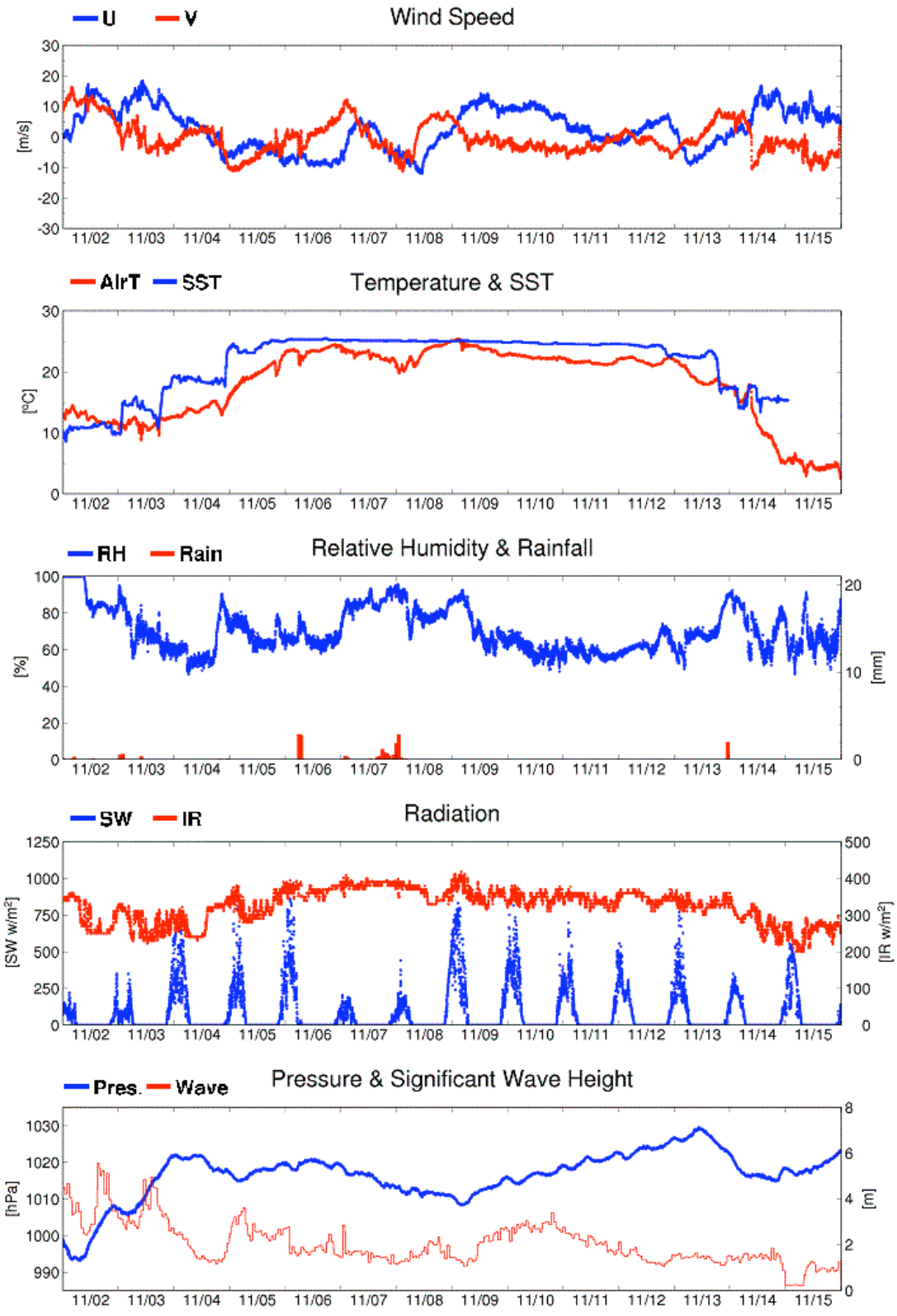

Fig.2.1.1-1 Continued

2.1.2 Ceilometer Observation

Katsuhisa MAENO (Global Ocean Development Inc., GODI)
Kazuho YOSHIDA (GODI)
Wataru TOKUNAGA (Mirai Crew)

(1) Objectives

The information of cloud base height and the liquid water amount around cloud base is important to understand the process on formation of the cloud. As one of the methods to measure them, the ceilometer observation was carried out.

(2) Parameters

1. Cloud base height [m].
2. Backscatter profile, sensitivity and range normalized at 30 m resolution.
3. Estimated cloud amount [oktas] and height [m]; Sky Condition Algorithm.

(3) Methods

We measured cloud base height and backscatter profile using ceilometer (CT-25K, VAISALA, Finland) throughout the MR10-06 cruise from the departure of Dutch Harbor on 18 October 2010 to arrival of Sekinehama on 16 November 2010.

Major parameters for the measurement configuration are as follows;
Laser source: Indium Gallium Arsenide (InGaAs) Diode
Transmitting wavelength: 905±5 mm at 25 degC
Transmitting average power: 8.9 mW
Repetition rate: 5.57 kHz
Detector: Silicon avalanche photodiode (APD)
Responsibility at 905 nm: 65 A/W
Measurement range: 0 ~ 7.5 km
Resolution: 50 ft in full range
Sampling rate: 60 sec
Sky Condition 0, 1, 3, 5, 7, 8 oktas (9: Vertical Visibility)
(0: Sky Clear, 1:Few, 3:Scattered, 5-7: Broken, 8: Overcast)

On the archive dataset, cloud base height and backscatter profile are recorded with the resolution of 30 m (100 ft).

(4) Preliminary results

Figure 2.1.2-1 shows the time series of the lowest, second and third cloud base height.

(5) Data archives

The raw data obtained in this cruise will be submitted to the Data Management Group (DMG) of JAMSTEC, and will be opened to the public via “R/V MIRAI Data Web Page” in JAMSTEC home page.

(6) Remarks

i. We did not collect data in the territorial waters of U.S.A in the following period.
19:00UTC 18 Oct. – 0:00UTC 19 Oct.2010

ii. Window cleaning;
22:34UTC 21 Oct. 2010, 05:11UTC 25 Oct. 2010,
04:58UTC 03 Nov. 2010, 00:08UTC 11 Nov. 2010

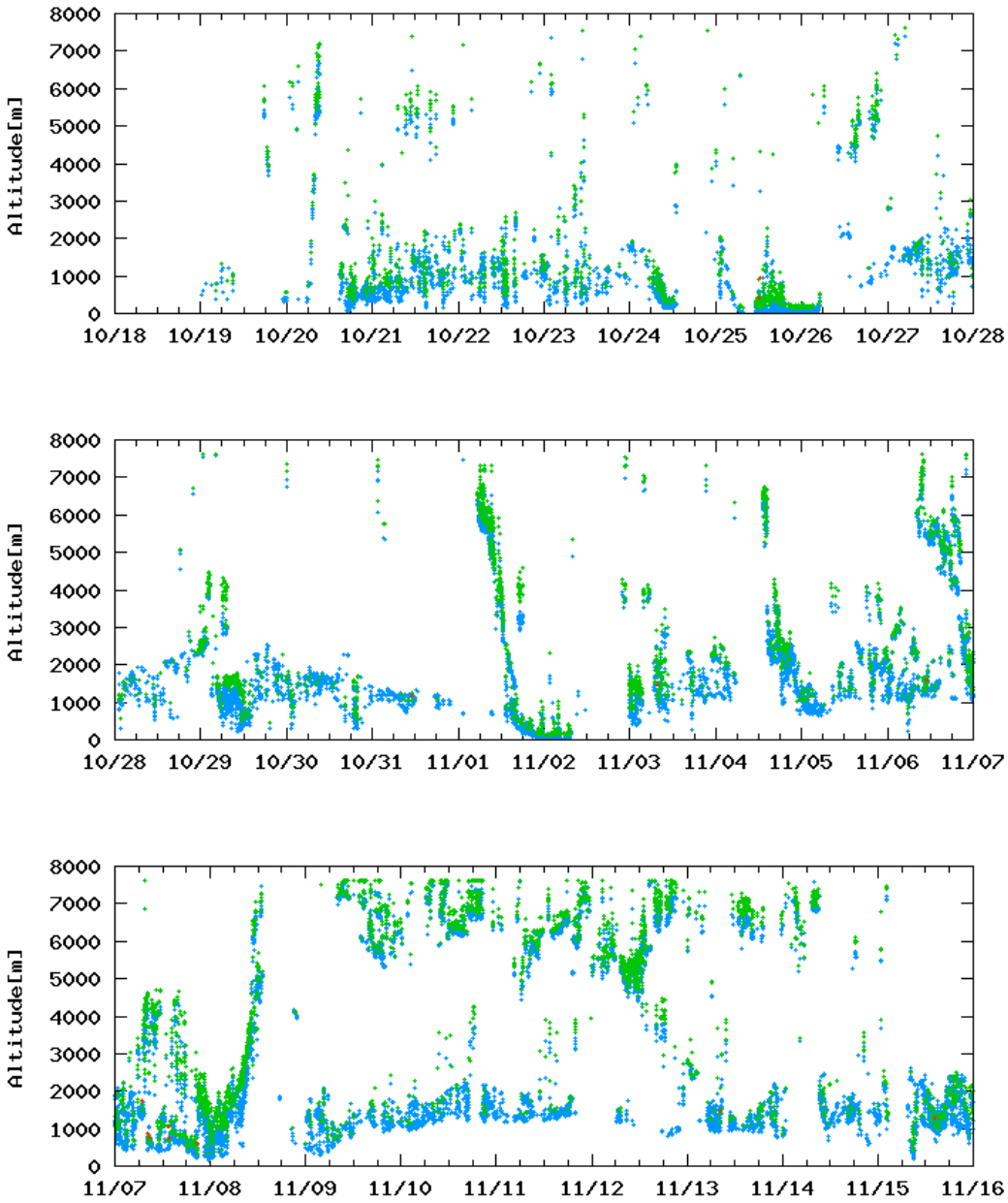

Fig.2.1.2-1 Lowest (blue), 2nd (green) and 3rd(red) cloud base height during the cruise.

2.1.3 Lidar observations of clouds and aerosols

Nobuo SUGIMOTO
(National Institute for Environmental Studies: NIES, not on board)
Ichiro MATSUI (NIES, not on board)
Atsushi SHIMIZU (NIES, not on board)
Tomoaki NISHIZAWA (NIES, not on board)
lidar operation was supported by Global Ocean Development Inc.

(1) Objectives

Objectives of the observations in this cruise is to study distribution and optical characteristics of ice/water clouds and marine aerosols using a two-wavelength lidar.

2) Measured parameters

- Vertical profiles of backscattering coefficient at 532 nm
- Vertical profiles of backscattering coefficient at 1064 nm
- Depolarization ratio at 532 nm

(3) Method

Vertical profiles of aerosols and clouds were measured with a two-wavelength lidar. The lidar employs a Nd:YAG laser as a light source which generates the fundamental output at 1064 nm and the second harmonic at 532 nm. Transmitted laser energy is typically 30 mJ per pulse at both of 1064 and 532 nm. The pulse repetition rate is 10 Hz. The receiver telescope has a diameter of 20 cm. The receiver has three detection channels to receive the lidar signals at 1064 nm and the parallel and perpendicular polarization components at 532 nm. An analog-mode avalanche photo diode (APD) is used as a detector for 1064 nm, and photomultiplier tubes (PMTs) are used for 532 nm. The detected signals are recorded with a transient recorder and stored on a hard disk with a computer. The lidar system was installed in a container which has a glass window on the roof, and the lidar was operated continuously regardless of weather. Every 10 minutes vertical profiles of four channels (532 parallel, 532 perpendicular, 1064, 532 near range) are recorded.

(4) Results

As lidar data has not been brought to NIES, a quick-look of lidar observation on November 6 is shown in Figure 1. Although data duration is one day, multi-layered structure of the atmosphere is depicted. Upper clouds appeared between 5-6 km, and aerosol layer were apparent below 2 km. It is interesting that cloud base in the aerosol layer was located at little lower altitude (1.5 km) compared with the top of aerosol layer (2km). Strong scattering after 21:00 was caused by raining.

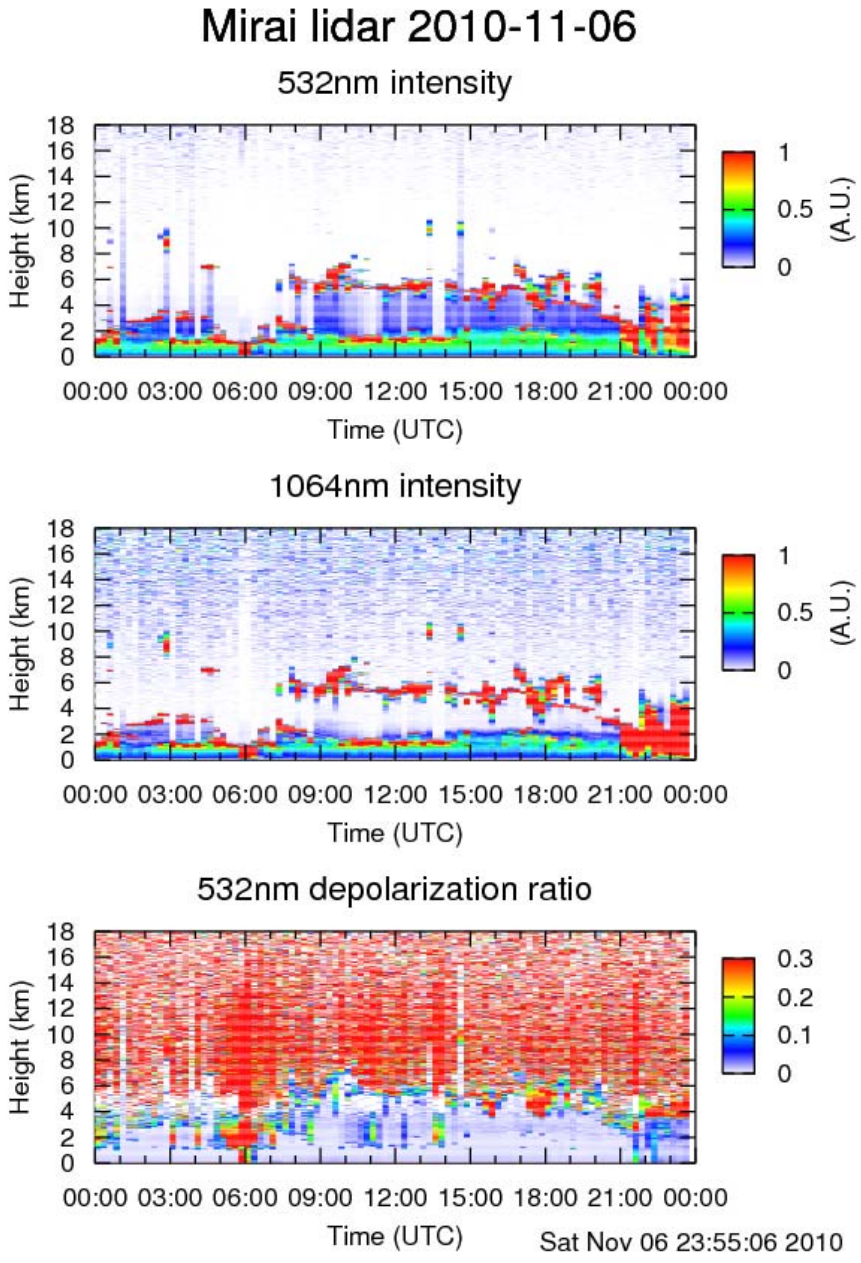

Figure 1: Time-height sections of (top) backscatter intensity at 532 nm, (middle) backscatter intensity at 1064 nm, and (bottom) volume depolarization ratio at 532 nm on November 6, 2010.

(5) Data archive

- raw data

lidar signal at 532 nm
lidar signal at 1064 nm
depolarization ratio at 532 nm
temporal resolution 10min/ vertical resolution 6 m
data period (UTC): October 19 – November 15, 2010

- processed data (plan)
  cloud base height, apparent cloud top height
  phase of clouds (ice/water)
  cloud fraction
  boundary layer height (aerosol layer upper boundary height)
  backscatter coefficient of aerosols
  particle depolarization ratio of aerosols

(6) Data policy and Citation

Contact NIES lidar team (nsugimot/i-matsui/shimizua/nisizawa@nies.go.jp) to utilize lidar data for productive use.

2.1.4 Optical characteristics of aerosol observed by sky-radiometer

Kazuma AOKI (University of Toyama) Principal Investigator / not onboard
Tadahiro HAYASAKA (Tohoku University) Co-worker / not onboard

(1) Objective

Objective of the observations in this aerosol is to study distribution and optical characteristics of marine aerosols by using a ship-borne sky radiometer (POM-01 MKII: PREDE Co. Ltd., Japan). Furthermore, collections of the data for calibration and validation to the remote sensing data were performed simultaneously.

(2) Methods and Instruments

Sky radiometer is measuring the direct solar irradiance and the solar aureole radiance distribution, has seven interference filters (0.34, 0.4, 0.5, 0.675, 0.87, 0.94, and 1.02 μm). Analysis of these data is performed by SKYRAD.pack version 4.2 developed by Nakajima *et al*. 1996.

@ Measured parameters
- Aerosol optical thickness at five wavelengths (400, 500, 675, 870 and 1020 nm)
- Ångström exponent
- Single scattering albedo at five wavelengths
- Size distribution of volume (0.01 μm – 20 μm)

GPS provides the position with longitude and latitude and heading direction of the vessel, and azimuth and elevation angle of sun. Horizon sensor provides rolling and pitching angles.

(3) Preliminary results

This study is not onboard. Data obtained in this cruise will be analyzed at University of Toyama.

(4)Data archives

Measurements of aerosol optical data are not archived so soon and developed, examined, arranged and finally provided as available data after certain duration. All data will archived at University of Toyama (K.Aoki, SKYNET/SKY: http://skyrad.sci.u-toyama.ac.jp/) after the quality check and submitted to JAMSTEC.

2.1.5 Tropospheric aerosol and gas profile observations by MAX-DOAS on a research vessel

Hisahiro TAKASHIMA (PI, JAMSTEC/RIGC, not on board)
Hitoshi IRIE (JAMSTEC/RIGC)
Yugo KANAYA (JAMSTEC/RIGC)

(1) Objectives

- To quantify typical background values of atmospheric aerosol and gas over the ocean
- To clarify transport processes from source over Asia to the ocean (and also clarify the gas emission from the ocean (including organic gas))
- To validate satellite measurements (as well as chemical transport model)

(2) Methods

Multi-Axis Differential Optical Absorption Spectroscopy (MAX-DOAS) is a passive remote sensing technique using scattered visible and ultraviolet (UV) solar radiation at several elevation angles. The MAX-DOAS system used in this study records spectra of scattered solar radiation every 0.5 second. Measurements were made at several elevation angles of 0, 3, 4, 5, 10, 20, 30, 70, 110, 150, 160, 170, 175, 176 and 177 degrees using a movable mirror, which repeated the same sequence of elevation angles every 30-min. The UV/visible spectra range was changed every min (284-423 nm and 391-528 nm). On the roof top of the anti-rolling system of R/V *Mirai*, the telescope unit was installed on a gimbal mount, which compensates for the pitch and roll of the ship. A sensor measuring pitch and roll of the telescope unit (10Hz) is used together to measure an offset of elevation angle due to incomplete compensation by the gimbal. The line of sight was in directions of the starboard and portside of the ship.

After measurements were made, we first selected spectrum data with an elevation angle offset less than ±0.2 degrees. For those spectra, DOAS spectral fitting was performed to quantify the slant column density (SCD), defined as the concentration integrated along the light path, for each elevation angle. In this analysis, SCDs of NO_2 (and other gases) and O_4 (O_2-O_2, collision complex of oxygen) were obtained together. Next, O_4 SCDs were converted to the aerosol optical depth (AOD) and the vertical profile of aerosol extinction coefficient (AEC) at a wavelength of 476 nm using an optimal estimation inversion method with a radiative transfer model. Using derived aerosol information, another inversion is performed to retrieve the tropospheric vertical column/profile of NO_2 and other gases.

(3) Preliminary results

These data for the whole cruise period will be analyzed.

(4) Data archives

The data will be submitted to the Marine-Earth Data and Information Department (MEDID) of JAMSTEC after the full analysis of the raw spectrum data is completed, which will be <2 years after the end of the cruise.

2.1.6 Water isotopes in atmospheric vapor, precipitation and sea surface water

Naoyuki KURITA (JAMSTEC) Principal Investigator（not on-board）
Katsuhisa MAENO (Global Ocean Development Inc.: GODI) Operator

(1) Objective

It is well known that the variability of stable water isotopes (HDO and $H_2{}^{18}O$) is closely related with the moisture origin and hydrological processes during the transportation from the source region to deposition site. Thus, water isotope tracer is recognized as the powerful tool to study of the hydrological cycles in the atmosphere. However, oceanic region is one of sparse region of the isotope data, it is necessary to fill the data to identify the moisture sources by using the isotope tracer. In this study, to fill this sparse observation area, intense water isotopes observation was conducted along the cruise track of MR10-06.

(2) Method

Following observation was carried out throughout this cruise.

- Atmospheric moisture sampling:

  Water vapor was sampled from the height about 20m above the sea level. The air was drawn at rate of 1.5-3.0 L/min through a plastic tube attached to top of the compass deck. The flow rate is regulated according to the water vapor content to collect the sample amount 9-32ml. The water vapor was trapped in a glass trap submerged into an ethanol cooled to 100 degree C by radiator, and then they are collected every 12 hour during the cruise. After collection, water in the trap was subsequently thawed and poured into the 6ml glass bottle.

- Rainwater sampling

  Rainwater samples gathered in rain/snow collector were collected just after precipitation events have ended. The collected sample was then transferred into glass bottle (6ml) immediately after the measurement of precipitation amount.

- Surface seawater sampling

  Seawater sample taken by the pump from 4m depth were collected in glass bottle (6ml) around the noon at the local time.

(3) Results

Sampling of water vapor for isotope analysis is summarized in Table 2.1.6-1 (41 samples). The detail of rainfall sampling (18 samples) is summarized in Table 2.1.6-2. Described rainfall amount is calculated from the collected amount of precipitation. Sampling of surface seawater taken by pump from 4m depths is summarized in Table 2.1.6-3 (26 samples).

(4) Data archive

Isotopes (HDO, $H_2{}^{18}O$) analysis will be done at RIGC/JAMSTEC, and then analyzed isotopes data will be submitted to JAMSTEC Data Integration and Analysis Group (DIAG).

Table 2.1.6-1 Summary of water vapor sampling for isotope analysis

Sample	Start Date	Start Time (UT)	End Date	End Time (UT)	Lon	Lat	T.M. (m^3)	Sam. (ml)	H2O ppm
V-1	10.19	0:00	10.19	17:03	171-45W	54-42N	3.05	11.0	4488
V-2	10.19	17:09	10.20	5:00	171-53W	55-29N	2.13	9.0	5258
V-3	10.20	5:02	10.20	18:02	178-45W	56-05N	2.33	10.0	5341
V-4	10.20	18:07	10.21	6:00	178-47E	55-56N	2.13	9.0	5258
V-5	10.21	6:05	10.21	19:00	174-39E	55-31N	2.32	8.0	4291
V-6	10.21	19:10	10.22	7:00	174-59E	54-19N	2.31	8.0	4310
V-7	10.22	7:04	10.22	20:00	169-50E	52-45N	2.32	8.0	4291
V-8	10.22	22:06	10.23	7:00	168-08E	51-19N	2.14	8.0	4652
V-9	10.23	21:04	10.23	21:00	164-45E	49-46N	2.32	8.0	4291
V-10	10.23	21:04	10.24	9:03	162-18E	48-27N	2.15	8.0	4630
V-11	10.24	9:04	10.24	21:02	159-59E	46-59N	2.15	10.0	5788
V-12	10.24	21:08	10.25	9:00	160-09E	46-55N	2.13	12.0	7011
V-13	10.25	9:02	10.26	0:00	159-52E	46-50N	2.13	17.0	9932
V-14	10.26	9:01	10.27	9:02	160-01E	46-49N	2.14	8.0	4652
V-15	10.27	9:05	10.28	8:59	159-58E	46-53N	2.13	7.0	4090
V-16	10.28	9:00	10.29	9:03	159-54E	46-55N	2.14	10.0	5815
V-17	10.29	9:11	10.30	9:00	159-47E	46-55N	2.90	10.0	4291
V-18	10.30	9:02	10.31	9:00	160-08E	47-00N	2.89	10.0	4306
V-19	10.31	9:03	11.1	9:00	159-54E	46-53N	2.90	10.0	4291
V-20	11.1	9:03	11.1	21:02	157-31E	45-06N	2.14	10.0	5815
V-21	11.1	21:06	11.2	9:00	155-04E	44-01N	2.16	21.0	12099
V-22	11.2	9:02	11.2	21:00	153-24E	42-54N	2.14	16.0	9304
V-23	11.2	21:04	11.3	9:00	151-43E	41-30N	2.19	14.0	7955
V-24	11.3	9:04	11.3	21:00	149-48E	40-11N	2.10	10.0	5926
V-25	11.3	21:06	11.4	9:00	147-02E	38-31N	2.14	10.0	5815
V-26	11.4	9:04	11.4	21:01	145-55E	36-26N	2.14	12.0	6978
V-27	11.4	21:05	11.5	9:00	145-05E	34-00N	2.15	20.0	11576
V-28	11.5	9:02	11.5	0:00	144-48E	30-54N	2.33	21.0	11216
V-29	11.5	22:05	11.6	10:01	145-00E	30-00N	2.14	26.0	15119
V-30	11.6	10:02	11.7	10:00	145-00E	30-00N	2.16	28.0	16132
V-31	11.7	10:01	11.8	10:00	145-00E	30-00N	2.14	32.0	18609
V-32	11.8	10:01	11.9	10:00	145-00E	30-00N	2.15	33.0	19101
V-33	11.9	10:06	11.10	10:00	145-01E	30-00N	2.14	25.0	14538
V-34	11.10	10:01	11.11	10:00	145-00E	30-00N	2.15	20.0	11576
V-35	11.11	10:05	11.12	10:00	144-42E	31-07N	2.15	20.0	11576

V-36	11.12	10:01	11.12	22:00	144-03E	33-32N	2.17	21.0	12043
V-37	11.12	22:05	11.13	10:02	143-34E	35-46N	2.15	21.0	12155
V-38	11.12	10:01	11.13	23:00	142-42E	38-20N	2.34	21.0	11168
V-39	11.13	23:04	11.14	11:00	142-11E	40-31N	2.15	19.0	10997
V-40	11.14	11:01	11.14	23:02	141-32E	40-35N	2.16	9.0	5185
V-41	11.14	23:05	11.15	23:05	141-17E	41-24N	4.32	14.0	4033

Table 2.1.6-2 Summary of precipitation sampling for isotope analysis.

	Date	Time (UT)	Lon	Lat	Date	Time (UT)	Lon	Lat	Rain (mm)
R-1	10.19	00:10	167-16W	54-14N	10.20	16:47	178-27W	56-02N	8.9
R-2	10.20	16:47	178-27W	56-02N	10.21	05:24	179-00E	55-57N	0.9
R-3	10.21	05:24	179-00E	55-57N	10.21	19:22	174-34E	55-30N	0.7
R-4	10.21	19:22	174-34E	55-30N	10.22	20:19	169-50E	52-45N	2.5
R-5	10.22	20:19	169-50E	52-45N	10.23	20:21	164-52E	49-49N	1.6
R-6	10.23	20:21	164-52E	49-49N	10.24	20:49	159-58E	46-59N	2.4
R-7	10.24	20:49	159-58E	46-59N	10.25	19:59	160-01E	46-53N	14.4
R-8	10.25	19:59	160-01E	46-53N	10.26	20:11	159-58E	46-51N	0.0
R-9	10.26	20:11	159-58E	46-51N	10.29	19:52	159-42E	47-05N	9.0
R-10	10.29	19:52	159-42E	47-05N	10.30	20:52	160-03E	47-00N	2.3
R-11	10.30	20:52	160-03E	47-00N	11.02	21:08	153-23E	42-53N	4.0
R-12	11.02	21:08	153-23E	42-53N	11.03	05:17	152-07E	42-00N	3.0
R-13	11.03	05:17	152-07E	42-00N	11.05	21:54	144-48E	30-56N	1.6
R-14	11.05	21:54	144-48E	30-56N	11.06	07:47	145-00E	30-00N	5.6
R-15	11.06	07:47	145-00E	30-00N	11.07	22:26	145-03E	30-01N	6.3
R-16	11.07	22:26	145-03E	30-01N	11.08	06:06	145-00E	30-00N	14.5
R-17	11.08	06:06	145-00E	30-00N	11.13	23:10	142-41E	38-21N	1.5
R-18	11.13	23:10	142-41E	38-21N	11.15	23:20	141-15E	41-22N	0.8

Table 2.1.6-3 Summary of water vapor sampling for isotope analysis

			(UTC)	LON	LAT
MR10-06 O-	1	10.19	21:00	172-58W	55-10N
MR10-06 O-	2	10.20	22:06	179-08W	56-09N
MR10-06 O-	3	10.21	23:00	173-38E	55-25N
MR10-06 O-	4	10.23	00:02	169-22E	52-30N
MR10-06 O-	5	10.24	01:00	163-58E	49-27N
MR10-06 O-	6	10.25	01:00	159-59E	46-59N
MR10-06 O-	7	10.26	01:03	160-02E	46-49N
MR10-06 O-	8	10.27	01:00	159-57E	46-52N

MR10-06 O-	9	10.28	01:18	160-00E	46-51N
MR10-06 O-	10	10.29	01:01	159-55E	46-53N
MR10-06 O-	11	10.30	01:03	159-47E	46-57N
MR10-06 O-	12	10.31	01:05	160-07E	46-57N
MR10-06 O-	13	11.1	01:01	159-54E	46-52N
MR10-06 O-	14	11.2	01:04	156-45E	44-36N
MR10-06 O-	15	11.3	01:00	152-40E	42-24N
MR10-06 O-	16	11.4	01:02	148-58E	39-41N
MR10-06 O-	17	11.5	01:20	145-32E	35-23N
MR10-06 O-	18	11.6	02:10	144-57E	30-04N
MR10-06 O-	19	11.7	02:05	144-58E	29-56N
MR10-06 O-	20	11.8	02:05	145-05E	30-03N
MR10-06 O-	21	11.9	02:00	145-00E	30-00N
MR10-06 O-	22	11.10	02:02	145-00E	30-00N
MR10-06 O-	23	11.11	02:00	144-58E	30-04N
MR10-06 O-	24	11.12	02:02	145-04E	30-06N
MR10-06 O-	25	11.13	03:57	143-44E	34-42N
MR10-06 O-	26	11.14	03:03	142-29E	39-04N

2.1.7 Air-sea surface eddy flux measurement

Osamu TSUKAMOTO (Okayama University) Principal Investigator * not on board
Hiroshi ISHIDA (Kobe University) * not on board
Fumiyoshi KONDO (University of Tokyo) * not on board
Yasuo KAMEI (Okayama University)
Katsuhisa MAENO (Global Ocean Development Inc. (GODI))
Kazuho YOSHIDA (Global Ocean Development Inc. (GODI))

(1) Objective

To better understand the air-sea interaction, accurate measurements of surface heat and fresh water budgets are necessary as well as momentum exchange through the sea surface. In addition, the evaluation of surface flux of carbon dioxide is also indispensable for the study of global warming. Sea surface turbulent fluxes of momentum, sensible heat, latent heat, and carbon dioxide were measured by using the eddy correlation method that is thought to be most accurate and free from assumptions. These surface heat flux data are combined with radiation fluxes and water temperature profiles to derive the surface energy budget.

(2) Instruments and Methods

The surface turbulent flux measurement system (Fig. 1) consists of turbulence instruments (Kaijo Co., Ltd.) and ship motion sensors (Kanto Aircraft Instrument Co., Ltd.). The turbulence sensors include a three-dimensional sonic anemometer-thermometer (Kaijo, DA-600) and an infrared hygrometer (LICOR, LI-7500). The sonic anemometer measures three-dimensional wind components relative to the ship. The ship motion sensors include a two-axis inclinometer (Applied Geomechanics, MD-900-T), a three-axis accelerometer (Applied Signal Inc., QA-700-020), and a three-axis rate gyro (Systron Donner, QRS-0050-100). LI7500 is a CO_2/H_2O turbulence sensor that measures turbulent signals of carbon dioxide and water vapor simultaneously. These signals are sampled at 10 Hz by a PC-based data logging system (Labview, National Instruments Co., Ltd.). By obtaining the ship speed and heading information through the Mirai network system it yields the absolute wind components relative to the ground. Combining wind data with the turbulence data, turbulent fluxes and statistics are calculated in a real-time basis. These data are also saved in digital files every 0.1 second for raw data and every 1 minute for statistic data.

(3) Observation log

The observation was carried out throughout this cruise.

(4) Data Policy and citation

All data are archived at Okayama University, and will be open to public after quality checks and corrections. Corrected data will be submitted to JAMSTEC Marine-Earth Data and Information Department.

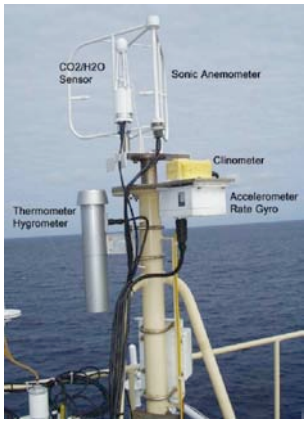

Fig. 1 Turbulent flux measurement system on the top deck of the foremast.

2.1.8 Measurements of DMS in seawater and atmosphere over the northern North Pacific

Ippei NAGAO (Nagoya University)

(1) Objective

An accurate estimation of the sea-air DMS flux is required to improve an estimation of the impact of DMS on the aerosol formation in the marine air. Thus far, the bulk method which is a traditional one but includes a large uncertainty has been used, because no devices of trace gases such as DMS have been available for the eddy correlation (EC) method, which is more accurate than the bulk method. Utilizing a chemiluminescence induced by reaction of DMS with fluorine (F_2), the fast measurement system of DMS for the EC method was developed and installed on R/V Mirai during the cruise of MR10-06. In this cruise, these two methods are applied to the DMS flux measurement over the northern North Pacific. Then the results of two methods will be analyzed to improve the DMS flux calculation. In addition, distributions of the DMS concentrations both in the atmosphere and seawater are measured to discuss the relationship with marine biological and chemical parameters.

(2) Methods

i. Measurement system by GC/FPD for the bulk method

Atmospheric DMS concentration

Sample air was introduced through 20 m long Teflon-tube (OD: 10mm, and ID: 8 mm) from the compass deck to the Environmental Research Laboratory of R/V Mirai with the flow rate at 30~36 L/min by sampling pump (Iwaki Co. Ltd.). This sample air was separated in the manifold to be introduced to the DMS analysis system with the flow rate at 100 ml/min. The sample air was then concentrated on the concentration tube packed with Tenax-GR (60/80 mesh, GL Science Co. Ltd.) at -75 deg C by liquid CO_2 after removing water vapor by perma pure dryer (MD-070-48F, GL Science Co. Ltd.). Then the concentration tube was abruptly heated to +180 deg C within 1.5 min and DMS trapped on Tenax-GR was introduced to Gas Chromatography equipped with a flame photometric detector (GC-14B, Shimadzu Co. Ltd.) by the carrier gas (ultra high purified (UHP) nitrogen (N_2) gas). Analysis column of this system was β-β' oxydipropionitrile glass column (ZO-1, Shimadzu Co. Ltd.). Temperature in the column oven was set to be 60 deg C. Calibration of this system was performed with DMS standard gas (5.16 ppmv, N_2 base, Nagoya-Kosan Co. Ltd.). The detection limit (DL) was estimated to be 30 pptv in 4.5 liter of STP. The precision was ±10%.

Seawater DMS concentration

100mL of seawater samples were taken to the brown glass bottles in the sea surface water monitoring laboratory of R/V Mirai. After overflow of seawater, the sample bottle was immediately sealed with butyl gum cap with care to exclude air bubbles. Then the analysis of DMS was performed on board within an hour by a purge and trap. A 30 ml of seawater sample was introduced into a degasification vessel by syringe through GF/F filter. Then sample water was sparged for 10 min by the UHP N_2 gas. The flow rate was about 120 ml/min. The extracted gas was then concentrated on the concentration tube (60/80 mesh Tenax-GR, GL Science Co. Ltd.). Then the determination of DMS was carried out by the same procedures as those for air samples. Reproducibility of this system was about ± 12%, and the detection limit was about 0.1 nM in 25 ml water sample.

Analysis of DMSP (DMSPp and DMSPd)

After gravitational filtration of 50ml of seawater with GF/F filter, GF/F filter was immersed into the solution of sodium hydroxide (5N,1.2ml) with 30ml Mili-Q water in the brown glass bottles. Analysis of DMSPp was performed with GC/FPD by purge and trap method. After conversion of DMSP to DMS through "hydrolysis" with NaOH, DMSPp was measured as DMS by purge and trap method. DMSPd was obtained by subtracting of the sum of DMS and DMSPp from the DMS-total. DMS-total was measured by addition of NaOH (2mL of NaOH) to a 50ml of seawater sample without filtration by GF/F. Storing this sample for 1~2 days in refrigerator, DMS-total was measured as DMS by purge and trap method as described above.

ii. Measurement system by fluorine induced chemiluminescence for the EC method

High speed sensor for DMS concentration based on its fast chemiluminescence reaction with molecular fluorine (F_2) was developed following the document by Hills et al [1998] to measure the atmospheric DMS concentration within a 0.1 second for the eddy correlation method. Intense chemiluminescence occurred upon reaction of F_2 with a sulfur-containing compound, as follows;

CH_3SCH_3 (DMS) + F_2 ➔ many steps ➔ $HCF^{\dagger}$ and HF* (R1)

$HCF^{\dagger}$ ➔ HCF + *hv* (λ=500~700 nm) (R2)

HF* ➔ HF + *hv* (λ=660~750 nm) (R3)

Emission in the wavelength range 500~750 nm was monitored with a photomultiplier tube (H7421 and R2228P, Hamamatsu Photonics, Co. Ltd.). Under suitable conditions, residence time of the sample air in the reaction cell was very short (much less than 0.1 sec). Assuming that reaction (R1) was a pseudo 1st order reaction, reaction (R1) was expected to almost complete within the residence time of sample air in the cell. Product gases were evacuated from the reaction cell and then scrubbed of F_2 and HF via a chemical trap, which converts excess F_2 to CF_4 on activated carbon. This system was installed on the top pf the foremast of R/V Mirai. Sample air was introduced from the top of the foremast through a Teflon-tube (OD: 8mm and c.a. 3m of length), and the sample air after analysis was exhausted outside. Signals of this reaction were recorded in personal computer. For calibration, the output of this reaction with DMS standard gas (0.76 ppmv) was also measured.

Estimation of Flux

The DMS fluxes by the bulk method and the EC method can be calculated as follows:

$$F_{bulk} = K_W (C_W - C_A / H_{DMS}) \quad \text{(Eq.1)}$$

$$F_{EC} = \frac{1}{T}\int_0^T w' C_A' dt \quad \text{(Eq.2)}$$

where Kw is the exchange coefficient of DMS at the sea surface. C_W and C_A are the DMS concentrations in the surface seawater and the atmosphere, respectively. H_{DMS} is the Henry constant of DMS. T is the time for integration (generally about 30min). w' and C_A' are the fluctuations of the vertical wind speed and the DMS concentration in the atmosphere from their average values, respectively. For the bulk method, C_W and C_A were measured by the GC/FPD system, and for the EC method, C_A variations within 0.1 sec were measured by the chemiluminescence system. The vertical component of wind speed as well as inclination and acceleration of ship movement measured by the

CO_2 flux measurement system by Okayama University will be used for the DMS flux calculation.

(3) Preliminary results

Figure 1 shows the vertical profiles of DMS and its precursors DMSPp and DMSPd in seawater at these stations measured by this GC/FPD system. Seawater DMS concentrations in the sub-arctic region (Stn004 and Stn 006 (K2)) were not so different from those in the subtropics (station 010 and station 011).The concentrations ranged from 0.5 to 1.5 nmol/L in the mixing layer. However, the DMSP concentrations in the body of phytoplankton (DMSPp) in the mixing layer were much higher in the subarctic (8~10 nmol/L) than those in the subtropics (2~5 nmol/L). As for DMSPd, no clear difference of the concentrations were observed between the subarctic and subtropics. Highest DMSPd (~8 nmol/L) was observed at the depth of 50m in the subtropics (station 011 (S1)). The marine biological and chemical data will be used to consistently elucidate all the results.

As for the atmospheric DMS concentrations, Figure 2 shows the variations in the atmospheric DMS concentrations measured by GC/FPD system. Atmospheric DMS concentration ranged from 50 to 200 pptv, and lower than those measured during the several cruises of Mirai over this area in summer season. The variations in the sea-air DMS flux and other parameters such as O3 concentration are required to elucidate these variations.

Figure 3 shows an example of the signal outputs of photon counting from the fluorine induced chemiluminescence method for fast measurement of atmospheric DMS concentration. Significant increases in the photon counts were observed when ambient marine air was introduced to this system as compared to the photon signals when zero air (UHP N_2 gas) was introduced. This increase in the photon levels can be attributed to the reaction of DMS with F_2. As mentioned above, maximum DMS concentration in the atmosphere was about 200 pptv and this level was around the detection limit of this F_2-chemiluminescence system. Consequently significant levels of signals from the chemiluminescence were obtained for only limited period of the cruise.

(4) Data archive

The data of atmospheric and seawater DMS concentrations will be submitted to the JAMSTEC DMO (Data Management Office).

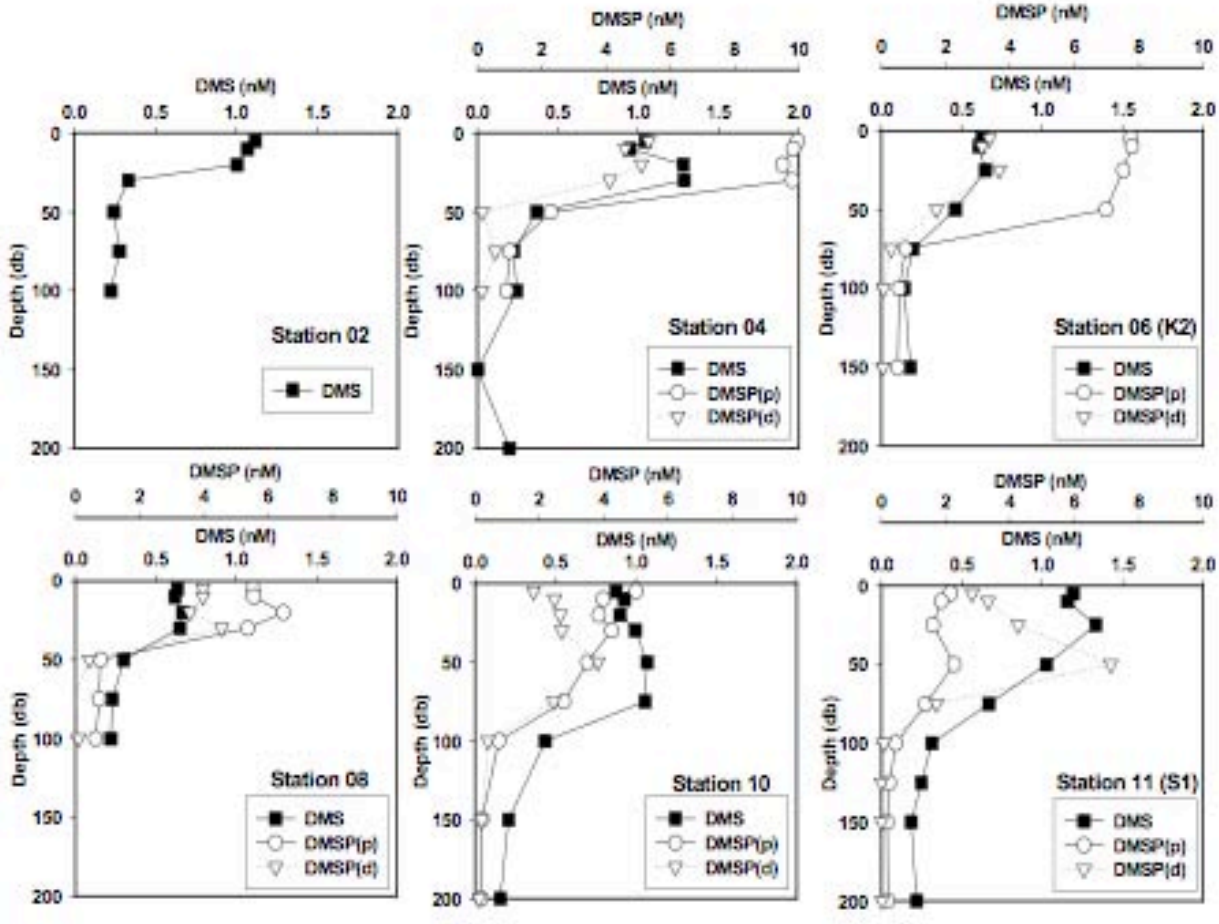

Figure 1. Vertical profiles of seawater DMS and DMSP concentrations at six stations during MR10-06 cruise. Filled square, open circle and triangle depict the concentrations of seawater DMS, DMSPp and DMSPd, respectively.

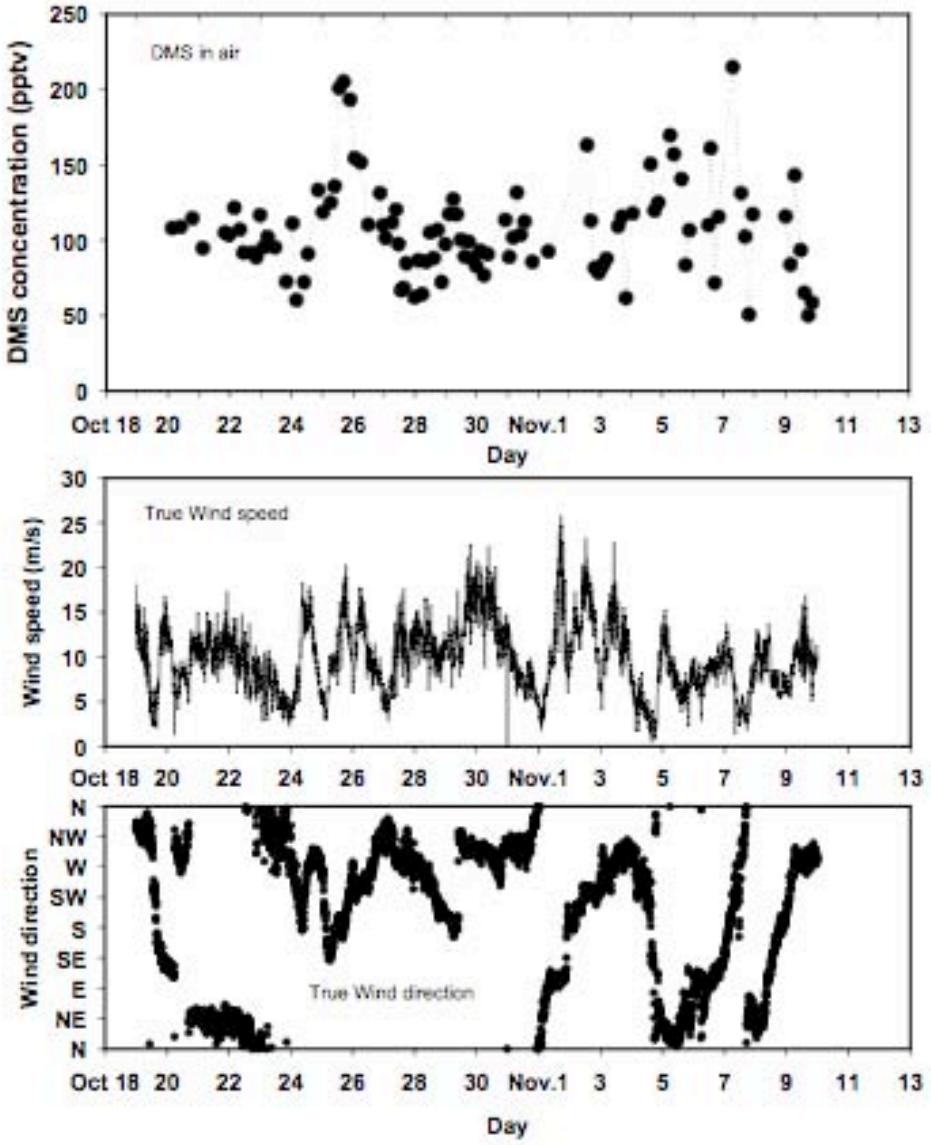

Figure 2 Time variations in the atmospheric DMS concentrations measured by GC/FPD system together with true wind speed and wind direction measured by the monitoring system of R/V Mira.

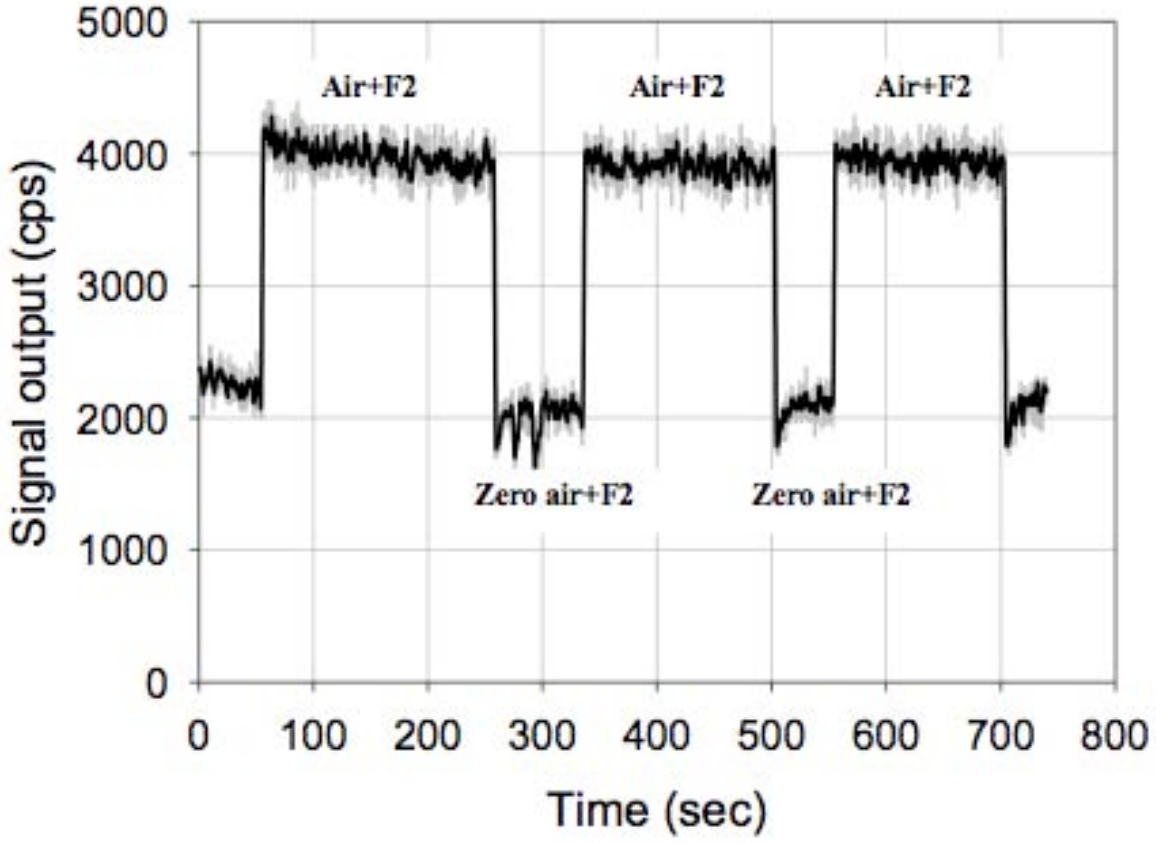

Figure 3. Photon signals emitted from chemiluminescence of sample air and zero gas with F_2. Gray line is the raw data obtained at every 0.1 sec, and thick black line is the data obtained by 1 sec -running mean. The difference the signals between those from reaction of air with F_2 and those from reaction of zero air is probably attributed to the reaction of DMS with F_2.

2.2 Physical oceanographic observation

2.2.1 CTD cast and water sampling

Masahide WAKITA (JAMSTEC MIO): Principal investigator
Kenichi KATAYAMA (MWJ): Operation leader
Hiroki USHIROMURA (MWJ)
Naoko TAKAHASHI (MWJ)
Tamami UENO (MWJ)

(1) Objective

Investigation of oceanic structure and water sampling.

(2) Methods

CTD/Carousel Water Sampling System, which is a 36-position Carousel water sampler (CWS) with Sea-Bird Electronics, Inc. CTD (SBE9plus), was used during this cruise. 12-liter Niskin Bottles, which were washed by alkaline detergent and 1 N HCl, were used for sampling seawater. The sensors attached on the CTD were temperature (Primary and Secondary), conductivity (Primary and Secondary), pressure, dissolved oxygen (Primary), RINKOIII (dissolved oxygen sensor), deep ocean standards thermometer, altimeter, fluorescence, and PAR sensor. Salinity was calculated by measured values of pressure, conductivity and temperature. The CTD/CWS was deployed from starboard on working deck.

The CTD raw data were acquired on real time using the Seasave-Win32 (ver.7.20g) provided by Sea-Bird Electronics, Inc. and stored on the hard disk of the personal computer. Seawater was sampled during the up cast by sending fire commands from the personal computer. We usually stop at each layer for 30 seconds to stabilize then fire. At the station KNTM01, bottles were fired without stopping from 1800 dbar due to rough sea.

29 casts of CTD measurements were conducted (table 2.2.1-1). No major problems were encountered during the operation.

Data processing procedures and used utilities of SBE Data Processing-Win32 (ver.7.18d) and SEASOFT were as follows:

(The process in order)

DATCNV: Convert the binary raw data to engineering unit data. DATCNV also extracts bottle information where scans were marked with the bottle confirm bit during acquisition. The duration was set to 4.4 seconds, and the offset was set to 0.0 seconds.
*At the station KNTM01, from 1800 dbar to surface, the duration was set to 1.0 seconds, and the offset was set to -0.5 seconds.

RINKOCOR(original module): Corrected the of hysteresis of RINKOIII voltage.

RINKOCORROS(original module): Corrected the of hysteresis of RINKOIII voltage bottle data.

BOTTLESUM: Create a summary of the bottle data. The data were averaged over 4.4 seconds.
*At the station KNTM01, from 1800 dbar to surface, the data were averaged over 1.0 second.

ALIGNCTD: Convert the time-sequence of sensor outputs into the pressure sequence to ensure that all calculations were made using measurements from the same parcel of water. Dissolved oxygen data are systematically delayed with respect to depth mainly because of the long time constant of the dissolved oxygen sensor and of an additional delay from the transit time of water in the pumped pluming line. This delay was compensated by 6 seconds

advancing dissolved oxygen sensor output (dissolved oxygen voltage) relative to the temperature data. RINKOIII data are also delayed by slightly slow response time to the sensor. The delay was compensated by 1 second advancing.

WILDEDIT: Mark extreme outliers in the data files. The first pass of WILDEDIT obtained an accurate estimate of the true standard deviation of the data. The data were read in blocks of 1000 scans. Data greater than 10 standard deviations were flagged. The second pass computed a standard deviation over the same 1000 scans excluding the flagged values. Values greater than 20 standard deviations were marked bad. This process was applied to pressure, depth, temperature, conductivity and dissolved oxygen voltage.

CELLTM: Remove conductivity cell thermal mass effects from the measured conductivity. Typical values used were thermal anomaly amplitude alpha = 0.03 and the time constant 1/beta = 7.0.

FILTER: Perform a low pass filter on pressure with a time constant of 0.15 second. In order to produce zero phase lag (no time shift) the filter runs forward first then backward

WFILTER: Perform a median filter to remove spikes in the fluorescence data. A median value was determined by 49 scans of the window.

SECTIONU (original module of SECTION): Select a time span of data based on scan number in order to reduce a file size. The minimum number was set to be the starting time when the CTD package was beneath the sea-surface after activation of the pump. The maximum number of was set to be the end time when the package came up from the surface.

LOOPEDIT: Mark scans where the CTD was moving less than the minimum velocity of 0.0 m/s (traveling backwards due to ship roll).

DESPIKE (original module): Remove spikes of the data. A median and mean absolute deviation was calculated in 1-dbar pressure bins for both down and up cast, excluding the flagged values. Values greater than 4 mean absolute deviations from the median were marked bad for each bin. This process was performed 2 times for temperature, conductivity, dissolved oxygen voltage (SBE43), and RINKOIII voltage.

DERIVE: Compute dissolved oxygen (SBE43).

BINAVG: Average the data into 1-dbar pressure bins.

DERIVE: Compute salinity, potential temperature, and sigma-theta.

SPLIT: Separate the data from an input .cnv file into down cast and up cast files.

Configuration file: MR1006A.con

Specifications of the sensors are listed below.

CTD: SBE911plus CTD system

Under water unit:

SBE9plus (S/N 09P27443-0677, Sea-Bird Electronics, Inc.)

Pressure sensor:

Digiquartz pressure sensor (S/N 79511)

Calibrated Date: 07 Jul. 2010

Temperature sensors:

Primary: SBE03-04/F (S/N 031525, Sea-Bird Electronics, Inc.)

Calibrated Date: 29 Jun. 2010

Secondary: SBE03-04/F (S/N 031464, Sea-Bird Electronics, Inc.)

Calibrated Date: 20 Jul. 2010

Conductivity sensors:

Primary: SBE04C (S/N 043036, Sea-Bird Electronics, Inc.)

Calibrated Date: 28 Jan. 2010

Secondary: SBE04C (S/N 042240, Sea-Bird Electronics, Inc.)

Calibrated Date: 10 Feb. 2010

Dissolved Oxygen sensors:

Primary: SBE43 (S/N 430330, Sea-Bird Electronics, Inc.)

Calibrated Date: 04 Jun. 2010

RINKOIII (S/N 006, Alec Electronics Co. Ltd.)

Calibrated Date: 10 Oct. 2010

Deep Ocean Standards Thermometer:

SBE35 (S/N 0045, Sea-Bird Electronics, Inc.)

Calibrated Date: 19 Aug. 2009

Altimeter:

Benthos PSA-916T (S/N 1100, Teledyne Benthos, Inc.)

Fluorescence:

Chlorophyll Fluorometer (S/N 3054, Seapoint Sensors, Inc.)

Photosynthetically Active Radiation:

PAR sensor (S/N 0049, Satlantic Inc.)

Calibrated Date: 22 Jan. 2009

Carousel water sampler:

SBE32 (S/N 3227443-0391, Sea-Bird Electronics, Inc.)

Deck unit:

SBE11plus (S/N 11P7030-0272, Sea-Bird Electronics, Inc.)

(3) Preliminary result

During this cruise, 29 casts of CTD observation were carried out. Date, time and locations of the CTD casts are listed in Table 2.2.1-1.

(4) Data archive

All raw and processed data files were copied onto DVD-ROM. The data will be submitted to the Data Management Office (DMO), JAMSTEC, and will be opened to public via “R/V MIRAI Data Web Page” in the JAMSTEC home page.

MR10-06 CTD Casttable

Stnnbr	Castno	Date(UTC)	Time(UTC)		BottomPosition		Depth	Wire Out	HT Above Bottom	Max Depth	Max Pressure	CTD Filename	Remark
		(mmddyy)	Start	End	Latitude	Longitude							
001	1	101910	22:52	23:44	55-14.25N	173-13.56W	3546.0	989.1	-	992.5	1003.9	001M01	
002	1	102010	20:03	22:52	56-08.46N	179-07.49W	3796.0	3808.3	8.1	3775.1	3845.2	002M01	
004	1	102310	01:28	02:22	52-24.02N	169-09.51E	5127.0	987.3	-	989.8	1002.8	004M01	
005	1	102410	02:32	03:23	49-23.71N	163-50.36E	5587.0	991.3	-	990.9	1001.4	005M01	
K02	1	102410	21:02	00:18	46-59.32N	159-58.49E	5214.0	5201.0	9.1	5195.5	5303.7	K02M01	
K02	2	102510	05:48	06:15	46-59.47N	160-02.94E	5226.0	301.9	-	300.7	304.8	K02M02	
K02	3	102510	17:05	17:47	46-53.20N	160-00.06E	5156.0	300.6	-	300.7	303.3	K02M03	
K02	4	102510	21:00	22:18	46-52.69N	160-01.96E	5166.0	1999.2	-	1976.1	2003.3	K02M04	
K02	5	102610	03:55	04:57	46-50.77N	160-02.81E	5221.0	1001.4	-	1001.0	1011.7	K02M05	
K02	6	102610	21:01	21:55	46-51.77N	159-56.10E	5167.0	999.0	-	1000.8	1013.8	K02M06	
K02	7	102610	23:34	02:27	46-51.66N	159-56.89E	5160.0	5012.5	-	5000.3	5102.4	K02M07	
K02	8	102810	07:34	07:46	46-52.47N	159-55.51E	5176.0	91.8	-	100.1	102.3	K02M08	
K02	9	102810	17:04	17:41	46-51.79N	159-59.42E	5153.0	298.7	-	300.6	303.4	K02M09	
KNT	1	110210	07:47	10:52	44-00.05N	155-00.35E	5316.0	5311.2	10.2	5294.8	5404.1	KNTM01	Due to rough sea, bottles were fired without stopping (from upcast 1800dbar)
008	1	110310	04:53	05:48	41-59.91N	152-07.16E	5236.0	985.1	-	991.2	1000.8	008M01	
009	1	110410	12:01	12:50	37-59.87N	146-29.41E	5414.0	992.8	-	992.0	1001.9	009M01	
010	1	110510	08:13	09:08	34-00.02N	145-04.90E	5737.0	989.8	-	991.4	1001.3	010M01	
S01	1	110610	06:53	08:04	30-00.08N	145-00.03E	5972.0	1979.0	-	1977.6	2000.5	S01M01	
S01	2	110610	20:33	00:18	30-00.16N	145-00.06E	5981.0	5940.6	9.4	5948.5	6073.9	S01M02	
S01	3	110710	09:14	09:39	30-00.09N	145-00.04E	5968.0	199.1	-	200.5	201.7	S01M03	
S01	4	110710	17:51	18:29	30-00.18N	144-59.81E	5969.0	300.9	-	300.8	302.9	S01M04	
S01	5	110710	22:55	23:47	30-00.74N	145-02.69E	5971.0	1000.9	-	1001.9	1011.1	S01M05	
S01	6	110810	05:58	08:55	29-59.99N	144-59.99E	5966.0	4914.3	-	4910.6	5002.2	S01M06	
S01	7	110910	04:06	04:23	29-59.97N	144-59.99E	5960.0	102.7	-	105.5	106.9	S01M07	
S01	8	110910	08:33	08:58	29-59.98N	145-00.05E	5968.0	197.9	-	200.6	202.0	S01M08	
S01	9	110910	10:12	10:23	29-59.95N	145-00.00E	5961.0	76.9	-	80.3	80.7	S01M09	
S01	10	110910	18:01	18:38	30-00.04N	145-00.09E	5965.0	298.0	-	300.4	302.9	S01M10	
S01	11	111010	03:01	03:58	30-00.06N	144-59.98E	5961.0	999.8	-	1001.6	1011.5	S01M11	
S01	12	111010	22:03	22:16	30-00.57N	145-04.07E	5951.0	200.4	-	201.1	202.7	S01M12	

2.2.2 Salinity measurement

Masahide WAKITA (JAMSTEC MIO): Principal investigator
Naoko TAKAHASHI (MWJ): Operation leader
Tamami UENO (MWJ)

(1) Objective

To measure bottle salinity obtained by CTD casts, bucket sampling, and The Continuous Sea Surface Water Monitoring System (TSG).

(2) Methods

a. Salinity Sample Collection

Seawater samples were collected with 12 liter Niskin-X bottles, bucket, and TSG. The salinity sample bottle of the 250ml brown grass bottle with screw cap was used for collecting the sample water. Each bottle was rinsed three times with the sample water, and was filled with sample water to the bottle shoulder. The salinity sample bottles for TSG were sealed with a plastic inner cap and a screw cap because we took into consideration the possibility of storage for about a month. These caps were rinsed three times with the sample water before use. The bottle was stored for more than 12 hours in the laboratory before the salinity measurement.

The number of samples are shown as follows ;

Table 2.2.2-1 The number of samples

Sampling type	Number of Samples
CTD and Bucket	311
TSG	21
Total	332

b. Instruments and Method

The salinity analysis on R/V MIRAI was carried out during the cruise of MR10-06 using the salinometer (Model 8400B “AUTOSAL” ; Guildline Instruments Ltd.: S/N 62827) with an additional peristaltic-type intake pump (Ocean Scientific International, Ltd.). A pair of precision digital thermometers (Model 9540 ; Guildline Instruments Ltd.:S/N66528 and 62525) were used. The thermometer monitored the ambient temperature and the bath temperature of the salinometer.

The specifications of AUTOSAL salinometer and thermometer are shown as follows ;

Salinometer (Model 8400B “AUTOSAL” ; Guildline Instruments Ltd.)

Measurement Range	:	0.005 to 42 (PSU)
Accuracy	:	Better than ±0.002 (PSU) over 24 hours without re-standardization
Maximum Resolution	:	Better than ±0.0002 (PSU) at 35 (PSU)

Thermometer (Model 9540 ; Guildline Instruments Ltd.)

Measurement Range	:	-40 to +180 deg C
Resolution	:	0.001
Limits of error ±deg C	:	0.01 (24 hours @ 23 deg C ±1 deg C)
Repeatability	:	±2 least significant digits

The measurement system was almost the same as Aoyama et al. (2002). The salinometer was operated in the air-conditioned ship's laboratory at a bath temperature of 24 deg C. The ambient temperature varied from approximately 21 deg C to 24 deg C, while the bath temperature was very stable and varied within +/- 0.001 deg C on rare occasion.

The measurement for each sample was done with the double conductivity ratio and defined as the median of 31 readings of the salinometer. Data collection was started 10 seconds after filling the cell with the sample and it took about 15 seconds to collect 31 readings by a personal computer. Data were taken for the sixth and seventh filling of the cell after rinsing 5 times. In the case of the difference between the double conductivity ratio of these two fillings being smaller than 0.00002, the average value of the double conductivity ratio was used to calculate the bottle salinity with the algorithm for practical salinity scale, 1978 (UNESCO, 1981). If the difference was greater than or equal to 0.00003, an eighth filling of the cell was done. In the case of the difference between the double conductivity ratio of these two fillings being smaller than 0.00002, the average value of the double conductivity ratio was used to calculate the bottle salinity. In the case of the double conductivity ratio of eighth filling did not satisfy the criteria above, we measured a ninth filling of the cell and calculated the bottle salinity. The measurement was conducted in about 4 - 12 hours per day and the cell was cleaned with soap after the measurement of the day.

(3)Preliminary Result

a. Standard Seawater

Standardization control of the salinometer was set to 462 and all measurements were done at this setting. The value of STANDBY was 24+5392 +/- 0002 and that of ZERO was 0.0+0000 +/- 0001. The conductivity ratio of IAPSO Standard Seawater batch P152 was

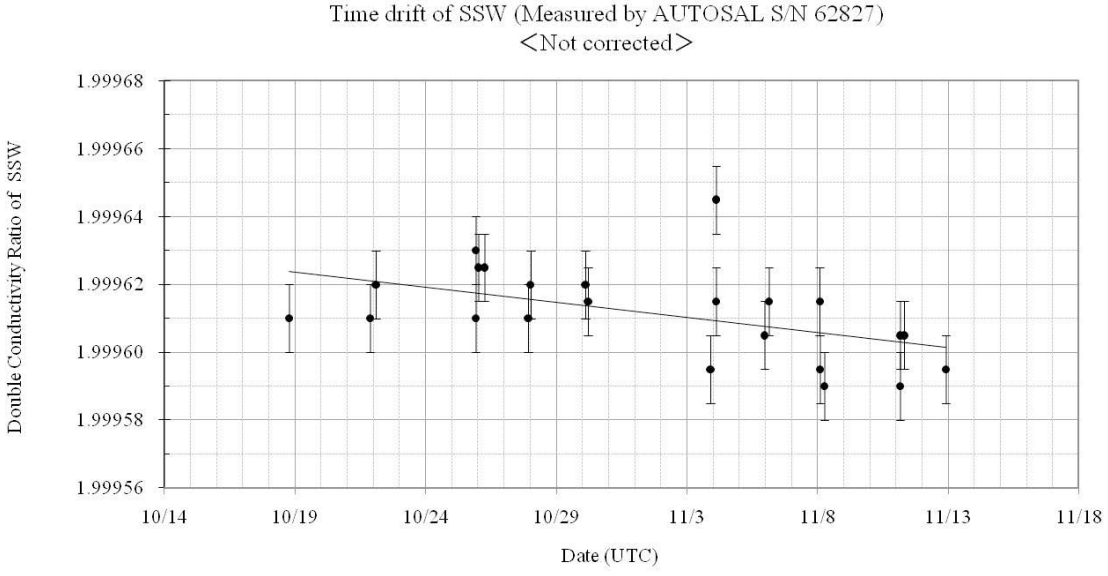

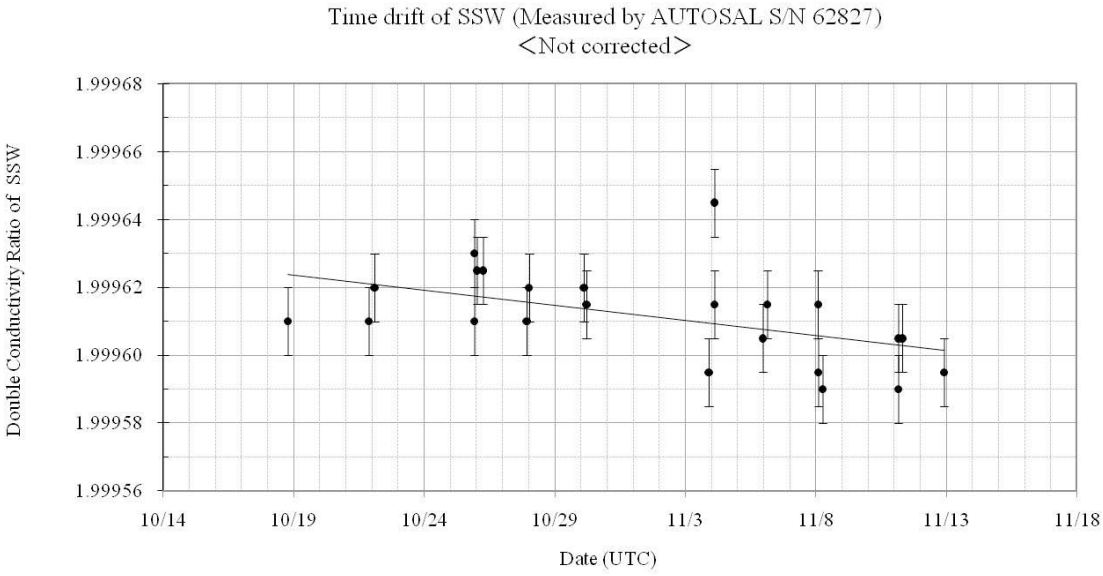

Fig. 2.2.2-1 The history of the double conductivity ratio
for the Standard Seawater batch P152(Before correction)

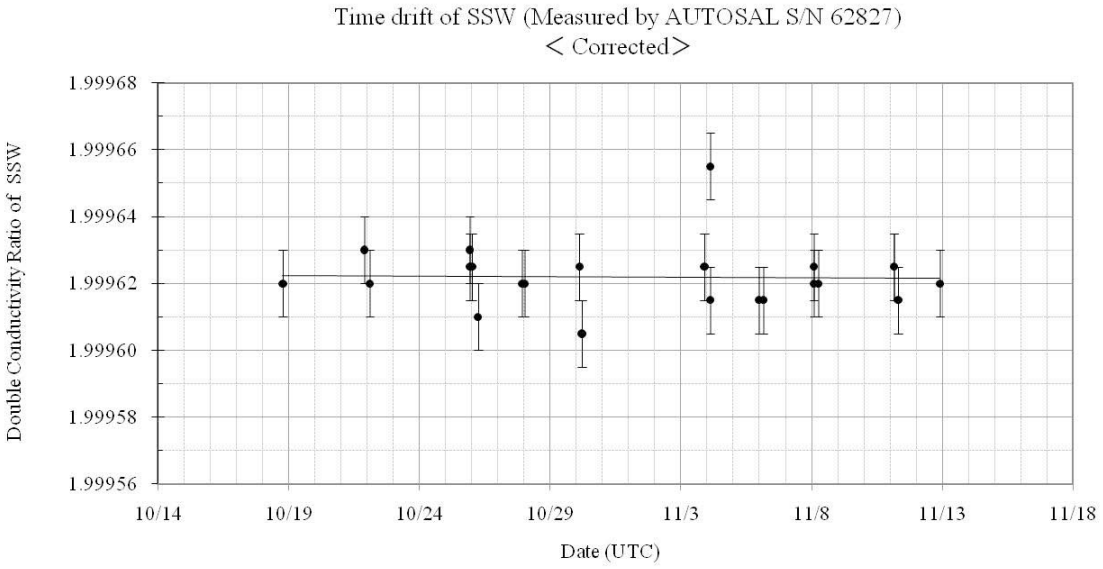

Fig. 2.2.2-2 The history of the double conductivity ratio
for the Standard Seawater batch P152(after correction)

b. Sub-Standard Seawater

Sub-standard seawater was made from deep-sea water filtered by a pore size of 0.45 micrometer and stored in a 20-liter container made of polyethylene and stirred for at least 24 hours before measuring. It was measured about every 6 samples in order to check for the possible sudden drifts of the salinometer.

c. Replicate Samples

We estimated the precision of this method using 30 pairs of replicate samples taken

from the same Niskin bottle. Fig.2.2.2-3 shows the histogram of the absolute difference between each pair of the replicate samples. There was 1 questionable measurement in the replicate samples. The average and the standard deviation of absolute deference among 30 pairs of replicate samples were 0.0003 and 0.0002 in salinity, respectively.

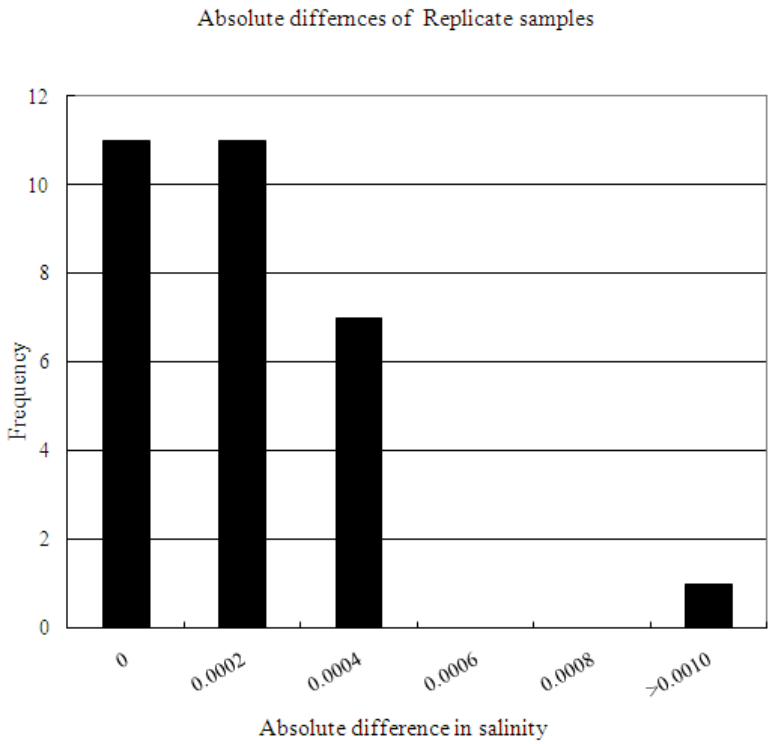

Fig. 2.2.2-3 The histogram of the double conductivity ratio
for the absolute difference of replicate samples

(4) Data archive

These raw datasets will be submitted to JAMSTEC Data Management Office (DMO).

(5) Reference

・Aoyama, M., T. Joyce, T. Kawano and Y. Takatsuki : Standard seawater comparison up to P129. Deep-Sea Research, I, Vol. 49, 1103～1114, 2002

・UNESCO : Tenth report of the Joint Panel on Oceanographic Tables and Standards. UNESCO Tech. Papers in Mar. Sci., 36, 25 pp., 1981

2.2.3. XBT/XCTD

Yoshimi KAWAI (JAMSTEC) Principal Investigator
Akira NAGAO (JAMSTEC)
Katsuhisa MAENO (GODI)
Kazuho YOSHIDA (GODI)
Chiho SUKIGARA (Nagoya University)

(1) Objectives

Investigation of the hydrographic and current structures in the Kuroshio Extension region, especially focusing on meso- and submeso-scale phenomena.

(2) Parameters

According to the manufacturer, Tsurumi-Seiki Co., Ltd., the range and accuracy of parameters measured by the XCTD (eXpendable Conductivity, Temperature, and Depth profiler) are as follows;

Parameter	Range	Accuracy
Conductivity	0-60 mS	±0.03 mS/cm
Temperature	−2-35 °C	±0.02 °C
Depth	0-1000 m	5 m or 2 % at depth, whichever is greater

(3) Methods

We measured temperature and salinity from the sea surface to the depth of 1000 m by using XCTD-1 probes and an on-board data converter, MK-130 (Tsurumi-Seiki Co., Ltd.) We intersected the Kuroshio Extension twice; southwestward from JKEO to KEO (E-line), and northwestward from S1 to W43 (W-line), casting probes by automatic or hand launchers. A total of 84 casts were performed, as shown in the observation summary (Table 2.2.3-1) and the XCTD site map (Fig. 2.2.3-1).

(4) Preliminary results

Both temperature and salinity profiles down to over 1000 m were obtained except for the sites of W03 and W11. At W03, the data were collected to 705 m. At W11, the temperature and salinity were measured down to 1000 and 800 m, respectively. The E- and W-lines well captured sections of a crest and a trough of the Kuroshio Extension, respectively. A clear baroclinic structure of the Kuroshio Extension and submeso-scale structures of salinity around the Kuroshio current axis can be recognized (Figs. 2.3.3-2 and 2.3.3-3).

(5) Data archives

These XCTD data have been submitted to the Data Integration and Analysis Group (DIAG) of JAMSTEC just after the cruise.

Table 2.2.3-1. Summary of the XCTD observations

Station No.	Date (YYYY/MM/DD)	Time (hh:mm)	Latitude	Longitude	Depth (m)
JKEO	2010.11.05	12:11	37-59.92N	146-29.40E	5414
E01	2010.11.05	14:13	37-49.99N	146-27.99E	4967
E02	2010.11.05	15:04	37-40.00N	146-23.88E	5525
E03	2010.11.05	15:56	37-29.99N	146-19.46E	5610
E04	2010.11.05	16:47	37-19.99N	146-15.14E	5637
E05	2010.11.05	17:47	37-07.76N	146-10.49E	5541
E06	2010.11.05	18:25	37-00.01N	146-07.67E	5464
E07	2010.11.05	19:14	36-49.99N	146-04.00E	5467
E08	2010.11.05	20:02	36-39.99N	146-00.13E	5470
E09	2010.11.05	20:45	36-29.99N	145-56.31E	5497
E10	2010.11.05	21:27	36-19.99N	145-52.73E	5527
E11	2010.11.05	22:07	36-10.00N	145-49.21E	5662
E12	2010.11.05	22:46	36-00.00N	145-45.37E	5713
E13	2010.11.05	23:28	35-50.01N	145-41.64E	5817
E14	2010.11.06	00:09	35-40.00N	145-38.00E	5839
E15	2010.11.06	00:52	35-29.99N	145-34.29E	5844
E16	2010.11.06	01:35	35-19.99N	145-30.91E	5797
E17	2010.11.06	02:18	35-10.00N	145-27.47E	5927
E18	2010.11.06	03:01	34-59.99N	145-24.15E	5884
E19	2010.11.06	03:44	34-49.99N	145-20.79E	5812
E20	2010.11.06	00:04	34-39.99N	145-17.85E	5855
E21	2010.11.06	05:11	34-29.99N	145-14.68E	5839
E22	2010.11.06	05:56	34-19.99N	145-11.45E	5817
E23	2010.11.06	06:40	34-09.99N	145-08.25E	5803
E24	2010.11.06	08:24	34-00.00N	145-04.92E	5734
E25	2010.11.06	09:58	33-49.99N	145-01.77E	5746
E26	2010.11.06	10:41	33-39.99N	144-58.22E	5787
E27	2010.11.06	11:24	33-29.98N	144-54.96E	5716
E28	2010.11.06	12:07	33-19.95N	144-51.70E	5662

E29	2010.11.06	12:49	33-09.99N	144-48.27E	5680
E30	2010.11.06	13:31	33-00.00N	144-45.05E	5649
E31	2010.11.06	14:14	32-50.00N	144-41.80E	5780
E32	2010.11.06	14:56	32-40.00N	144-38.67E	5928
E33	2010.11.06	15:38	32-29.98N	144-35.36E	5589
KEO	2010.11.06	16:05	32-23.68N	144-33.37E	5740
S1	2010.11.13	04:32	30-02.87N	145-02.38E	5962
W01	2010.11.13	05:09	30-10.01N	144-59.78E	5943
W02	2010.11.13	06:00	30-20.01N	144-55.97E	5970
W03	2010.11.13	06:52	30-30.01N	144-52.61E	5991
W04	2010.11.13	07:42	30-40.01N	144-49.61E	6092
W05	2010.11.13	08:33	30-50.18N	144-46.88E	6012
W06	2010.11.13	09:23	31-00.02N	144-44.07E	5969
W07	2010.11.13	10:15	31-10.06N	144-41.39E	5718
W08	2010.11.13	11:07	31-20.01N	144-39.15E	5634
W09	2010.11.13	11:58	31-30.01N	144-38.10E	5572
W10	2010.11.13	12:48	31-40.02N	144-33.34E	5600
W11	2010.11.13	13:38	31-50.00N	144-30.59E	5802
W12	2010.11.13	14:28	32-00.01N	144-27.90E	5828
W13	2010.11.13	15:18	32-09.99N	144-25.16E	5853
W14	2010.11.13	16:08	32-20.00N	144-22.36E	5795
W15	2010.11.13	16:58	32-29.99N	144-19.65E	5690
W16	2010.11.13	17:47	32-39.99N	144-17.08E	5704
W17	2010.11.13	18:37	32-50.00N	144-14.30E	5661
W18	2010.11.13	19:25	33-00.01N	144-11.68E	5531
W19	2010.11.13	20:14	33-10.01N	144-09.02E	5489
W20	2010.11.13	21:04	33-20.00N	144-06.30E	5517
W21	2010.11.13	21:53	33-30.00N	144-03.50E	5605
W22	2010.11.13	22:42	33-40.01N	144-00.82E	5638
W23	2010.11.13	23:31	33-50.00N	143-58.12E	5691
W24	2010.11.14	00:22	34-00.03N	143-55.38E	5438
W25	2010.11.14	01:13	34-10.00N	143-52.49E	4233
W26	2010.11.14	02:04	34-20.01N	143-49.48E	1864

W27	2010.11.14	02:55	34-30.00N	143-46.96E	5683
W28	2010.11.14	03:46	34-40.00N	143-44.30E	5652
W29	2010.11.14	04:36	34-50.02N	143-41.38E	5696
W30	2010.11.14	05:25	35-00.02N	143-38.52E	5646
W31	2010.11.14	06:15	35-10.01N	143-35.72E	5563
W32	2010.11.14	07:13	35-20.01N	143-35.23E	5587
W33	2010.11.14	08:26	35-30.00N	143-38.39E	5653
W34	2010.11.14	09:30	35-40.01N	143-37.88E	5629
W35	2010.11.14	10:23	35-50.01N	143-32.10E	5998
W36	2010.11.14	11:16	36-00.02N	143-26.56E	3726
W37	2010.11.14	12:02	36-10.02N	143-21.28E	6398
W38	2010.11.14	12:58	36-20.02N	143-16.39E	6823
W39	2010.11.14	13:46	36-30.02N	143-13.31E	7215
W40	2010.11.14	14:34	36-39.99N	143-10.60E	7415
W41	2010.11.14	15:22	36-50.00N	143-08.10E	6485
W42	2010.11.14	16:11	36-59.99N	143-06.19E	5964
W43	2010.11.14	17:01	37-10.00N	143-02.96E	4958
W44	2010.11.14	17:50	37-20.00N	142-59.20E	4368
W45	2010.11.14	18:39	37-30.00N	142-55.90E	3157
W46	2010.11.14	19:28	37-40.10N	142-53.11E	2175

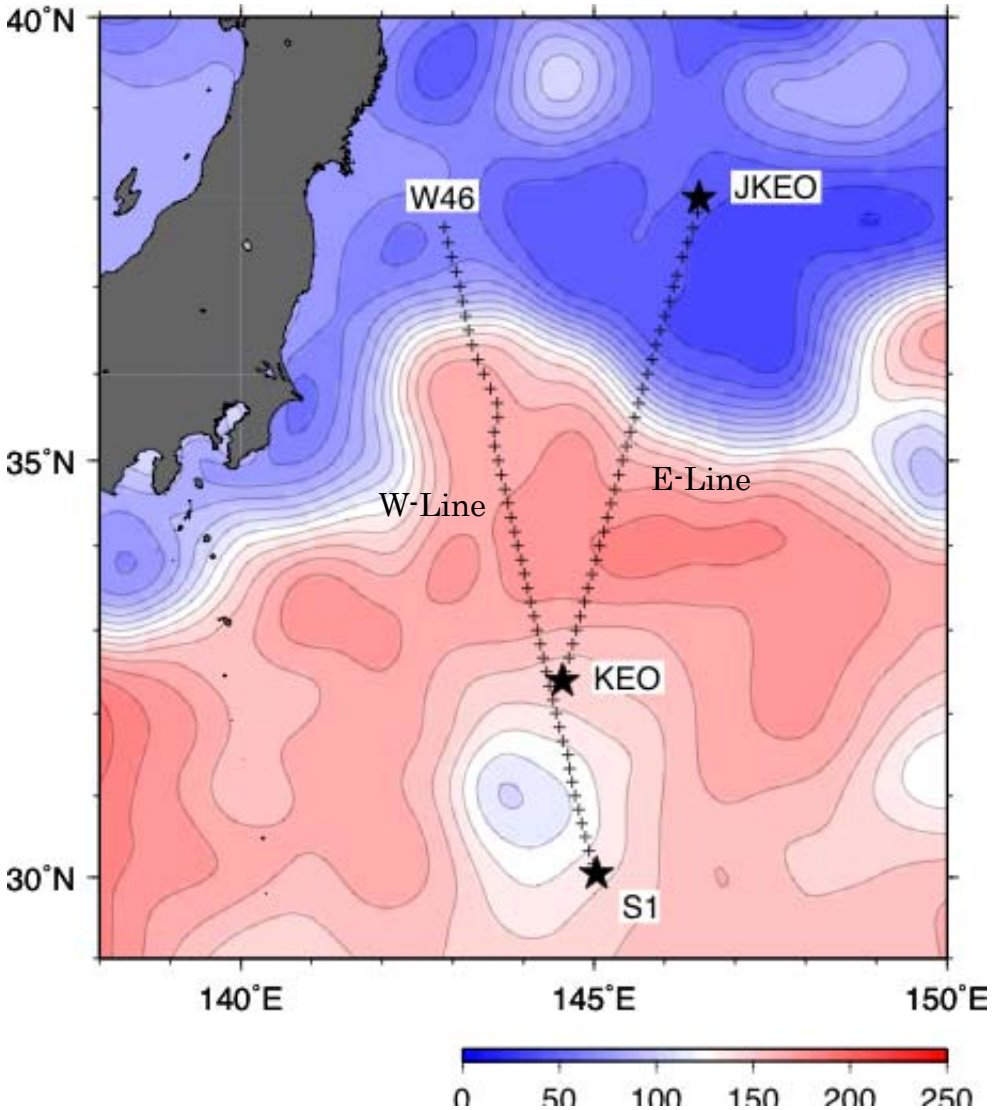

Figure 2.2.3-1. Location of the XCTD sites and absolute sea-surface height (cm) on November 10, 2010 obtained from AVISO data. Contour interval is 10 cm.

a

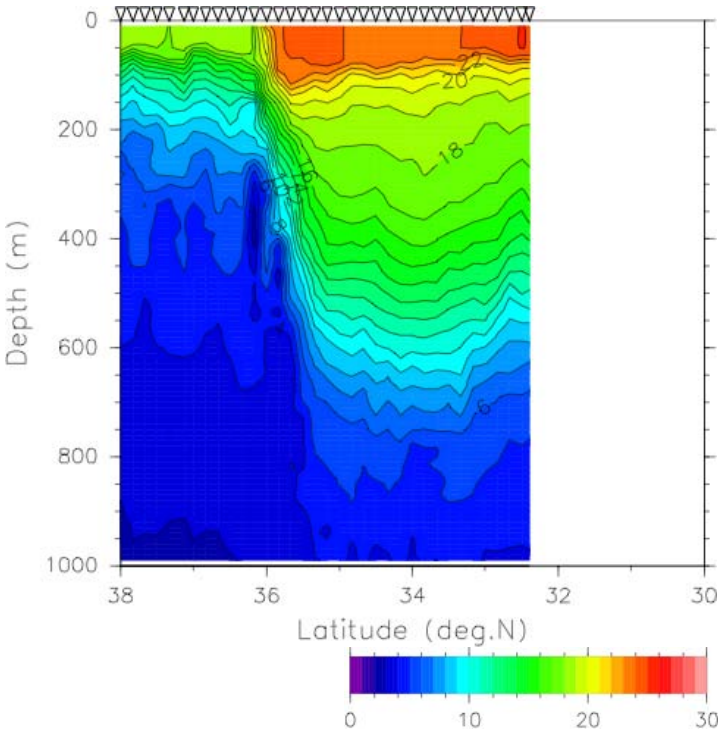

b

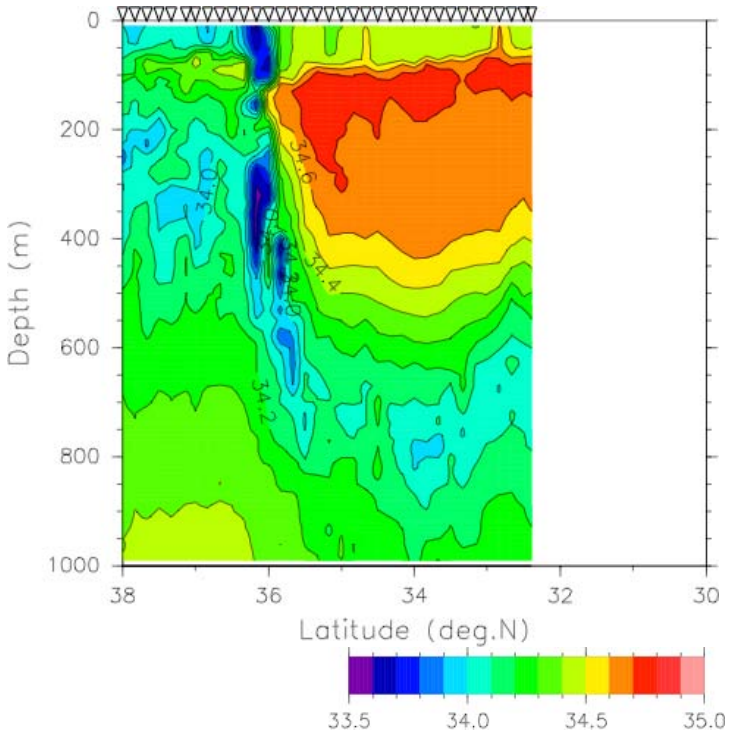

Figure 2.2.3-2. Sections of (a) potential temperature and (b) salinity at the E-line. Contour intervals in (a) and (b) are 1˚C and 0.2, respectively.

a

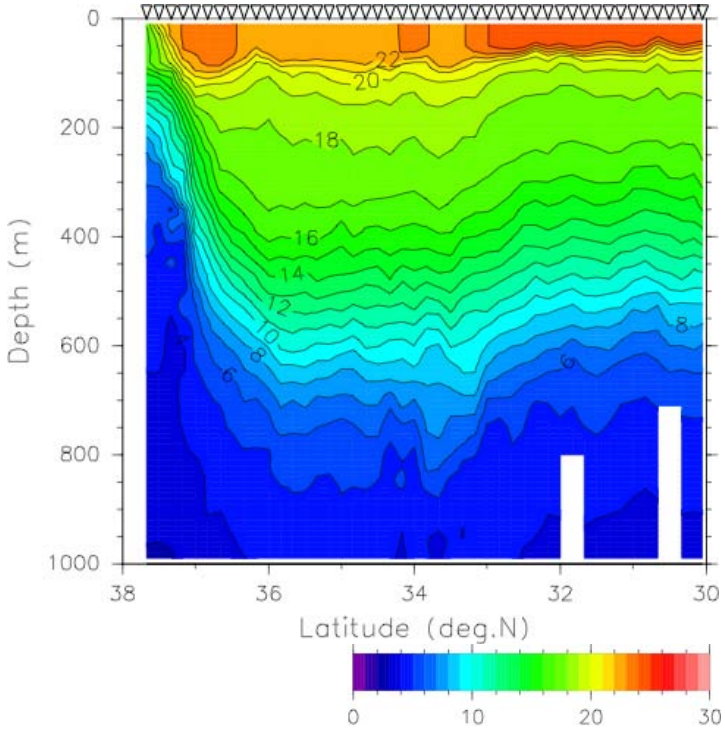

b

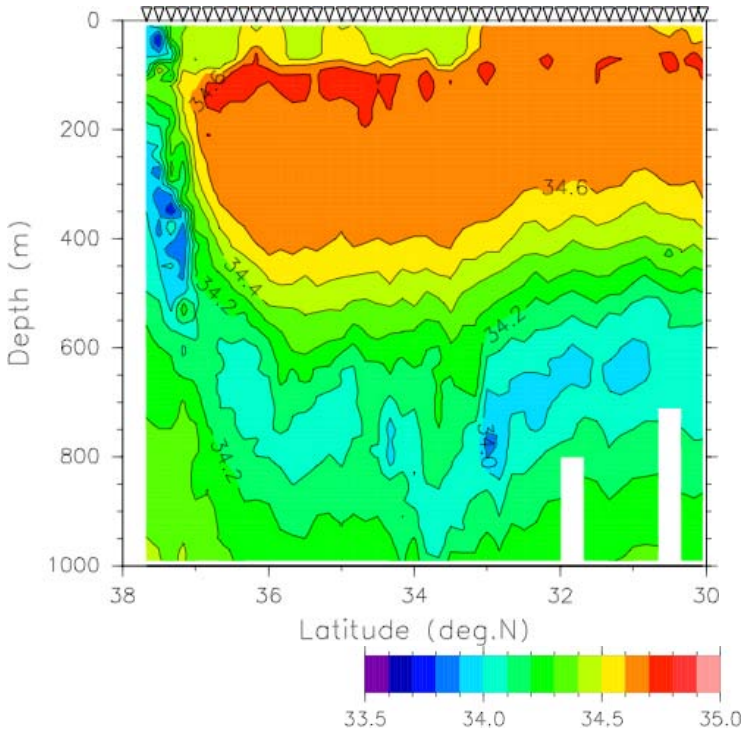

Figure 2.2.3-3. Same as Fig. 2.2.3-2 but for the W-line.

2.2.4 Shipboard ADCP

Katsuhisa MAENO (Global Ocean Development Inc., GODI)
Kazuho YOSHIDA (GODI)
Wataru TOKUNAGA (Mirai Crew)

(1) Objective

To obtain continuous measurement of the current profile along the ship's track.

(2) Methods

Upper ocean current measurements were made throughout MR10-06 cruise, using the hull-mounted Acoustic Doppler Current Profiler (ADCP) system that is permanently installed on the R/V MIRAI. For most of its operation, the instrument was configured for water-tracking mode recording. Bottom-tracking mode, interleaved bottom-ping with water-ping, was made in shallower water region to get the calibration data for evaluating transducer misalignment angle. The system consists of following components;

i) R/V MIRAI has installed the Ocean Surveyor for vessel-mount (acoustic frequency 75 kHz; Teledyne RD Instruments). It has a phased-array transducer with single ceramic assembly and creates 4 acoustic beams electronically. We mounted the transducer head rotated to a ship-relative angle of 45 degrees azimuth from the keel
ii) For heading source, we use ship's gyro compass (Tokimec, Japan), continuously providing heading to the ADCP system directory. Additionally, we have Inertial Navigation System (INS) which provide high-precision heading, attitude information, pitch and roll, are stored in ".N2R" data files with a time stamp.
iii) DGPS system (Trimble SPS751 & StarFixXP) providing position fixes.
iv) We used VmDas version 1.42 (TRD Instruments) for data acquisition.
v) To synchronize time stamp of ping with GPS time, the clock of the logging computer is adjusted to GPS time every 1 minute
vi) We have placed ethylene glycol into the fresh water to prevent freezing in the sea chest.
vii) The sound speed at the transducer does affect the vertical bin mapping and vertical velocity measurement, is calculated from temperature, salinity (constant value; 35.0 psu) and depth (6.5 m; transducer depth) by equation in Medwin (1975).

Data was configured at 8-m intervals starting 23-m below the surface. Every ping was recorded as raw ensemble data (.ENR). Also, 60 seconds and 300 seconds averaged data were recorded as short term average (.STA) and long term average (.LTA) data, respectively. Major parameters for the measurement (Direct Command) are shown Table 2.2.4-1 Major parameters.

(3) Preliminary results

Fig.2.2.4-1 shows an hour averaged surface (100 – 150m) current vector along the ship track. In this cruise, the data quality was not in good condition When you use ADCP data, it is highly recommended to check the status data (correlation, echo amplitude and error velocity).

(4) Data archive

These data obtained in this cruise will be submitted to the Data Management Group

(DMG) of JAMSTEC, and will be opened to the public via “R/V MIRAI Data Web Page” in JAMSTEC home page.

(5) Remarks

1) We did not collect data in the following periods.

00:16 – 01:19UTC 26 Oct.

20:51 – 21:40UTC 29 Oct.

Table 2.2.4-1 Major parameters

Bottom-Track Commands	
BP = 001	Pings per Ensemble (almost less than 1000m depth) 08:52 UTC, 14 Nov. – 00:10 UTC, 16 Nov.
BP = 000	Disable bottom-track ping (almost over 1000m depth) 00:00 UTC, 19 Oct. – 08:51 UTC, 14 Nov
Environmental Sensor Commands	
EA = +04500	Heading Alignment (1/100 deg)
EB = +00000	Heading Bias (1/100 deg)
ED = 00065	Transducer Depth (0 - 65535 dm)
EF = +001	Pitch/Roll Divisor/Multiplier (pos/neg) [1/99 - 99]
EH = 00000	Heading (1/100 deg)
ES = 35	Salinity (0-40 pp thousand)
EX = 00000	Coord Transform (Xform:Type; Tilts; 3Bm; Map)
EZ = 10200010	Sensor Source (C; D; H; P; R; S; T; U) C (1): Sound velocity calculates using ED, ES, ET (temp.) D (0): Manual ED H (2): External synchro P (0), R (0): Manual EP, ER (0 degree) S (0): Manual ES T (1): Internal transducer sensor U (0): Manual EU
Timing Commands	
TE = 00:00:02.00	Time per Ensemble (hrs:min:sec.sec/100)
TP = 00:02.00	Time per Ping (min:sec.sec/100)
Water-Track Commands	
WA = 255	False Target Threshold (Max) (0-255 count)
WB = 1	Mode 1 Bandwidth Control (0=Wid, 1=Med, 2=Nar)
WC = 120	Low Correlation Threshold (0-255)
WD = 111 110 000	Data Out (V; C; A; PG; St; Vsum; Vsum^2;#G;P0)
WE = 1000	Error Velocity Threshold (0-5000 mm/s)
WF = 0800	Blank After Transmit (cm)
WG = 001	Percent Good Minimum (0-100%)
WI = 0	Clip Data Past Bottom (0 = OFF, 1 = ON)
WJ = 1	Rcvr Gain Select (0 = Low, 1 = High)
WM = 1	Profiling Mode (1-8)
WN = 100	Number of depth cells (1-128)
WP = 00001	Pings per Ensemble (0-16384)
WS = 0800	Depth Cell Size (cm)
WT = 000	Transmit Length (cm) [0 = Bin Length]
WV = 0390	Mode 1 Ambiguity Velocity (cm/s radial)

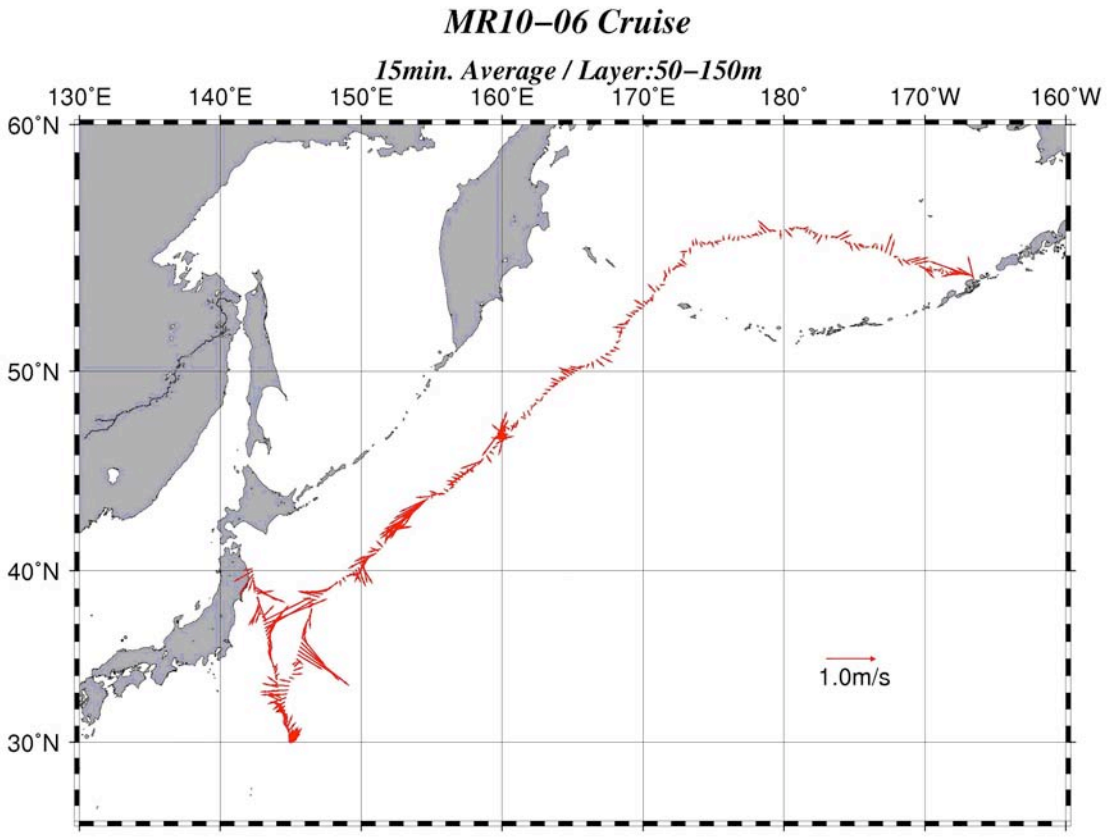

Fig. 2.2.4-1 An hour averaged surface (50-150 m) current vector along the ship track

.

2.3 Sea surface water monitoring

Masahide WAKITA (JAMSTEC): Principal Investigator
Hironori SATO (Marine Works Japan Co. Ltd): Operation Leader

(1) Objective

Our purpose is to obtain temperature, salinity, dissolved oxygen, and fluorescence data continuously in near-sea surface water.

(2) Parameters

Temperature (surface water)
Salinity (surface water)
Dissolved oxygen (surface water)
Fluorescence (surface water)

(3) Instruments and Methods

The Continuous Sea Surface Water Monitoring System (Marine Works Japan Co. Ltd.) has five sensors and automatically measures temperature, salinity, dissolved oxygen and fluorescence in near-sea surface water every one minute. This system is located in the "*sea surface monitoring laboratory*" and connected to shipboard LAN-system. Measured data, time, and location of the ship were stored in a data management PC. The near-surface water was continuously pumped up to the laboratory from about 4.5 m water depth and flowed into the system through a vinyl-chloride pipe. The flow rate of the surface seawater was adjusted to be 5 dm^3 min^{-1}.

a. Instruments

Software

Seamoni-kun Ver.1.10

Sensors

Specifications of the each sensor in this system are listed below.

Temperature and Conductivity sensor

Model:	SBE-45, SEA-BIRD ELECTRONICS, INC.
Serial number:	4557820-0319
Measurement range:	Temperature -5 to +35 ^oC
	Conductivity 0 to 7 S m^{-1}
Initial accuracy:	Temperature 0.002 ^oC
	Conductivity 0.0003 S m^{-1}
Typical stability (per month):	Temperature 0.0002 ^oC
	Conductivity 0.0003 S m^{-1}
Resolution:	Temperatures 0.0001 ^oC
	Conductivity 0.00001 S m^{-1}

Bottom of ship thermometer

Model:	SBE 38, SEA-BIRD ELECTRONICS, INC.
Serial number:	3857820-0540

Measurement range: -5 to +35 ^{o}C
Initial accuracy: ±0.001 ^{o}C
Typical stability (per 6 month): 0.001 ^{o}C
Resolution: 0.00025 ^{o}C

Dissolved oxygen sensor
Model: OPTODE 3835, AANDERAA Instruments.
Serial number: 1233
Measuring range: 0 - 500 μmol dm^{-3}
Resolution: <1 μmol dm^{-3}
Accuracy: <8 μmol dm^{-3} or 5% whichever is greater
Settling time: <25 s

Fluorometer
Model: 10-AU, TURNER DESIGNS
Serial number: 5562 FRXX

b. Measurements

Periods of measurement during MR10-06 are listed in Table 2.3-1.

Table 2.3-1. Events list of the Sea surface water monitoring during MR10-06

System Date [UTC]	System Time [UTC]	Events	Remarks
2010/10/19	01:14	All the measurements started and data was available.	start
2010/11/14	04:00	All the measurements stopped.	end

(5) Preliminary Result

Preliminary data of temperature, salinity, dissolved oxygen and fluorescence at sea surface is shown in Fig. 2.3-1.

We took the surface water samples to compare sensor data with bottle data of salinity, dissolved oxygen and fluorescence. The results are shown in Figs. 2.3-2 - 4. All the salinity samples were analyzed by the Guideline 8400B “AUTOSAL” (see 2.2.2), and dissolve oxygen samples were analyzed by Winkler method (see 2.4), and fluorescence were analyzed by 10-AU (see 3.3.1).

(6) Data archive

All data will be submitted to Chief Scientist.

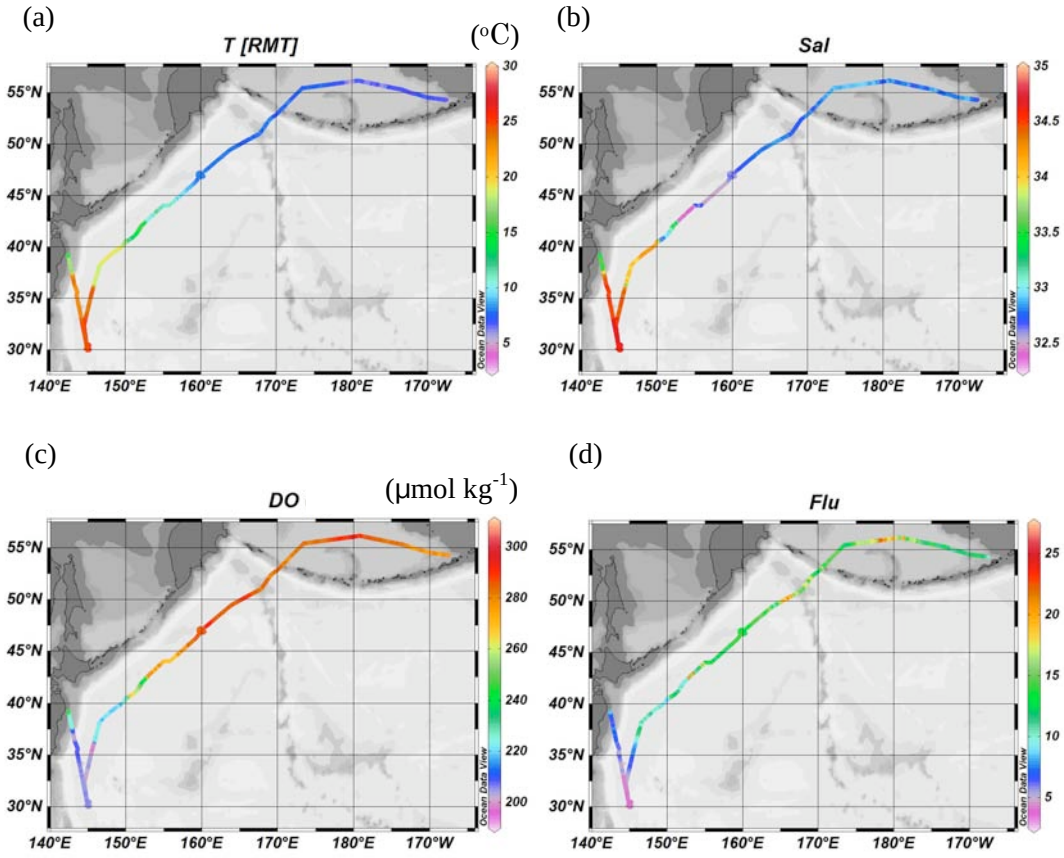

Fig. 2.3-1. Spatial and temporal distribution of (a) temperature, (b) salinity, (c) dissolved oxygen and (d) fluorescence in MR10-06 cruise.

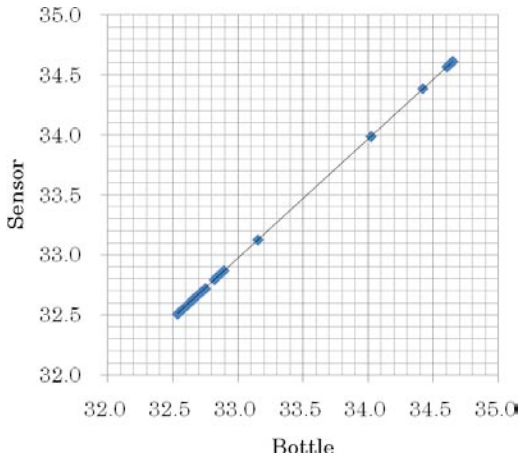

Fig. 2.3-2. Correlation of salinity between sensor data and bottle data.

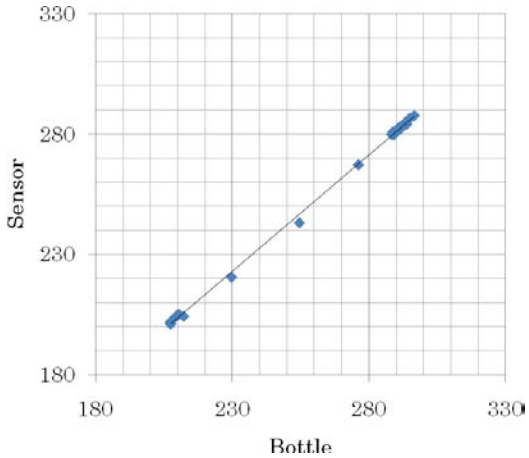

Fig. 2.3-3. Correlation of dissolved oxygen between sensor data and bottle data.

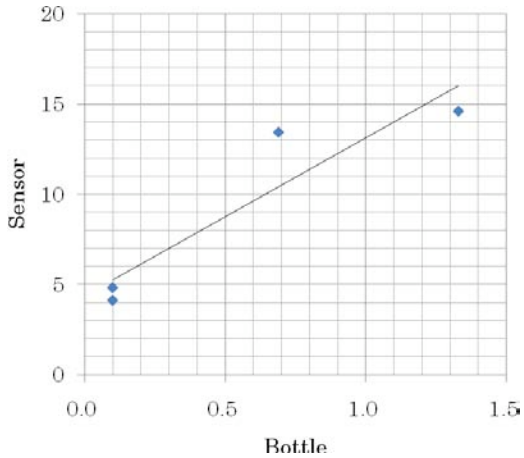

Fig. 2.3-4. Correlation of fluorescence between sensor data and bottle data.

2.4 Dissolved oxygen

Masahide WAKITA (JAMSTEC): Principal Investigator
Hironori SATO (Marine Works Japan Co. Ltd): Operation Leader

(1) Objectives

Determination of dissolved oxygen in seawater by Winkler titration.

(2) Parameter

Dissolved Oxygen

(3) Instruments and Methods

Following procedure is based on an analytical method, entitled by "Determination of dissolved oxygen in sea water by Winkler titration", in the WHP Operations and Methods (Dickson, 1996).

a. Instruments

Burette for sodium thiosulfate and potassium iodate;

APB-510 manufactured by Kyoto Electronic Co. Ltd. / 10 cm^3 of titration vessel

Detector;

Automatic photometric titrator (DOT-01) manufactured by Kimoto Electronic Co. Ltd.

Software;

DOT controller Ver.2.2.1

b. Reagents

Pickling Reagent I: Manganese chloride solution (3 mol dm^{-3})
Pickling Reagent II: Sodium hydroxide (8 mol dm^{-3}) / sodium iodide solution (4 mol dm^{-3})
Sulfuric acid solution (5 mol dm^{-3})
Sodium thiosulfate (0.025 mol dm^{-3})
Potassium iodide (0.001667 mol dm^{-3})
CSK standard of potassium iodide:
Lot TSK3592, Wako Pure Chemical Industries Ltd., 0.0100N

c. Sampling

Seawater samples were collected with Niskin bottle attached to the CTD-system and surface bucket sampler. Seawater for oxygen measurement was transferred from sampler to a volume calibrated flask (ca. 100 cm^3). Three times volume of the flask of seawater was overflowed. Temperature was measured by digital thermometer during the overflowing. Then two reagent solutions (Reagent I and II) of 0.5 cm^3 each were added immediately into the sample flask and the stopper was inserted carefully into the flask. The sample flask was then shaken vigorously to mix the contents and to disperse the precipitate finely throughout. After the precipitate has settled at least halfway down the flask, the flask was shaken again vigorously to disperse the precipitate. The sample flasks containing pickled samples were stored in a laboratory until they were titrated.

d. Sample measurement

At least two hours after the re-shaking, the pickled samples were measured on board. 1 cm^3 sulfuric acid solution and a magnetic stirrer bar were added into the sample flask and stirring began. Samples were titrated by sodium thiosulfate solution whose morality was determined by potassium iodate solution. Temperature of sodium thiosulfate during titration was recorded by a digital thermometer. During this cruise, we measured dissolved oxygen concentration using 2 sets of the titration apparatus. Dissolved oxygen concentration ($\mu mol\ kg^{-1}$) was calculated by sample temperature during seawater sampling, salinity of the CTD sensor, flask volume, and titrated volume of sodium thiosulfate solution without the blank. When we measured low concentration samples, titration procedure was adjusted manually.

e. Standardization and determination of the blank

Concentration of sodium thiosulfate titrant was determined by potassium iodate solution. Pure potassium iodate was dried in an oven at 130 ^oC. 1.7835 g potassium iodate weighed out accurately was dissolved in deionized water and diluted to final volume of 5 dm^3 in a calibrated volumetric flask (0.001667 mol dm^{-3}). 10 cm^3 of the standard potassium iodate solution was added to a flask using a volume-calibrated dispenser. Then 90 cm^3 of deionized water, 1 cm^3 of sulfuric acid solution, and 0.5 cm^3 of pickling reagent solution II and I were added into the flask in order. Amount of titrated volume of sodium thiosulfate (usually 5 times measurements average) gave the morality of sodium thiosulfate titrant.

The oxygen in the pickling reagents I (0.5 cm^3) and II (0.5 cm^3) was assumed to be 3.8 x 10^{-8} mol (Murray *et al.*, 1968). The blank due to other than oxygen was determined as follows. 1 and 2 cm^3 of the standard potassium iodate solution were added to two flasks respectively using a calibrated dispenser. Then 100 cm^3 of deionized water, 1 cm^3 of sulfuric acid solution, and 0.5 cm^3 of pickling reagent solution II and I each were added into the flask in order. The blank was determined by difference between the first (1 cm^3 of KIO_3) titrated volume of the sodium thiosulfate and the second (2 cm^3 of KIO_3) one. The results of 3 times blank determinations were averaged.

Table 2.4.-1 shows results of the standardization and the blank determination during this cruise.

Table 2.4-1 Results of the standardization and the blank determinations during this cruise.

Date	KIO_3 ID	$Na_2S_2O_3$	DOT-01(No.1)		DOT-01(No.2)		Stations
			E.P.	Blank	E.P.	Blank	
2010/10/18	20091216-06-10	20100702-1	3.932	-0.002	3.933	-0.004	Stn.001, 002
2010/10/21	20091216-06-11	20100702-1	3.935	0.001	3.936	-0.002	Stn.004
2010/10/23	20100630-01-02	20100702-1	3.941	0.000	3.939	-0.001	Stn.005, K2cast1, 3
2010/10/28	20100630-01-03	20100702-1	3.941	0.001	3.939	0.000	Stn.K2cast9
2010/11/1	20100630-01-04	20100702-1	3.943	0.001	3.942	0.000	Stn.KNT, 008, 009
2010/11/6	20100630-01-05	20100702-1	3.941	0.002	3.940	-0.002	Stn.010, S1cast1, 2, 4, 10
2010/11/12	20100630-01-06	20100702-1	3.943	0.003	3.938	-0.002	
2010/11/12	CSK	20100702-1	3.941	0.003	3.937	-0.002	

f. Repeatability of sample measurement

Replicate samples were taken at every CTD casts. Total amount of the replicate sample pairs of good measurement was 37 The standard deviation of the replicate measurement was 0.20 $\mu mol\ kg^{-1}$ that was calculated by a procedure in Guide to best practices for ocean CO_2 measurements Chapter4 SOP23 Ver.3.0 (2007). Results of replicate samples were shown in

Table 2.4-2 and this diagram shown in Fig. 2.4-1 and -2.

Table 2.4-2 Results of the replicate sample measurements

Layer	Number of replicate sample pairs	Oxygen concentration (μmol kg^{-1}) Standard Deviation.
1000m>=	28	0.22
>1000m	9	0.11
All	37	0.20

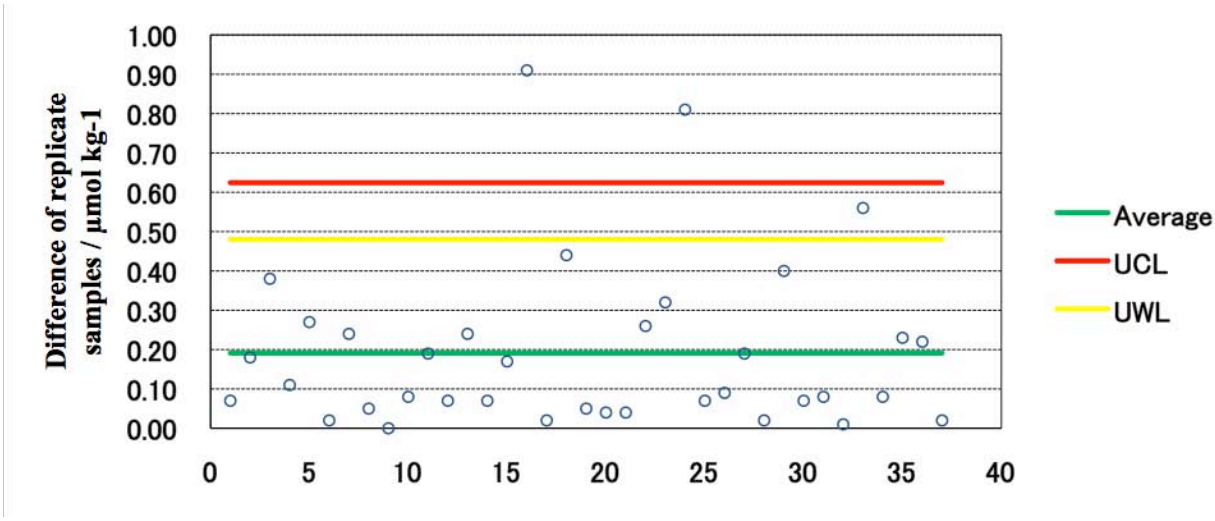

Fig. 2.4-1 Differences of replicate samples against sequence number

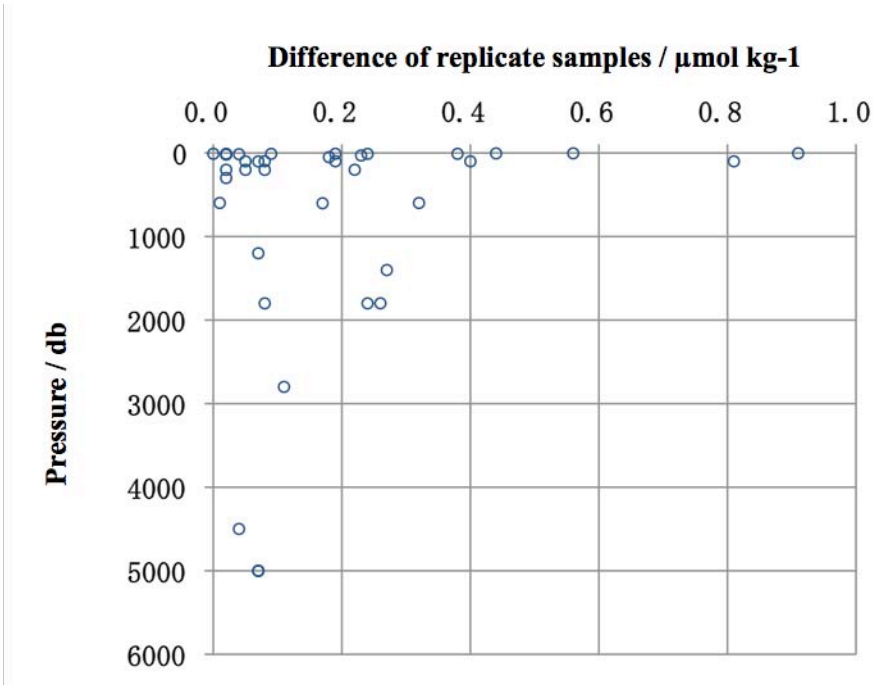

Fig. 2.4-2 Differences of replicate samples against pressure

(4) Data archive

All data will be submitted to Chief Scientist.

(5) References

Dickson, A.G., Determination of dissolved oxygen in sea water by Winkler titration. (1996)

Dickson, A.G., Sabine, C.L. and Christian, J.R. (Eds.), Guide to best practices for ocean CO2 measurements. (2007)

Culberson, C.H., WHP Operations and Methods July-1991 “Dissolved Oxygen”, (1991)

Japan Meteorological Agency, Oceanographic research guidelines（Part 1）. (1999)

KIMOTO electric CO. LTD., Automatic photometric titrator DOT-01 Instruction manual

2.5 Nutrients

Michio AOYAMA
(Meteorological Research Institute / Japan Meteorological Agency)
Junji MATSUSHITA (Department of Marine Science, Marine Works Japan Ltd.)
Ai TAKANO (Department of Marine Science, Marine Works Japan Ltd.)

(1) Objectives

The objectives of nutrients analyses during the R/V Mirai MR10-06 cruise in the North Pacific Ocean are as follows:

- Describe the present status of nutrients concentration with excellent comparability.
- Provide excellent nutrients data to biologist onboard MR10-06 to help their study.

(2) Parameters

The determinants are nitrate, nitrite, phosphate, silicate and ammonia in the North Pacific Ocean.

(3) Summary of nutrients analysis

We made 14 QuAAtro runs for the samples at 16 stations in MR10-06. The total amount of layers of the seawater sample reached up to 291 for MR10-06. We made duplicate measurement at all layers. The station locations for nutrients measurement is shown in Figure 2.5.1

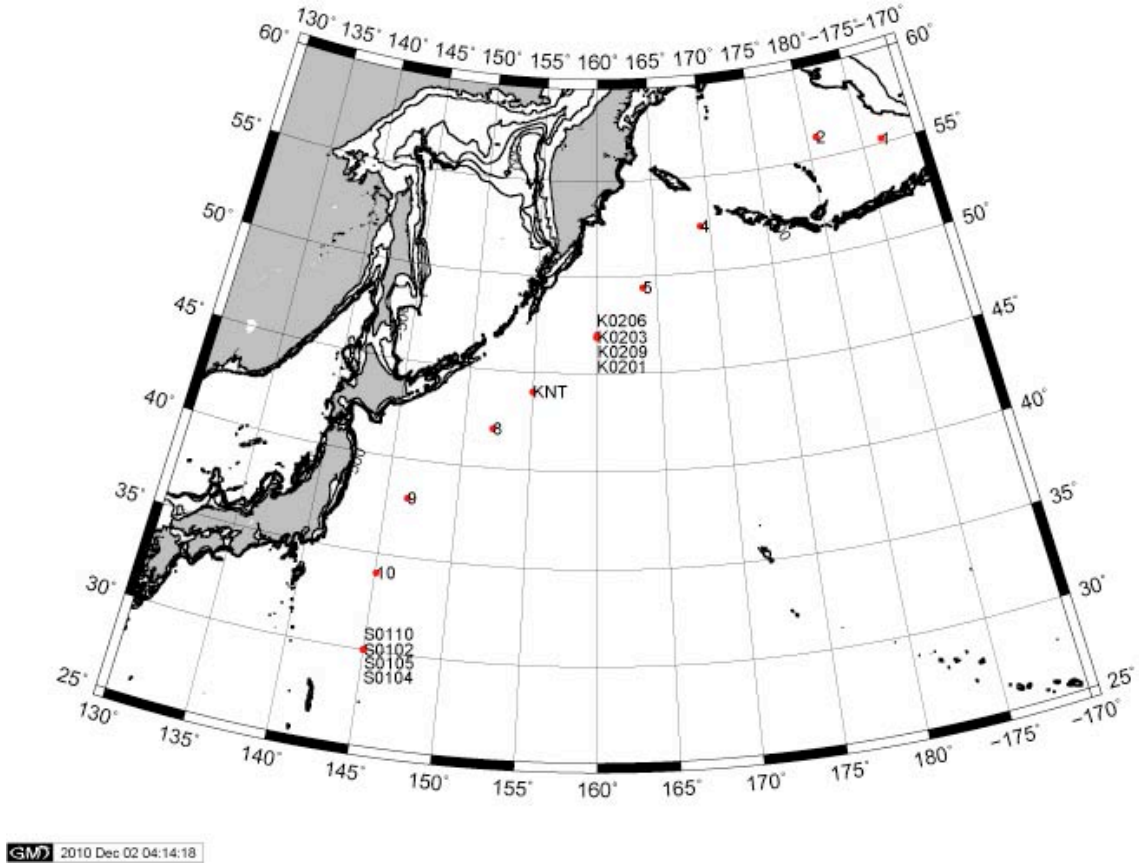

Figure 2.5.1 Sampling positions of nutrients sample.

(4) Instrument and Method

a. Analytical detail using QuAAtro system

The phosphate analysis is a modification of the procedure of Murphy and Riley (1962).

Molybdic acid is added to the seawater sample to form phosphomolybdic acid which is in turn reduced to phosphomolybdous acid using L-ascorbic acid as the reductant.

Nitrate + nitrite and nitrite are analyzed according to the modification method of Grasshoff (1970). The sample nitrate is reduced to nitrite in a cadmium tube inside of which is coated with metallic copper. The sample stream with its equivalent nitrite is treated with an acidic, sulfanilamide reagent and the nitrite forms nitrous acid which reacts with the sulfanilamide to produce a diazonium ion. N-1-Naphthylethylene-diamine added to the sample stream then couples with the diazonium ion to produce a red, azo dye. With reduction of the nitrate to nitrite, both nitrate and nitrite react and are measured; without reduction, only nitrite reacts. Thus, for the nitrite analysis, no reduction is performed and the alkaline buffer is not necessary. Nitrate is computed by difference.

The silicate method is analogous to that described for phosphate. The method used is essentially that of Grasshoff et al. (1983), wherein silicomolybdic acid is first formed from the silicate in the sample and added molybdic acid; then the silicomolybdic acid is reduced to silicomolybdous acid, or "molybdenum blue," using ascorbic acid as the reductant. The analytical methods of the nutrients, nitrate, nitrite, silicate and phosphate, during this cruise are same as the methods used in (Kawano et al. 2009).

The ammonia in seawater is mixed with an alkaline containing EDTA, ammonia as gas state is formed from seawater. The ammonia (gas) is absorbed in sulfuric acid by way of 0.5 μm pore size membrane filter (ADVANTEC PTFE) at the dialyzer attached to analytical system. The ammonia absorbed in sulfuric acid is determined by coupling with phenol and hypochlorite to form indophenols blue. Wavelength using ammonia analysis is 630 nm, which is absorbance of indophenols blue.

The flow diagrams and reagents for each parameter are shown in Figures 2.5.2 to 2.5.6.

b. Nitrate + Nitrite Reagents

Imidazole (buffer), 0.06 M (0.4 % w/v)

Dissolve 4 g imidazole, $C_3H_4N_2$, in ca. 1000 ml DIW; add 2 ml concentrated HCl. After mixing, 1 ml Triton®X-100 (50 % solution in ethanol) is added.

Sulfanilamide, 0.06 M (1 % w/v) in 1.2M HCl

Dissolve 10 g sulfanilamide, 4-$NH_2C_6H_4SO_3H$, in 900 ml of DIW, add 100 ml concentrated HCl. After mixing, 2 ml Triton®X-100 (50 % solution in ethanol) is added.

N-1-Napthylethylene-diamine dihydrochloride, 0.004 M (0.1 %f w/v)

Dissolve 1 g NED, $C_{10}H_7NHCH_2CH_2NH_2 \cdot 2HCl$, in 1000 ml of DIW and add 10 ml concentrated HCl. After mixing, 1 ml Triton®X-100 (50 % solution in ethanol) is added. This reagent is stored in a dark bottle.

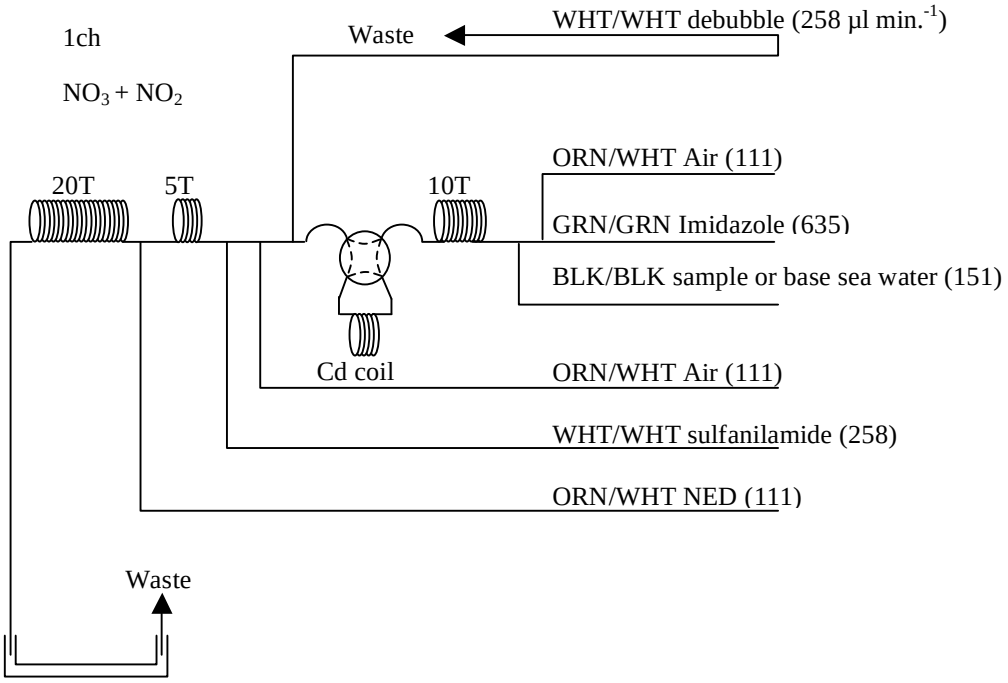

1.0 mm I.D. × 10.0 mm

550 nm

Figure 2.5.2 NO_3+NO_2 (1ch.) Flow diagram.

c. Nitrite Reagents

Sulfanilamide, 0.06 M (1 % w/v) in 1.2 M HCl

Dissolve 10g sulfanilamide, 4-$NH_2C_6H_4SO_3H$, in 900 ml of DIW, add 100 ml concentrated HCl. After mixing, 2 ml Triton®X-100 (50 % solution in ethanol) is added.

N-1-Napthylethylene-diamine dihydrochloride, 0.004 M (0.1 % w/v)

Dissolve 1 g NED, $C_{10}H_7NHCH_2CH_2NH_2 \cdot 2HCl$, in 1000 ml of DIW and add 10 ml concentrated HCl. After mixing, 1 ml Triton®X-100 (50 % solution in ethanol) is added. This reagent is stored in a dark bottle.

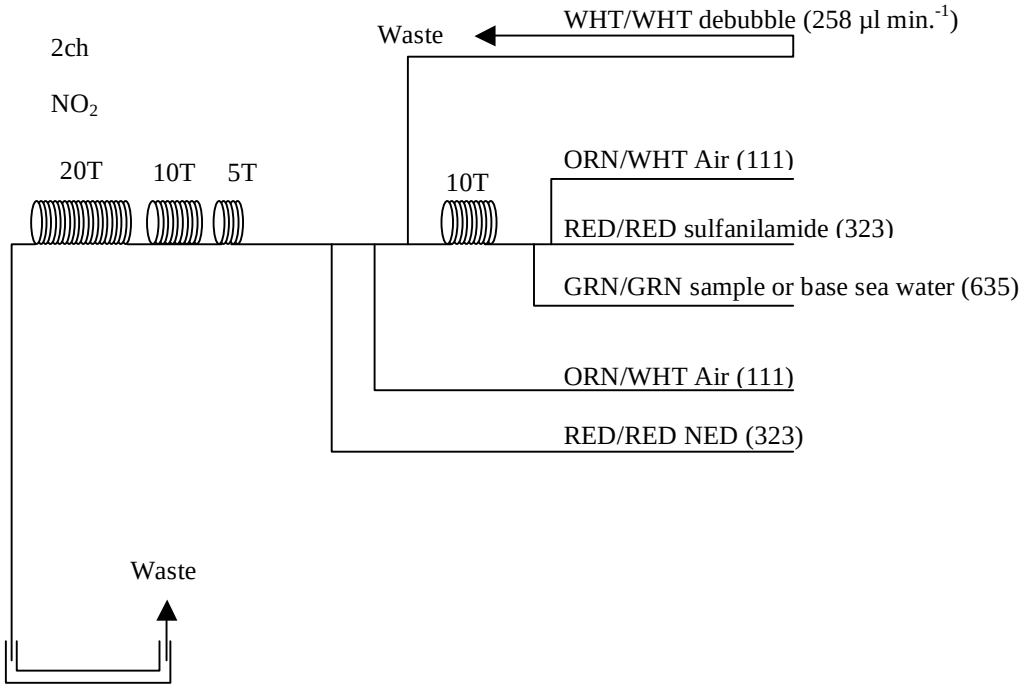

1.0 mm I.D. × 10.0 mm or 30.0 mm

550 nm

Figure 2.5.3 NO_2 (2ch.) Flow diagram.

d. Silicate Reagents

Molybdic acid, 0.06 M (2 % w/v)

Dissolve 15 g disodium molybdate(VI) dihydrate, $Na_2M_oO_4 \cdot 2H_2O$, in 980 ml DIW, add 8 ml concentrated H_2SO_4. After mixing, 20 ml sodium dodecyl sulphate (15 % solution in water) is added.

Oxalic acid, 0.6 M (5 % w/v)

Dissolve 50 g oxalic acid anhydrous, HOOC: COOH, in 950 ml of DIW.

Ascorbic acid, 0.01M (3 % w/v)

Dissolve 2.5g L (+)-ascorbic acid, $C_6H_8O_6$, in 100 ml of DIW. Stored in a dark bottle and freshly prepared before every measurement.

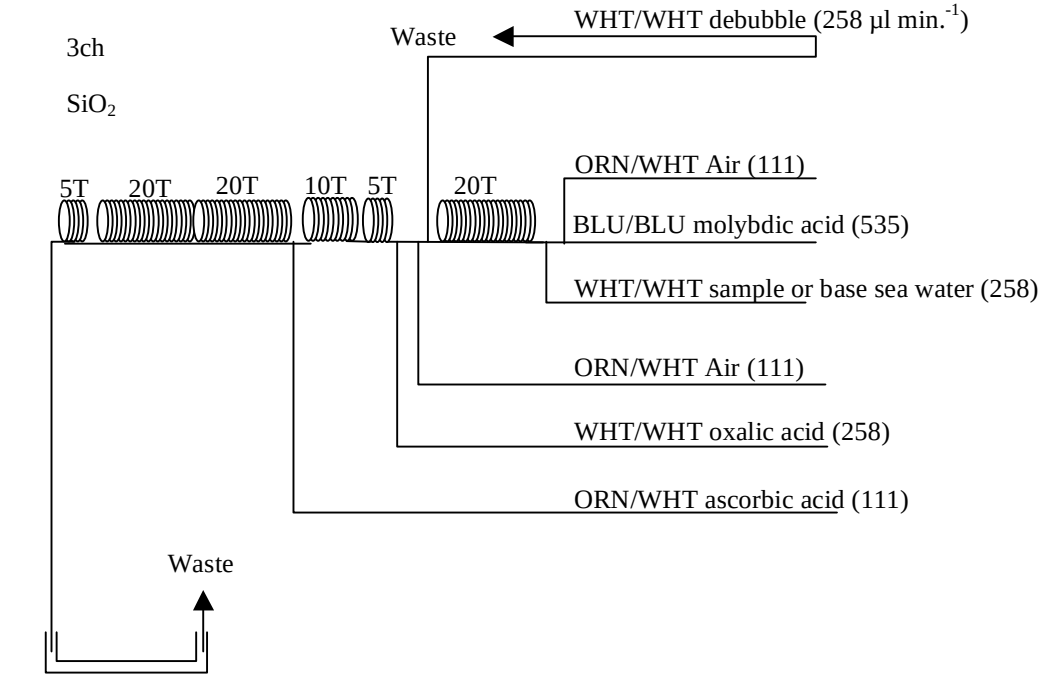

Figure 2.5.4 SiO_2 (3ch.) Flow diagram.

e. Phosphate Reagents

Stock molybdate solution, 0.03M (0.8 % w/v)

Dissolve 8 g disodium molybdate(VI) dihydrate, $Na_2M_oO_4 \cdot 2H_2O$, and 0.17 g antimony potassium tartrate, $C_8H_4K_2O_{12}Sb_2 \cdot 3H_2O$, in 950 ml of DIW and add 50 ml concentrated H_2SO_4.

Mixed Reagent

Dissolve 0.8 g L (+)-ascorbic acid, $C_6H_8O_6$, in 100 ml of stock molybdate solution. After mixing, 2 ml sodium dodecyl sulphate (15 % solution in water) is added. Stored in a dark bottle and freshly prepared before every measurement.

Reagent for sample dilution

Dissolve sodium chloride, NaCl, 10 g in ca. 950 ml of DIW, add 50 ml acetone and 4 ml concentrated H_2SO_4. After mixing, 5 ml sodium dodecyl sulphate (15 % solution in water) is added.

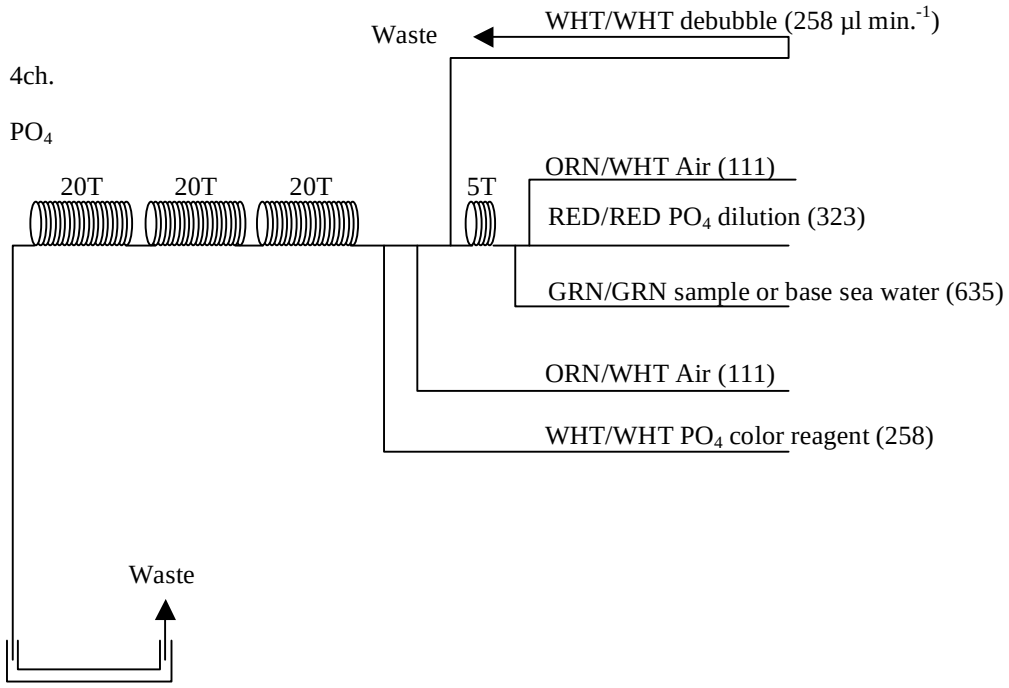

1.0 mm I.D. × 10.0 mm or 30.0 mm

880 nm

Figure 2.5.5 PO_4 (4ch.) Flow diagram.

f. Ammonia Reagents

EDTA

Dissolve 25 g EDTA (ethylenediaminetetraacetatic acid tetrasodium salt), $C_{10}H_{12}N_2O_8Na_4 \cdot 4H_2O$, and 2 g boric acid, H_3BO_3, in 200 ml of DIW. After mixing, 1 ml Triton®X-100 (30 % solution in DIW) is added. This reagent is prepared at a week about.

NaOH

Dissolve 5 g sodium hydroxide, NaOH, and 16 g EDTA in 100 ml of DIW. This reagent is prepared at a week about.

Stock Nitroprusside

Dissolved 0.25 g sodium pentacyanonitrosylferrate(II), $Na_2[Fe(CN)_5NO]$, in 100 ml of DIW and add 0.2 ml 1N H_2SO_4. Stored in a dark bottle and prepared at a month about.

Nitroprusside solution

Mixed 4 ml stock nitroprusside and 5 ml 1N H_2SO_4 in 500 ml of DIW. After mixing, 1 ml Triton®X-100 (30 % solution in DIW) is added. This reagent is stored in a dark bottle and prepared at every 2 or 3 days.

Alkaline phenol

Dissolved 10 g phenol, C_6H_5OH, 5 g sodium hydroxide and citric acid, $C_6H_8O_7$, in 200 ml DIW. Stored in a dark bottle and prepared at a week about.

NaClO solution

Mixed 3 ml sodium hypochlorite solution, NaClO, in 47 ml DIW. Stored in a dark bottle and fleshly prepared before every measurement. This reagent is prepared 0.3% available chlorine.

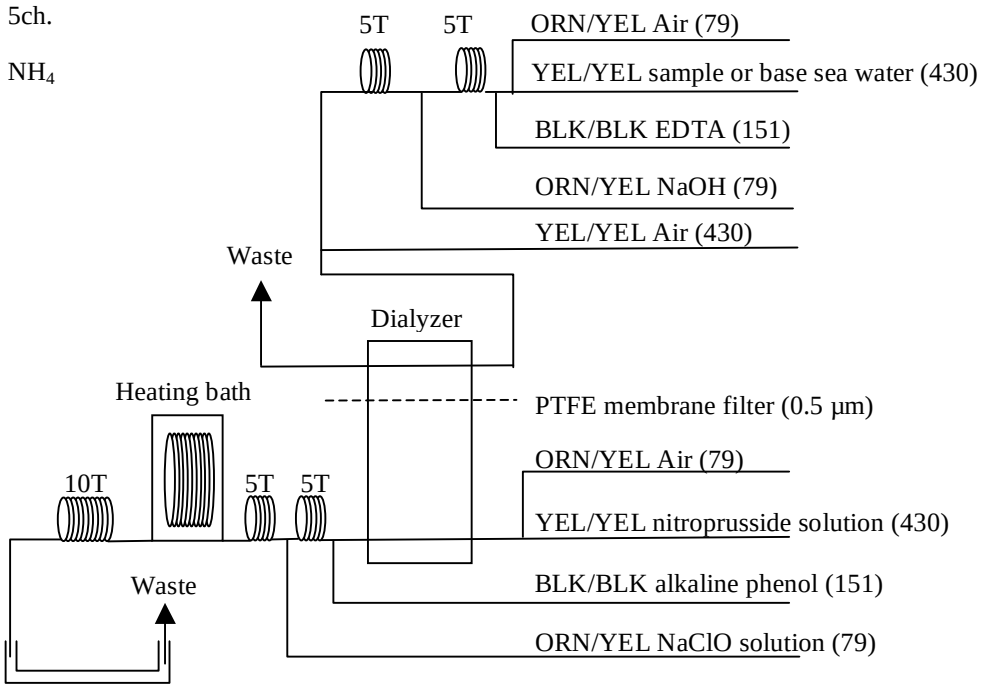

Figure 2.5.6 NH_4 (5ch.) Flow diagram.

g. Sampling procedures

Sampling of nutrients followed that oxygen, salinity and trace gases. Samples were drawn into two of virgin 10 ml polyacrylates vials without sample drawing tubes. These were rinsed three times before filling and vials were capped immediately after the drawing. The vials are put into water bath adjusted to ambient temperature, 25 ± 1 deg. C, in about 30 minutes before use to stabilize the temperature of samples in MR10-06.

No transfer was made and the vials were set an auto sampler tray directly. Samples were analyzed after collection basically within 24 hours in MR10-06.

h. Data processing

Raw data from QuAAtro were treated as follows:

- Check baseline shift.
- Check the shape of each peak and positions of peak values taken, and then change the positions of peak values taken if necessary.
- Carry-over correction and baseline drift correction were applied to peak heights of each samples followed by sensitivity correction.
- Baseline correction and sensitivity correction were done basically using liner regression.
- Load pressure and salinity from CTD data to calculate density of seawater.
- Calibration curves to get nutrients concentration were assumed second order equations.

(5) Nutrients standards

a. Volumetric laboratory ware of in-house standards

All volumetric glass ware and polymethylpentene (PMP) ware used were gravimetrically calibrated. Plastic volumetric flasks were gravimetrically calibrated at the temperature of use within 0 to 4 K.

Volumetric flasks

Volumetric flasks of Class quality (Class A) are used because their nominal tolerances are 0.05 % or less over the size ranges likely to be used in this work. Class A flasks are made of borosilicate glass, and the standard solutions were transferred to plastic bottles as quickly as possible after they are made up to volume and well mixed in order to prevent excessive dissolution of silicate from the glass. PMP volumetric flasks were gravimetrically calibrated and used only within 0 to 4 K of the calibration temperature.

The computation of volume contained by glass flasks at various temperatures other than the calibration temperatures were done by using the coefficient of linear expansion of borosilicate crown glass.

Because of their larger temperature coefficients of cubical expansion and lack of tables constructed for these materials, the plastic volumetric flasks were gravimetrically calibrated over the temperature range of intended use and used at the temperature of calibration within 0 to 4 K. The weights obtained in the calibration weightings were corrected for the density of water and air buoyancy.

Pipettes and pipettors

All pipettes have nominal calibration tolerances of 0.1 % or better. These were gravimetrically calibrated in order to verify and improve upon this nominal tolerance.

b. Reagents, general considerations

Specifications

For nitrate standard, “potassium nitrate 99.995 suprapur®” provided by Merck, CAS No.: 7757-91-1, was used.

For phosphate standard, “potassium dihydrogen phosphate anhydrous 99.995 suprapur®” provided by Merck, CAS No.: 7778-77-0, was used.

For nitrite standard, “sodium nitrate” provided by Wako, CAS No.: 7632-00-0, was used. And assay of nitrite was determined according JIS K8019 and assays of nitrite salts were 98.04 %. We use that value to adjust the weights taken.

For the silicate standard, we use “Silicon standard solution SiO_2 in NaOH 0.5 mol/l CertiPUR®” provided by Merck, CAS No.: 1310-73-2, of which lot number is HC814662 and HC074650 are used. The silicate concentration is certified by NIST-SRM3150 with the uncertainty of 0.5 %. Factor of HC074650 is signed 1.000, however we reassigned the factor as 0.975 from the result of comparison among HC814662, HC074650 and RMNS.

For ammonia standard, “ammonia sulfate” provided by Wako, CAS No.: 7783-20-2, was used.

Ultra pure water

Ultra pure water (Milli-Q) freshly drawn was used for preparation of reagent, standard solutions and for measurement of reagent and system blanks.

Low-nutrients seawater (LNSW)

Surface water having low nutrient concentration was taken and filtered using 0.45 μm pore size membrane filter. This water is stored in 20 liter cubitainer with paper box. The concentrations of nutrient of this water were measured carefully in Jul 2008.

c. Concentrations of nutrients for A, B and C standards

Concentrations of nutrients for A, B and C standards are set as shown in Table 2.5.1. The C standard is prepared according recipes as shown in Table 2.5.2. All volumetric laboratory tools were calibrated prior the cruise as stated in chapter (5). Then the actual concentration of nutrients in each fresh standard was calculated based on the ambient, solution temperature and determined factors of volumetric laboratory wares.

The calibration curves for each run were obtained using 4 levels, C-1, C-2, C-3 and C-4.

Table 2.5.1 Nominal concentrations of nutrients for A, B and C standards.

	A	B	C-1	C-2	C-3	C-4	C-5
NO_3 (μM)	22000	900	0.03	9	28	46	55
NO_2 (μM)	4000	20	0.00	0.2	0.6	1	1.2
SiO_2 (μM)	36000	2800	0.80	28	80	140	170
PO_4 (μM)	3000	60	0.03	0.6	1.8	3	3.6
NH_4 (μM)	4000	200	0.00	0.0	2	4	6

Table 2.5.2 Working calibration standard recipes.

C Std.	B-1 Std.	B-2 Std.	B-3 Std.	DIW
C-1	0 ml	0 ml	0 ml	75 ml
C-2	5 ml	5 ml	0 ml	65 ml
C-3	15 ml	15 ml	5 ml	40 ml
C-4	25 ml	25 ml	10 ml	15 ml
C-5	30 ml	30 ml	15 ml	0 ml

B-1 Std.: Mixture of nitrate, silicate and phosphate

B-2 Std.: Nitrite

B-3 Std.: Ammonia

d. Renewal of in-house standard solutions

In-house standard solutions as stated in paragraph c were renewed as shown in Table 2.5.3(a) to (c).

Table 2.5.3(a) Timing of renewal of in-house standards.

NO_3, NO_2, SiO_2, PO_4, NH_4	Renewal
A-1 Std. (NO_3)	maximum 1 month
A-2 Std. (NO_2)	maximum 1 month
A-3 Std. (SiO_2)	commercial prepared solution
A-4 Std. (PO_4)	maximum 1 month
A-5 Std. (NH_4)	maximum 1 month
B-1 Std. (mixture of NO_3, SiO_2, PO_4)	8 days
B-2 Std. (NO_2)	8 days
B-3 Std. (NH_4)	8 days

Table 2.5.3(b) Timing of renewal of working calibration standards.

C Std.	Renewal
C Std. (mixture of B-1 , B-2 and B-3 Std.)	24 hours

Table 2.5.3(c) Timing of renewal of in-house standards for reduction estimation.

Reduction estimation	Renewal

D-1 Std. (3600 μM NO_3)	8 days
43 μM NO_3	when C Std. renewed
47 μM NO_2	when C Std. renewed

(6) Reference material of nutrients in seawater

To get the more accurate and high quality nutrients data to achieve the objectives stated above, huge numbers of the bottles of the reference material of nutrients in seawater (hereafter RMNS) are prepared (Aoyama et al., 2006, 2007, 2008, 2009). In the previous worldwide expeditions, such as WOCE cruises, the higher reproducibility and precision of nutrients measurements were required (Joyce and Corry, 1994). Since no standards were available for the measurement of nutrients in seawater at that time, the requirements were described in term of reproducibility. The required reproducibility was 1 %, 1 to 2 %, 1 to 3 % for nitrate, phosphate and silicate, respectively. Although nutrient data from the WOCE one-time survey was of unprecedented quality and coverage due to much care in sampling and measurements, the differences of nutrients concentration at crossover points are still found among the expeditions (Aoyama and Joyce, 1996, Mordy et al., 2000, Gouretski and Jancke, 2001). For instance, the mean offset of nitrate concentration at deep waters was 0.5 μmol kg^{-1} for 345 crossovers at world oceans, though the maximum was 1.7 μmol kg^{-1} (Gouretski and Jancke, 2001). At the 31 crossover points in the Pacific WHP one-time lines, the WOCE standard of reproducibility for nitrate of 1 % was fulfilled at about half of the crossover points and the maximum difference was 7 % at deeper layers below 1.6 deg. C in potential temperature (Aoyama and Joyce, 1996).

a. RMNS for this cruise

RMNS lots BA, AY, AX, BD, BE, BF and BG, which cover full range of nutrients concentrations in the North Pacific Ocean are prepared. These RMNS assignment were completely done based on random number. The RMNS bottles were stored at a room in the ship, REAGENT STORE, where the temperature was maintained around 20 deg. C.

b. Assigned concentration for RMNSs

We assigned nutrients concentrations for RMNS lots BA, AY, AX, BD, BE, BF and BG as shown in Table 2.5.4.

Table 2.5.4 Assigned concentration of RMNSs.

unit: μmol kg^{-1}

	Nitrate	Phosphate	Silicate	Nitrite	Ammonia
BA	0.07	0.061	1.61	0.02	0.97
AY	5.61	0.516	29.40	0.63	0.81
AX	21.44	1.614	58.05	0.35	0.69
BD	29.74	2.176	64.43	0.03	2.45
BE	36.70	2.662	99.20	0.03	-
BF	41.39	2.809	150.61	0.02	-
BG	36.85	2.570	254.42	0.06	-

(7) Quality control

a. Precision of nutrients analyses during the cruise

Precision of nutrients analyses during the cruise was evaluated based on the 5 to 7 measurements, which are measured every 5 to 13 samples, during a run at the concentration of C-4 std. Summary of precisions are shown as shown in Table 2.5.5. Analytical precisions previously evaluated were 0.08 % for nitrate, 0.10 % for phosphate and 0.07 % for silicate in CLIVAR P21 revisited cruise of MR09-01 cruise in 2009, respectively. During this cruise, analytical precisions were 0.07% for nitrate, 0.07 % for phosphate, 0.11 % for silicate and 0.24 % for ammonia in terms of median of precision, respectively. Then we can conclude that the analytical precisions for nitrate, phosphate and silicate were maintained throughout this cruise.

Table 2.5.5 Summary of precision based on the replicate analyses.

	Nitrate	Nitrite	Phosphate	Silicate	Ammonia
	CV %	CV %	CV %	CV %	CV%
Median	0.07	0.11	0.07	0.11	0.24
Mean	0.08	0.14	0.08	0.12	0.23
Maximum	0.18	0.35	0.17	0.23	0.28
Minimum	0.03	0.04	0.03	0.05	0.13
N	16	16	16	16	6

b. Carry over

We can also summarize the magnitudes of carry over throughout the cruise. These are small enough within acceptable levels as shown in Table 2.5.6.

Table 2.5.6 Summary of carry over throughout MR10-06.

	Nitrate	Nitrite	Phosphate	Silicate	Ammonia
	%	%	%	%	%
Median	0.11	0.00	0.09	0.15	0.31
Mean	0.09	0.03	0.10	0.17	0.39
Maximum	0.19	0.18	0.20	0.38	0.92
Minimum	0.01	0.00	0.01	0.06	0.16
N	16	16	16	16	6

(8) Problems/improvements occurred and solutions.

a. Deterioration of pump tubes of QuAAtro

We used pump tubes of QuAAtro, standard pump tube by BL TEC. The pump tube, especially sample line, was deteriorated at 40 to 80 hours. Therefore, we need to examine a material of the pump tube.

b. Precipitation at ammonia line

There was a precipitation at the point of mixed seawater sample, EDTA and NaOH in ammonia line. We need to examine the quantity of EDTA.

c. Noises accompanying the ship's rolling at the rough weather

When the rough weather, noises were detected in all parameter chart. We attached a damper for removed vibration under the QuAAtro. However, we could not remove noises completely.

(9) Station list

Table 2.5.7 List of stations

Cruise	Station	Cast	Year	Month	Date	Latitude		Longitude	
MR1006	001	01	2010	10	20	55.238	N	186.774	E
MR1006	002	01	2010	10	22	56.141	N	180.875	E
MR1006	004	01	2010	10	23	52.400	N	169.159	E
MR1006	005	01	2010	10	25	49.395	N	163.839	E
MR1006	K02	01	2010	10	25	46.989	N	159.975	E
MR1006	K02	03	2010	10	26	46.887	N	160.001	E

MR1006	K02	06	2010	10	26	46.863	N	159.935	E
MR1006	K02	09	2010	10	28	46.863	N	159.990	E
MR1006	KNT	01	2010	11	3	44.001	N	155.006	E
MR1006	008	01	2010	11	3	41.999	N	152.119	E
MR1006	009	01	2010	11	5	37.998	N	146.490	E
MR1006	010	01	2010	11	6	34.000	N	145.082	E
MR1006	S01	02	2010	11	7	30.000	N	145.001	E
MR1006	S01	04	2010	11	8	30.003	N	144.997	E
MR1006	S01	05	2010	11	8	30.012	N	145.045	E
MR1006	S01	10	2010	11	9	30.001	N	145.002	E

(10) Data archive

All data will be submitted to JAMSTEC Data Integration and Analyses Group (DIAG) and is currently under its control.

References

Aminot, A. and Kerouel, R. 1991. Autoclaved seawater as a reference material for the determination of nitrate and phosphate in seawater. Anal. Chim. Acta, 248: 277-283.

Aminot, A. and Kirkwood, D.S. 1995. Report on the results of the fifth ICES intercomparison exercise for nutrients in sea water, ICES coop. Res. Rep. Ser., 213.

Aminot, A. and Kerouel, R. 1995. Reference material for nutrients in seawater: stability of nitrate, nitrite, ammonia and phosphate in autoclaved samples. Mar. Chem., 49: 221-232.

Aoyama M., and Joyce T.M. 1996, WHP property comparisons from crossing lines in North Pacific. In Abstracts, 1996 WOCE Pacific Workshop, Newport Beach, California.

Aoyama, M., 2006: 2003 Intercomparison Exercise for Reference Material for Nutrients in Seawater in a Seawater Matrix, Technical Reports of the Meteorological Research Institute No.50, 91pp, Tsukuba, Japan.

Aoyama, M., Susan B., Minhan, D., Hideshi, D., Louis, I. G., Kasai, H., Roger, K., Nurit, K., Doug, M., Murata, A., Nagai, N., Ogawa, H., Ota, H., Saito, H., Saito, K., Shimizu, T., Takano, H., Tsuda, A., Yokouchi, K., and Agnes, Y. 2007. Recent Comparability of Oceanographic Nutrients Data: Results of a 2003 Intercomparison Exercise Using Reference Materials. Analytical Sciences, 23: 1151-1154.

Aoyama M., J. Barwell-Clarke, S. Becker, M. Blum, Braga E. S., S. C. Coverly,E. Czobik, I. Dahllof, M. H. Dai, G. O. Donnell, C. Engelke, G. C. Gong, Gi-Hoon Hong, D. J. Hydes, M. M. Jin, H. Kasai, R. Kerouel, Y. Kiyomono, M. Knockaert, N. Kress, K. A. Krogslund, M. Kumagai, S. Leterme, Yarong Li, S. Masuda, T. Miyao, T. Moutin, A. Murata, N. Nagai, G.Nausch, M. K. Ngirchechol, A. Nybakk, H. Ogawa, J. van Ooijen, H. Ota, J. M. Pan, C. Payne, O. Pierre-Duplessix, M. Pujo-Pay, T. Raabe, K. Saito, K. Sato, C. Schmidt, M. Schuett, T. M. Shammon, J. Sun, T. Tanhua, L. White, E.M.S. Woodward, P. Worsfold, P. Yeats, T. Yoshimura, A.Youenou, J. Z. Zhang, 2008: 2006 Intercomparison Exercise for Reference Material for Nutrients in Seawater in a Seawater Matrix, Technical Reports of the

Meteorological Research Institute No. 58, 104pp.
Gouretski, V.V. and Jancke, K. 2001. Systematic errors as the cause for an apparent deep water property variability: global analysis of the WOCE and historical hydrographic data・REVIEW ARTICLE, Progress In Oceanography, 48: Issue 4, 337-402.
Grasshoff, K., Ehrhardt, M., Kremling K. et al. 1983. Methods of seawater anylysis. 2nd rev. Weinheim: Verlag Chemie, Germany, West.
Joyce, T. and Corry, C. 1994. Requirements for WOCE hydrographic programmed data reporting. WHPO Publication, 90-1, Revision 2, WOCE Report No. 67/91.
Kawano, T., Uchida, H. and Doi, T. WHP P01, P14 REVISIT DATA BOOK, (Ryoin Co., Ltd., Yokohama, 2009).
Kirkwood, D.S. 1992. Stability of solutions of nutrient salts during storage. Mar. Chem., 38 : 151-164.
Kirkwood, D.S. Aminot, A. and Perttila, M. 1991. Report on the results of the ICES fourth intercomparison exercise for nutrients in sea water. ICES coop. Res. Rep. Ser., 174.
Mordy, C.W., Aoyama, M., Gordon, L.I., Johnson, G.C., Key, R.M., Ross, A.A., Jennings, J.C. and Wilson. J. 2000. Deep water comparison studies of the Pacific WOCE nutrient data set. Eos Trans-American Geophysical Union. 80 (supplement), OS43.
Murphy, J., and Riley, J.P. 1962. Analytica chim. Acta 27, 31-36.
Uchida, H. & Fukasawa, M. WHP P6, A10, I3/I4 REVISIT DATA BOOK Blue Earth Global Expedition 2003 1, 2, (Aiwa Printing Co., Ltd., Tokyo, 2005).

2.6 pH measurement

Masahide WAKITA (JAMSTEC MIO): Principal Investigator
Minoru KAMATA (MWJ)

(1) Objective

Since the global warming is becoming an issue world-widely, studies on the greenhouse gases such as CO_2 are drawing high attention. The ocean plays an important role in buffering the increase of atmospheric CO_2, and studies on the exchange of CO_2 between the atmosphere and the sea becomes highly important. Oceanic biosphere, especially primary production, has an important role concerned to oceanic CO_2 cycle through its photosynthesis and respiration. However, the diverseness and variability of the biological system make difficult to reveal their mechanism and quantitative understanding of CO_2 cycle. Dissolved CO_2 in water alters its appearance into several species, but the concentrations of the individual species of CO_2 system in solution cannot be measured directly. However, two of the four measurable parameters (alkalinity, total dissolved inorganic carbon, pH and pCO_2) can estimate each concentration of CO_2 system (Dickson et al., 2007). Seawater acidification associated with CO_2 uptake into the ocean possibly changes oceanic ecosystem and CO_2 garners in Ocean recently. We here report on board measurements of pH during MR10-06 cruise.

(2) Method

(2)-1 Seawater sampling

Seawater samples were collected with CTD system mounted 12 liter Niskin bottles and a bucket at 4 stations. Seawater was sampled in a 100 ml glass bottle that was previously soaked in 5 % non-phosphoric acid detergent (pH13) solution at least 3 hours and was cleaned by fresh water for 5 times and Milli-Q ultrapure water for 3 times. A sampling silicone rubber tube with PFA tip was connected to the Niskin bottle when the sampling was carried out. The glass bottles were filled from the bottom smoothly, without rinsing, and were overflowed for 2 times bottle volume (about 10 seconds) with care not to leave any bubbles in the bottle. The water in the bottle was sealed by a glass made cap gravimetrically fitted to the bottle mouth without additional force. After collecting the samples on the deck, the bottles were carried into the lab and put in the water bath kept about 25 deg C before the measurement.

(2)-2 Seawater analyses

pH (-log[H+]) of the seawater was measured potentiometrically in the glass bottles. The pH / Ion meter (Radiometer PHM240) is used to measure the electromotive force (e.m.f.) between the glass electrode cell (Radiometer pHG201) and the reference electrode cell (Radiometer REF201) in the sample with its temperature controlled to 25 $\pm$ 0.05 deg C.

Ag, AgCl reference electrode | solution of KCl || test solution | H+ -glass electrode.

To calibrate the electrodes, the TRIS buffer (Lot=100715-1: pH=8.0906 pH units at 25 deg C, Delvalls and Dickson, 1998) and AMP buffer (Lot=100720-1: pH=6.7838 pH units at 25 deg C, DOE, 1994) in the synthetic seawater (Total hydrogen ion concentration scale) were applied. pH_T of seawater sample (pH_{spl}) is calculated from the expression:

$$pH_{spl} = pH_{TRIS} + (E_{TRIS} - E_{spl}) / ER$$

where electrode response ER is calculated as follows:

$$ER = (E_{AMP} - E_{TRIS}) / (pH_{TRIS} - pH_{AMP})$$

ER value should be equal to the ideal Nernst value as follows:

ER = RT LN(10) / F = 59.16 mV / pH units at 25 deg C

(3) Preliminary results

A replicate analysis of seawater sample was made at 50, 300, 1600, and 3500 dbar depth (deep cast) or 5% irradiance depth, and 125 m depth (shallow cast). The difference between each pair of analyses was plotted on a range control chart (see Figure 2.6-1). The average of the difference was 0.001 pH units (n = 23 pairs) with its standard deviation of 0.001 pH units. These values were lower than the value recommended by Guide (Dickson et al., 2007).

(4) Data Archive

All data will be submitted to JAMSTEC and is currently under its control.

(5) Reference

DOE (1994), Handbook of methods for the analysis of the various parameters of the carbon dioxide system in sea water; version 2, A. G. Dickson & C. Goyet, Eds., ORNS/CDIAC-74

DelValls, T. A. and Dickson, A. G., 1998. The pH of buffers based on 2-amino-2-hydroxymethyl-1,3-propanediol (‘tris’) in synthetic sea water. Deep-Sea Research I 45, 1541-1554.

Dickson, A. G., C. L. Sabine and J. R. Christian, Eds. (2007): Guide to best practices for ocean CO_2 measurements, PICES Special Publication 3, 199pp.

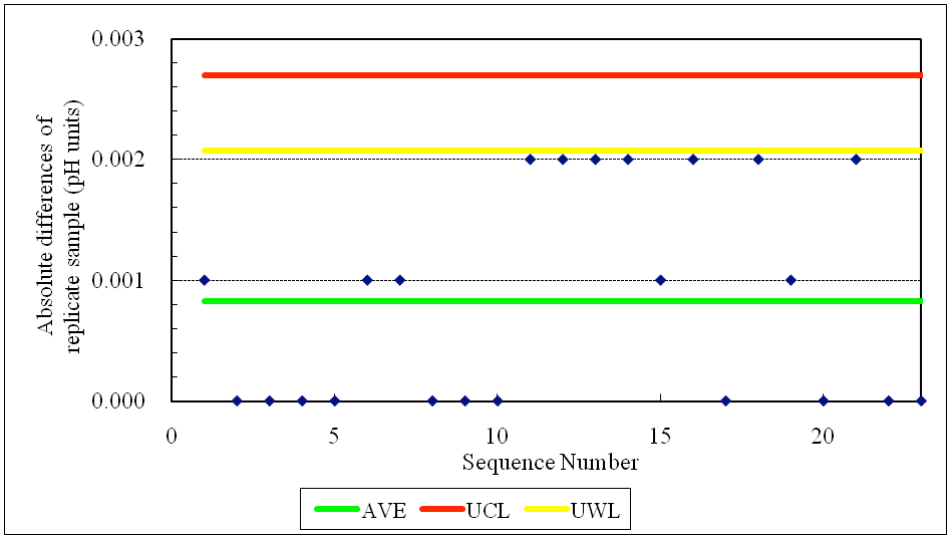

Figure 2.6-1 Range control chart of the absolute differences of replicate measurements of pH carried out during the cruise. AVE represents the average value, UCL upper control limit (UCL = AVE * 3.267), and UWL upper warning limit (UWL = AVE * 2.512) (Dickson et al., 2007).

2.7. Dissolved inorganic carbon-DIC

Masahide WAKITA (JAMSTEC MIO): Principal Investigator
Yoshiko ISHIKAWA (MWJ)
Hatsumi AOYAMA (MWJ)

(1) Objective

Concentrations of CO_2 in the atmosphere are now increasing at a rate of 1.5 ppmv y^{-1} owing to human activities such as burning of fossil fuels, deforestation, and cement production. It is an urgent task to estimate as accurately as possible the absorption capacity of the oceans against the increased atmospheric CO_2, and to clarify the mechanism of the CO_2 absorption. The ocean plays an important role in buffering the increase of atmospheric CO_2 and oceanic biosphere, especially primary production, has an important role concerned to oceanic CO_2 cycle through its photosynthesis and respiration. However, the diverseness and variability of the biological system make difficult to reveal their mechanism and quantitative understanding of CO_2 cycle. When CO_2 dissolves in water, chemical reaction takes place and CO_2 alters its appearance into several species. Unfortunately, concentrations of the individual species of CO_2 system in solution cannot be measured directly. There are, however, four parameters that could be measured; total alkalinity, total dissolved inorganic carbon, pH and pCO_2. When more than two of the four parameters are measured, the concentration of CO_2 system in the water can be estimated (Dickson et al., 2007). We here report on-board measurements of DIC performed during the MR10-06 cruise.

(2) Methods, Apparatus and Performance

(2)-1 Seawater sampling

Seawater samples were collected by 12 liter Niskin bottles mounted on the CTD/Carousel system at 4 stations. Among these stations, deep and shallow casts were carried out for 2 stations. When shallow casts were performed, surface seawater samples were also collected by a bucket. Seawater was sampled in a 300 ml glass bottle (SCHOTT DURAN) that was previously soaked in 5 % non-phosphoric acid detergent (pH = 13) solution at least 3 hours and was cleaned by fresh water for 5 times and Milli-Q deionized water for 3 times. A sampling silicone rubber with PFA tip was connected to the Niskin bottle when the sampling was carried out. The glass bottles were filled from the bottom, without rinsing, and were overflowed for 20 seconds. They were sealed using the 29 mm polyethylene inner lids with care not to leave any bubbles in the bottle. After collecting the samples on the deck, the glass bottles were carried to the lab to be measured. Within one hour after the sampling, 3ml of the sample (1 % of the bottle volume) was removed from the glass bottle and poisoned with 100 μl of over saturated solution of mercury chloride. Then the samples were sealed with the 31.9 mm polyethylene inner lids and stored in a refrigerator at approximately 5deg C until analyzed. Before the analysis, the samples were put in the water bath kept about 20deg C for one hour.

(2)-2 Seawater analysis

Measurements of DIC were made with total CO_2 measuring system (Nippon ANS, Inc.). The system comprise of seawater dispensing system, a CO_2 extraction system and a coulometer (Model 5012, UIC, Inc.)

The seawater dispensing system has an auto-sampler (6 ports), which dispenses the seawater from a glass bottle to a pipette of nominal 21ml volume. The pipette was kept at 20 ± 0.05 degC by a water jacket, in which water circulated from a thermostatic water bath (RTE 10,

Thermo) set at 20 degC.

The CO_2 dissolved in a seawater sample is extracted in a stripping chamber of the CO_2 extraction system by adding phosphoric acid (10 % v/v). The stripping chamber is made approx. 25 cm long and has a fine frit at the bottom. The certain amount of acid is taken to the constant volume tube and added to the stripping chamber from its bottom by pressurizing an acid bottle with nitrogen gas (99.9999 %). After the acid is transferred to the stripping chamber, a seawater sample kept in a pipette is introduced to the stripping chamber by the same method as that for an acid. The seawater and phosphoric acid are stirred by the nitrogen bubbles through a fine frit at the bottom of the stripping chamber. The CO_2 stripped in the chamber is carried by the nitrogen gas (flow rates of 140 ml min^{-1}) to the coulometer through two electric dehumidifiers (kept at 0.5 degC) and a chemical desiccant ($Mg(ClO_4)_2$).

The measurement sequence such as 1.5 % CO_2 gas in a nitrogen base, system blank (phosphoric acid blank), and seawater samples (6 samples) was programmed to repeat. The measurement of 1.5 % CO_2 gas was made to monitor response of coulometer solutions (from UIC, Inc.).

(3) Preliminary results

During the cruise, 245 samples were analyzed for DIC. A replicate analysis was performed at the interval decided beforehand and the difference between each pair of analyses was plotted on a range control chart (Figure 2.7-1). The average of the differences was 0.7 μ mol/kg (n=23). The standard deviation was 0.6 μ mol kg^{-1}, which indicates that the analysis was accurate enough according to Guide to best practices for ocean CO_2 measurements (Dickson et al., 2007).

(4) Data Archive

These data obtained in this cruise will be submitted to the Data Management Office (DMO) of JAMSTEC, and will opened to the public via “R/V Mirai Data Web Page” in JAMSTEC home page.

(5) Reference

Dickson, A. G., Sabine, C. L. & Christian, J. R. (2007), Guide to best practices for ocean CO_2 measurements; PICES Special Publication 3, 199pp.

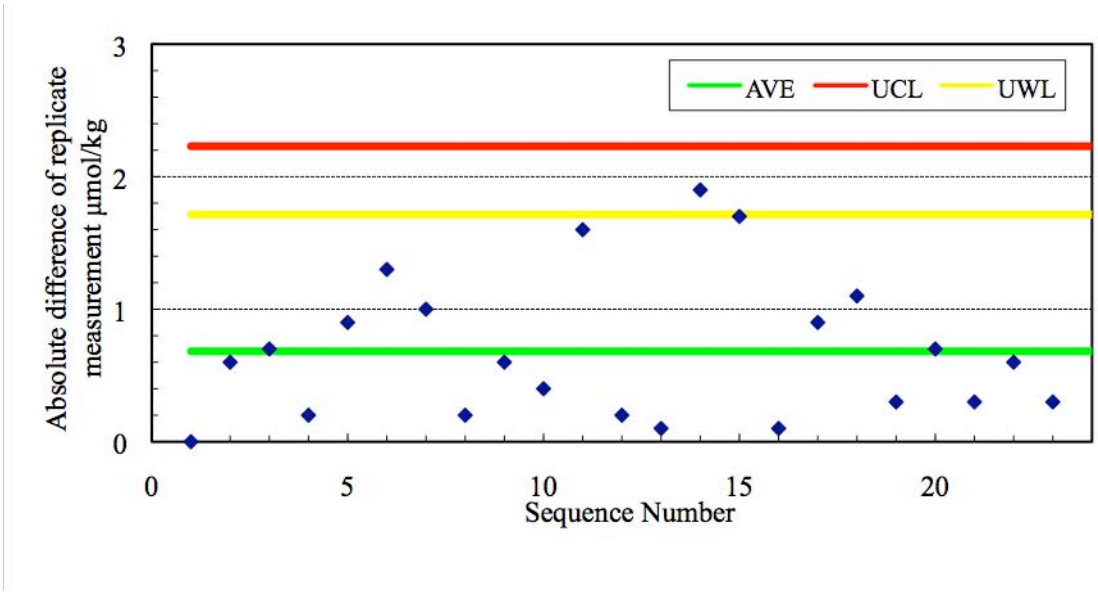

Figure 2.7-1 Range control chart of the absolute differences of replicate measurements of DIC carried out during this cruise. UCL and UWL represents the upper control limit (UCL=AVE*3.267) and upper warning limit (UWL=AVE*2.512), respectively.

2.8 Total Alkalinity

Masahide WAKITA (JAMSTEC MIO) :Principal Investigator
Yoshiko ISHIKAWA (MWJ)
Hatsumi AOYAMA (MWJ)

(1) Objective

Since the global warming is becoming an issue world-widely, studies on green house gases such as CO_2 are drawing high attention. Because the ocean plays an important role in buffering the increase of atmospheric CO_2, surveys on the exchange of CO_2 between the atmosphere and the sea becomes highly important. When CO_2 dissolves in water, chemical reaction takes place and CO_2 alters its appearance into several species. Unfortunately, concentrations of the individual species of CO_2 system in solution cannot be measured directly. There are, however, four parameters that could be measured; total alkalinity, total dissolved inorganic carbon, pH and pCO_2. When two of the four parameters are measured, the concentration of CO_2 system in the water could be estimated (Dickson et al., 2007). We here report on-board measurements of total alkalinity performed during the MR10-06 cruise.

(2) Measured Parameters

Total Alkalinity, TA

(3) Apparatus and performance

(3)-1 Seawater sampling

Seawater samples were collected by 12 liter Niskin bottles mounted on the CTD/Carousel Water Sampling System at 4 stations. Among these stations, deep and shallow casts were carried out for 2 stations. When shallow casts were performed, surface seawater samples were also collected by a bucket. A sampling silicone rubber with PFA tip was connected to the Niskin bottle when the sampling was carried out. The 125 ml borosilicate glass bottles (SHOTT DURAN) were filled from the bottom smoothly, without rinsing, and were overflowed for 2 times bottle volume (10 seconds) with care not to leave any bubbles in the bottle. These bottles were pre-washed by soaking in 5 % non-phosphoric acid detergent (pH = 13) for more than 3 hours and then rinsed 5 times with tap water and 3 times with Milli-Q deionized water. After collecting the samples on the deck, the bottles were carried into the lab to be measured. The samples were stored in a refrigerator at approximately 5 deg C until being analyzed. Before the analysis, the samples were put in the water bath kept about 25 deg C for one hour.

(3)-2 Seawater analysis

Measurement of alkalinity was made using a spectrophotometric system (Nippon ANS, Inc.) using a scheme of Yao and Byrne (1998). The sample seawater of approx. 40ml is transferred from a sample bottle into the titration cell kept at 25 deg C in a thermostated compartment. Then, the sample seawater circulated through the line between the titration and pH cells in the spectrophotometer (Carry 50 Scan, Varian) via dispensing unit by a peristaltic pump. The length and volume of the pH cell are 8 cm and 13 ml, respectively, and its temperature is kept at 25 deg C in a thermostated compartment. The TA is calculated by measuring two sets of absorbance at three wavelengths (750, 616 and 444 nm). One is the absorbance of seawater sample before injecting an acid with indicator solution (bromocresol

green) and another is the one after the injection. For mixing the acid with indicator solution and the seawater sufficiently, they are circulated through the line by a peristaltic pump 7 and half minutes before the measurement.

The TA is calculated based on the following equation:

$$pH_T = 4.2699 + 0.002578 * (35 - S) + \log ((R(25) - 0.00131) / (2.3148 - 0.1299 * R(25))) - \log (1 - 0.001005 * S), \quad (1)$$

$$A_T = (N_A * V_A - 10 \wedge pH_T * DensSW(T, S) * (V_S + V_A)) * (DensSW(T, S) * V_S)^{-1}, \quad (2)$$

where R(25) represents the difference of absorbance at 616 and 444 nm between before and after the injection. The absorbance of wavelength at 750 nm is used to subtract the variation of absorbance caused by the system. DensSW (T, S) is the density of seawater at temperature (T) and salinity (S), N_A the concentration of the added acid, V_A and V_S the volume of added acid and seawater, respectively.

To keep the high analysis precision, some treatments were carried out during the cruise. The acid with indicator solution stored in 1 L DURAN bottle is kept in a bath with its temperature of 25 deg C, and about 10 ml of it is discarded at first before the batch of measurement. For mixing the seawater and the acid with indicator solution sufficiently, TYGON tube used on the peristaltic pump was periodically renewed. Absorbance measurements were done 10 times during each analysis, and the stable last five and three values are averaged and used for above listed calculation for before and after the injection, respectively.

(4) Preliminary results

A few replicate samples were taken at most of stations and the difference between each pair of analyses was plotted on a range control chart (see Figure 2.8-1). The average of the difference was 0.6 μmol kg^{-1} (n=23). The standard deviation was 0.5 μmol kg^{-1}, which indicates that the analysis was accurate enough according to Guide to best practices for ocean CO_2 measurements (Dickson et al., 2007).

(5) Data Archive

These data obtained in this cruise will be submitted to the Data Management Office (DMO) of JAMSTEC, and will opened to the public via “R/V Mirai Data Web Page” in JAMSTEC home page.

(6) References

Yao, W. and Byrne, R. H. (1998), Simplified seawater alkalinity analysis: Use of linear array spectrometers. Deep-Sea Research Part I, Vol. 45, 1383-1392.

Dickson, A. G., Sabine, C. L. & Christian, J. R. (2007), Guide to best practices for ocean CO_2 measurements; PICES Special Publication 3, 199pp.

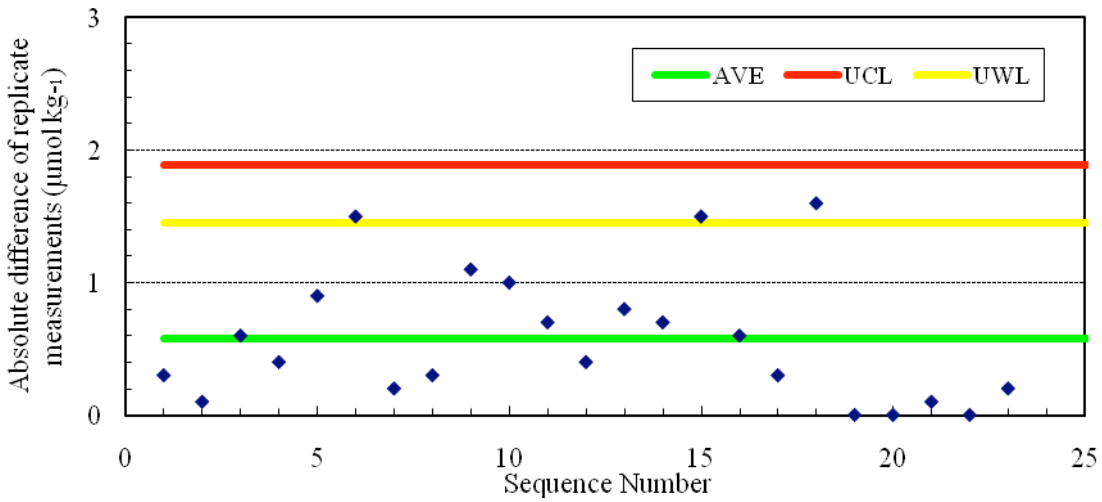

Figure 2.8-1 Range control chart of the absolute differences of replicate measurements carried out in the analysis of TA during the MR10-06 cruise. UCL and UWL represents the upper control limit (UCL=AVE*3.267) and upper warning limit (UWL=AVE*2.512), respectively.

2.9 Underway pCO_2

Masahide WAKITA (JAMSTEC MIO) :Principal Investigator
Yoshiko ISHIKAWA (MWJ)
Hatsumi AOYAMA (MWJ)

(1) Objectives

Concentrations of CO_2 in the atmosphere are increasing at a rate of 1.5 ppmv y^{-1} owing to human activities such as burning of fossil fuels, deforestation, and cement production. It is an urgent task to estimate as accurately as possible the absorption capacity of the oceans against the increased atmospheric CO_2, and to clarify the mechanism of the CO_2 absorption, because the magnitude of the anticipated global warming depends on the levels of CO_2 in the atmosphere, and because the ocean currently absorbs 1/3 of the 6 Gt of carbon emitted into the atmosphere each year by human activities.

Since the global warming is becoming an issue world-widely, studies on green house gases such as CO_2 are drawing high attention. Because the ocean plays an important role in buffering the increase of atmospheric CO_2, surveys on the exchange of CO_2 between the atmosphere and the sea becomes highly important. When CO_2 dissolves in water, chemical reaction takes place and CO_2 alters its appearance into several species. Unfortunately, concentrations of the individual species of CO_2 system in solution cannot be measured directly. There are, however, four parameters that could be measured; total alkalinity, total dissolved inorganic carbon, pH and pCO_2. When more than two of the four parameters are measured, the concentration of CO_2 system in the water can be estimated (Dickson et al., 2007). We here report on board measurements of pCO_2 performed during MR10-06 cruise.

(2) Methods, Apparatus and Performance

Concentrations of CO_2 in the atmosphere and the sea surface were measured continuously during the cruise using an automated system with a non-dispersive infrared gas analyzer (NDIR; MLT 3T-IR).

The automated system was operated by on one and a half hour cycle. In one cycle, standard gasses, marine air and equilibrated air with surface seawater within the equilibrator were analyzed subsequently. The concentrations of the standard gas were 300.043, 349.954, 400.326 and 450.078 ppm.

To measure marine air concentrations (mol fraction) of CO_2 in dry air (xCO_2-air), marine air sampled from the bow of the ship (approx.30 m above the sea level) was introduced into the NDIR by passing through a mass flow controller which controls the air flow rate at about 0.5 L min^{-1}, a cooling unit, a perma-pure dryer (GL Sciences Inc.) and a desiccant holder containing $Mg(ClO_4)_2$.

To measure surface seawater concentrations of CO_2 in dry air (xCO_2-sea), marine air equilibrated with a stream of seawater within the equilibrator was circulated with a pump at 0.7-0.8 L min^{-1} in a closed loop passing through two cooling units, a perma-pure dryer and a desiccant holder containing $Mg(ClO_4)_2$. The seawater taken by a pump from the intake placed at the approx. 4.5m below the sea surface flowed at a rate of 5-6 L min^{-1} in the equilibrator. After that, the equilibrated air was introduced into the NDIR.

(3) Preliminary results

The track observed pCO_2 is shown in Figure 2.9-1. Concentrations of CO_2 (xCO_2) of marine air and surface seawater are shown in Fig. 2.9-2.

(4) Data Archive

These data obtained in this cruise will be submitted to the Data Management Office (DMO) of JAMSTEC, and will opened to the public via “R/V Mirai Data Web Page” in JAMSTEC home page.

(5) Reference

Dickson, A. G., Sabine, C. L. & Christian, J. R. (2007), Guide to best practices for ocean CO_2 measurements; PICES Special Publication 3, 199pp.

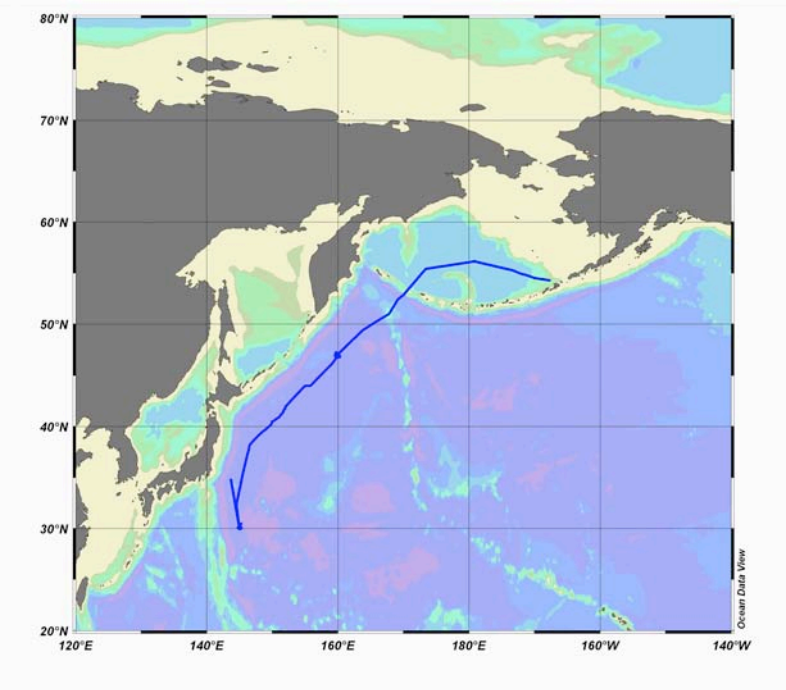

Figure 2.9-1 Observation map

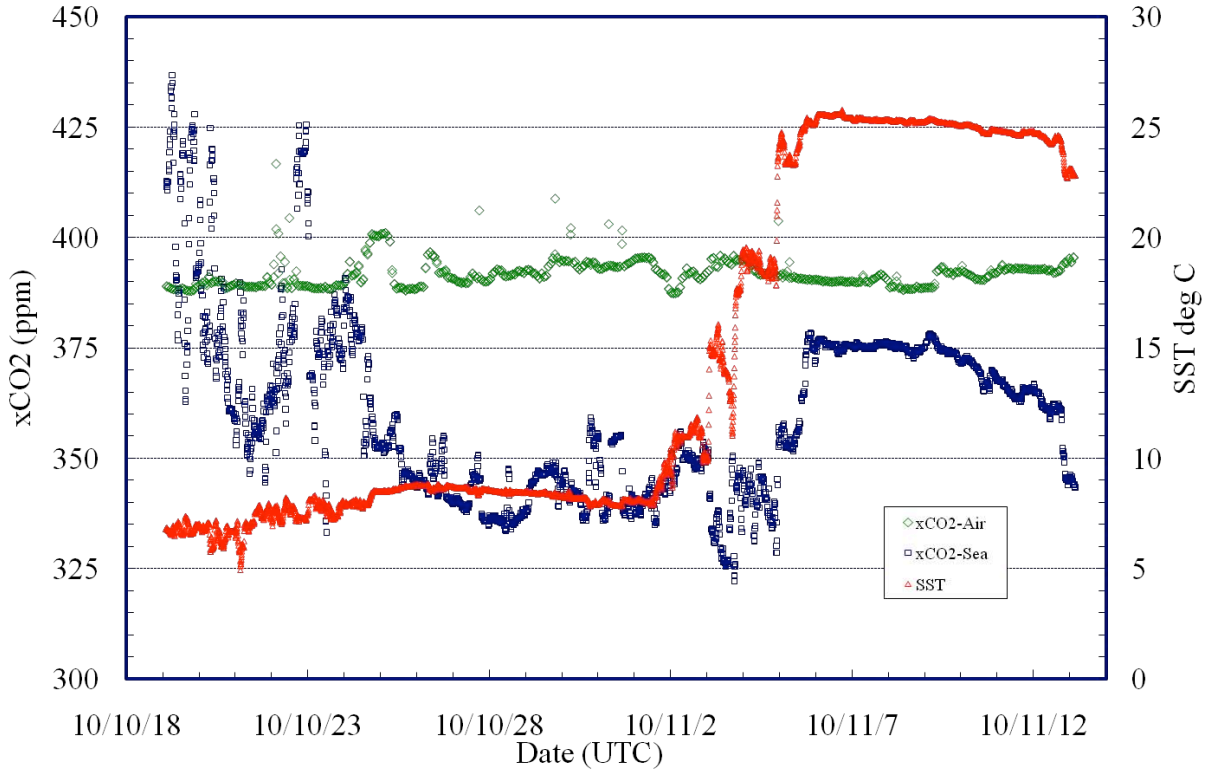

Figure 2.9-2 Temporal variations of atmospheric and oceanic CO_2 concentration (xCO_2). Green dots represent atmosphere xCO_2 variation and blue oceanic xCO_2. SST variation (red) is also shown.

3. Special observation

3.1 BGC mooring

Makio HONDA (JAMSTEC)
Hajime KAWAKAMI (JAMSTEC)
Toru IDAI (MWJ)
Kenichi KATAYAMA (MWJ)
Daiki USHIROMURA (MWJ)
Naoko TAKAHASHI (MWJ)
Tamami UENO (MWJ)
Yasumi YAMADA (MWJ)

3.1.1 Recovery and deployment

The one BGC mooring system was designed for biogeochemistry at Station K-2 and S-1 in the Western Subarctic Gyre. We recovered BGC mooring at Station K-2 and S-1 which were deployed at MR10-01 and deployed BGC mooring at Station K-2 and S-1. K-2 is 47N / 160E, where is close to station KNOT and, however, structure of water mass is more stable than station KNOT. Before deployment, sea floor topography was surveyed with Sea Beam. In order to place the top of mooring systems 150m depth, precise water depths for mooring positions was measured by an altimeter (Datasonics PSA900D) mounted on CTD / CWS. Mooring works took approximately 5 hours for each mooring system. After sinker was dropped, we positioned the mooring systems by measuring the slant ranges between research vessel and the acoustic releaser. The position of the mooring is finally determined as follow:

Table 3.1-1 Mooring positions for respective mooring systems

	Recovery	Deployment	Recovery	Deployment
Station & type	K-2 BGC	K-2 BGC	S-1 BGC	S-1 BGC
Mooring Number	K2BGC100215	K2BGC101031	S1BGC100203	S1BGC101111
Working Date	Oct. 25th 2010	Oct. 31st 2010	Nov. 6th 20101	Nov. 11th 2010
Latitude	47° 00.34 N	47° 00.37 N	30° 03.88 N	30° 03.92 N
Longitude	159° 58.24 E	159° 58.24 E	144° 57.96 E	144° 57.98 E
Sea Beam Depth	5,206 m	5,218 m	5,926 m	5,927 m

The BGC mooring consists of a 64” syntactic top float with 3,000 lbs (1,360 kg) buoyancy, instruments, wire and nylon ropes, glass floats (Benthos 17” glass ball), dual releasers (Edgetech) and 4,660 lbs (2,116 kg). sinker with mace plate. Two ARGOS compact mooring locators and one submersible recovery strobe are mounted on the top float. This mooring system was planned to keep the following time-series observational instruments are mounted approximately 150 m below sea surface. It is 10 m longer than real depth because recovered depth sensor which was installed on the Sediment trap shows 10 m deeper than our expected by mooring tilt.

On the BGC mooring, 3 Sediment Traps are installed on the 200 m, 500 m and 5,000 m. Extra CTD (SBE-37) and Do Sensor (Arec) are mounted on the dual acoustic releasers.

Also extra RIGO Depth Sensor is mounted on the Nichiyu Sediment Trap at K-2.

Details for each instrument are described later (section 3.2). Serial numbers for instruments are as follows:

Table 3.1-2 Serial numbers of instruments

	Recover		Deployment	
Station and type	K-2 BGC	S-1 BGC	K-2 BGC	S-1 BGC
Mooring Number	K2BGC100215	S1BGC100203	K2BGC101031	S1BGC101111
ARGOS	18842 / 52111	18840 / 52112	18842 / 52111	18841 / 52112
ARGOS ID	18577 / 5373	18558 / 5374	18577 / 5373	18570 / 5374
Strobe	233	N02-044	N02-043	N02-044
Sediment Trap×3				
Nichiyu (200m)	ST98025	ST98080	ST98025	ST98080
Rigo Depth Sensor	DP1142	-	DP1158	-
Mark7-21 (500m)	0256	10292	989	No ID
Mark7-21(5000m)	989	878	10558-01	878
Releaser	27805	27809	27824	28533
Releaser	28509	28386	28531	27825
SBE-37	2731	2730	2731	2730
AREC DO sensor	005	003	005	003

Table 3.1-3 Recovery BGC Mooring Record at K-2

Project	Time-Series		Depth	5,206.2	m
Area	North Pacific		Planned Depth	5,216.2	m
Station	K-2 BGC		Length	5,068.2	m
Target Position	**47°00.350 N**		Depth of Buoy	150	m
	159°58.326 E		Period	1	year
ACOUCTIC RELEASERS					
Type	Edgetech		Edgetech		
Serial Number	27805		28509		
Receive F.	11.0	kHz	11.0	kHz	
Transmit F.	14.0	kHz	14.0	kHz	
RELEASE C.	**344611**		**335704**		
Enable C.	360631		377142		
Disable C.	360677		377161		
Battery	2 years		2 years		
Release Test	OK		OK		
RECOVERY					
Recorder	Yasumi Yamada		Work Distance	3.4	Nmile
Ship	R/V MIRAI		Send Enable C.	1:41	
Cruise No.	MR10-06		Slant Renge	-	msec
Date	2010/10/25		Send Release C.	1:41	
Weather	o		Discovery Buoy	1:43	
Wave Hight	2.4	m	Pos. of Top Buoy	47°00.30	N
Depth	5,223	m		159°58.65	E
Ship Heading	<120>		Pos. of Start	47°00.82	N
Ship Ave.Speed	0.8	knot		159°58.66	E
Wind	<230> 4.3	m/s	Pos. of Finish	46°59.54	N
Current	<010> 0.4	cm/sec		160°02.53	E

Table 3.1-4 Recovery BGC Mooring Record at S-1

Project	Time-Series	Depth	5,910.0	m
Area	North Pacific	Planned Depth	5,900.0	m
Station	S-1 BGC	Length	5,752.3	m

Target Position	**30°03.8656**	**N**	Depth of Buoy	150	m
	144°58.0275	**E**	Period	1	year
ACOUCTIC RELEASERS					
Type	Edgetech		Edgetech		
Serial Number	27809		28386		
Receive F.	11.0	kHz	11.0	kHz	
Transmit F.	14.0	kHz	14.0	kHz	
RELEASE C.	**344535**		**354501**		
Enable C.	360320		376513		
Disable C.	360366		376530		
Battery	2 years		2 years		
Release Test	OK		OK		
RECOVERY					
Recorder	Yasumi Yamada		Work Distance	2.2	Nmile
Ship	R/V MIRAI		Send Enable C.	1:39	
Cruise No.	MR10-06		Slant Renge	5,822	m
Date	2010/11/6		Send Release C.	1:44	
Weather	C		Discovery Buoy	1:46	
Wave Hight	2.0	m	Pos. of Top Buoy	30°03.98	N
Depth	5,936	m		144°57.94	E
Ship Heading	<140>		Pos. of Start	30°04.30	N
Ship Ave.Speed	0.5	knot		144°57.74	E
Wind	<088> 6.3	m/s	Pos. of Finish	30°03.80	N
Current	<343> 0.4	cm/sec		144°59.07	E

Table 3.1-5 Deployment BGC Mooring Record at K-2

Project	Time-Series		Depth	5,206.2	m
Area	North Pacific		Planned Depth	5,216.2	m
Station	K-2 BGC		Length	5,068.2	m
Target Position	**47°00.350**	**N**	Depth of Buoy	150	m
	159°58.326	**E**	Period	1	year
ACOUCTIC RELEASERS					
Type	Edgetech		Edgetech		
Serial Number	27824		28531		
Receive F.	11.0	kHz	11.0	kHz	
Transmit F.	14.0	kHz	12.0	kHz	
RELEASE C.	**344674**		**223065**		
Enable C.	361121		200405		
Disable C.	361167		200426		
Battery	2 years		2 years		
Release Test	OK		OK		
DEPLOYMENT					
Recorder	Yasumi Yamada		Start	6.6	Nmile
Ship	R/V MIRAI		Overshoot	560	m
Cruise No.	MR10-06		Let go Top Buoy	1:58	
Date	2010/10/31		Let go Anchor	5:35	
Weather	o		Sink Top Buoy	6:05	
Wave Hight	3.9	m	Pos. of Start	46°57.22	N
Seabeam Depth	5,218	m		160°06.47	E
Ship Heading	<300>		Pos. of Drop. Anc.	47°00.52	N
Ship Ave.Speed	1.9	knot		159°57.94	E
Wind	<297> 12.0	m/s	Pos. of Mooring	47°00.37	N
Current	<150> 0.3	cm/sec		159°58.23	E

Table 3.1-6 Deployment BGC Mooring Record at S-1

Project	Time-Series	Depth	5,910.0	m

Area	North Pacific		Planned Depth	5,900.0	m
Station	S-1 BGC		Length	5,752.3	m
Target Position	**30°03.8656**	**N**	Depth of Buoy	150	m
	144°58.0275	**E**	Period	1	year
ACOUCTIC RELEASERS					
Type	Edgetech		Edgetech		
Serial Number	28533		27825		
Receive F.	11.0	kHz	11.0	kHz	
Transmit F.	14.0	kHz	14.0	kHz	
RELEASE C.	**223307**		**344176**		
Enable C.	201054		356736		
Disable C.	201077		356770		
Battery	2 years		2 years		
Release Test	OK		OK		
DEPLOYMENT					
Recorder	Yasumi Yamada		Start	6.1	Nmile
Ship	R/V MIRAI		Overshoot	600	m
Cruise No.	MR10-06		Let go Top Buoy	22:33	
Date	2010/11/10		Let go Anchor	1:52	
Weather	c		Sink Top Buoy	2:30	
Wave Hight	3.0	m	Pos. of Start	30°00.64	N
Seabeam Depth	5,927	m		145°03.88	E
Ship Heading	<302>		Pos. of Drop. Anc.	30°04.03	N
Ship Ave.Speed	1.1	knot		144°57.72	E
Wind	<298> 7.2	m/s	Pos. of Mooring	30°03.92	N
Current	<001> 0.2	cm/sec		144°57.98	E

Table 3.1-7 detail of Recovery BGC Mooring system at K-2

	Description	S/N	Joint	Item Length (m)	Item Weight (kg)	Mooring Length (m)	Mooring Weight (kg)	Above Bottom (m)	Mooring Depth (m)	
1	64" Syntatic Sphere	025162-01		2.27	-1360.78		-1360.78	5068.12	148.08	**150**
2	Hardware		I	0.28	3.63	2.55	-1357.15	5065.85	150.35	
3	**5** Meters 16mm			5.00	27.80	7.55	-1329.35	5065.57	150.63	
4	Hardware		F	0.25	2.40	7.80	-1326.95	5060.57	155.63	
5	3-TON Miller Swivel			0.16	3.17	7.96	-1323.78	5060.33	155.87	
6	Hardware		A	0.24	1.90	8.20	-1321.88	5060.17	156.03	
7	**40** Meters 5/16" Wire	C-1		40.08	8.54	48.27	-1313.33	5059.93	156.27	
8	Hardware		A	0.24	1.90	48.51	-1311.43	5019.85	196.35	
9	**3** Meters 5/16" Wire	C-4		3.00	0.64	51.51	-1310.79	5019.61	196.59	
10	Hardware		L	0.24	2.19	51.75	-1308.60	5016.61	199.59	
11	Sediment Trap	ST98025	Y	3.79	55.68	55.54	-1252.92	5016.37	199.83	**200**
12	Hardware		E	0.06	0.70	55.60	-1252.22	5012.58	203.62	
13	**3.0** Meters 13mm			3.00	7.71	58.60	-1244.51	5012.52	203.68	
14	Hardware		A	0.24	1.90	58.84	-1242.61	5009.52	206.68	
15	3-TON Miller Swivel			0.16	3.17	59.00	-1239.44	5009.28	206.92	
16	Hardware		A	0.24	1.90	59.24	-1237.54	5009.12	207.08	
17	**200** Meters 5/16" Wire	T-05		200.63	42.77	259.87	-1194.77	5008.88	207.32	
18	Hardware		A	0.24	1.90	260.11	-1192.87	4808.25	407.95	
19	**88** Meters 5/16" Wire	T09-B1		88.17	18.80	348.28	-1174.07	4808.01	408.19	
20	Hardware		A	0.24	1.90	348.52	-1172.17	4719.84	496.36	
21	**3** Meters 5/16" Wire	C-5		3.00	0.64	351.52	-1171.53	4719.60	496.60	
22	Hardware		L	0.24	2.19	351.76	-1169.34	4716.60	499.60	
23	Sediment Trap	0256	Y	3.83	55.70	355.59	-1113.64	4716.36	499.84	**500**
24	Hardware		E	0.06	0.70	355.65	-1112.94	4712.53	503.67	
25	**2.0** Meters 13mm			2.00	5.14	357.65	-1107.80	4712.47	503.73	
26	Hardware		A	0.24	1.90	357.89	-1105.90	4710.47	505.73	
27	3-TON Miller Swivel			0.16	3.17	358.05	-1102.73	4710.23	505.97	
28	Hardware		A	0.24	1.90	358.29	-1100.83	4710.07	506.13	

29	**1000** Meters 12mm	SK1000-1		1000.00	31.00	1358.29	-1069.83	4709.83	506.37	
30	Hardware		A	0.24	1.90	1358.53	-1067.93	3709.83	1506.37	
31	**1000** Meters 12mm	SK1000-2		1000.00	31.00	2358.53	-1036.93	3709.59	1506.61	
32	Hardware		A	0.24	1.90	2358.77	-1035.03	2709.59	2506.61	
33	4-17" Glassballs on			4.00	-91.32	2362.77	-1126.35	2709.35	2506.85	
34	Hardware		A	0.24	1.90	2363.01	-1124.45	2705.35	2510.85	
35	4-17" Glassballs on			4.00	-91.32	2367.01	-1215.77	2705.11	2511.09	
36	Hardware		A	0.24	1.90	2367.25	-1213.87	2701.11	2515.09	
37	**1000** Meters 12mm	SK1000-3		1000.00	31.00	3367.25	-1182.87	2700.87	2515.33	
38	Hardware		A	0.24	1.90	3367.49	-1180.97	1700.87	3515.33	
39	**500** Meters 12mm	SK500-1		500.00	15.50	3867.49	-1165.47	1700.63	3515.57	
40	Hardware		A	0.24	1.90	3867.73	-1163.57	1200.63	4015.57	
41	**300** Meters 12mm	SK300-1		300.00	9.30	4167.73	-1154.27	1200.39	4015.81	
42	Hardware		D	0.23	1.65	4167.96	-1152.62	900.39	4315.81	
43	**200** Meters 1/4" Wire	T09-E5		200.56	28.20	4368.52	-1124.42	900.16	4316.04	
44	Hardware		D	0.23	1.65	4368.75	-1122.77	699.60	4516.60	
45	4-17" Glassballs on			4.00	-91.32	4372.75	-1214.09	699.37	4516.83	
46	Hardware		D	0.23	1.65	4372.98	-1212.44	695.37	4520.83	
47	**200** Meters 1/4" Wire	T08-H2		200.36	28.17	4573.34	-1184.27	695.14	4521.06	
48	Hardware		C	0.21	1.33	4573.55	-1182.94	494.78	4721.42	
49	**50** Meters 1/4" Wire			50.00	7.03	4623.55	-1175.91	494.57	4721.63	
50	Hardware		C	0.21	1.33	4623.76	-1174.58	444.57	4771.63	
51	**35** Meters 1/4" Wire			35.00	4.92	4658.76	-1169.66	444.36	4771.84	
52	Hardware		D	0.23	1.65	4658.99	-1168.01	409.36	4806.84	
53	**3** Meters 5/16" Wire	C-6		3.00	0.64	4661.99	-1167.37	409.13	4807.07	
54	Hardware		L	0.20	1.33	4662.19	-1166.04	406.13	4810.07	
55	Sediment Trap	989	Y	3.80	55.70	4665.99	-1110.33	405.93	4810.27	**4810.8**
56	Hardware		E	0.06	0.70	4666.05	-1109.63	402.13	4814.07	
57	**4.0** Meters 13mm			4.00	10.28	4670.05	-1099.35	402.07	4814.13	
58	Hardware		A	0.24	1.90	4670.29	-1097.45	398.07	4818.13	
59	3-TON Miller Swivel			0.16	3.17	4670.46	-1094.29	397.83	4818.37	
60	Hardware		D	0.23	1.65	4670.69	-1092.64	397.67	4818.53	
61	**300** Meters 1/4" Wire	T07-F		300.63	42.27	4971.32	-1050.36	397.44	4818.76	
62	Hardware		C	0.21	1.33	4971.53	-1049.03	96.80	5119.40	
63	**20** Meters 1/4" Wire			20.00	2.81	4991.53	-1046.22	96.59	5119.61	
64	Hardware		H	0.22	1.65	4991.75	-1044.57	76.59	5139.61	
65	5 Meters 16mm			5.00	27.80	4996.75	-1016.77	76.37	5139.83	
66	Hardware		B	0.24	2.00	4996.99	-1014.77	71.37	5144.83	
67	4-17" Glassballs on			4.00	-79.36	5000.99	-1094.13	71.14	5145.06	
68	Hardware		B	0.24	2.00	5001.22	-1092.13	67.14	5149.06	
69	4-17" Glassballs on			4.00	-79.36	5005.22	-1171.49	66.90	5149.30	
70	Hardware		B	0.24	2.00	5005.46	-1169.49	62.90	5153.30	
71	4-17" Glassballs on			4.00	-79.36	5009.46	-1248.85	62.67	5153.53	
72	Hardware		B	0.24	2.00	5009.69	-1246.85	58.67	5157.53	
73	4-17" Glassballs on			4.00	-79.36	5013.69	-1326.21	58.43	5157.77	
74	Hardware		B	0.24	2.00	5013.93	-1324.21	54.43	5161.77	
75	4-17" Glassballs on			4.00	-79.36	5017.93	-1403.57	54.20	5162.00	
76	Hardware		B	0.24	2.00	5018.16	-1401.57	50.20	5166.00	
77	4-17" Glassballs on			4.00	-79.36	5022.16	-1480.93	49.96	5166.24	
78	Hardware		B	0.24	2.00	5022.40	-1478.93	45.96	5170.24	
79	4-17" Glassballs on			4.00	-79.36	5026.40	-1558.29	45.73	5170.47	
80	Hardware		B	0.24	2.00	5026.63	-1556.29	41.73	5174.47	
81	5 Meters 16mm			5.00	27.80	5031.63	-1528.49	41.49	5174.71	
82	Hardware		B	0.24	2.00	5031.87	-1526.49	36.49	5179.71	
83	3-TON Miller Swivel			0.16	3.20	5032.03	-1523.29	36.26	5179.94	
84	Hardware		F	0.25	2.40	5032.27	-1520.89	36.09	5180.11	
85	Dual EGG Acoustic		J	1.95	66.04	5034.22	-1454.85	35.85	5180.35	
86	Hardware		F	0.25	2.40	5034.46	-1452.45	33.90	5182.30	
87	5 Meters 16mm			5.00	27.80	5039.46	-1424.65	33.66	5182.54	

88	Hardware		G	0.26	2.85	5039.72	-1421.80	28.66	5187.54	
89	**20** Meters 1" Nylon			21.92	6.54	5061.64	-1415.26	28.40	5187.80	
90	Hardware		G	0.26	2.85	5061.90	-1412.41	6.48	5209.72	
91	5 Meters 16mm			5.00	27.80	5066.90	-1384.61	6.22	5209.98	
92	Hardware		G	0.26	2.85	5067.16	-1381.76	1.22	5214.98	**Design**
93	2.116 Ton Anchor			0.96	2116.46	5068.12	734.70	0.96	5215.24	**Depth**
	OVERALL			**5068.12**					5216.20	**5216.2**

Table 3.1-8 detail of Recovery BGC Mooring system at S-1

	Description	S/N	Joint	Item Length (m)	Item Weight (kg)	Mooring Length (m)	Mooring Weight (kg)	Above Bottom (m)	Mooring Depth (m)	
1	64" Syntatic Sphere	015162-03		2.27	-1360.78		-1360.78	5752.30	157.70	**150**
2	Hardware		I	0.28	3.63	2.55	-1357.15	5750.03	159.97	
3	**5** Meters 16mm			5.00	27.80	7.55	-1329.35	5749.75	160.25	
4	Hardware		F	0.25	2.40	7.80	-1326.95	5744.75	165.25	
5	3-TON Miller Swivel			0.16	3.17	7.96	-1323.78	5744.50	165.50	
6	Hardware		A	0.24	1.90	8.20	-1321.88	5744.34	165.66	
7	**40** Meters 5/16" Wire	E-②		40.08	8.54	48.27	-1313.33	5744.10	165.90	
8	Hardware		A	0.24	1.90	48.51	-1311.43	5704.02	205.98	
9	**3** Meters 5/16" Wire			3.00	0.64	51.51	-1310.79	5703.78	206.22	
10	Hardware		L	0.24	2.19	51.75	-1308.60	5700.78	209.22	
11	Sediment Trap	ST98080	Y	3.79	55.68	55.54	-1252.92	5700.54	209.46	**200**
12	Hardware		E	0.06	0.70	55.60	-1252.22	5696.75	213.25	
13	**4.0** Meters 13mm			4.00	10.28	59.60	-1241.94	5696.69	213.31	
14	Hardware		A	0.24	1.90	59.84	-1240.04	5692.69	217.31	
15	3-TON Miller Swivel			0.16	3.17	60.00	-1236.87	5692.45	217.55	
16	Hardware		A	0.24	1.90	60.24	-1234.97	5692.29	217.71	
17	**200** Meters 5/16"	T09-A1		200.33	42.71	260.58	-1192.26	5692.05	217.95	
18	Hardware		A	0.24	1.90	260.82	-1190.36	5491.72	418.28	
19	**88** Meters 5/16" Wire	T09-B2		88.16	18.79	348.98	-1171.57	5491.48	418.52	
20	Hardware		A	0.24	1.90	349.22	-1169.67	5403.32	506.68	
21	**3** Meters 5/16" Wire			3.00	0.64	352.22	-1169.03	5403.08	506.92	
22	Hardware		L	0.24	2.19	352.46	-1166.84	5400.08	509.92	
23	Sediment Trap ML	10292	Y	3.80	55.70	356.26	-1111.14	5399.84	510.16	**500**
24	Hardware		E	0.06	0.70	356.32	-1110.44	5396.04	513.96	
25	**1.0** Meters 13mm			1.00	2.57	357.32	-1107.87	5395.98	514.02	
26	Hardware		A	0.24	1.90	357.56	-1105.97	5394.98	515.02	
27	3-TON Miller Swivel			0.16	3.17	357.72	-1102.80	5394.74	515.26	
28	Hardware		A	0.24	1.90	357.96	-1100.90	5394.58	515.42	
29	**1000** Meters 12mm	SK1000-4		1000.00	31.00	1357.96	-1069.90	5394.34	515.66	
30	Hardware		A	0.24	1.90	1358.20	-1068.00	4394.34	1515.66	
31	**1000** Meters 12mm	SK1000-5		1000.00	31.00	2358.20	-1037.00	4394.10	1515.90	
32	Hardware		A	0.24	1.90	2358.44	-1035.10	3394.10	2515.90	
33	4-17" Glassballs on			4.00	-91.32	2362.44	-1126.42	3393.86	2516.14	
34	Hardware		A	0.24	1.90	2362.68	-1124.52	3389.86	2520.14	
35	4-17" Glassballs on			4.00	-91.32	2366.68	-1215.84	3389.62	2520.38	
36	Hardware		A	0.24	1.90	2366.92	-1213.94	3385.62	2524.38	
37	**1000** Meters 12mm	SK1000-6		1000.00	31.00	3366.92	-1182.94	3385.38	2524.62	
38	Hardware		A	0.24	1.90	3367.16	-1181.04	2385.38	3524.62	
39	**500** Meters 12mm	SK500-2		500.00	15.50	3867.16	-1165.54	2385.14	3524.86	
40	Hardware		A	0.24	1.90	3867.40	-1163.64	1885.14	4024.86	
41	**300** Meters 12mm	SK300-2		300.00	9.30	4167.40	-1154.34	1884.90	4025.10	
42	Hardware		D	0.23	1.65	4167.63	-1152.69	1584.90	4325.10	
43	**200** Meters 1/4" Wire	T09-E3		200.56	28.20	4368.19	-1124.49	1584.67	4325.33	
44	Hardware		D	0.23	1.65	4368.42	-1122.84	1384.11	4525.89	
45	4-17" Glassballs on			4.00	-91.32	4372.42	-1214.16	1383.88	4526.12	
46	Hardware		D	0.23	1.65	4372.65	-1212.51	1379.88	4530.12	
47	**200** Meters 1/4" Wire	T09-E2		200.56	28.20	4573.21	-1184.30	1379.65	4530.35	

48	Hardware		C	0.21	1.33	4573.42	-1182.97	1179.09	4730.91	
49	**50** Meters 1/4" Wire			50.00	7.03	4623.42	-1175.94	1178.88	4731.12	
50	Hardware		C	0.21	1.33	4623.63	-1174.61	1128.88	4781.12	
51	**35** Meters 1/4" Wire			35.00	4.92	4658.63	-1169.69	1128.67	4781.33	
52	Hardware		D	0.23	1.65	4658.86	-1168.04	1093.67	4816.33	
53	**3** Meters 5/16" Wire			3.00	0.64	4661.86	-1167.40	1093.44	4816.56	
54	Hardware		L	0.20	1.33	4662.06	-1166.07	1090.44	4819.56	
55	Sediment Trap	878	Y	3.84	55.70	4665.90	-1110.37	1090.24	4819.76	**4810.8**
56	Hardware		E	0.06	0.70	4665.96	-1109.67	1086.40	4823.60	
57	**1.0** Meters 13mm			1.00	2.57	4666.96	-1107.10	1086.34	4823.66	
58	Hardware		A	0.24	1.90	4667.20	-1105.20	1085.34	4824.66	
59	3-TON Miller Swivel			0.16	3.17	4667.36	-1102.03	1085.10	4824.90	
60	Hardware		D	0.23	1.65	4667.59	-1100.38	1084.94	4825.06	
61	**500** Meters 1/4" Wire	T08-F8		501.75	70.55	5169.33	-1029.83	1084.71	4825.29	
62	Hardware		C	0.21	1.33	5169.54	-1028.50	582.97	5327.03	
63	**300** Meters 1/4" Wire	T09-D1		300.85	42.30	5470.39	-986.20	582.76	5327.24	
64	Hardware		C	0.21	1.33	5470.60	-984.87	281.91	5628.09	
65	**200** Meters 1/4" Wire	T09-E1		200.55	28.20	5671.15	-956.67	281.70	5628.30	
66	Hardware		H	0.22	1.65	5671.38	-955.02	81.14	5828.86	
67	5 Meters 16mm			5.00	27.80	5676.38	-927.22	80.92	5829.08	
68	Hardware		B	0.24	2.00	5676.61	-925.22	75.92	5834.08	
69	2-17" Glassballs on			2.00	-39.68	5678.61	-964.90	75.69	5834.31	
70	Hardware		B	0.24	2.00	5678.85	-962.90	73.69	5836.31	
71	4-17" Glassballs on			4.00	-79.36	5682.85	-1042.26	73.45	5836.55	
72	Hardware		B	0.24	2.00	5683.08	-1040.26	69.45	5840.55	
73	4-17" Glassballs on			4.00	-79.36	5687.08	-1119.62	69.22	5840.78	
74	Hardware		B	0.24	2.00	5687.32	-1117.62	65.22	5844.78	
75	4-17" Glassballs on			4.00	-79.36	5691.32	-1196.98	64.98	5845.02	
76	Hardware		B	0.24	2.00	5691.55	-1194.98	60.98	5849.02	
77	4-17" Glassballs on			4.00	-79.36	5695.55	-1274.34	60.75	5849.25	
78	Hardware		B	0.24	2.00	5695.79	-1272.34	56.75	5853.25	
79	4-17" Glassballs on			4.00	-79.36	5699.79	-1351.70	56.51	5853.49	
80	Hardware		B	0.24	2.00	5700.02	-1349.70	52.51	5857.49	
81	4-17" Glassballs on			4.00	-79.36	5704.02	-1429.06	52.28	5857.72	
82	Hardware		B	0.24	2.00	5704.26	-1427.06	48.28	5861.72	
83	4-17" Glassballs on			4.00	-79.36	5708.26	-1506.42	48.04	5861.96	
84	Hardware		B	0.24	2.00	5708.49	-1504.42	44.04	5865.96	
85	4-17" Glassballs on			4.00	-79.36	5712.49	-1583.78	43.81	5866.19	
86	Hardware		B	0.24	2.00	5712.73	-1581.78	39.81	5870.19	
87	5 Meters 16mm			5.00	27.80	5717.73	-1553.98	39.57	5870.43	
88	Hardware		B	0.24	2.00	5717.96	-1551.98	34.57	5875.43	
89	3-TON Miller Swivel			0.16	3.20	5718.12	-1548.78	34.34	5875.66	
90	Hardware		F	0.25	2.40	5718.37	-1546.38	34.17	5875.83	
91	Dual EGG Acoustic		J	1.95	66.04	5720.31	-1480.33	33.93	5876.07	
92	Hardware		F	0.25	2.40	5720.56	-1477.93	31.98	5878.02	
93	5 Meters 16mm			5.00	27.80	5725.56	-1450.13	31.74	5878.26	
94	Hardware		G	0.26	2.85	5725.82	-1447.28	26.74	5883.26	
95	**20** Meters 1" Nylon	09-24-20-25		20.00	5.96	5745.82	-1441.32	26.48	5883.52	
96	Hardware		G	0.26	2.85	5746.08	-1438.47	6.48	5903.52	
97	5 Meters 16mm			5.00	27.80	5751.08	-1410.67	6.22	5903.78	
98	Hardware		G	0.26	2.85	5751.34	-1407.82	1.22	5908.78	**Design**
99	2.116 Ton Anchor			0.96	2116.46	5752.30	708.64	0.96	5909.04	**Depth**
	OVERALL			**5752.30**					5910.00	**5900**

Table 3.1-9 detail of Deployment BGC Mooring system at K-2

	Description	S/N	Joint	Item Length (m)	Item Weight (kg)	Mooring Length (m)	Mooring Weight (kg)	Above Bottom (m)	Mooring Depth (m)	
1	64" Syntatic Sphere			2.27	-1360.78		-1360.78	5067.20	149.00	**150**

2	Hardware		K	0.28	3.63	2.55	-1357.15	5064.93	151.27	
3	3-TON Miller Swivel			0.16	3.17	2.71	-1353.98	5064.65	151.55	
4	Hardware		G	0.13	1.80	2.84	-1352.18	5064.49	151.71	
5	**5** Meters 16mm			5.00	27.80	7.84	-1324.38	5064.36	151.84	
6	Hardware		D	0.12	1.40	7.96	-1322.98	5059.36	156.84	
7	**38** Meters 5/16" Wire	T10_B-1		38.07	8.12	46.03	-1314.86	5059.24	156.96	
8	Hardware		D	0.12	1.40	46.15	-1313.46	5021.17	195.03	
9	**3** Meters 5/16" Wire			3.00	0.64	49.15	-1312.82	5021.05	195.15	
10	Hardware		M	0.06	0.70	49.21	-1312.12	5018.05	198.15	
11	Sediment Trap		Y	3.79	55.68	53.00	-1256.44	5017.99	198.21	**200**
12	Hardware		G	0.13	1.80	53.13	-1254.64	5014.20	202.00	
13	3-TON Miller Swivel			0.16	3.17	53.29	-1251.47	5014.07	202.13	
14	Hardware		G	0.13	1.80	53.42	-1249.67	5013.91	202.29	
15	**4.0** Meters 13mm			4.00	10.28	57.42	-1239.39	5013.78	202.42	
16	Hardware		D	0.12	1.40	57.54	-1237.99	5009.78	206.42	
17	**200** Meters 5/16" Wire	T10_A-1		200.39	42.72	257.94	-1195.27	5009.66	206.54	
18	Hardware		D	0.12	1.40	258.06	-1193.87	4809.27	406.93	
19	**88** Meters 5/16" Wire	T09_B-3		88.16	18.79	346.22	-1175.07	4809.15	407.05	
20	Hardware		D	0.12	1.40	346.34	-1173.67	4720.99	495.21	
21	**3** Meters 5/16" Wire			3.00	0.64	349.34	-1173.03	4720.87	495.33	
22	Hardware		M	0.06	0.70	349.40	-1172.33	4717.87	498.33	
23	Sediment Trap		Y	3.83	55.70	353.23	-1116.63	4717.81	498.39	**500**
24	Hardware		G	0.13	1.80	353.36	-1114.83	4713.98	502.22	
25	3-TON Miller Swivel			0.16	3.17	353.52	-1111.66	4713.85	502.35	
26	Hardware		G	0.13	1.80	353.65	-1109.86	4713.68	502.52	
27	**4.0** Meters 13mm			4.00	10.28	357.65	-1099.58	4713.55	502.65	
28	Hardware		D	0.12	1.40	357.77	-1098.18	4709.55	506.65	
29	**1000** Meters 12mm	SK1000-7		1000.00	35.00	1357.77	-1063.18	4709.43	506.77	
30	Hardware		D	0.12	1.40	1357.89	-1061.78	3709.43	1506.77	
31	**1000** Meters 12mm	SK1000-8		1000.00	35.00	2357.89	-1026.78	3709.31	1506.89	
32	Hardware		D	0.12	1.40	2358.01	-1025.38	2709.31	2506.89	
33	4-17" Glassballs on			4.00	-91.32	2362.01	-1116.70	2709.19	2507.01	
34	Hardware		F	0.24	1.90	2362.25	-1114.80	2705.19	2511.01	
35	4-17" Glassballs on			4.00	-91.32	2366.25	-1206.12	2704.95	2511.25	
36	Hardware		D	0.12	1.40	2366.37	-1204.72	2700.95	2515.25	
37	**1000** Meters 12mm	SK1000-9		1000.00	35.00	3366.37	-1169.72	2700.83	2515.37	
38	Hardware		D	0.12	1.40	3366.49	-1168.32	1700.83	3515.37	
39	**500** Meters 12mm	SK500-3		500.00	17.50	3866.49	-1150.82	1700.71	3515.49	
40	Hardware		D	0.12	1.40	3866.61	-1149.42	1200.71	4015.49	
41	**300** Meters 12mm	SK300-3		300.00	10.50	4166.61	-1138.92	1200.59	4015.61	
42	Hardware		B	0.11	1.10	4166.72	-1137.82	900.59	4315.61	
43	**200** Meters 1/4" Wire	T10_F-1		200.59	28.21	4367.30	-1109.62	900.48	4315.72	
44	Hardware		B	0.11	1.10	4367.41	-1108.52	699.90	4516.30	
45	4-17" Glassballs on			4.00	-91.32	4371.41	-1199.84	699.79	4516.41	
46	Hardware		B	0.11	1.10	4371.52	-1198.74	695.79	4520.41	
47	**200** Meters 1/4" Wire	T10_F-2		200.59	28.21	4572.12	-1170.53	695.68	4520.52	
48	Hardware		A	0.10	0.80	4572.21	-1169.73	495.09	4721.11	
49	**50** Meters 1/4" Wire	T10_G-1		50.15	7.05	4622.36	-1162.68	494.99	4721.21	
50	Hardware		A	0.10	0.80	4622.46	-1161.88	444.84	4771.36	
51	**35** Meters 1/4" Wire	T10_H-1		35.11	4.94	4657.56	-1156.94	444.75	4771.45	
52	Hardware		B	0.11	1.10	4657.67	-1155.84	409.64	4806.56	
53	**3** Meters 5/16" Wire			3.00	0.64	4660.67	-1155.20	409.53	4806.67	
54	Hardware		M	0.06	0.70	4660.73	-1154.50	406.53	4809.67	
55	Sediment Trap		Y	3.80	55.70	4664.53	-1098.80	406.47	4809.73	**4810.8**
56	Hardware		G	0.13	1.80	4664.66	-1097.00	402.67	4813.53	
57	3-TON Miller Swivel			0.16	3.17	4664.82	-1093.83	402.54	4813.66	
58	Hardware		E	0.12	1.50	4664.94	-1092.33	402.38	4813.82	
59	**6.5** Meters 13mm			6.50	16.71	4671.44	-1075.63	402.26	4813.94	
60	Hardware		A	0.10	0.80	4671.53	-1074.83	395.76	4820.44	

61	**300** Meters 1/4" Wire	T10_E-2		300.90	42.31	4972.44	-1032.52	395.67	4820.53	
62	Hardware		A	0.10	0.80	4972.53	-1031.72	94.76	5121.44	
63	**20** Meters 1/4" Wire	I-1		20.05	2.82	4992.58	-1028.90	94.67	5121.53	
64	Hardware		A	0.10	0.80	4992.67	-1028.10	74.62	5141.58	
65	**5** Meters 1/4" Wire			5.00	0.70	4997.67	-1027.40	74.53	5141.67	
66	Hardware		B	0.11	1.10	4997.78	-1026.30	69.53	5146.67	
67	5 Meters 16mm			5.00	27.80	5002.78	-998.50	69.42	5146.78	
68	Hardware		H	0.23	2.00	5003.01	-996.50	64.42	5151.78	
69	4-17" Glassballs on			4.00	-79.36	5007.01	-1075.86	64.19	5152.01	
70	Hardware		H	0.23	2.00	5007.24	-1073.86	60.19	5156.01	
71	4-17" Glassballs on			4.00	-79.36	5011.24	-1153.22	59.96	5156.24	
72	Hardware		H	0.23	2.00	5011.47	-1151.22	55.96	5160.24	
73	4-17" Glassballs on			4.00	-79.36	5015.47	-1230.58	55.73	5160.47	
74	Hardware		H	0.23	2.00	5015.70	-1228.58	51.73	5164.47	
75	4-17" Glassballs on			4.00	-79.36	5019.70	-1307.94	51.50	5164.70	
76	Hardware		H	0.23	2.00	5019.93	-1305.94	47.50	5168.70	
77	4-17" Glassballs on			4.00	-79.36	5023.93	-1385.30	47.27	5168.93	
78	Hardware		H	0.23	2.00	5024.16	-1383.30	43.27	5172.93	
79	4-17" Glassballs on			4.00	-79.36	5028.16	-1462.66	43.04	5173.16	
80	Hardware		D	0.12	1.40	5028.28	-1461.26	39.04	5177.16	
81	5 Meters 16mm			5.00	27.80	5033.28	-1433.46	38.92	5177.28	
82	Hardware		G	0.13	1.80	5033.41	-1431.66	33.92	5182.28	
83	3-TON Miller Swivel			0.16	3.20	5033.58	-1428.46	33.79	5182.41	
84	Hardware		I	0.14	2.20	5033.72	-1426.26	33.62	5182.58	
85	Dual EGG Acoustic		L	1.95	66.04	5035.66	-1360.21	33.48	5182.72	
86	Hardware		G	0.13	1.80	5035.79	-1358.41	31.54	5184.66	
87	5 Meters 16mm			5.00	27.80	5040.79	-1330.61	31.41	5184.79	
88	Hardware		J	0.15	2.45	5040.94	-1328.16	26.41	5189.79	
89	**20** Meters 1" Nylon			20.00	5.96	5060.94	-1322.20	26.26	5189.94	
90	Hardware		J	0.15	2.45	5061.09	-1319.75	6.26	5209.94	
91	5 Meters 16mm			5.00	27.80	5066.09	-1291.95	6.11	5210.09	
92	Hardware		J	0.15	2.45	5066.24	-1289.50	1.11	5215.09	**Design**
93	2.116 Ton Anchor			0.96	2116.46	5067.20	826.96	0.96	5215.24	**Depth**
	OVERALL			**5067.20**					5216.20	**5216.2**

Table 3.1-10 detail of Deployment BGC Mooring system at S-1

	Description	S/N	Joint	Item Length (m)	Item Weight (kg)	Mooring Length (m)	Mooring Weight (kg)	Above Bottom (m)	Mooring Depth (m)	
1	64" Syntatic Sphere			2.27	-1360.78		-1360.78	5760.30	149.70	**150**
2	Hardware		K	0.28	3.63	2.55	-1357.15	5758.03	151.97	
3	3-TON Miller Swivel			0.16	3.17	2.71	-1353.98	5757.75	152.25	
4	Hardware		G	0.13	1.80	2.84	-1352.18	5757.59	152.41	
5	**5** Meters 16mm			5.00	27.80	7.84	-1324.38	5757.46	152.54	
6	Hardware		D	0.12	1.40	7.96	-1322.98	5752.46	157.54	
7	**38** Meters 5/16" Wire	T10_B-2		38.07	8.12	46.03	-1314.86	5752.34	157.66	
8	Hardware		D	0.12	1.40	46.15	-1313.46	5714.26	195.74	
9	**3** Meters 5/16" Wire			3.00	0.64	49.15	-1312.82	5714.14	195.86	
10	Hardware		M	0.06	0.70	49.21	-1312.12	5711.14	198.86	
11	Sediment Trap		Y	3.79	55.68	53.00	-1256.44	5711.08	198.92	**200**
12	Hardware		G	0.13	1.80	53.13	-1254.64	5707.29	202.71	
13	3-TON Miller Swivel			0.16	3.17	53.29	-1251.47	5707.16	202.84	
14	Hardware		G	0.13	1.80	53.42	-1249.67	5707.00	203.00	
15	**4.0** Meters 13mm			4.00	10.28	57.42	-1239.39	5706.87	203.13	
16	Hardware		D	0.12	1.40	57.54	-1237.99	5702.87	207.13	
17	**200** Meters 5/16"	T10_A-2		200.38	42.72	257.92	-1195.27	5702.75	207.25	
18	Hardware		D	0.12	1.40	258.04	-1193.87	5502.38	407.62	
19	**88** Meters 5/16" Wire	T09_B-4		88.16	18.79	346.20	-1175.08	5502.26	407.74	
20	Hardware		D	0.12	1.40	346.32	-1173.68	5414.10	495.90	

21	**3** Meters 5/16" Wire			3.00	0.64	349.32	-1173.04	5413.98	496.02	
22	Hardware		M	0.06	0.70	349.38	-1172.34	5410.98	499.02	
23	Sediment Trap		Y	3.83	55.70	353.21	-1116.64	5410.92	499.08	**500**
24	Hardware		G	0.13	1.80	353.34	-1114.84	5407.09	502.91	
25	3-TON Miller Swivel			0.16	3.17	353.50	-1111.67	5406.96	503.04	
26	Hardware		G	0.13	1.80	353.63	-1109.87	5406.80	503.20	
27	**4.0** Meters 13mm			4.00	10.28	357.63	-1099.59	5406.67	503.33	
28	Hardware		D	0.12	1.40	357.75	-1098.19	5402.67	507.33	
29	**1000** Meters 12mm	SK1000-10		1000.00	35.00	1357.75	-1063.19	5402.55	507.45	
30	Hardware		D	0.12	1.40	1357.87	-1061.79	4402.55	1507.45	
31	**1000** Meters 12mm	SK1000-11		1000.00	35.00	2357.87	-1026.79	4402.43	1507.57	
32	Hardware		D	0.12	1.40	2357.99	-1025.39	3402.43	2507.57	
33	4-17" Glassballs on			4.00	-91.32	2361.99	-1116.71	3402.31	2507.69	
34	Hardware		F	0.24	1.90	2362.23	-1114.81	3398.31	2511.69	
35	4-17" Glassballs on			4.00	-91.32	2366.23	-1206.13	3398.07	2511.93	
36	Hardware		D	0.12	1.40	2366.35	-1204.73	3394.07	2515.93	
37	**1000** Meters 12mm	SK1000-12		1000.00	35.00	3366.35	-1169.73	3393.95	2516.05	
38	Hardware		D	0.12	1.40	3366.47	-1168.33	2393.95	3516.05	
39	**500** Meters 12mm	SK500-4		500.00	17.50	3866.47	-1150.83	2393.83	3516.17	
40	Hardware		D	0.12	1.40	3866.59	-1149.43	1893.83	4016.17	
41	**300** Meters 12mm	SK300-4		300.00	10.50	4166.59	-1138.93	1893.71	4016.29	
42	Hardware		B	0.11	1.10	4166.70	-1137.83	1593.71	4316.29	
43	**200** Meters 1/4" Wire	T10_F-3		200.57	28.20	4367.27	-1109.62	1593.60	4316.40	
44	Hardware		B	0.11	1.10	4367.38	-1108.52	1393.03	4516.97	
45	4-17" Glassballs on			4.00	-91.32	4371.38	-1199.84	1392.92	4517.08	
46	Hardware		B	0.11	1.10	4371.49	-1198.74	1388.92	4521.08	
47	**200** Meters 1/4" Wire	T10_F-4		200.59	28.21	4572.08	-1170.54	1388.81	4521.19	
48	Hardware		A	0.10	0.80	4572.18	-1169.74	1188.21	4721.79	
49	**50** Meters 1/4" Wire	T10_G-2		50.15	7.05	4622.33	-1162.69	1188.12	4721.88	
50	Hardware		A	0.10	0.80	4622.42	-1161.89	1137.97	4772.03	
51	**35** Meters 1/4" Wire	T10_H-2		35.10	4.94	4657.52	-1156.95	1137.87	4772.13	
52	Hardware		B	0.11	1.10	4657.63	-1155.85	1102.78	4807.22	
53	**3** Meters 5/16" Wire			3.00	0.64	4660.63	-1155.21	1102.67	4807.33	
54	Hardware		M	0.06	0.70	4660.69	-1154.51	1099.67	4810.33	
55	Sediment Trap		Y	3.80	55.70	4664.49	-1098.81	1099.61	4810.39	**4810.8**
56	Hardware		G	0.13	1.80	4664.62	-1097.01	1095.81	4814.19	
57	3-TON Miller Swivel			0.16	3.17	4664.78	-1093.84	1095.68	4814.32	
58	Hardware		E	0.12	1.50	4664.90	-1092.34	1095.52	4814.48	
59	**1.0** Meters 13mm			1.00	2.57	4665.90	-1089.77	1095.40	4814.60	
60	Hardware		A	0.10	0.80	4665.99	-1088.97	1094.40	4815.60	
61	**500** Meters 1/4" Wire	T10-D		501.46	70.51	5167.45	-1018.46	1094.30	4815.70	
62	Hardware		A	0.10	0.80	5167.55	-1017.66	592.85	5317.15	
61	**300** Meters 1/4" Wire	T10_E-1		300.90	42.31	5468.44	-975.35	592.75	5317.25	
62	Hardware		A	0.10	0.80	5468.54	-974.55	291.85	5618.15	
63	**200** Meters 1/4" Wire	T10_F-5		200.58	28.20	5669.12	-946.35	291.76	5618.24	
64	Hardware		A	0.10	0.80	5669.21	-945.55	91.18	5818.82	
65	**10** Meters 1/4" Wire	adj		10.00	1.41	5679.21	-944.14	91.08	5818.92	
64	Hardware		A	0.10	0.80	5679.31	-943.34	81.08	5828.92	
65	**5** Meters 1/4" Wire			5.00	0.70	5684.31	-942.64	80.99	5829.01	
66	Hardware		B	0.11	1.10	5684.42	-941.54	75.99	5834.01	
67	5 Meters 16mm			5.00	27.80	5689.42	-913.74	75.88	5834.12	
68	Hardware		H	0.23	2.00	5689.65	-911.74	70.88	5839.12	
69	2-17" Glassballs on			2.00	-39.68	5691.65	-951.42	70.65	5839.35	
70	Hardware		H	0.23	2.00	5691.88	-949.42	68.65	5841.35	
71	4-17" Glassballs on			4.00	-79.36	5695.88	-1028.78	68.42	5841.58	
70	Hardware		H	0.23	2.00	5696.11	-1026.78	64.42	5845.58	
71	4-17" Glassballs on			4.00	-79.36	5700.11	-1106.14	64.19	5845.81	
70	Hardware		H	0.23	2.00	5700.34	-1104.14	60.19	5849.81	
71	4-17" Glassballs on			4.00	-79.36	5704.34	-1183.50	59.96	5850.04	

72	Hardware	H	0.23	2.00	5704.57	-1181.50	55.96	5854.04	
73	4-17" Glassballs on		4.00	-79.36	5708.57	-1260.86	55.73	5854.27	
74	Hardware	H	0.23	2.00	5708.80	-1258.86	51.73	5858.27	
75	4-17" Glassballs on		4.00	-79.36	5712.80	-1338.22	51.50	5858.50	
76	Hardware	H	0.23	2.00	5713.03	-1336.22	47.50	5862.50	
77	4-17" Glassballs on		4.00	-79.36	5717.03	-1415.58	47.27	5862.73	
78	Hardware	H	0.23	2.00	5717.26	-1413.58	43.27	5866.73	
79	4-17" Glassballs on		4.00	-79.36	5721.26	-1492.94	43.04	5866.96	
80	Hardware	D	0.12	1.40	5721.38	-1491.54	39.04	5870.96	
81	5 Meters 16mm		5.00	27.80	5726.38	-1463.74	38.92	5871.08	
82	Hardware	G	0.13	1.80	5726.51	-1461.94	33.92	5876.08	
83	3-TON Miller Swivel		0.16	3.20	5726.67	-1458.74	33.79	5876.21	
84	Hardware	I	0.14	2.20	5726.81	-1456.54	33.62	5876.38	
85	Dual EGG Acoustic	L	1.95	66.04	5728.76	-1390.49	33.48	5876.52	
86	Hardware	G	0.13	1.80	5728.89	-1388.69	31.54	5878.46	
87	5 Meters 16mm		5.00	27.80	5733.89	-1360.89	31.41	5878.59	
88	Hardware	J	0.15	2.45	5734.04	-1358.44	26.41	5883.59	
89	**20** Meters 1" Nylon		20.00	5.96	5754.04	-1352.48	26.26	5883.74	
90	Hardware	J	0.15	2.45	5754.19	-1350.03	6.26	5903.74	
91	5 Meters 16mm		5.00	27.80	5759.19	-1322.23	6.11	5903.89	
92	Hardware	J	0.15	2.45	5759.34	-1319.78	1.11	5908.89	**Design**
93	2.116 Ton Anchor		0.96	2116.46	5760.30	796.68	0.96	5909.04	**Depth**
	OVERALL		**5760.30**					5910.00	**5910**

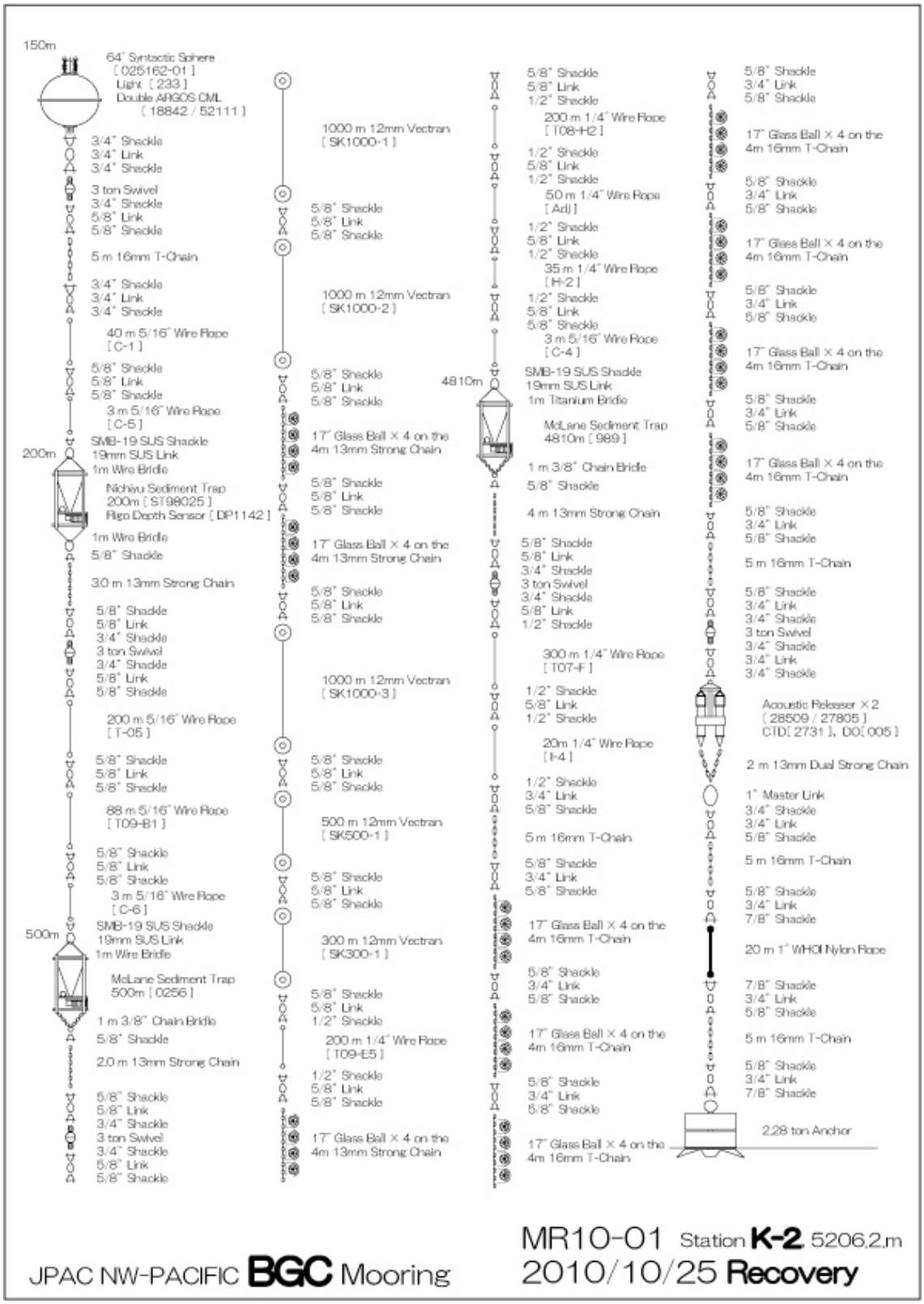

Fig. 3.1-1 Recovery BGC Mooring Figure at K-2

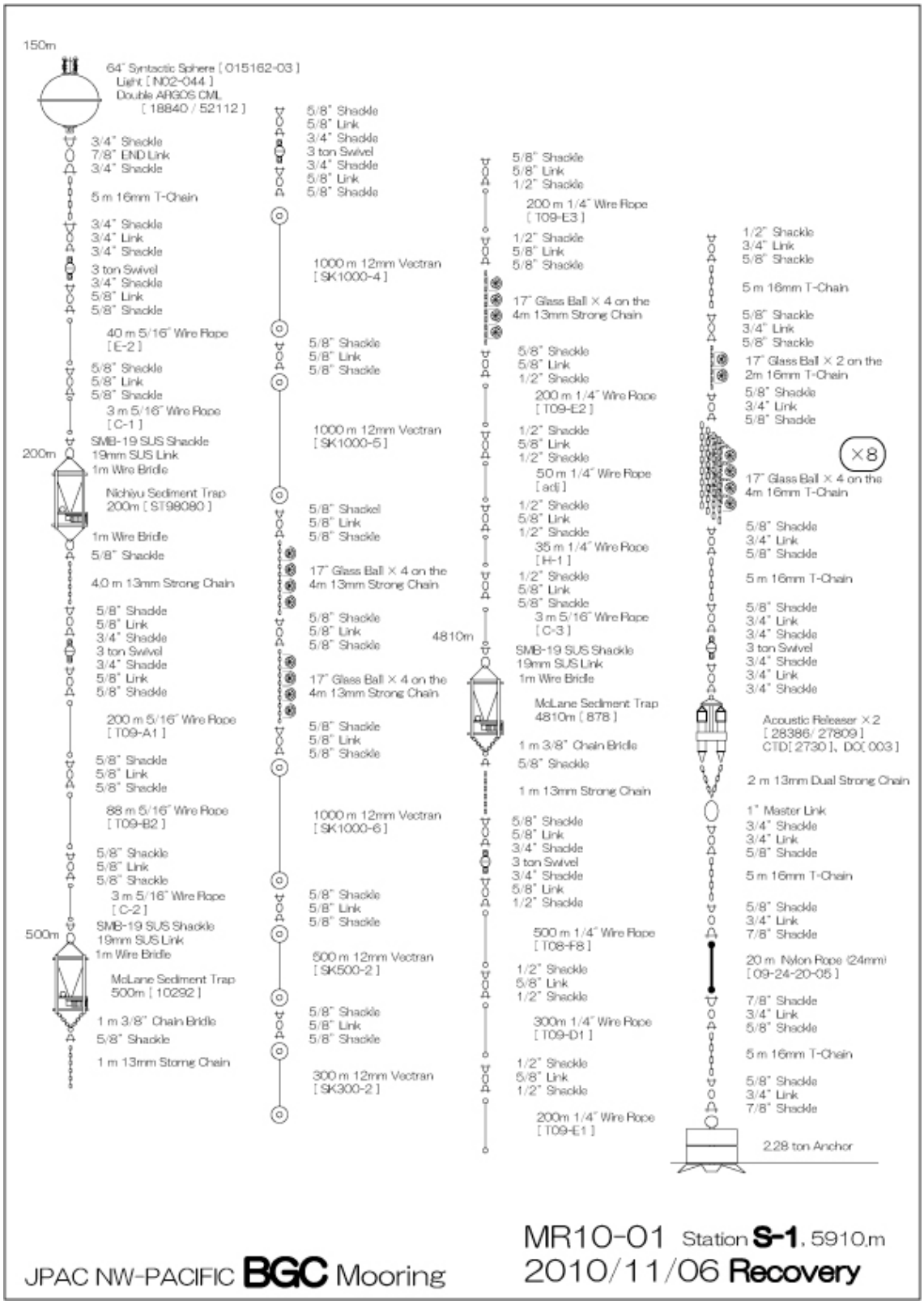

Fig. 3.1-2 Recovery BGC Mooring Figure at S-1

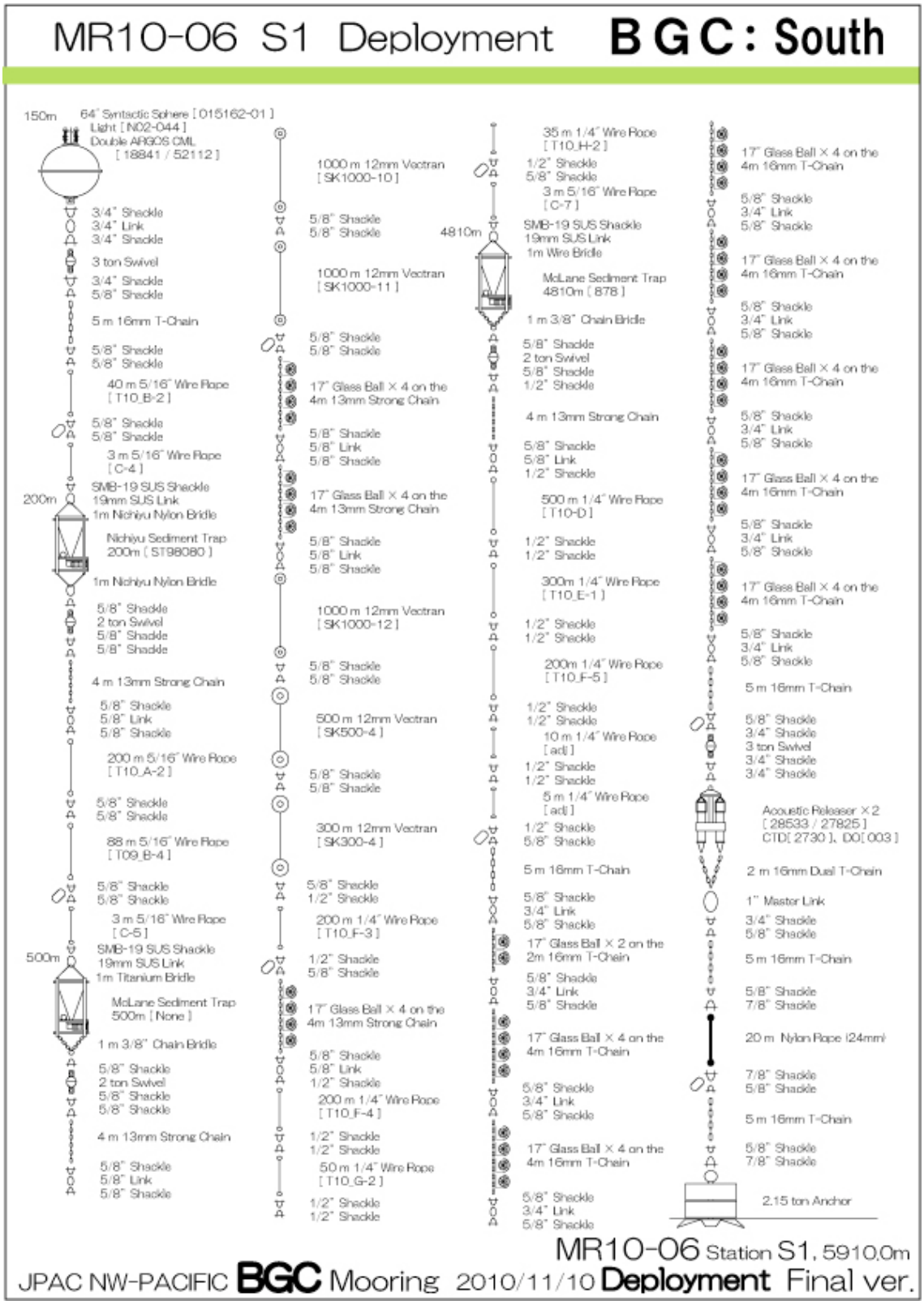

Fig. 3.1-3 Deployment BGC Mooring Figure at K-2

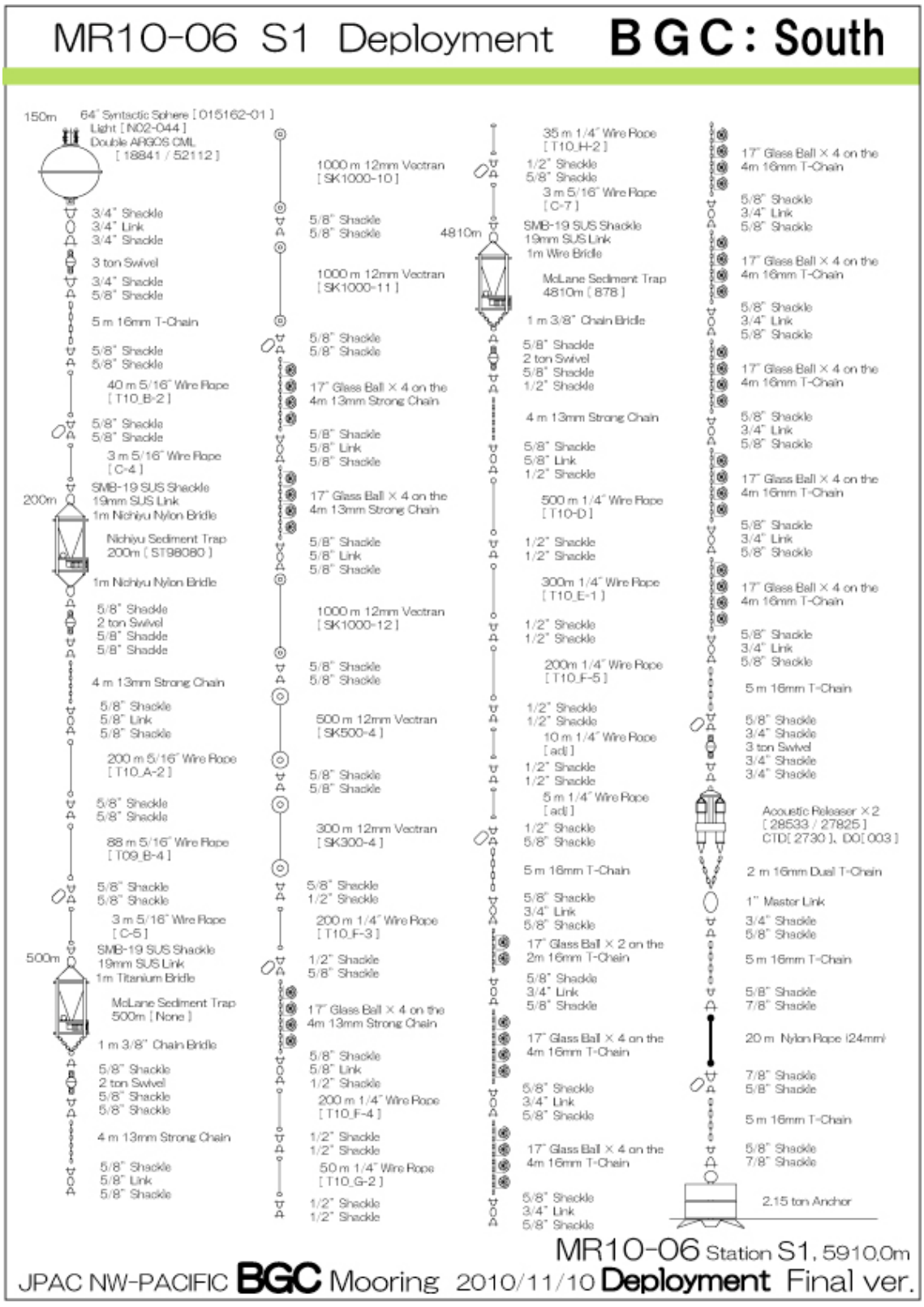

Fig. 3.1-4 Deployment BGC Mooring Figure at S-1

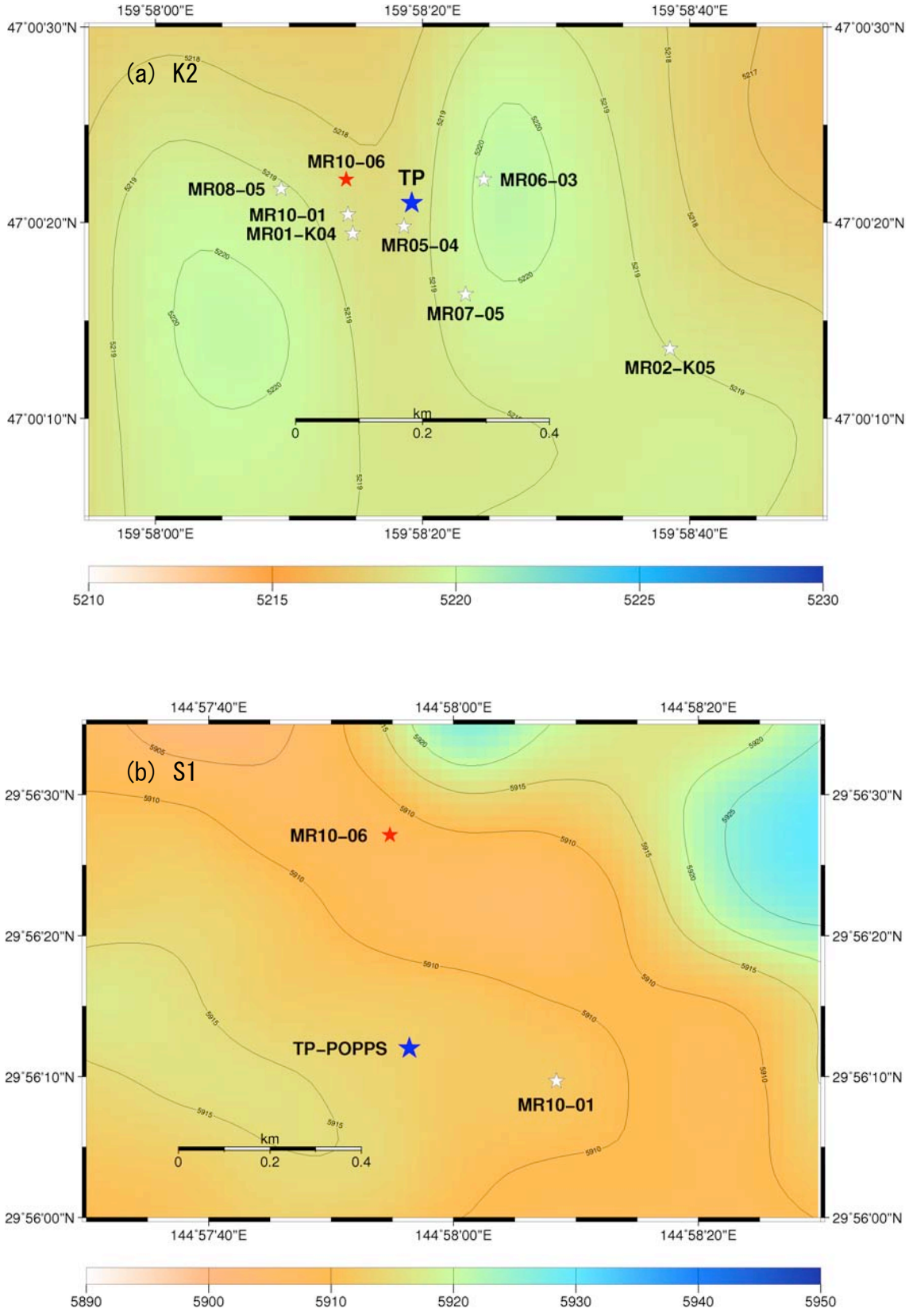

Fig. 3.1.5 Deployed positions of BGC mooring (a) K2, (b) S1

3.1.2 Instruments

On mooring systems, the following instruments are installed.

(1) ARGOS CML (Compact Mooring Locator)

The Compact Mooring Locator is a subsurface mooring locator based on SEIMAC's Smart Cat ARGOS PTT (Platform Terminal Transmitter) technology. Using CML, we can know when our mooring has come to the surface and its position. The CML employs a pressure sensor at the bottom. When the CML is turned ON, the transmission is started immediately every 90 seconds and then when the pressure sensor works ON by approximately 10 dbar, the transmission is stopped. When the top buoy with the CML comes to the surface, the pressure sensor will work OFF and the transmission will be started. Smart Cat transmissions will be initiated at this time, allowing us to locate our mooring. Depending on how long the CML has been moored, it will transmit for up to 120 days on a 90 second repetition period. Battery life, however, is affected by how long the CML has been moored prior to activation. A longer pre-activation mooring will mean less activation life.

Principle specification is as follows:

(Specification)

Transmitter:	Smart Cat PTT
Operating Temp.:	+35 [deg] to –5 [deg]
Standby Current:	80 microamps
Smart Cat Freq.:	401.650 MHz
Battery Supply:	7-Cell alkaline D-Cells
Ratings:	+10.5VDC nom., 10 Amp Hr
Hull:	6061-T6 Aluminum
Max Depth:	1,000 m
Length:	22 inches
Diameter:	3.4 inches
Upper flange:	5.60 inches
Dome:	Acrylic
Buoyancy:	-2.5 (negative) approx.
Weight	12 pounds approx.

(2) Submersible Recovery Strobe

The NOVATECH Xenon Flasher is intended to aid in the marking or recovery of oceanographic instruments, manned vehicles, remotely operated vehicles, buoys or structures. Due to the occulting (firing closely spaced bursts of light) nature of this design, it is much more visible than conventional marker strobes, particularly in poor sea conditions.

(Specification)

Repetition Rate:	Adjustable from 2 bursts per second to 1 burst every 3 seconds.
Burst Length:	Adjustable from 1 to 5 flashes per burst. 100 ms between flashes nominal.
Battery Type:	C-cell alkaline batteries.
Life:	Dependent on repetition rate and burst length. 150 hours with a one flash burst every 2 seconds.
Construction:	Awl-grip painted, Hard coat anodized 6061 T-6 aluminum housing.
Max. Depth:	7,300m
Daylight-off:	User selected, standard

Pressure Switch:	On at surface, auto off when submerged below 10m.
Weight in Air:	4 pounds
Weight in Water:	2 poundsOutside
Diameter:	1.7 inches nominal
Length:	21-1/2 inches nominal

(3) Depth Sensor

RMD Depth sensor is digital memory type and designed for mounting on the plankton net and instrument for mooring and so on. It is small and right weight for easy handling. Sampling interval is chosen between 2 and 127 seconds or 1 and 127 minutes and sampled Time and Depth data. The data is converted to personal computer using exclusive cable (printer interface).

(Specification)

Model:	RMD-500
Operating Depth:	0 ~ 500m
Precision:	0.5% (F.S.)
Accuracy:	1/1300
Memory:	65,534 data (128kbyte)
Battery:	lithium battery (CR2032) DC6V
Battery Life:65,000 data or less than 1 year	
Sample interval:	2 ~ 127 seconds or 1 ~ 127 minutes
Broken Pressure:	20MPa
Diameter:	50mm
Length:	150mm
Main Material:	vinyl chloride resin
Cap material:	polyacetal resin
Weight:	280g

(4) CTD SBE-37

The SBE 37-SM MicroCAT is a high-accuracy conductivity and temperature (pressure optional) recorder with internal battery and memory. Designed for moorings or other long duration, fixed-site deployments, the MicroCAT includes a standard serial interface and nonvolatile FLASH memory. Constructed of titanium and other non-corroding materials to ensure long life with minimum maintenance, the MicroCAT's depth capability is 7000 meters; it is also available with an optional 250-meter plastic *ShallowCAT* housing.

(Specification)

Measurement Range

Conductivity: 0 - 7 S/m (0 - 70 mS/cm)

Temperature: -5 to 35 °C

Optional Pressure: 7000 (meters of deployment depth capability)

Initial Accuracy

Conductivity: 0.0003 S/m (0.003 mS/cm)

Temperature: 0.002 °C

Optional Pressure: 0.1% of full scale range

Typical Stability (per month)

Conductivity: 0.0003 S/m (0.003 mS/cm)

Temperature: 0.0002 °C

Optional Pressure: 0.004% of full scale range

Resolution

Conductivity: 0.00001 S/m (0.0001 mS/cm)

Temperature: 0.0001 °C

Optional Pressure: 0.002% of full scale range

Time Resolution 1 second

Clock Accuracy 13 seconds/month

Quiescent Current * 10 microamps

Optional External Input Power 0.5 Amps at 9-24 VDC

Housing, Depth Rating, and Weight (without pressure sensor)

Standard Titanium, 7000 m (23,000 ft)

Weight in air: 3.8 kg (8.3 lbs)

Weight in water: 2.3 kg (5.1 lbs)

(sampling parameter)

Sampling start time:	Oct. 28th 2008 01:00:00
Sampling interval:	1800 seconds

(5) AREC DO Sensor

AREC DO (Compact Optode) sensor is digital memory type and designed for mounting on the plankton net and instrument for mooring and so on. It is small and right weight for easy handling. Sampling interval is chosen 1 second or 1, 2 and 10 minutes. The data is converted to personal computer using exclusive cable (serial port).

(Specification)

Model:	COMPACT-Optode
Sensor Type:	Fluorescence quenching
Operating Range:	0 ~ 120%
Precision:	0.4%
Accuracy:	within 5%
Memory:	2Mbyte flash memory
Battery:	lithium battery 7Ah
Battery Life:	172800 data
Sample interval:	1,2,5,10,15,20 and 30 seconds
Diameter:	54mm
Length:	272mm
Main Material:	titanium
Weight in water:	0.6kg
Broken Pressure:	60MPa

3.1.3 Sampling schedule

Sediment traps at stations K2 and S1 will collect samples (sinking particles) on the following schedule.

K2

	21cup		26cup	
	500 m, 4810 m		200m	
Int	12		12	
1	2010.11.1	1	2010.11.1	
2	2010.11.13	2	2010.11.13	
3	2010.11.25	3	2010.11.25	
4	2010.12.7	4	2010.12.7	
5	2010.12.19	5	2010.12.19	
6	2010.12.31	6	2010.12.31	
7	2011.1.12	7	2011.1.12	
8	2011.1.24	8	2011.1.24	
9	2011.2.5	9	2011.2.5	
10	2011.2.17	10	2011.2.17	
11	2011.3.1	11	2011.3.1	
12	2011.3.13	12	2011.3.13	
13	2011.3.25	13	2011.3.25	
14	2011.4.6	14	2011.4.6	
15	2011.4.18	15	2011.4.18	
16	2011.4.30	16	2011.4.30	interval
		17	2011.5.6	6 days
17	2011.5.12	18	2011.5.12	
		19	2011.5.18	
18	2011.5.24	20	2011.5.24	
		21	2011.5.30	
19	2011.6.5	22	2011.6.5	
		23	2011.6.11	
20	2011.6.17	24	2011.6.17	
		25	2011.6.23	
21	2011.6.29	26	2011.6.29	
	2011.7.11		2011.7.11	

S1

	21cup		26cup	
	500 m, 4810 m		200m	
Int	12		12	
1	2010.11.13	1	2010.11.13	
2	2010.11.25	2	2010.11.25	
3	2010.12.7	3	2010.12.7	
4	2010.12.19	4	2010.12.19	
5	2010.12.31	5	2010.12.31	
6	2011.1.12	6	2011.1.12	
7	2011.1.24	7	2011.1.24	
8	2011.2.5	8	2011.2.5	
9	2011.2.17	9	2011.2.17	
10	2011.3.1	10	2011.3.1	interval
		11	2011.3.7	6 days
11	2011.3.13	12	2011.3.13	
		13	2011.3.19	
12	2011.3.25	14	2011.3.25	
		15	2011.3.31	
13	2011.4.6	16	2011.4.6	
		17	2011.4.12	
14	2011.4.18	18	2011.4.18	
		19	2011.4.24	
15	2011.4.30	20	2011.4.30	
16	2011.5.12	21	2011.5.12	
17	2011.5.24	22	2011.5.24	
18	2011.6.5	23	2011.6.5	
19	2011.6.17	24	2011.6.17	
20	2011.6.29	25	2011.6.29	
21	2011.7.11	26	2011.7.11	
	2011.7.23		2011.7.23	

	K2
Deployment date	2010.10.31
MR11-04 start date	2011.6.27
Recovery date	ca. 2011.6.29

	S1
Deployment date	2010.11.11
MR11-04 start date	2011.6.27
Recovery date	ca. 2011.7.11

3.1.4 Preliminary results

(1) 200 m sediment trap depth

Depth of 200m sediment trap at station K2 was monitored by a depth sensor (RIGO RMD). Just after sediment trap mooring system was deployed, the trap depth was approximately 218 m, which was approximately 10 m deeper than designed depth (Fig. 3.1.4.1a). The trap depth varied largely from 222 m and 213 m between middle February and late June. Then variation of trap depth became smaller. When variation of trap depth is carefully observed, it was clarified that the trap depth varied following the tidal variability (figure inserted in Fig. 3.1.4.1 a). In general, the trap depth tended to be shallower (from 218 m and 212 m). It might be attributed to the stretch of Vectran and wire ropes used during mooring with high tension. During 2007-2008 and 2008-2010 deployments, 200 m trap was deepened by 350 - 400 m in August or September (see MR08-05 and MR10-01 preliminary cruise reports). However such depth change did not occurred this time (February – November 2010). The difference between the previous mooring system and this mooring system was that the top buoy was located at around 30 m previously while it was located at around 150 m this time.

Depth of 200 m sediment trap at station S1was also monitored by a depth sensor (Nichiyu Giken depth sensor). Although sensitivity of this depth sensor was not so high, it was monitored that depth of 200 m sediment trap also tended to be shallower from 210 m (at early February just after deployment) to 195 m (early November) with small variation (Fig. 3.1.4.1b).

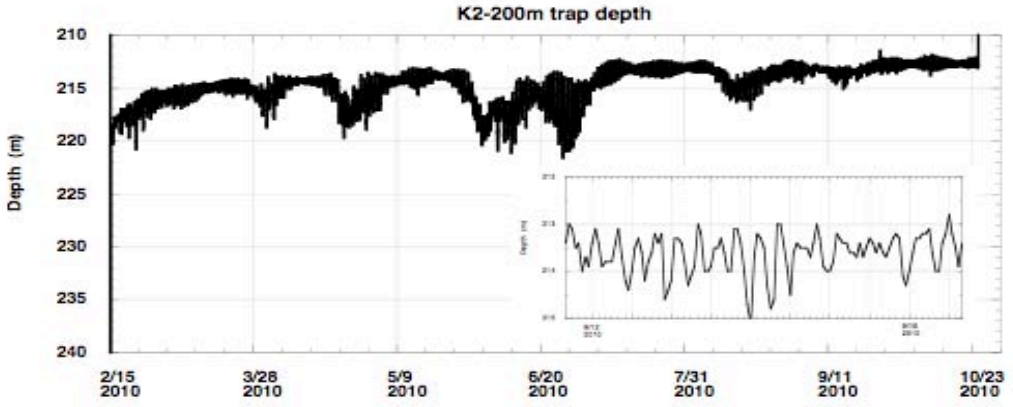

Fig. 3.1.4.1 (a) Depth of 200 m sediment trap at station K2. Figure inserted is time-series variation of depth between 12 – 18 September 2010.

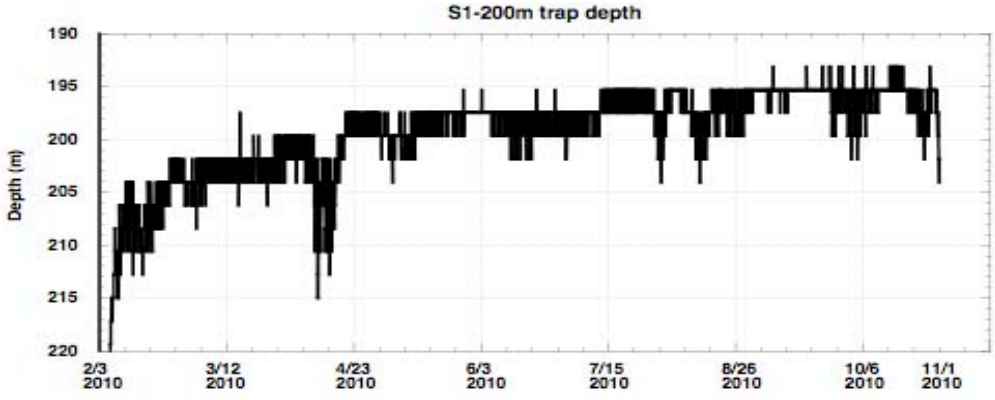

Fig. 3.1.4.1 (b) Depth of 200 m sediment trap at station S1

(2) Sediment trap

Seasonal sinking particle fluxes were collected at approximately 200 m, 500 m and 5000 m at stations K2 and S1 between February and October 2010. In order to know seasonal variability of sinking particle flux qualitatively onboard, heights of collected particles in collecting cups were measured with a scale. Particles collected at 200 m mainly consist of creature larger than 1 mm such as small fish, shrimp and large zooplankton. Thus these materials might not be sinking particles, but "swimmer".

(Station K2)

Sinking particle flux at 200 m started to increase from 22 February (start date of sample collection) and peaked at around middle May (Fig. 3.1.4.2a). Sinking particle flux at 200 m also increased in autumn centering early September. Sinking particle flux at 500 m show similar seasonal variability to that at 200 m with some differences: period of flux peak was delayed by one cup period (12 days), and peak in autumn was smaller than that observed at 200 m (Fig. 3.1.4.2.b). The first peak also appeared at 5000 m with time lag (12 days) from 500 m flux peak (Fig. 3.1.4.2.c). If sinking particle flux at 500 m arrived at 5000 m after 12 days, sinking velocity can be estimated to be approximately 375 m day^{-1}. After high flux was observed, little sinking particles were collected by 5000 m sediment trap. It is likely attributed not to that sinking particle fluxes were very small, but to "the clogging" of 5000 m sediment trap after high flux.

(Station S1)

Sinking particle flux at 200 m increased in late April 2010 (Fig. 3.1.4.2.d). Small flux peak was also observed in late February and early March. Small flux peak was observed in March at 500 m (Fig. 3.1.4.2.e). On the other hand, clear flux increase at 5000 m was not observed (Fig. 3.1.4.2.f). Compared to fluxes at station K2, seasonal variability and flux of sinking particles was very small at station S1.

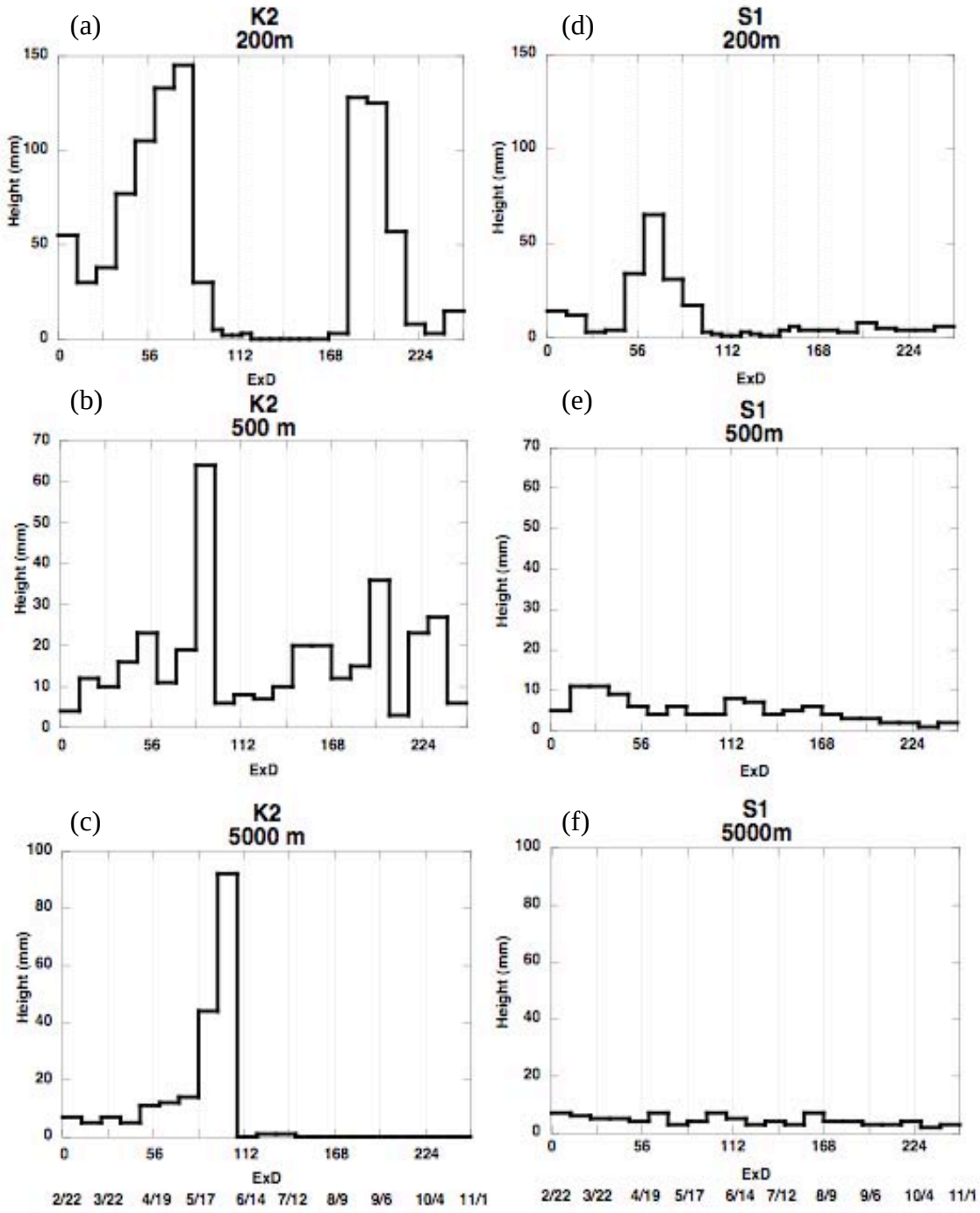

Fig. 3.1.4.2 Visual estimation of total mass flux at respective depths at station K2 (left side figures) and S1 (right side figures)

3.2 Underwater profiling buoy system (Primary productivity profiler)

Tetsuichi FUJIKI (JAMSTEC)
Toru IDAI (MWJ)
Tetsuya NAKAMURA (Nichiyu Giken Kogyo)

(1) Objective

An understanding of the variability in phytoplankton productivity provides a basic knowledge of how aquatic ecosystems are structured and functioning. The primary productivity of the world oceans has been measured mostly by the radiocarbon tracer method or the oxygen evolution method. As these traditional methods use the uptake of radiocarbon into particulate matter or changes in oxygen concentration in the bulk fluid, measurements require bottle incubations for periods ranging from hours to a day. This methodological limitation has hindered our understanding of the variability of oceanic primary productivity. To overcome these problems, algorithms for estimating primary productivity by using satellite ocean color imagery have been developed and improved. However, one of the major obstacles to the development and improvement of these algorithms is a lack of *in situ* primary productivity data to verify the satellite estimates.

During the past decade, the utilization of active fluorescence techniques in biological oceanography has brought marked progress in our understanding of phytoplankton photosynthesis in the oceans. Above all, fast repetition rate (FRR) fluorometry reduces the primary electron acceptor (Q_a) in photosystem (PS) II by a series of subsaturating flashlets and can measure a single turnover fluorescence induction curve in PSII. The PSII parameters derived from the fluorescence induction curve provide information on the physiological state related to photosynthesis and can be used to estimate gross primary productivity. FRR fluorometry has several advantages over the above-mentioned traditional methods. Most importantly, because measurements made by FRR fluorometry can be carried out without the need for time-consuming bottle incubations, this method enables real-time high-frequency measurements of primary productivity. In addition, the FRR fluorometer can be used in platform systems such as moorings, drifters, and floats.

The current study aimed to assess the vertical and temporal variations in PSII parameters and primary productivity in the western Pacific, by using an underwater profiling buoy system that uses the FRR fluorometer (system name: Primary productivity profiler)

(2) Methods

a) Primary productivity profiler

The primary productivity profiler (original design by Nichiyu Giken Kogyo) consisted mainly of an observation buoy equipped with a submersible FRR fluorometer (Diving Flash, Kimoto Electric), a scalar irradiance sensor (QSP-2200, Biospherical Instruments), a CTD sensor (MCTD, Falmouth Scientific) and a dissolved oxygen sensor (Compact Optode, Alec Electronics), an underwater winch, an acoustic Doppler current profiler (Workhorse Long Ranger, Teledyne RD Instruments) and an acoustic releaser (Fig. 1). The observation buoy moved between the winch depth and the surface at a rate of 0.2 m s^{-1} and measured the vertical profiles of phytoplankton fluorescence, irradiance, temperature, salinity and dissolved oxygen. The profiling rate of the observation buoy was set to 0.2 m s^{-1} to detect small-scale variations (approx. 0.5 m) in the vertical profile. To minimize biofouling of instruments, the underwater

winch was placed below the euphotic layer so that the observation buoy was exposed to light only during the measurement period. In addition, the vertical migration of observation buoy reduced biofouling of instruments.

b) Measurement principle of FRR fluorometer

The FRR fluorometer consists of closed dark and open light chambers that measure the fluorescence induction curves of phytoplankton samples in darkness and under actinic illumination. To allow relaxation of photochemical quenching of fluorescence, the FRR fluorometer allows samples in the dark chamber to dark adapt for about 1 s before measurements. To achieve cumulative saturation of PSII within 150 μs — i.e., a single photochemical turnover — the instrument generates a series of subsaturating blue flashes at a light intensity of 25 mmol quanta m^{-2} s^{-1} and a repetition rate of about 250 kHz s^{-1}. The PSII parameters are derived from the single-turnover-type fluorescence induction curve by using the numerical fitting procedure described by Kolber et al. (1998). Analysis of fluorescence induction curves measured in the dark and light chambers provides PSII parameters such as fluorescence yields, photochemical efficiency and effective absorption cross section of PSII, which are indicators of the physiological state related to photosynthesis. Using the PSII parameters, the rate of photosynthetic electron transport and the gross primary productivity can be estimated.

c) Site description and observations

The primary productivity profiler deployed at station K2 in MR10-01 (Fig. 2) was recovered on 28 October 2010 (UTC). At station S1, the primary productivity profiler was newly-deployed on 7 November 2010 (UTC) (Fig. 3, target position: 29° 56.16 N, 144° 58.14 E, 5912 m; actual position: 29° 56.45 N, 144° 57.91 E, 47°N, 5912 m). At station S1, the measurements began on 11 November 2010 and will continue until 15 Febrary 2011.

Measurement schedule at station S1 (Japan time)

1. 10/11/10 02:00	2. 10/11/10 11:00	3. 10/11/11 11:00	4. 10/11/13 02:00
5. 10/11/13 11:00	6. 10/11/14 11:00	7. 10/11/16 02:00	8. 10/11/16 11:00
9. 10/11/17 11:00	10. 10/11/19 02:00	11. 10/11/19 11:00	12. 10/11/20 11:00
13. 10/11/22 02:00	14. 10/11/22 11:00	15. 10/11/23 11:00	16. 10/11/25 02:00
17. 10/11/25 11:00	18. 10/11/26 11:00	19. 10/11/28 02:00	20. 10/11/28 11:00
21. 10/11/29 11:00	22. 10/12/01 02:00	23. 10/12/01 11:00	24. 10/12/02 11:00
25. 10/12/04 02:00	26. 10/12/04 11:00	27. 10/12/05 11:00	28. 10/12/07 02:00
29. 10/12/07 11:00	30. 10/12/08 11:00	31. 10/12/10 02:00	32. 10/12/10 11:00
33. 10/12/11 11:00	34. 10/12/13 02:00	35. 10/12/13 11:00	36. 10/12/14 11:00
37. 10/12/16 02:00	38. 10/12/16 11:00	39. 10/12/17 11:00	40. 10/12/19 02:00
41. 10/12/19 11:00	42. 10/12/20 11:00	43. 10/12/22 02:00	44. 10/12/22 11:00
45. 10/12/23 11:00	46. 10/12/25 02:00	47. 10/12/25 11:00	48. 10/12/26 11:00
49. 10/12/28 02:00	50. 10/12/28 11:00	51. 10/12/29 11:00	52. 10/12/31 02:00
53. 10/12/31 11:00	54. 11/01/01 11:00	55. 11/01/03 02:00	56. 11/01/03 11:00
57. 11/01/04 11:00	58. 11/01/06 02:00	59. 11/01/06 11:00	60. 11/01/07 11:00
61. 11/01/09 02:00	62. 11/01/09 11:00	63. 11/01/10 11:00	64. 11/01/12 02:00
65. 11/01/12 11:00	66. 11/01/13 11:00	67. 11/01/15 02:00	68. 11/01/15 11:00
69. 11/01/16 11:00	70. 11/01/18 02:00	71. 11/01/18 11:00	72. 11/01/19 11:00

73. 11/01/21 02:00	74. 11/01/21 11:00	75. 11/01/22 11:00	76. 11/01/24 02:00
77. 11/01/24 11:00	78. 11/01/25 11:00	79. 11/01/27 02:00	80. 11/01/27 11:00
81. 11/01/28 11:00	82. 11/01/30 02:00	83. 11/01/30 11:00	84. 11/01/31 11:00
85. 11/02/02 02:00	86. 11/02/02 11:00	87. 11/02/03 11:00	88. 11/02/05 02:00
89. 11/02/05 11:00	90. 11/02/06 11:00	91. 11/02/08 02:00	92. 11/02/08 11:00
93. 11/02/09 11:00	94. 11/02/11 02:00	95. 11/02/11 11:00	96. 11/02/12 11:00
97. 11/02/14 02:00	98. 11/02/14 11:00	99. 11/02/15 11:00	

To gain a better understanding of observational data from primary productivity profiler, separately from the primary productivity profiler, we moved up and down a submersible FRR fluorometer between surface and 100~200 m at both the stations K2 and S1 using a ship winch, and measured the vertical and spatial variation in PSII parameters. In addition, the potential photosynthetic activity of phytoplankton assemblage was measured using a desktop type FRR fluorometer.

(3) Preliminary results

The operating condition (up and down) of observation buoy in the primary productivity profiler recovered from station K2 was shown in figure 4.

(4) Data archives

The data will be submitted to JAMSTEC Data Management Office.

(5) References

Kolber, Z. S., O. Prášil and P. G. Falkowski. 1998. Measurements of variable chlorophyll fluorescence using fast repetition rate techniques: defining methodology and experimental protocols. *Biochim. Biophys. Acta*. 1367: 88-106.

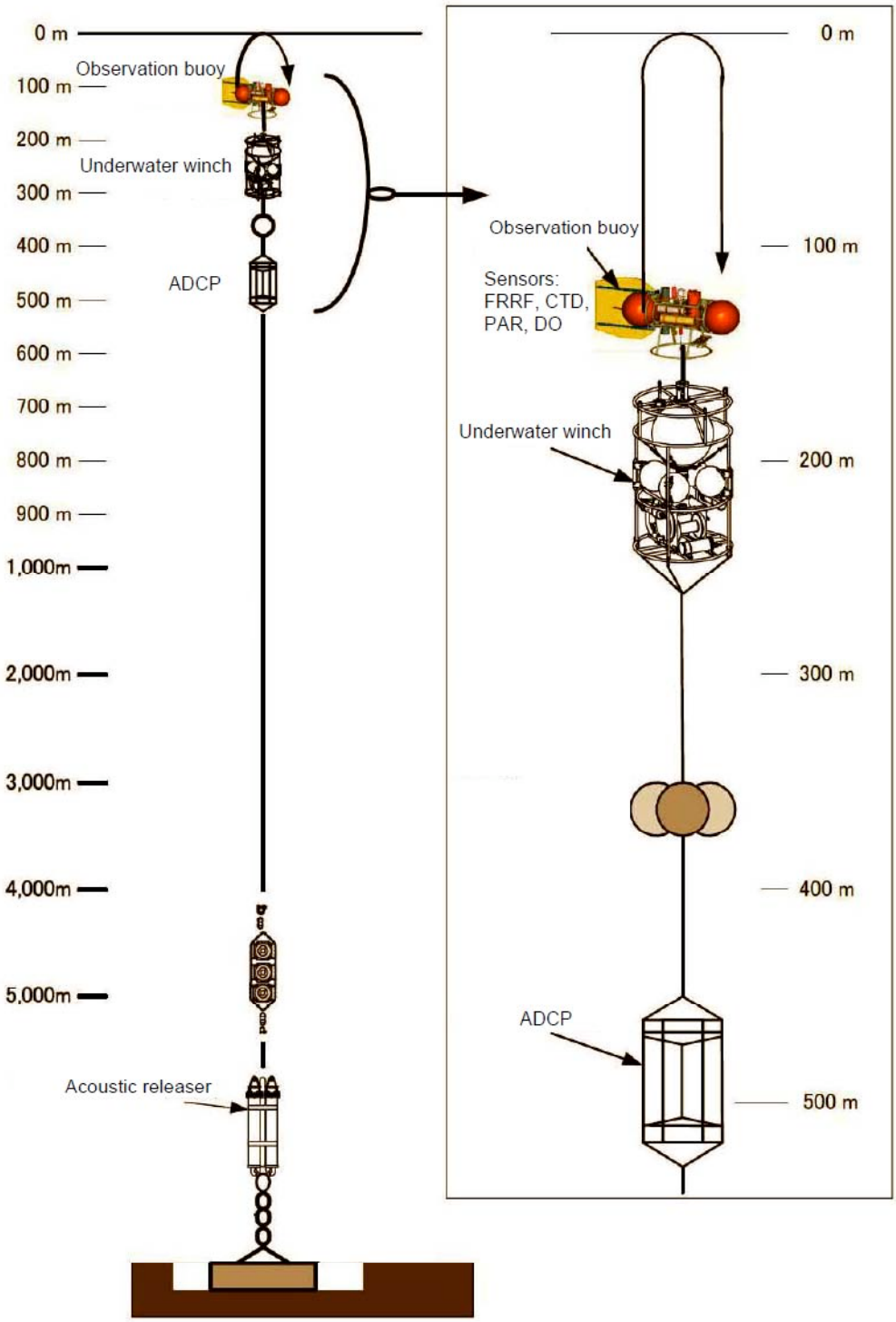

Figure 1a. Schematic diagram of the primary productivity profiler.

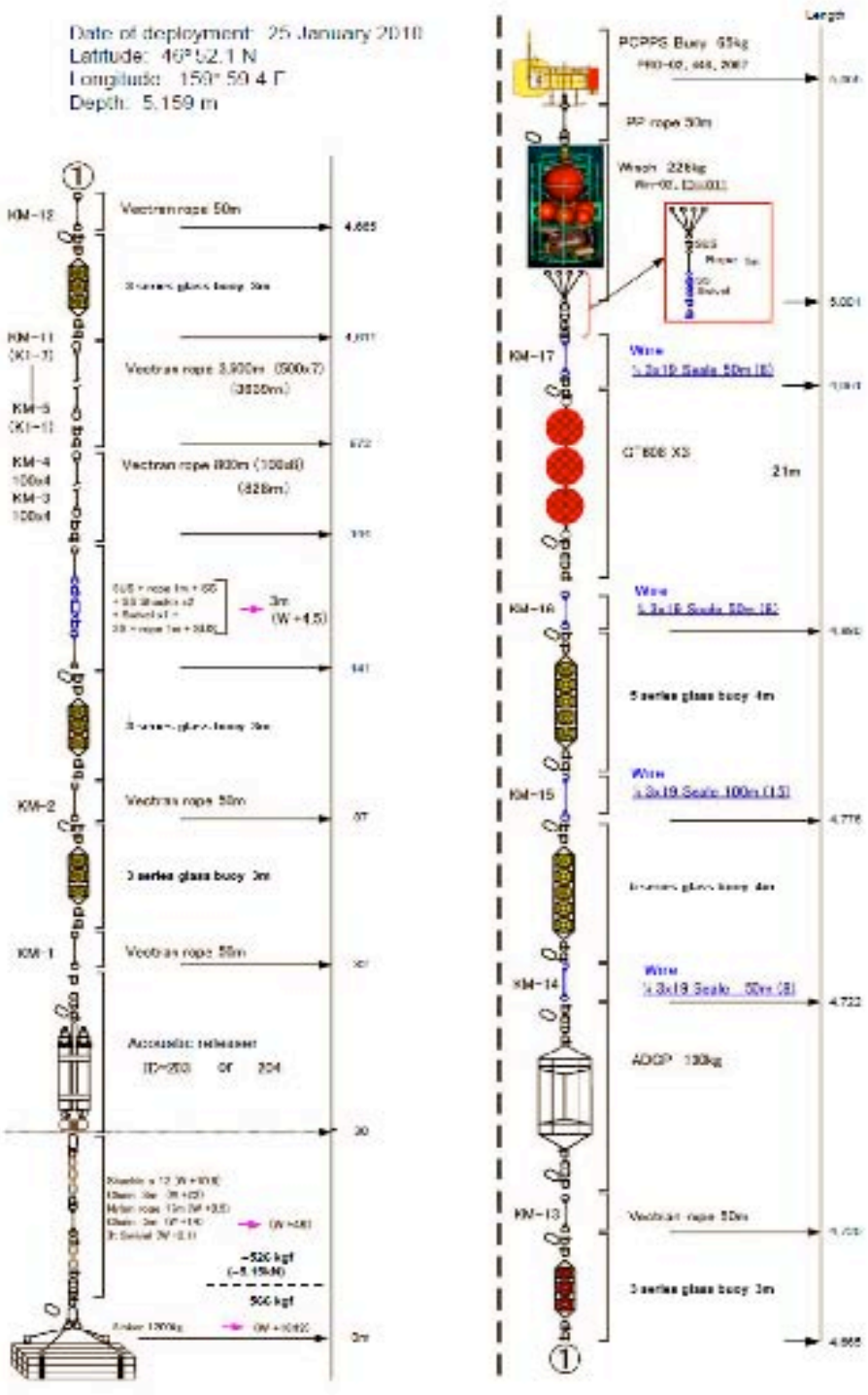

Figure 2. Detailed design of the primary productivity profiler at station K2 deployed in MR10-01.

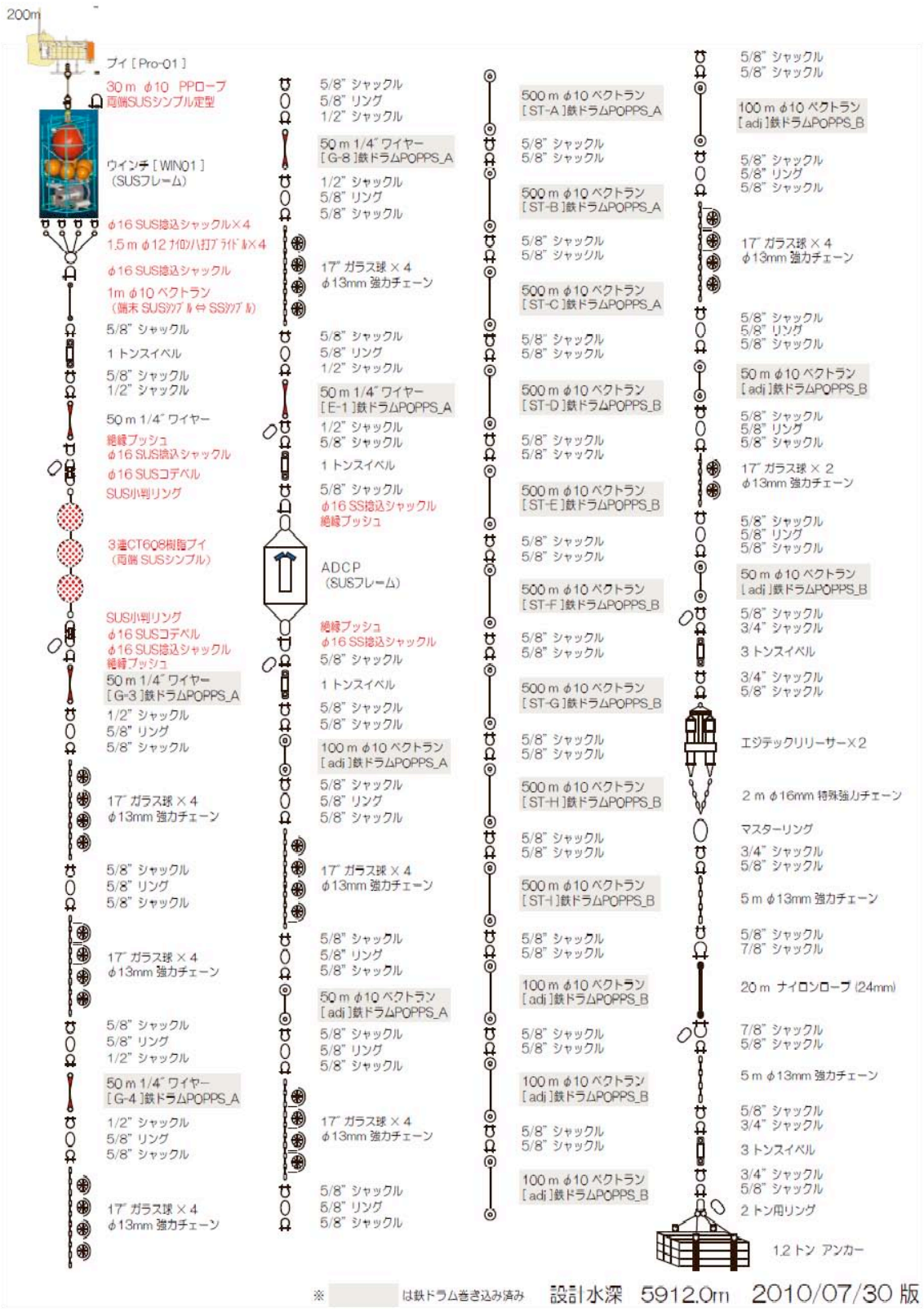

Figure 3. Detailed design of the primary productivity profiler deployed at station S1.

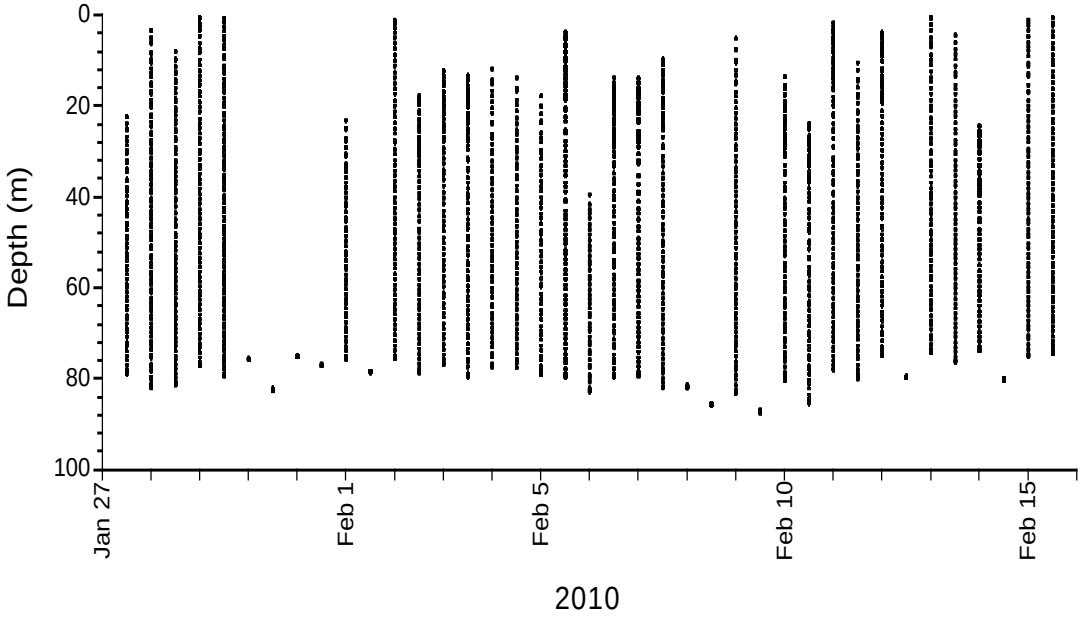

Figure 4. The operating condition (up and down) of observation buoy in the primary productivity profiler recovered from station K2.

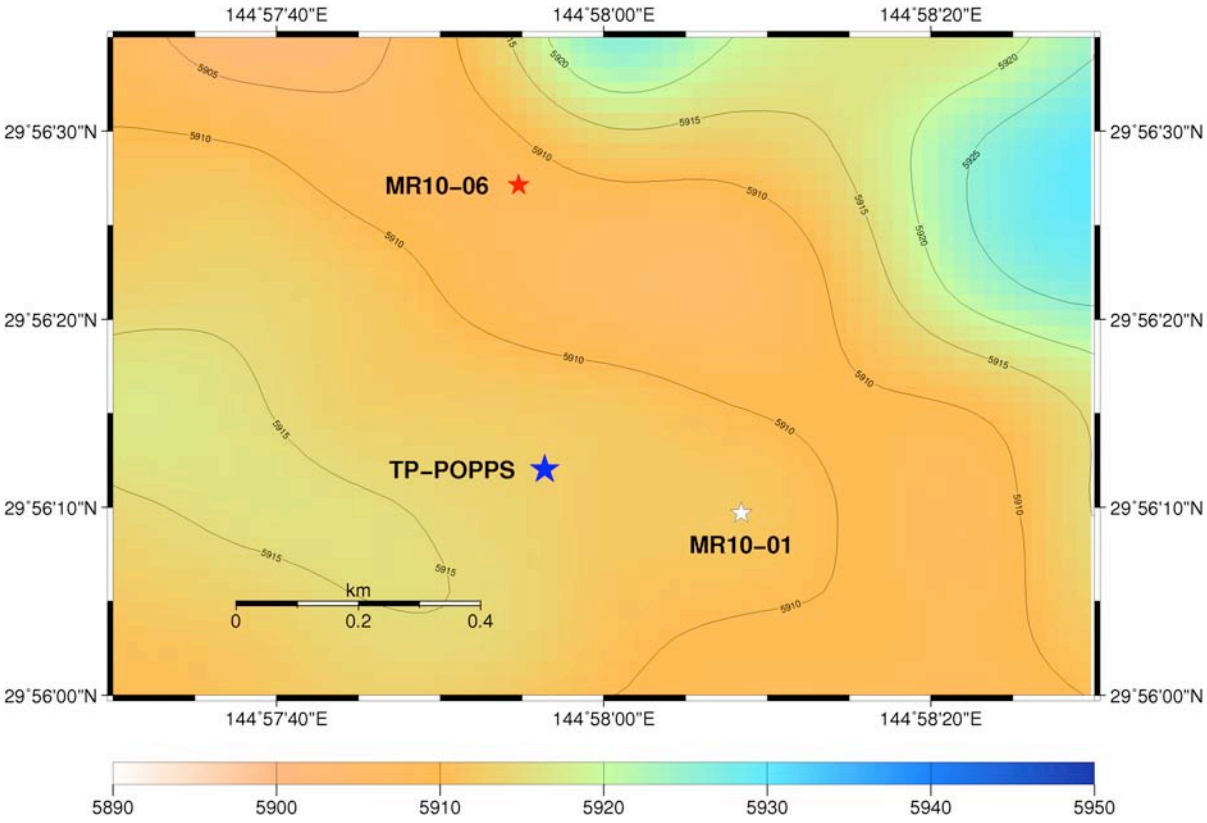

Figure 5. S1-POPPS deployed position.

3.3 Phytoplankton

3.3.1 Chlorophyll *a* measurements by fluorometric determination

Kazuhiko MATSUMOTO **(JAMSTEC); Principal Investigator**
Masahiro ORUI **(MWJ); Operation Leader**

1. Objective

Phytoplankton biomass can estimate as the concentration of chlorophyll *a* (chl-*a*), because all oxygenic photosynthetic plankton contain chl-*a*. Phytoplankton exist various species in the ocean, but the species are roughly characterized by their cell size. The objective of this study is to investigate the vertical distribution of phytoplankton and their size fractionations as chl-*a* by using the fluorometric determination.

2. Sampling

Samplings of total chl-*a* were conducted from 10 depths between the surface and 200 m at all observational stations. At the cast for primary production, water samples were collected at eight depths from among the surface, 0.5%, 1%, 2.5%, 5%, 10%, 25%, 50% light depths relative to the surface and at three other depths between the surface and 200 m at the station of K2 and S1.

3. Instruments and Methods

Water samples (0.5L) for total chl-*a* were filtered (<0.02 MPa) through 25mm-diameter Whatman GF/F filter. Size-fractionated chl-*a* were obtained by sequential filtration (<0.02 MPa) of 1-L water sample through 10-µm, 3-µm and 1-µm polycarbonate filters (47-mm diameter) and Whatman GF/F filter (25-mm diameter). Phytoplankton pigments retained on the filters were immediately extracted in a polypropylene tube with 7 ml of N,N-dimethylformamide (Suzuki and Ishimaru, 1990). Those tubes were stored at –20°C under the dark condition to extract chl-*a* for 24 hours or more.

Fluorescences of each sample were measured by Turner Design fluorometer (10-AU-005), which was calibrated against a pure chl-*a* (Sigma-Aldrich Co.). We applied two kind of fluorometric determination for the samples of total chl-*a*: “Non-acidification method” (Welschmeyer, 1994) and “Acidification method” (Holm-Hansen *et al*., 1965). Size-fractionated samples were applied only “Non-acidification method”. Analytical conditions of each method were listed in table 1.

4. Preliminary Results

The results of total chl-*a* at station K2 and S1 were shown in Figure 1 and 2. The results of size fractionated chl-*a* were shown in Figure3.

6. Data archives

The processed data file of pigments will be submitted to the JAMSTEC Data Integration and Analysis Group (DIAG) within a restricted period. Please ask PI for the latest information.

7. Reference

Suzuki, R., and T. Ishimaru (1990), An improved method for the determination of phytoplankton chlorophyll using N, N-dimethylformamide, *J. Oceanogr. Soc. Japan*, 46, 190-194.

Holm-Hansen, O., Lorenzen, C. J., Holmes, R.W. and J. D. H. Strickland (1965), Fluorometric determination of chlorophyll. *J. Cons. Cons. Int. Explor. Mer.* 30, 3-15.

Welschmeyer, N. A. (1994), Fluorometric analysis of chlrophyll *a* in the presence of chlorophyll *b* and pheopigments. *Limnol. Oceanogr.* 39, 1985-1992.

Table 1. Analytical conditions of "Non-acidification method" and "Acidification method" for chlorophyll *a* with Turner Designs fluorometer (10-AU-005).

	Non-acidification method	Acidification method
Excitation filter (nm)	436	340-500
Emission filter (nm)	680	>665
Lamp	Blue Mercury Vapor	Daylight White

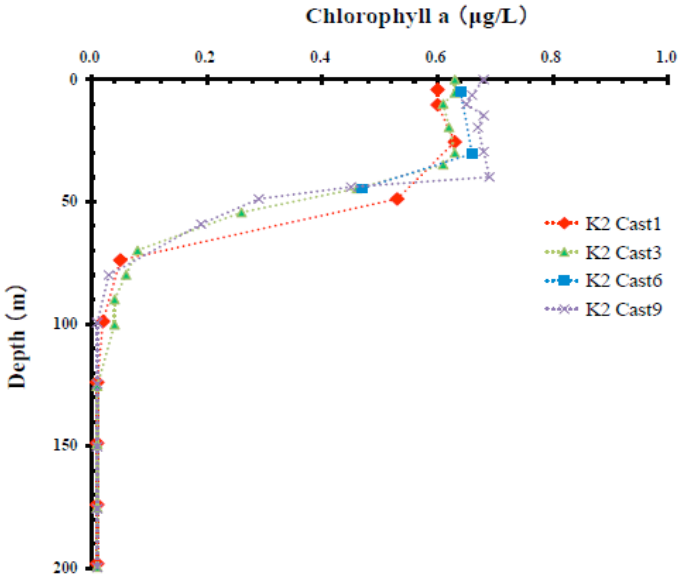

Figure 1. Vertical distribution of chlorophyll *a* at Stn.K2

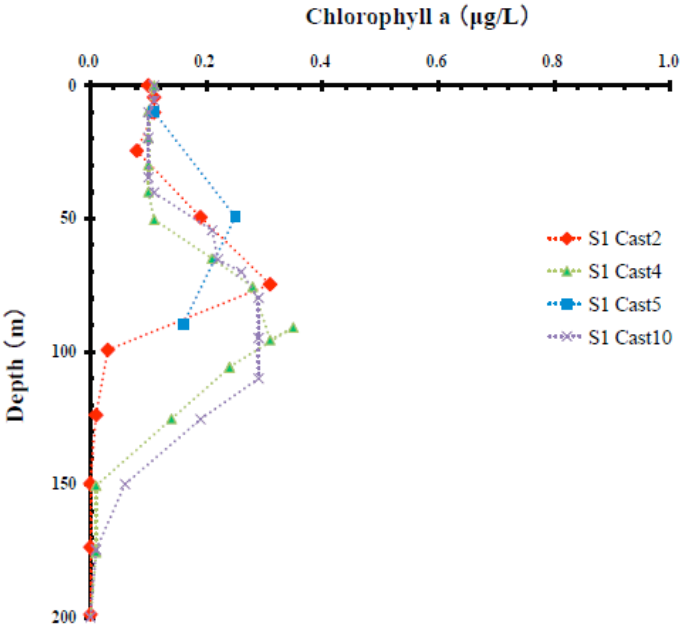

Figure 2. Vertical distribution of chlorophyll *a* at Stn.S1

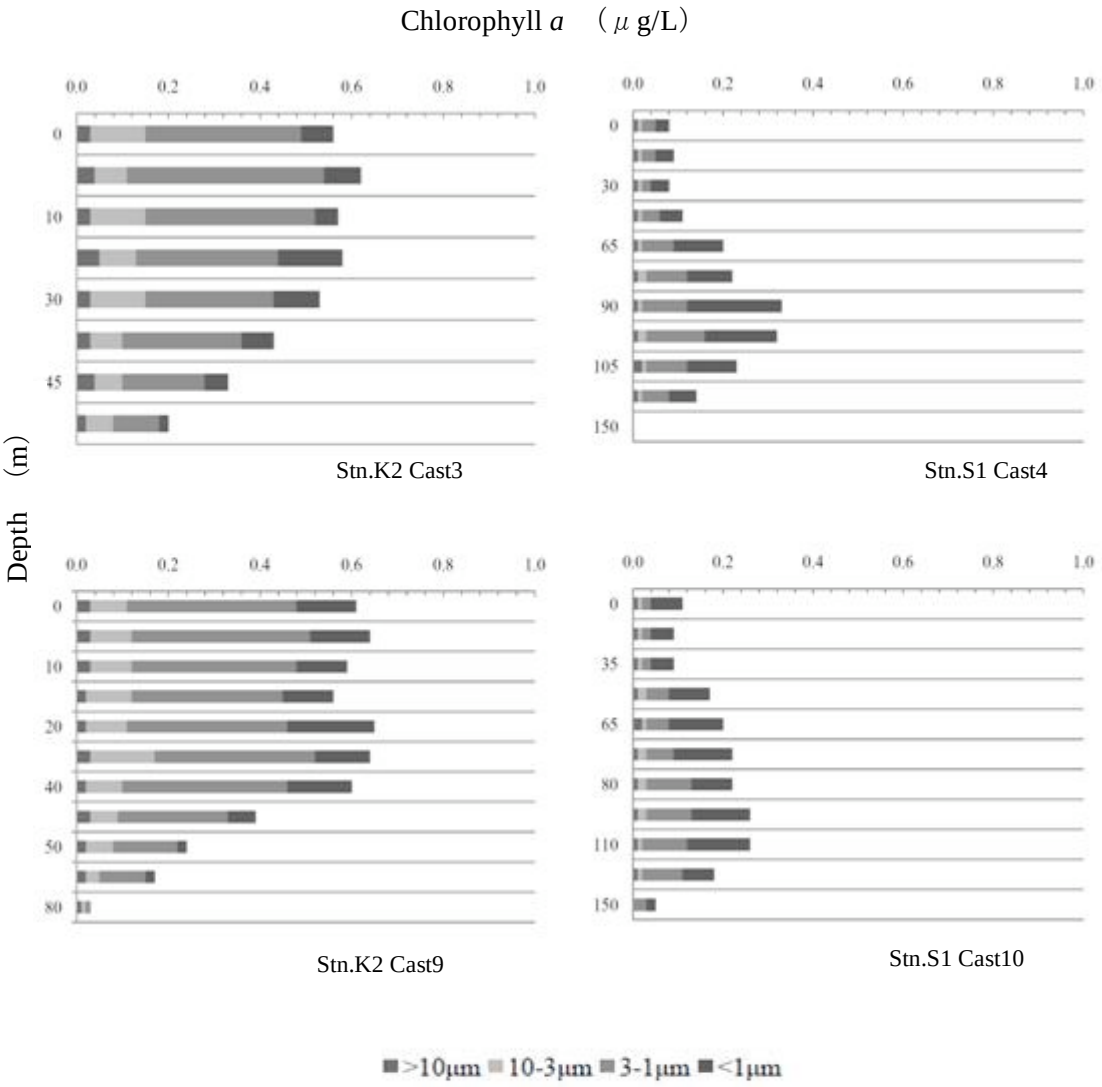

Figure 3. Vertical distribution of size-fractionated chlorophyll *a*

3.3.2. HPLC measurements of marine phytoplankton pigments

Kazuhiko MATSUMOTO (JAMSTEC RIGC)
Shoko TATAMISASHI (MWJ)

(1) Objective

The chemotaxonomic assessment of phytoplankton populations present in natural seawater requires taxon-specific algal pigments as good biochemical markers. A high-performance liquid chromatography (HPLC) measurement is an optimum method for separating and quantifying phytoplankton pigments in natural seawater.

In this cruise, we measured the marine phytoplankton pigments by HPLC to investigate the marine phytoplankton community structure in the northwestern Pacific Ocean.

(2) Methods, Apparatus and Performance

Seawater samples were collected at 10 depths, which were determined by the light intensity as 100, 50, 25, 10, 5, 2.5, 1,0.5% and Chlorophyll Max of surface incident irradiance during shallow-cast using Niskin bottles, except for the surface water (100%), which was taken by a bucket. The water samples (5L) were filtrated at a vacuum-pressure below 0.02MPa through the 47 mm-diameter Whatman GF/F filter. To remove retaining seawater in the sample filters, GF/F filters were vacuum-dried in a freezer (0 °C) within 6 hours. Subsequently, phytoplankton pigments retained on a filter were extracted in a glass tube with 4 ml of N,N-dimethylformamide (HPLC-grade) for at least 24 hours in a freezer (-20 °C), and analyzed by HPLC within a few days.

Residua cells and filter debris were removed through polypropylene syringe filter (pore size: 0.2 μm) before the analysis. The samples (500μl) were injected from the auto-sampler of pure water (150μl) and internal standard (10μl) with the extracted pigments (350μl). Phytoplankton pigments were quantified based on C8 column method containing pyridine in the mobile phase (Zapata *et al*., 2000). The eluant linear gradients of this method were modified slightly to be fit for our system.

(ⅰ) HPLC System

HPLC System was composed by Agilent1200 modular system G1311A Quaternary pump (low-pressure mixing system), G1329A auto-sampler and G1315D photodiode array detector.

(ⅱ) Stationary phase

Analytical separations were performed using a YMC C_8 column (150×4.6 mm). The column was thermostatted at 35 °C in the column heater box.

(ⅲ) Mobile phases

The eluant A was a mixture of methanol : acetonitrile : aqueous pyridine solution (0.25M pyridine) (50 : 25 : 25 v : v : v). The eluant B was a mixture of methanol : acetonitrile : acetone (20 : 60 : 20 v : v : v). Organic solvents for mobile phases were used reagents of HPLC-grade.

(ⅳ) Calibrations

HPLC was calibrated using the standard pigments (Table 1). The solvents of pigment

standards were displaced to N,N-dimethylformamide and the concentrations were determined with spectrophotometer by using its extinction coefficient.

(v) Internal standard

Ethyl-apo-8'-carotenoate was added into the samples prior to the injection as the internal standard. Keep the area values of internal standard at a stable condition (Figure 1). The average of area values was 166±3.46 (n=117), the coefficient of variation was 2.1%.

(vi) Pigment detection and identification

Chlorophylls and carotenoids were detected by photodiode array spectroscopy (350~800nm). Pigment concentrations were calculated from the chromatogram area at different four channels (Table 1).

First channel was allocated at 664 nm of wavelength, the absorption maximum for Divinyl Chlorophyll *a* and Chlorophyll *a*. Second channel was allocated at 462nm, the absorption maximum for Chlorophyll *b*.Third channel was allocated at 440nm, the absorption maximum for [3,8-Divinyl]-Protochlorophyllide. Fourth channel was allocated at 450.0 nm for other pigments.

(3) Preliminary results

Vertical profiles of major pigments at the station of Stn.K2 and Stn.S1. Shown in Figure 2~3. Chlorophyll *a* , Chlorophyll *b* , 19'-Hexanoyloxyfucoxanthin are roughly represented as the abundance of total phytoplankton, green algae, diatoms, and haptophytes, respectively . Zeaxanthin, Divinyl Chlorophyll *a* are roughly represented the Prochlorophyta, respectively.

(4) Data archives

The processed data file of pigments will be submitted to the Data Management Office (DMO) within a restricted period. Please ask PI for the latest information.

(5) Reference

Zapata M, Rodriguez F, Garrido JL (2000) Separation of chlorophylls and carotenoids from marine phytoplankton : a new HPLC method using a reversed phase C8 column and pyridine-containing mobile phases. Mar. Ecol. Prog. Ser. 195 : 29-45

Table 1. Retention time and wavelength of identification for pigment standards.

No.	Pigment	Productions	Retention Time (minute)	Wavelength of identification (nm)
1	Chlorophyll *c3*	DHI Co.	8.425	462
2	Chlorophyllide *a*	DHI Co.	10.350	664
3	[3,8-Divinyl]-Protochlorophyllide	DHI Co.	11.045	440
4	Chlorophyll *c2*	DHI Co.	11.641	450
5	Peridinin	DHI Co.	14.599	462
6	Pheophorbide *a*	DHI Co.	16.909	664
7	19'-butanoyloxyfucoxanthin	DHI Co.	18.021	450
8	Fucoxanthin	DHI Co.	19.332	450
9	Neoxanthin	DHI Co.	19.681	440
10	Prasinoxanthin	DHI Co.	21.026	450
11	19'-hexanoyloxyfucoxanthin	DHI Co.	21.843	450
12	Violaxanthin	DHI Co.	21.864	440
13	Diadinoxanthin	DHI Co.	24.495	450
14	Antheraxanthin	DHI Co.	25.922	450
15	Alloxanthin	DHI Co.	27.165	450
16	Diatoxanthin	DHI Co.	28.093	450
17	Zeaxanthin	DHI Co.	28.838	450
18	Lutein	DHI Co.	29.015	450
19	Ethyl-apo-8’-carotenoate	DHI Co.	30.871	462
20	Crocoxanthin	DHI Co.	32.946	450
21	Chlorophyll *b*	SIGMA Co.	33.383	462
22	Divinyl Chlorophyll *a*	DHI Co.	34.693	664
23	Chlorophyll *a*	SIGMA Co.	34.966	664
24	Pheophytin a	DHI Co.	37.374	664
25	Alpha-carotene	DHI Co.	38.032	450
26	Beta-carotene	WACO Ltd.	38.286	450

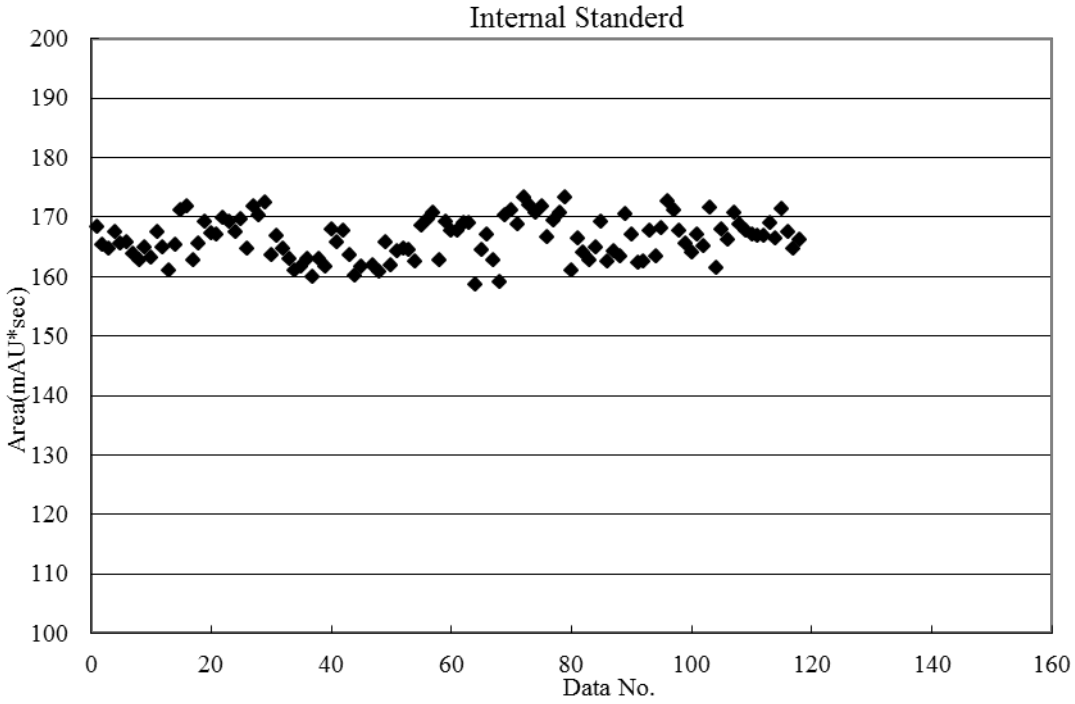

Figure 1. Variabilities of the chromatogram areas for the internal standard.

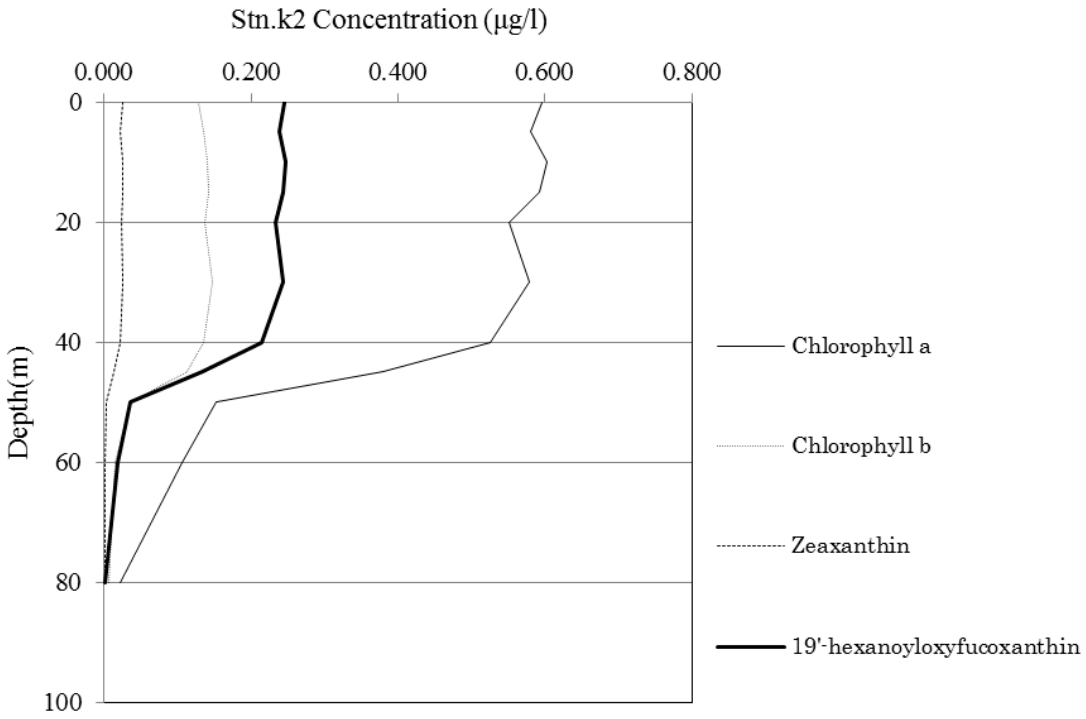

Figuare 2. Vertical distributions of phytoplankton pigments (µg/l) at the Chlorophyll *a* ,Chlorophyll *b*,19'-Hexanoyloxyfucoxanthin and Zeaxanthin by Stn.K2

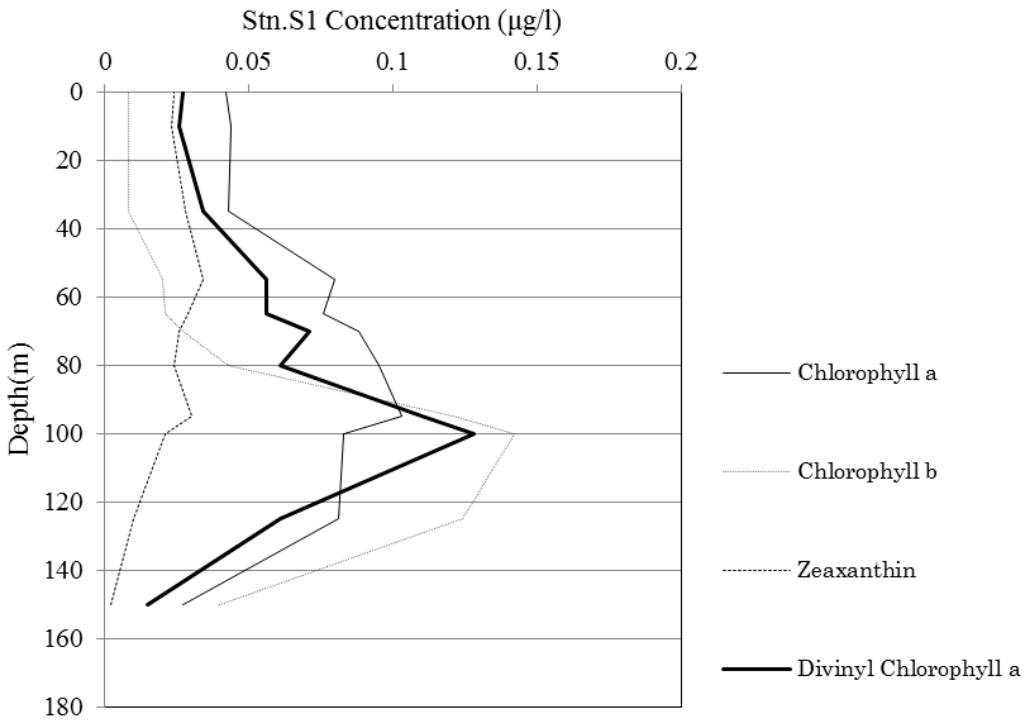

Figuare 2. Vertical distributions of phytoplankton pigments (μg/l) at the Chlorophyll *a* ,Chlorophyll *b*, Divinyl Chlorophyll *a* and Zeaxanthin by Stn.S1

3.3.3 Phytoplankton abundance

Kazuhiko MATSUMOTO (JAMSTEC)

(1) Objectives

The main objective of this study is to estimate phytoplankton abundances and their taxonomy in the subarctic gyre and the subtropical gyre in the western North Pacific. Phytoplankton abundances were measured with two kinds of methods: microscopy for large size phytoplankton and flowcytometry for small size phytoplankton.

(2) Sampling

Samplings were conducted using Niskin bottles, except for the surface water, which was taken by a bucket. Samplings were carried out at the two observational stations of K2 and S1.

(3) Methods

1) Microscopy

Water samples were placed in 500 ml plastic bottle at station K2 and in 1000 ml plastic bottle at station S1. Samples were fixed with neutral-buffered formalin solution (1% final concentration). The microscopic measurements are scheduled after the cruise.

2) Flowcytometry

2)-1 Equipment

The flowcytometry system used in this research was BRYTE HS system (Bio-Rad Laboratories Inc). System specifications are follows:

Light source: 75W Xenon arc lamp
Excitation wavelength: 350-650 nm
Detector: high-performance PMT
Analyzed volume: 75 µl
Flow rate: 10 µl min^{-1}
Sheath fluid: Milli-Q water
Filter block: B2 as excitation filter block, OR1 as fluorescence separator block
B2 and OR1 have ability as follows:

B2:	Excitation filter	390-490 nm
	Beam-splitter	510 nm
	Emission filter	515-720 nm
OR1:	Emission filter 1	565-605 nm
	Beam-splitter	600 nm
	Emission filter 2	>615 nm

2)-2 Measurements

The water samples were fixed immediately with glutaraldehyde (1% final concentration) and stored in the dark at 4°C. The analysis by the flow cytometer was acquired on board within 24 hours after the sample fixation. Calibration was achieved with standard beads of 0.356 – 9.146 µm (Polysciences, Inc.). Standard beads of 2.764 µm were added into each sample prior to the injection of flow cytometer as internal standard. Phytoplankton cell populations were estimated from the forward light scatter signal. Acquired data were

stored in list mode file and analyzed with WinBryte software. Phytoplankton are classified with prokaryotic cyanobacteria (*Prochlorococcus* and *Synechococcus*) and other eukaryotes on the basis of scatter and fluorescence signals. *Synechococcus* is discriminated by phycoerythrin as the orange fluorescence, while other phytoplankton are recognized by chlorophylls as the red fluorescence without the orange fluorescence. *Prochlorococcus* and picoeukaryotes were distinguished with their cell size, but it was difficult to identify the abundance of *Prochlorococcus* accurately in the surface mixed layer due to its decreased chlorophyll fluorescence. The cell size was estimated using the empirically-determined relationship between cell diameter (d_{cell}) and bead diameter (d_{bead}) with the forward light scatter signal (FS) by Blanchot *et al*., (2001) as follows.

$$d_{cell} = d_{bead} (FS)^{1/5}$$

(4) Preliminary result

The vertical profile of phytoplankton group identified by flow cytometer at station K2 is shown in Figure 1. *Prochlorococcus* was not observed in this station. The mean cell size of *Synechococcus* (SYN) was estimated to 0.9 – 1.1 μm, and the population of eukaryotic phytoplankton for EUK-1, EUK-2 and EUK-3 were isolated in cell size of 1.0 – 1.6 μm, 1.7 – 3.7 μm and >3.8 μm, respectively.

(5) Data Archive

All data will be submitted to Data Integration and Analysis Group (DIAG), JAMSTEC. Please ask PI for the latest information.

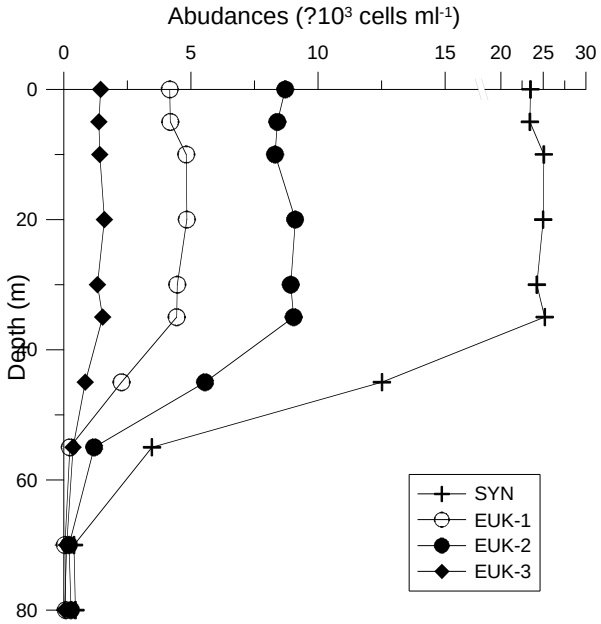

Figure 1. Vertical profile of phytoplankton abundances at K2

3.3.4 Primary production and new production

Kazuhiko MATSUMOTO (JAMSTEC)
Ai YASUDA (MWJ)
Miyo IKEDA (MWJ)
Kanako YOSHIDA (MWJ)

(1) Objective

Quantitative assessment of temporal and spatial variation in carbon and nitrate uptake in the surface euphotic layer should be an essential part of biogeochemical studies in the western North Pacific. Primary production (PP) was measured as incorporation of inorganic C^{13}, and new production (NP), measurement of nitrate uptake rate was conducted with ^{15}N stable isotope tracer at K2 and S1 stations.

(2) Methods

1) Sampling, incubation bottle and filter

Seawater samples were collected using Teflon-coated and acid-cleaned Niskin bottles, except for the surface water, which was taken by a bucket. Sampling depths were determined by the light intensity at eight depths from among the surface, 0.5%, 1%, 2.5%, 5%, 10%, 25%, 50% light depths relative to the surface obtained by SPMR sensor. Seawater samples were placed into acid-cleaned clear polycarbonate bottles in duplicate for PP and NP, and in a single for the dark and the time-zero samples. The time-zero sample was filtered immediately after the addition of ^{13}C and ^{15}N solution. Filtration of seawater sample was conducted with precombusted glass fiber filters (Whatman GF/F 25 mm) with temperature of 450 degree C for at least 4 hours.

2) Incubation

Each bottle was spiked with sufficient $NaH^{13}CO_3$ just before incubation so that ^{13}C enrichment was about 10% of ambient dissolved inorganic carbon as final concentration of 0.2 mmol dm^{-3} (Table 3.3.4-1). The ^{15}N-enriched NO_3, $K^{15}NO_3$ solution, was injected to the incubation bottles (except PP bottles), resulting that the final concentration of ^{15}N enrichment was about 10% of ambient nitrate (Table 3.3.4-2). Incubation was begun at predawn and continued for 24 h, generally by the simulated *in situ* method. The simulated *in situ* method was conducted in the on-deck bath cooled by running surface seawater for the samples within the mixed layer or by immersion cooler for the samples below the mixed layer. The light environment of each bottle in the simulated *in situ* method was adjusted using blue film corresponding to the light levels at the sampling depths. The incubation by the *in situ* method was conducted for PP at the station of S1. In the *in situ* method, bottles were placed appropriate depths on a line attached to a drifting buoy.

3) Measurement

After 24 hours incubation, samples were filtered though GF/F filter, and the filters were kept in a freezer (-20 degree C) on board until analysis. Before analysis, the filters were dried in the oven (45 degree C) for at least 20 hours, and inorganic carbon was removed by acid treatment in a HCl vapor bath for 30 minutes. During the cruise, all samples were measured by a mass spectrometer ANCA-SL system at MIRAI.

Instruments: preprocessing equipment ROBOPLEP-SL (Europa Scientific Ltd.; now SerCon Ltd.)
stable isotope ratio mass spectrometer EUROPA20-20 (Europa Scientific Ltd.; now SerCon Ltd.)
Methods: Dumas method, Mass spectrometry
Precision: All specifications are for n=5 samples.
It is a natural amount and five time standard deviation of the analysis as for amount 100 μg of the sample. We measured repeatability 5 times in this cruise. ^{13}C (0.08 – 0.16 ‰), ^{15}N (0.24 – 0.37 ‰)
Reference Material: The third-order reference materials L-aspartic acid (SHOKO Co., Ltd.)

4) Calculation

(a) Primary Production

Based on the balance of ^{13}C, assimilated organic carbon (ΔPOC) is expressed as follows (Hama *et al*., 1983):

$$^{13}C_{(POC)} * POC = {}^{13}C_{(sw)} * \Delta POC + (POC - \Delta POC) * {}^{13}C_{(0)}$$

This equation is converted to the following equation;

$$\Delta POC = POC * ({}^{13}C_{(POC)} - {}^{13}C_{(0)}) / ({}^{13}C_{(sw)} - {}^{13}C_{(0)})$$

where $^{13}C_{(POC)}$ is concentration of ^{13}C of particulate organic carbon after incubation, *i.e.*, measured value(%). $^{13}C_{(0)}$ is that of particulate organic carbon before incubation, *i.e.*, that for samples as a blank.
$^{13}C_{(sw)}$ is concentration of 13C of ambient seawater with a tracer. This value for this study was determined based on the following calculation;

$$^{13}C_{(sw)}\ (\%) = [(TDIC * 0.011) + 0.0002] / (TDIC + 0.0002) * 100$$

where TDIC is concentration of total dissolved inorganic carbon at respective bottle depth(mol dm^{-3}) and 0.011 is concentration of ^{13}C of natural seawater (1.1%). 0.0002 is added ^{13}C (mol) as a tracer. Taking into account for the discrimination factor between ^{13}C and ^{12}C (1.025), primary production (PP) was, finally, estimated by

$$PP = 1.025 * \Delta POC$$

(b) New production

NO_3 uptake rate or new production (NP) was estimated with following equation:

$$NP\ (\mu g\ dm^{-3}\ day^{-1}) = ({}^{15}N_{excess} * PON) / ({}^{15}N_{enrich}) / day$$

where $^{15}N_{excess}$, PON and $^{15}N_{enrich}$ are excess ^{15}N (measured ^{15}N minus ^{15}N natural abundance, 0.366 atom%) in the post-incubation particulate sample (%), particulate nitrogen content of the sample after incubation (mg dm^{-3}) and ^{15}N enrichment in the dissolved fraction (%), respectively.

(3) Preliminary results

Fig. 3.3.4.1 and 3.3.4.2 show the vertical profile of primary production (PP) and the diurnal change of photosynthetically available radiation (PAR) observed by PUV-510B (Biospherical Instruments Inc.).

(4) Data archives

All data will be submitted to Data Integration and Analyses Group (DIAG), JAMSTEC.

Table 3.3.4-1 Sampling cast table and spike ^{13}C concentration

Incubation type	Station	CTD cast No.	$NaH^{13}CO_3$ (mmol dm^{-3})
SIS	K2	6	0.2
SIS	K2	9	0.2
SIS	S1	4	0.2
IS	S1	4	0.2
SIS	S1	10	0.2

Table 3.3.4-2 Sampling cast table and spike ^{15}N concentration

Incubation type	Station	CTD cast No.	Light Intensity	$K^{15}NO_3$ (μmol dm^{-3})
SIS	K2	6	100 % - 1.0 % 0.5 %	1.2 1.5
SIS	K2	9	100 % - 1.0 % 0.5 %	1.0 1.4
SIS	S1	4	100 % - 10 % 5.0% - 2.5 % 1.0% 0.5 %	0.005 0.01 0.2 0.35
SIS	S1	10	100 % - 5.0 % 2.5 % - 1.0% 0.5 %	0.005 0.01 0.1

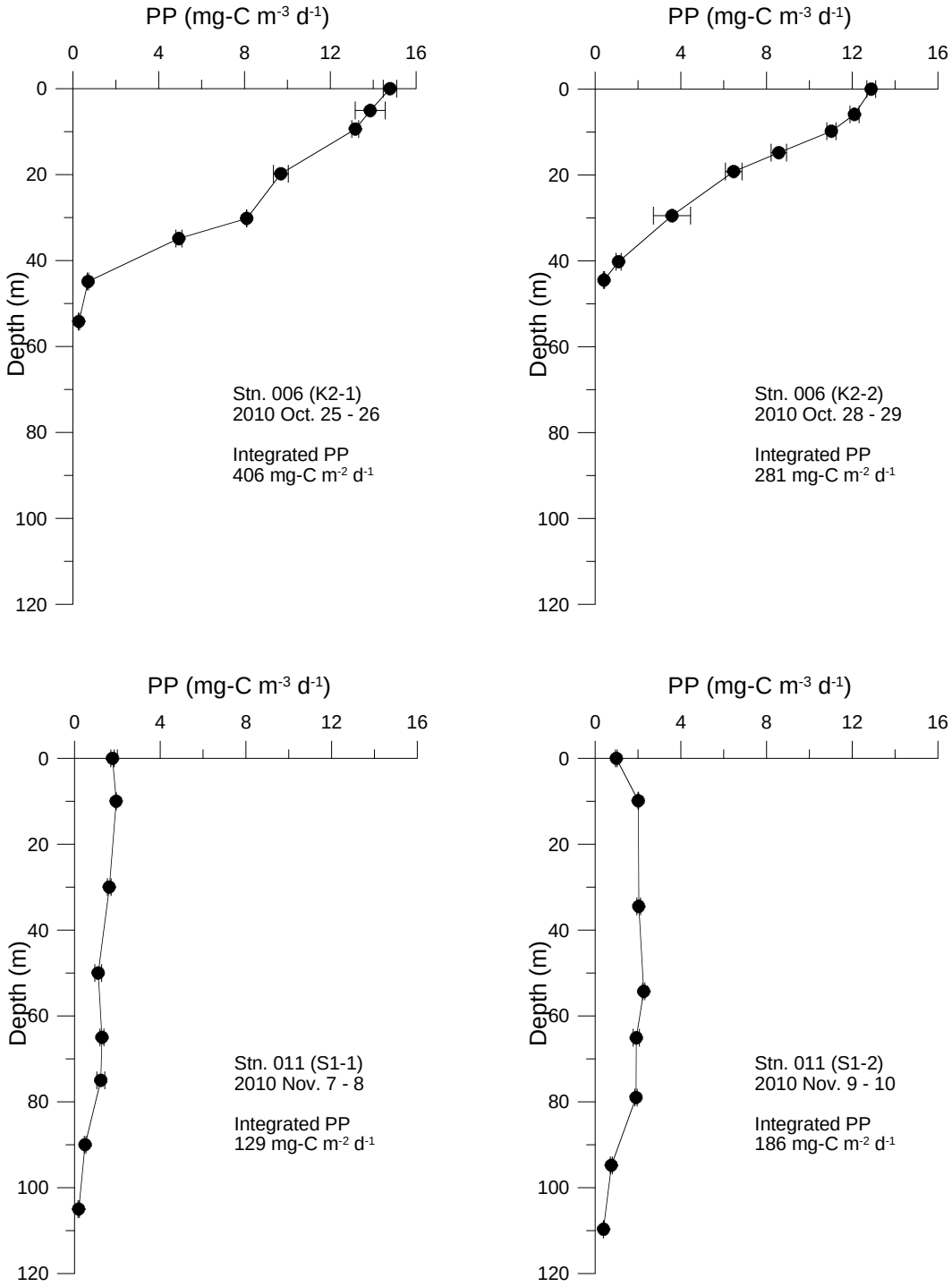

Figure 3.3.4.1 Vertical profile of primary production

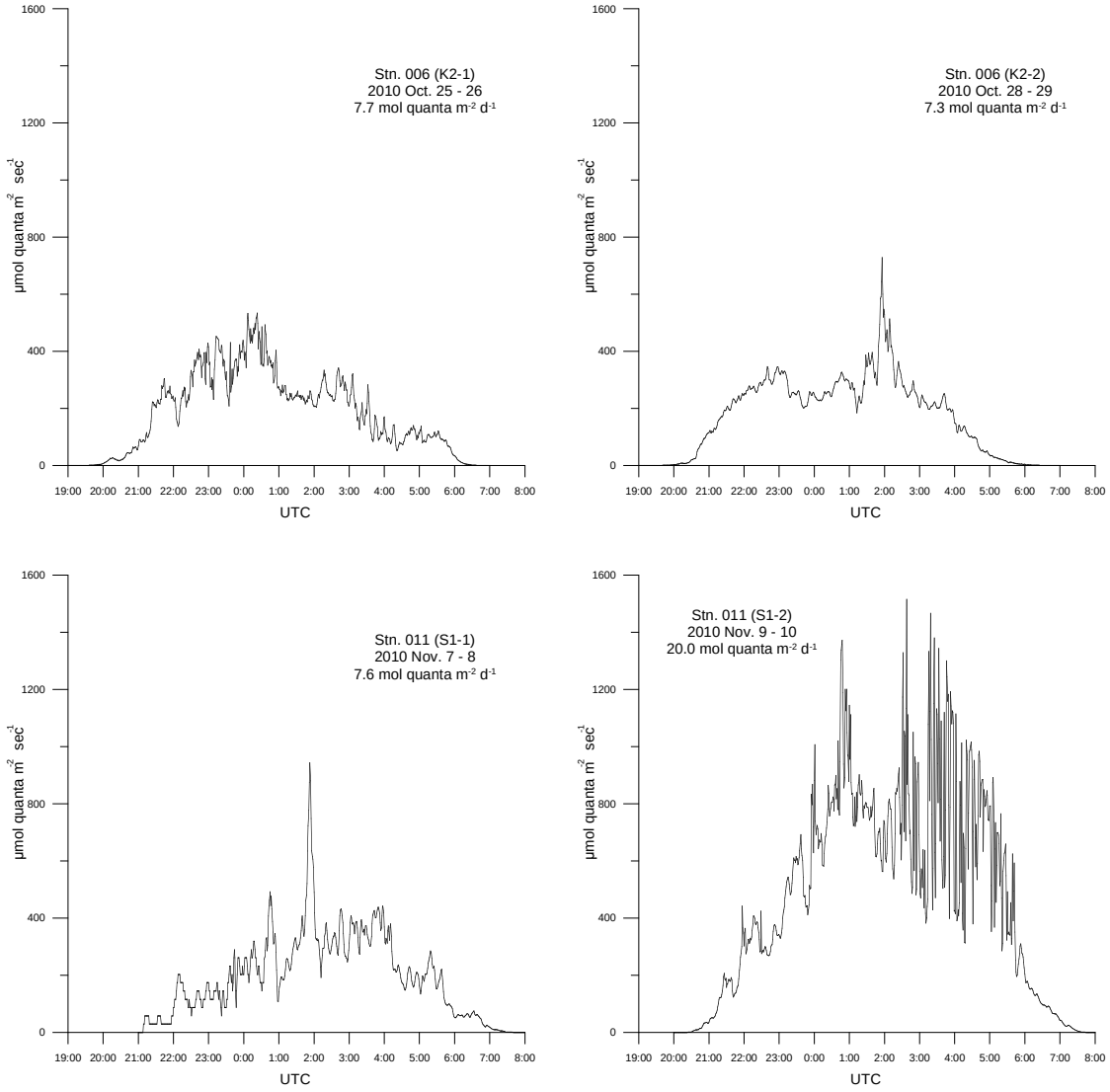

Figure 3.3.4.2 Photosynthetically available radiation (PAR) during incubation experiment

3.3.5 P vs. E curve

Kazuhiko MATSUMOTO (MIO)
Ai YASUDA (MWJ)
Miyo IKEDA (MWJ)
Kanako YOSHIDA (MWJ)

(1) Objectives

The objective of this study is to estimate the relationship between phytoplankton photosynthetic rate (P) and scalar irradiance (E) in the western North Pacific.

(2)Methods

1) Sampling

Samplings were carried out at two observational stations of K2 and S1. Sample water was collected at three depths of different irradiance level, using Teflon-coated and acid-cleaned Niskin bottles.

2) Incubation

Three incubators filled in water were used, illuminated at one end by a 500W halogen lamp. Water temperature was controlled by circulating water cooler (Fig. 3.3.5-1). Water samples were poured into acid-cleaned clear nine flasks (approx. 1 liter) and arranged in the incubator linearly against the lamp after adding the isotope solutions. The isotope solutions of 0.2 mmol dm^{-3} (final concentration) of $NaH^{13}CO_3$ solution were spiked. All flasks were controlled light intensity by shielding with a neutral density filter on lamp side. The light intensities inside the flasks were shown in Table 3.3.5. The incubations were begun at about local noon and continued for 3 h. Filtration of seawater sample was conducted with glass fiber filters (Whatman GF/F 25 mm) which precombusted with temperature of 450 degree C for at least 4 hours.

3) Measurement

After the incubation, samples were treated as same as the primary production experiment. During the cruise, all samples were measured by a mass spectrometer ANCA-SL system at MIRAI. The analytical function and parameter values used to describe the relationship between the photosynthetic rate (P) and scalar irradiance (E) are best determined using a least-squares procedure from the following equation.

$$P = P_{max}(1-e^{-\alpha E/Pmax})e^{-b\alpha E/Pmax}$$: (Platt et al., 1980)

where, P_{max} is the light-saturated photosynthetic rate, α is the initial slope of the P vs. E curve, b is a dimensionless photoinhibition parameter.

(3) Preliminary results

The *P – E* curves obtained at the stations of K2 and S1 are shown in Fig. 3.3.5-2 and 3.3.5-3.

(4) Data archives

All data will be submitted to Data Integration and Analyses Group (DIAG),

JAMSTEC.

(5) Reference

Platt, T., Gallegos, C.L. and Harrison, W.G., 1980. Photoinhibition of photosynthesis in natural assemblages of marine phytoplankton. *Journal of Marine Research*, 38, 687-701.

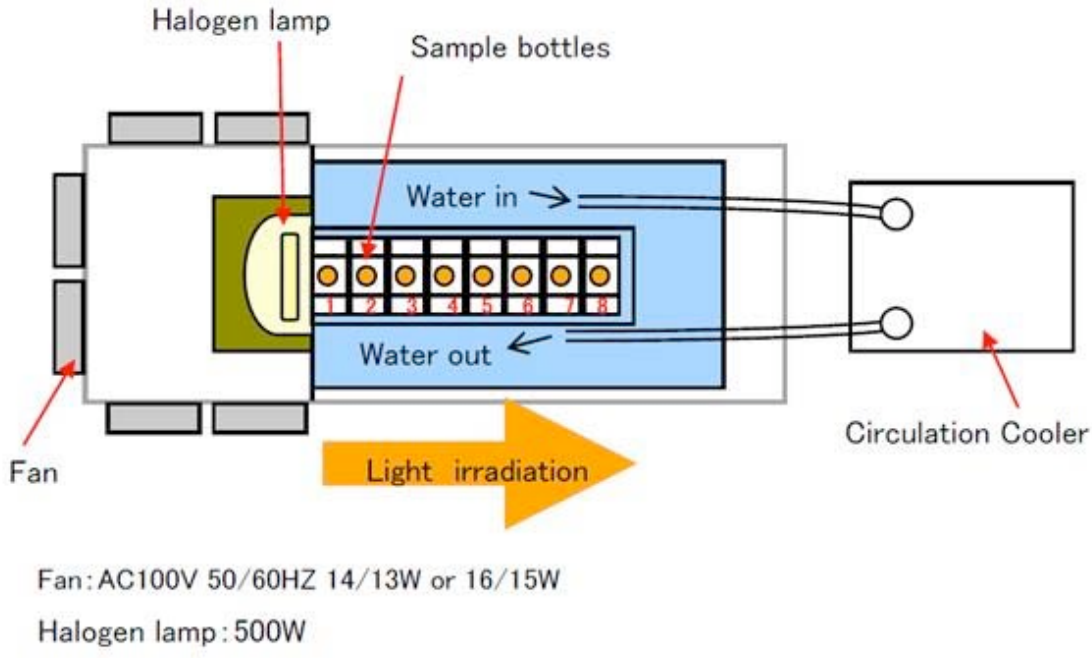

Fig. 3.3.5-1 Look down view of Incubator for Photosynthesis and irradiation curve

Table 3.3.5 Light Intensity of P vs. E measurements

	Bath A	Bath B	Bath C
Bottle No.	Light intensity (µE m^{-2} sec^{-1})		
1	2050	2050	2000
2	1000	1050	1000
3	470	500	460
4	210	220	200
5	100	100.0	92
6	47	44.0	46
7	20	20.0	20.5
8	8	8.2	8.4
9	0	0	0

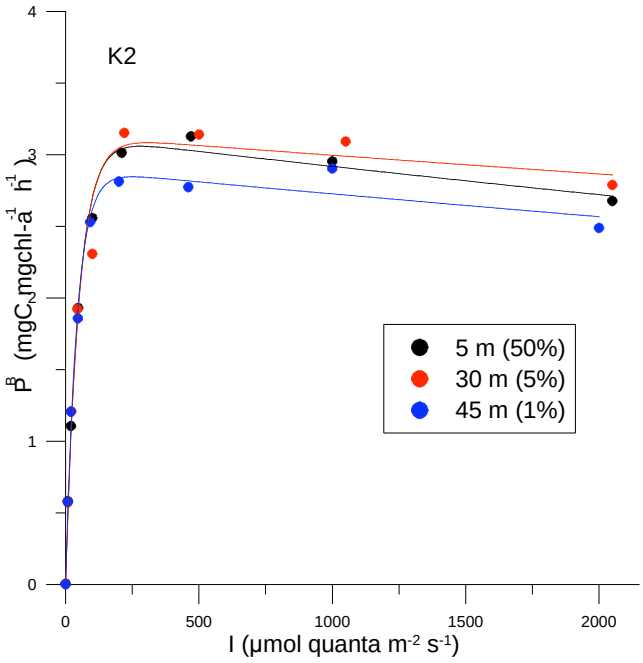

Fig. 3.3.5-2

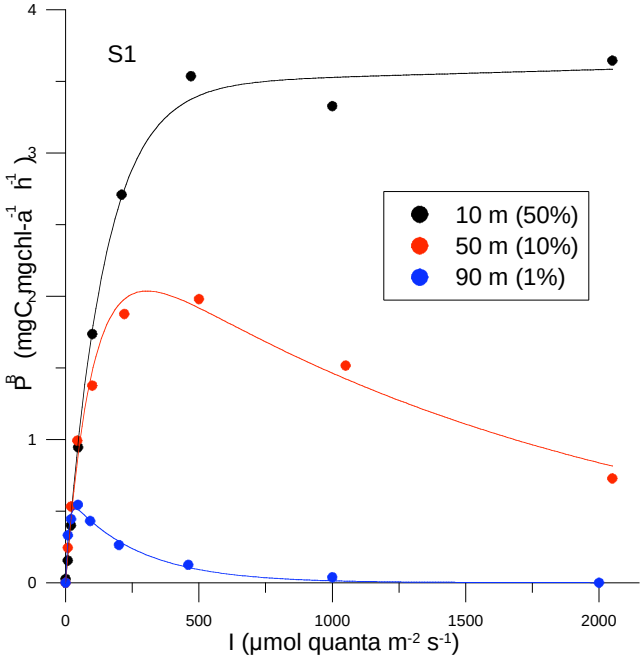

Fig. 3.3.5-3

3.3.6. Oxygen evolution (gross primary productivity)

Tetsuichi FUJIKI (JAMSTEC)
Hironori SATO (MWJ)

(1) Objective

Primary productivity in the world's oceans has been measured mostly by the carbon tracer or oxygen evolution methods. In incubations of 24 hours, the former method provides the values closest to net primary productivity (NPP), while the latter comes closest to gross primary productivity (GPP). The GPP is defined as total amount of oxygen released by phytoplankton photosynthesis. The NPP/GPP ratio provides fundamental information on the metabolic balance and carbon cycle in the ocean. In the MR10-06, the GPP was measured using the light–dark bottle method at the stations K2 and S1.

(2) Methods

In the same cast as the ^{13}C uptake experiment (section 3.3.4), seawater samples were collected from eight depths corresponding to light levels of approximately 100, 50, 25, 10, 5, 2.5, 1 and 0.5% of surface light intensity, using a bucket (surface only). Seawater samples were carefully transferred from Niskin bottle into volume calibrated flasks (ca. 100 cm^3). At each light depth, three light and three dark bottles were incubated under light condition that simulated those of the original sampling depth as the ^{13}C uptake experiment. The dark bottles were wrapped with aluminum foil. After 24 h incubation, the light and dark bottles were fixed immediately. Fixing, storage, reagent preparation, measurement and standardization were followed the dissolve oxygen section (2.4). The GPP was estimated by adding the dark respiration in dark bottles to the net oxygen evolution in light bottles.

(3) Preliminary results

The vertical profiles of GPP measured at stations K2 and S1 were shown in figure 3.3.6.1.

(4) Data archives

The data will be submitted to Data Integration and Analyses Group (DIAG), JAMSTEC.

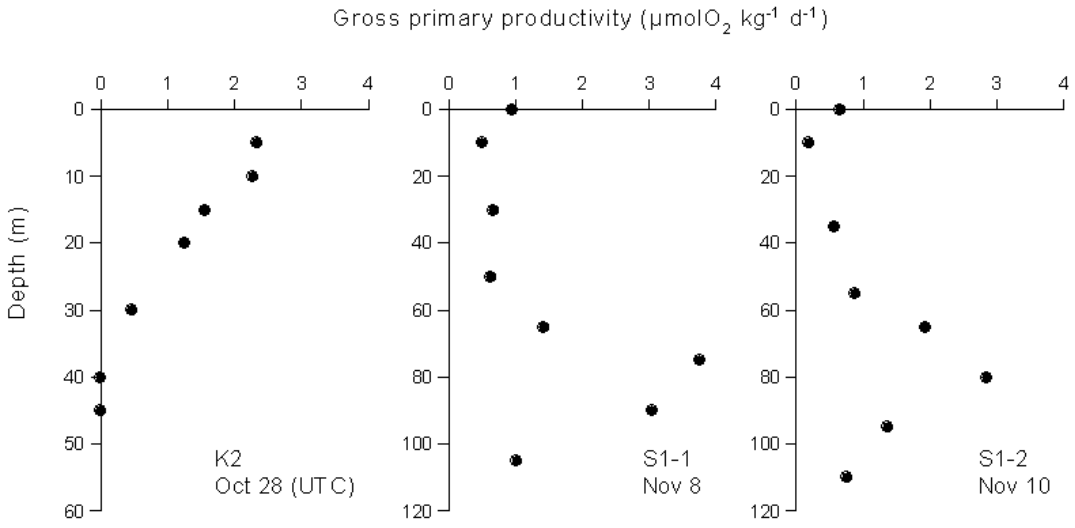

Figure 3.3.6.1. Vertical profiles of gross primary productivity (GPP) at stations K2 and S1.

3.4 Optical measurement

Makio HONDA (JAMSTEC RIGC)
Kazuhiko MATSUMOTO (JAMSTEC RIGC)

(1) Objective

The objective of this measurement is to investigate the air and underwater light conditions at respective stations and to determine depths for *in situ* or simulated *in situ* measurement of primary production by using carbon stable isotope (C-13) during late autumn. In addition, optical data can be used for the validation of satellite data.

(2) Description of instruments deployed

The instrument consisted of the SeaWiFS Profiling Multichannel Radiometer (SPMR) and SeaWiFS Multichannel Surface Reference (SMSR). The SPMR was deployed in a free fall mode through the water column (see right picture). The SPMR profiler called "Free Fall" has a 13 channel irradiance sensors (Ed), a 13 channel radiance sensors (Lu), tilt sensor, and fluorometer. The SMSR has a 13 channel irradiance sensors (Es) and tilt meter (Table 1). These instruments observed the vertical profiles of visible and ultra violet light and chlorophyll concentration.

Table 1. Center wavelength (nm) of the SPMR/SMSR

Es	379.5	399.6	412.2	442.8	456.1	490.9	519.0	554.3	564.5	619.5	665.6	683.0	705.9
Ed	380.0	399.7	412.4	442.9	455.2	489.4	519.8	554.9	565.1	619.3	665.5	682.8	705.2
Lu	380.3	399.8	412.4	442.8	455.8	489.6	519.3	554.5	564.6	619.2	665.6	682.6	704.5

Optical measurements by Free Fall were conducted at our time-series station K2 and S1. Measurements should be ideally conducted at median time. However observations were conducted irregularly because of limited ship-time and other observation's convenience (Table 2). The profiler was dropped twice a each deployment to a depth of 200 m. The SMSR was mounted on the anti-rolling system's deck and was never shadowed by any ship structure. The profiler descended at an average rate of 1.0 m/s with tilts of less than 3 degrees except near surface.

Observed data was analyzed by using software "Satlantic PPROSOFT 6" and extinction rate and photosynthetically available radiation (PAR) were computed.

Table 2 Locations of optical observation and principle characteristics
(Date and Time in LST: UTC+11hr at station K2 and UTC+10hr at station S1)

Date and Time	Station	Lat./Long.	Surface PAR (quanta cm^{-2} sec^{-1})	Euphotic layer* (m)	Memo
2010.10.25 12:02	K2	47N/160E	8.7×10^{15}	~ 56	1 day before PP incubation #1
2010.10.28 11:22	K2	47N/160E	5.2×10^{16}	~ 45	during PP incubation #1
2010.10.29 14:55	K2	47N/160E	9.5×10^{15}	~ 56	1 day before PP incubation #2
2010.11.07 11:27	S1	30N/145E	1.2×10^{16}	~ 100	1 day before PP incubation #1
2010.11.08 10:00	S1	30N/145E	1.5×10^{16}	~ 101	during PP incubation #1
2010.11.09 14:41	S1	30N/145E	6.4×10^{16}	~ 103	1 day before PP incubation #2
2010.11.10 11:27	S1	30N/145E	5.3×10^{16}	~ 102	during PP incubation #2

* Euphotic layer: 0.5% of surface PAR

(3) Preliminary result

We deployed “Free Fall sensor” three times at station K2 and four times at station S1 (Table 2). Surface PAR ranged from approximately 8.7×10^{15} to 6.4×10^{15} quanta cm^{-2} sec^{-1} and surface PAR at S1 was higher than that at K2 on average (2.37×10^{16} and 3.67×10^{16} quanta cm^{-2} sec^{-1} at K2 and S1, respectively). The euphotic layers ,that is defined as water depth with 0.5 % of surface PAR, were approximately 50 m at station K2 and 100 m at station S1. It is likely attributed to the amount of particulate materials, *i.e.* phytoplankton, in the water column: the amount of phytoplankton was likely smaller at S1 than those at K2 although surface PAR was higher at S1.

(4) Data archive

Optical data were filed on two types of file.

(BIN file) digital data of upwelling radiance and downwelling irradiance each 1 m from near surface to approximately 100 m for respective wave-lengths with surface PAR data during “Free Fall” deployment

(PAR file) in situ PAR each 1 m from near surface to approximately 100 m with extinction coefficient with surface PAR data during “Free Fall” deployment

These data files will be submitted to JAMSTEC Data Integration and Analyses Group (DIAG).

3.5 Drifting sediment trap

3.5.1 Drifting mooring system

Hajime KAWAKAMI (JAMSTEC MIO)
Makio C. HONDA (JAMSTEC RIGC)

In order to conduct drifting sediment trap experiment at stations K2 and S1, drifting mooring system (drifter) was deployed. This drifter consists of radar reflector, GPS radio buoy (Taiyo TGB-100), flush light, surface buoy, ropes and sinker. On this system, “Knauer” type sediment trap at 4 layers were installed together. Thanks to the effort by MWJ technicians, drifting mooring system was upgraded on board. The configuration is shown in Fig. 3.5.1-1.

The drifter was deployed at 20:14 on 28 October (UTC) at station K2 and at 21:09 on 8 November (UTC) at station S1. The drifter was recovered after 3 days. The drifter’s position was monitored by using GPS radio buoy (Taiyo TGB-100). Fig. 3.5.1-2 shows tracks of the drifter. In general, the drifter tended to drift eastward and northward at stations K2 and S1, respectively.

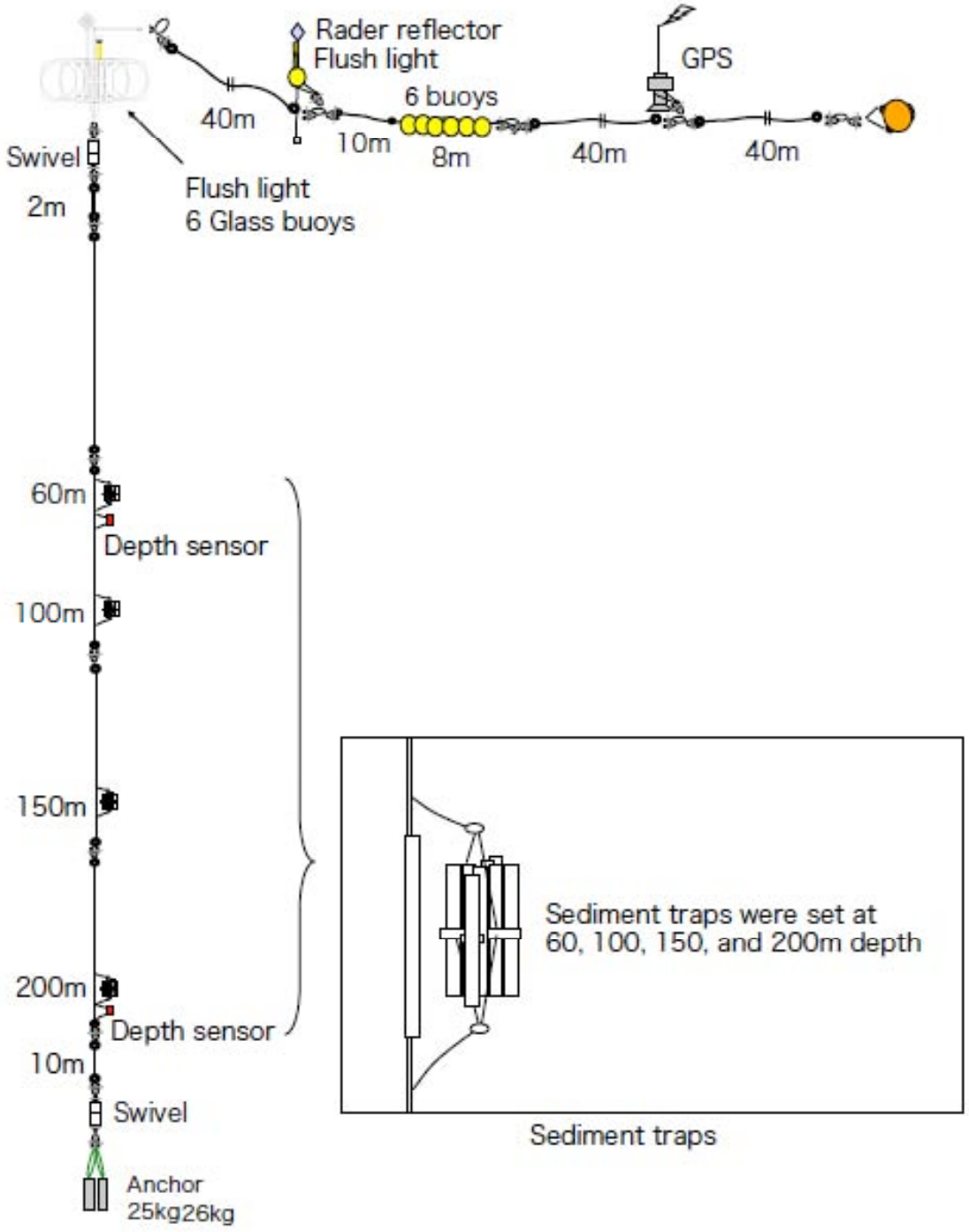

Fig. 3.5.1-1 Drifting mooring system at stations K2 and S1.

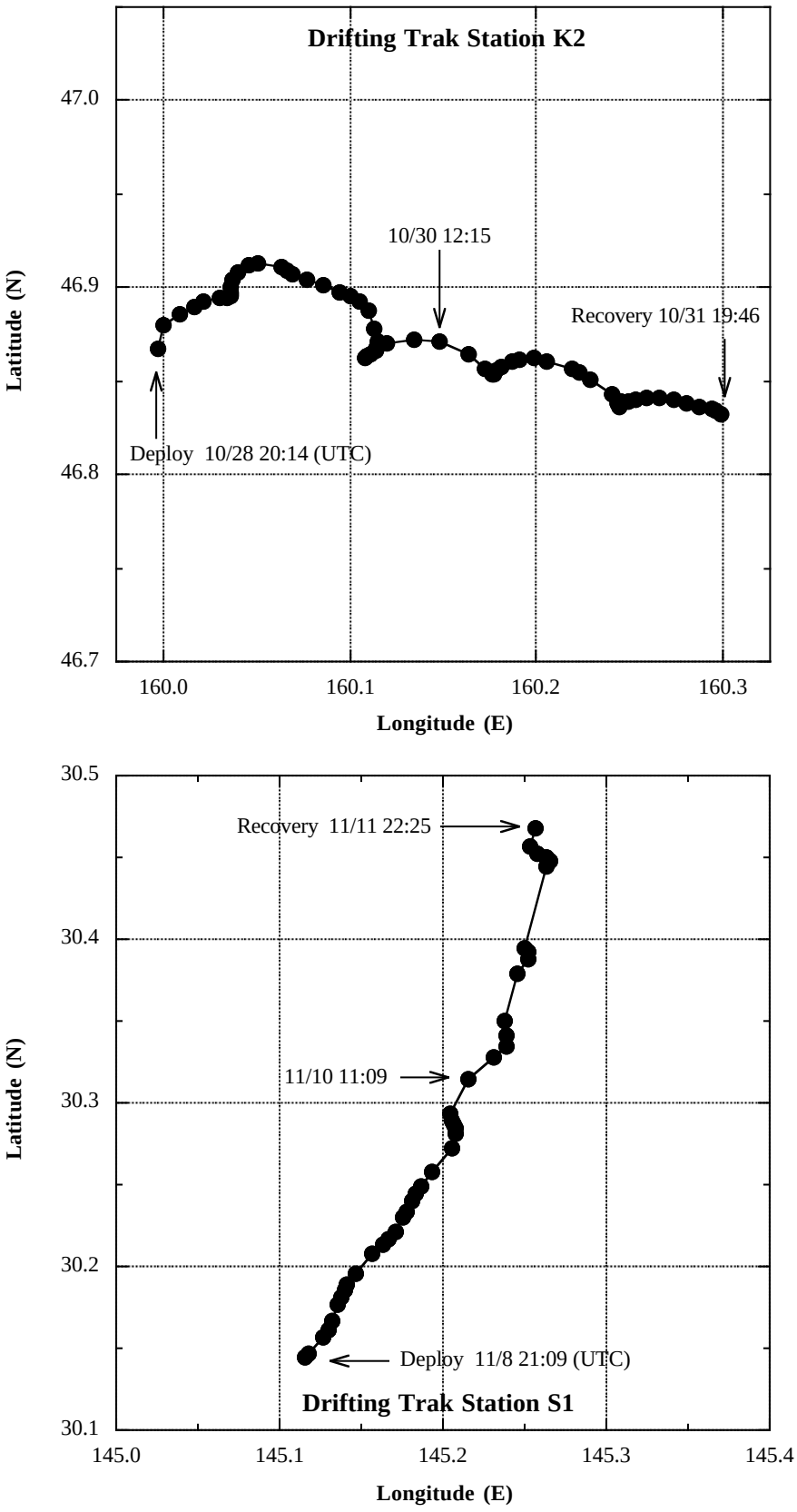

Fig. 3.5.1-2 Track of drifter (GPS buoy) at stations K2 and S1.

3.5.2 Drifting sediment trap of JAMSTEC

Hajime KAWAKAMI (JAMSTEC MIO)
Makio HONDA (JAMSTEC MARITEC)

In order to collect sinking particles and measure carbon flux, and zooplankton, “Knauer type” cylindrical sediment trap (Photo 3.5.2-1) was deployed at stations K2 and S1 where measurement of primary productivity was conducted. This trap consists of 8 individual transparent policarbonate cylinders with baffle (collection area: ca. 0.0038 m^2, aspect ratio: 620 mm length / 75 mm width = 8.27), which was modified from Knauer (1979). Before deployment, each trap was filled with filtrated surface seawater, which salinity is adjusted to ~ 39 PSU by addition of NaCl (addition of 100 mg NaCl to 20 L seawater) were placed in tubes. These were located at approximately 60 m, 100 m, 150 m and 200 m. After recovery, sediment traps were left for half hour to make collected particles settle down to the bottle. After seawater in acrylic tube was dumped using siphonic tube, collecting cups were took off. Two cups of samples at each layer were given to the team of Kagoshima Univ. to determine fecal pellets. Four cups of samples at each layer were filtered thorough Nuclepore filter with a pore size of 0.4μm and GF/F filter by two cups, for respective purpose (total mass flux, trace elements, total particulate carbon, and particulate organic carbon). The other samples were added buffered formalin for archive. The filter and archive samples were kept in freezer and refrigerator by the day when these were analyzed, respectively. At 60 m depth of station K2, a cup of samples were divided to each object, because four cups of samples were lose owing to rough condition of sea.

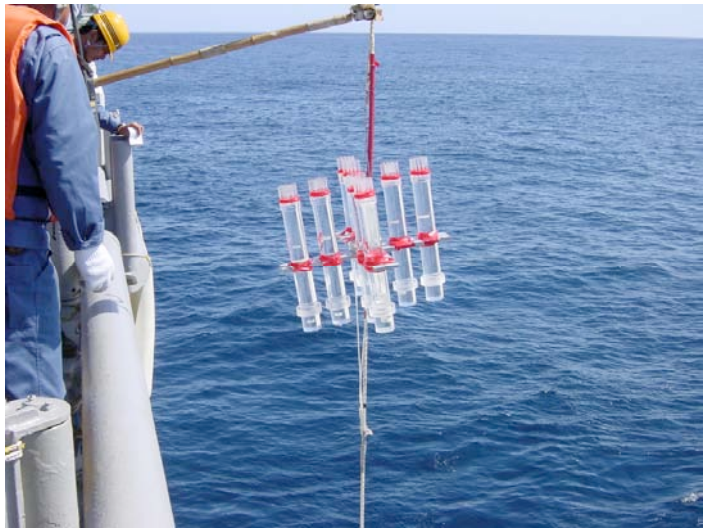

Photo 3.5.2-1 Drifting Sediment Trap.

3.5.3 Vertical changes of fecal pellets

Toru KOBARI (Kagoshima University)
Keisuke UNNO (Kagoshima University)

(1) Objective

Sinking particles includes phytoplankton aggregates, fecal pellets, feeding mucus and carcass of zooplankton and crustacean molts (e.g. Flower and Knauer, 1986). Especially, zooplankton fecal pellets can significantly contribute to vertical flux of particulate organic carbon (POC) and are a key component of the biological pump (Bishop et al., 1977; Lampitt et al., 1990; Silver and Gowing, 1991; Carroll et al., 1998; Turner, 2002). Fecal pellets are changed by zooplankton ingestion (coprophagy), fragmentation via sloppy feeding or swimming activity (coprorhexy) and loosening of membrane (coprochaly) during sinking (Paffenhöfer and Strickland, 1970; Lampitt et al., 1990; Noji et al., 1991). These processes largely affect transfer efficiency of POC flux (Wilson et al., 2008). It has been believed that fecal pellets are declined by bacterial decomposition (Honjo and Roman, 1978; Arístegui et al., 2002) and/or coprophagy/coprorhexy of small copepods such as cyclopoids and poecilostomatoids for last two decades (González and Smetacek, 1994; Suzuki et al., 2003; Svensen and Nejstgraard, 2003; Huskin et al., 2004; Poulsen and Kiørboe, 2006). In recent years, however, these copepods showed minor contributions to coprophagy/coprorhexy from the field observations (Iversen and Poulsen, 2007) and laboratory experiments (Reigstad et al., 2005), and heterotrophic microbes consume fecal pellets (Poulsen and Iversen, 2008). Thus, we should re-consider how fecal pellets are declined or changed during sinking from surface to mesopelagic depths.

In the present study, we investigated vertical differences of flux, shape and volume of fecal pellets from drifting sediment trap experiments to evaluate how fecal pellets were changed.

(2) Methods

Knauer-type sediment traps were deployed at 60, 100, 150 and 200 m at K2 and S1 in the Northwestern Pacific Ocean for 48 hours during the Mirai cruise (MR10-06) from 18 October to 16 November 2010. The sediment traps were constructed from 8 cylinders (opening diameter of 10 cm and 50 cm height) with a baffle to reduce turbulence, mounted on a polyvinylchloride frame. A 200-mL sample cup was attached to the bottom of each cylinder via screw threads. The sample cup was filled with a brine solution.

Once traps were recovered, samples for particle organic carbon (POC) flux were preserved at 4^{o}C until filtration. To avoid pellet breakage during processing, samples for POC flux were not screened; i.e. swimmers were picked out under a stereo dissecting microscope. These samples were filtered through a pre-combusted and pre-weighed Whatman GF/F filter under vacuum pressure less than 10kPa and rinsed with Milli-Q water. Samples for fecal pellet (FP) flux were fixed with 5% buffered

formaldehyde solution.

(3) Preliminary results

During the cruise, we collected 7 samples for POC flux 8 samples for FP flux were collected (Table). In the land laboratory, carbon and nitrogen contents will be measured from these filter samples. For fixed samples, number, shape and volume will be measured under a stereo dissecting microscope.

Table. Summary list of oceanographic observations and samplings during MR10-06.

Samplings/Observations	Analyses	Stat		End		Depth (m)	No. of	Reference
		Date	Time	Date	Time		samples	
K2								
Drifting Sediment Trap	FP	29 Oct	06:30	01 Nov	06:30	60/100/150/200	4	
	CFux						3	No sample for 60m
CTD-CMS	FPD/TC	25 Oct	16:46	25 Oct	17:53	15	-	
	FPD/TC	28 Oct	18:31	28 Oct	19:08	20	-	
	DE	26 Oct	4:01	26-Oct	5:44	5	-	
	DE	29 Oct	04:01	29 Oct	06:05	5	-	
CTD-CMS	Pico	26 Oct	04:01	26 Oct	05:44	0/5/10/20/30/35/45/55	24	Sample is for FCM
	Nano						8	
	Micro						8	
Single NORPAC	FPD	25 Oct	18:00	25 Oct	18:15	0-20	-	
	FPD	28 Oct	18:25	28 Oct	18:40	0-40	-	
Twin NORPAC	Macro	26 Oct	14:25	26 Oct	14:40	0-200	1	
	GP						1	
	Macro	27 Oct	09:05	27 Oct	09:20	0-200	1	
	GP						1	
	Macro	27 Oct	18:58	27 Oct	19:15	0-200	1	
	GP						1	
IONESS	Macro	29 Oct	11:00	29 Oct	13:52	0-1000	8	Split is 1/4
	Macro	29 Oct	21:07	29 Oct	23:38	0-1000	8	Split is 1/4
	Macro	01 Nov	10:58	01 Nov	13:50	0-1000	8	Split is 1/4
Bottle experiments	FPD	25 Oct	20:00	26 Oct	20:00	-	15	Cyclopoids are used
	FPD	28 Oct	20:30	29 Oct	22:20	-	15	Cyclopoids are used
	TC (Pico)	25 Oct	20:00	26 Oct	20:00	-	80	Sample is for FCM
	TC (CHL)						20	
	TC (Pico)	28 Oct	20:20	29 Oct	20:20	-	80	Sample is for FCM
	TC (CHL)						20	
	DE	26 Oct	06:30	27 Oct	06:30	-	48	Sample is for FCM
	DE	29 Oct	06:15	30 Oct	06:15	-	48	Sample is for FCM
S1								
Drifting Sediment Trap	FP	09 Nov	07:00	12 Nov	08:00	60/100/150/200	4	
	CFlux						4	
CTD-CMS	FPD/TC	07 Nov	19:11	07 Nov	20:12	70	-	
	FPD/TC	09 Nov	20:10	09 Nov	20:44	80	-	
	DE	08 Nov	03:48	08 Nov	05:42	96	-	
	DE	09 Nov	18:30	09 Nov	19:36	90	-	
Bucket	DE	06 Nov	17:35	06 Nov	17:51	0	-	
	DE	09 Nov	09:28	09 Nov	09:42	0	-	
CTD-CMS	Pico	10 Nov	03:58	10 Nov	05:48	0/10/35/55/65/80/95/110	24	Sample is for FCM
	Nano						8	
	Micro						8	
Single NORPAC	FPD	07 Nov	19:00	07 Nov	19:10	0-100	-	
	FPD	09 Nov	20:00	09 Nov	20:10	0-100	-	
Twin NORPAC	Macro	08 Nov	08:26	08 Nov	08:41	0-200	1	
	GP						1	
	Macro	08 Nov	19:56	08 Nov	20:20	0-200	1	
	GP						1	
	Macro	10 Nov	15:37	10 Nov	15:55	0-200	1	
	GP						1	
	Macro	11 Nov	19:56	11 Nov	20:15	0-200	1	
	GP						1	
IONESS	Macro	08 Nov	11:15	08 Nov	14:02	0-1000	8	Split is 1/4
	DW						8	Split is 1/8
	Macro	10 Nov	21:04	11 Nov	00:04	0-1000	8	Split is 1/4
	DW						8	Split is 1/8
	Macro	11 Nov	21:09	12 Nov	00:09	0-1000	7	Split is 1/4, No sample for 100-150m
	DW						-	Samples will be made from 1/4 sample
	Macro	12 Nov	11:07	12 Nov	14:04	0-1000	8	Split is 1/4
	DW						-	Samples will be made from 1/4 sample
In situ experiments	FPD	07 Nov	21:50	08 Nov	22:45	-	15	Poecilostomatoids are used
	FPD	09 Nov	22:30	10 Nov	22:50	-	15	Poecilostomatoids are used
	TC (Pico)	07 Nov	21:50	08 Nov	21:50	-	80	Sample is for FCM
	TC (CHL)						20	
	TC (Pico)	09 Nov	21:30	10 Nov	21:30	-	80	Sample is for FCM
	TC (CHL)						20	
	DE	06 Nov	18:50	07 Nov	18:50	-	48	Sample is for FCM
	DE	08 Nov	06:30	09 Nov	06:30	-	48	Sample is for FCM
	DE	09 Nov	10:40	10 Nov	10:40	-	48	Sample is for FCM
	DE	09 Nov	20:30	10 Nov	19:30	-	48	Sample is for FCM
Abbreviations	FPD	Fecal pellet analyses						
	DE	Dilution experiments						
	Pico	Microscopic analyses for picoplankton						
	Nano	Microscopic analyses for nanozooplankton						
	Micro	Microscopic analyses for microplankton						
	Macro	Microscopic analyses for macrozooplankton						
	GP	Gut pigment analyses						
	FPD	Fecal pellet decomposition						
	TC	Trophic cascading						
	DM	Dry mass measurement						

(4) Reference

Aristegui, J., Duarte, C.M., Agusti, S., Doval, M., Alvarez-Salgado, X.A., Hansell, D.A. (2002). Dissolved organic carbon support of respiration in the dark ocean. Science, 298, 1967-1967.

Bishop, J.K., Edmond, J.M., Ketten, D.R., Bacon, M.P., Silker, W.B. (1977). Thechemistry, biology, and vertical flux of particulate matter from the upper 400m of the equatorial Atlantic Ocean. Deep-Sea Research, 24, 511-548.

Carroll, M.L., Miquel, J.-C., Fowler, S.W. (1998). Seasonal patterns and depth-specific trends of zooplankton fecal pellet fluxes in the Northwestern Mediterranean Sea. Deep-Sea Research I, 45, 1303–1318.

González, H. E., Smetacek, V. (1994). The possible role of the cyclopoid copepod Oithona in retarding vertical flux of zooplankton fecal material. Marine Ecology Progress Series, 113, 233-246.

Flower, S.W., Knauer, G.A. (1986). Role of large particles in the transport of elements and organic compounds through the oceanic water column. Progress in Oceanography. 16, 147-194.

Honjo, S., Roman, M. R. (1978). Marine copepod fecal pellets: production, preservation and sedimentation. Journal of Marine Research, 36, 45-57.

Huskin, I., Viesca, L., Anado´ n, R. (2004). Particle flux in the Subtropical Atlantic near the Azores: influence of mesozooplankton. Journal of Plankton Research, 26, 403-415.

Iversen, M. H., Poulsen, M. R. (2007). Coprorhexy, coprophagy, and coprochaly in the copepods *Calanus helgolandicus*, *Pseudocalanus elongates*, and *Oithona similis*. Marine Ecology Progress Series, 350, 79-89.

Lampitt, R.S., Noji, T.T., von Bodungen, B. (1990). What happens to zooplankton faecal pellets? Implications for material flux. Marine Biology, 104, 15-23.

Noji, T. T., Estep, K. W., MacIntyre, F., Norrbin, F. (1991). Image analysis of faecal material grazed upon by three species of copepods: evidence for coprohexy, coprophagy, and coprochaly. Journal of the Marine Biological Association of the United Kingdom, 71, 465-480.

Paffenhöfer, G.-A ., Strickland, J. D. H. (1970). A note on the feeding of *Calanus helgolandicus* on detritus. Marine Biology, 5, 97-99.

Poulsen, L. K., Kiørboe, T. (2006). Vertical flux and degradation rates of copepod fecal pellets in a zooplankton community dominated by small copepods. Marine Ecology Progress Series, 323, 195-204.

Poulsen, M. R., Iversen, M. H. (2008). Degradation of copepod fecal pellets: key role of protozooplankton. Marine Ecology Progress Series, 367, 1-13.

Reigstad, M., Riser, C. W., Svensen, C. (2005). Fate of copepod faecal pellets and the role of Oithona spp. Marine Ecology Progress Series, 304, 265-270.

Silver, M.W., Gowing, M.M. (1991). The “particle” flux: origins and biological components. Oceanography, 26, 75-113.

Suzuki, H., Sasaki, H., Fukuchi, M. (2003). Loss processes of sinking fecal pellets of zooplankton in the mesopelagic layers of the Antarctic marginal ice zone. Journal of

Oceanography, 59, 809-818.
Svensen, C., Nejstgaard, J. C. (2003). Is sedimentation of copepod faecal pellets determined by cyclopoids? Evidence from enclosed ecosystems. Journal of Plankton Research, 25, 917-926.
Turner, J.T. (2002). Zooplankton fecal pellets, marine snow and sinking phytoplankton blooms. Aquatic Microbial Ecology, 27, 57-102.
Wilson, S. E., Steinberg, D. K., Buesseler, K. O. (2008). Changes in fecal pellet characteristics with depth as indicators of zooplankton repackaging of particles in the mesopelagic zone of the subtropical and subarctic North Pacific Ocean. Deep-Sea Research II, 55, 1636-1647.

3.6 Po-210 and export flux

Hajime KAWAKAMI (JAMSTEC MIO)
Makio HONDA (JAMSTEC MIO)

(1) Purpose of the study

The fluxes of POC were estimated from Particle-reactive radionuclide (^{210}Po) and their relationship with POC in the western North Pacific Ocean.

(2) Sampling

Seawater and suspended particulate sampling for ^{210}Po, ^{210}Pb, and POC: 2 stations (stations K2 and S1) and 16 depths (10m, 20m, 30m, 50m, 75m, 100m, 150m, 200m, 300m, 400m, 500m, 600m, 700m, 800m, 900m, and 1000m) at each station.

Seawater samples (10 L for ^{210}Po and ^{210}Pb) were taken from Hydrocast at each depth. The seawater samples for ^{210}Po were filtered through polypropylene cartridge filters with a pore size of 0.8 μm on board immediately after water sampling.

In situ filtering (suspended particulate) samples were taken from large volume pump sampler (Large Volume Pump WTS-6-1-142V, McLane Inc.). Approximately 200L and 800L seawater was filtered through glass-fiber filter with a pore size of 0.7 μm at each station at 10–200m depths and 300–1000m depths, respectively. The filter samples were divided for ^{210}Po and POC.

(3) Chemical analyses

Dissolved and particulate ^{210}Po was absorbed on 25mm silver disks electrically, and were measured by α-ray counter (Octéte, Seiko EG&G Co. Ltd.). For total (dissolved + particulate) ^{210}Pb measurement, the same procedure was applied to the seawater samples 18 months later, when ^{210}Po come to radioactive equilibrium with ^{210}Pb.

POC was measured with an elemental analyzer (Perkin-Elmer model 2400II) in land-based laboratory.

(4) Preliminary result

The distributions of ^{210}Po and POC will be determined as soon as possible after this cruise. This work will help further understanding of particle dynamics at the euphotic layer and twilight zone.

3.7 Settling velocity of particles in the twilight zone

Yoshihisa MINO (NAGOYA UNIV. HyARC)
Chiho SUKIGARA (NAGOYA UNIV. HyARC)

(1) Objective

Sinking particles have been considered as the most important vehicle, by which the biological pump sequesters carbon in the ocean interior (Buesseler et al., 2007). As the particles sink they undergo the remineralization processes (fragmented into non-sinking ones and consumed by bacteria etc.) in the twilight zone, which leads to POC flux attenuation with depth. A large number of sediment trap studies have revealed that POC flux attenuation varied seasonally and regionally (Berelson, 2001), so it is required to understand this variability in order to better quantify the magnitude of biological pump. Recent studies pointed out the significance of particle settling velocity, varying three orders of magnitude, as a parameter affecting the flux attenuation (Armstrong et al., 2002, 2009; Trull et al., 2008).

This study aim to determine the settling velocity (SV) of particles collected by sediment trap at ~100 and 200 m depth for the subarctic (station K2) and subtropical (S1) North Pacific Ocean, for further understanding the carbon transfer in the twilight zone.

(2) Methods

Particulate samples were collected in the drifting sediment trap experiments conducted during this cruise（see the chapter 3.5 for details on trap experiments）. The depth of sample collection is 85-95, 185-195m at K2, and 90, 185m at S1.

Here we applied the elutriation method (Peterson et al. 2005) to fractionate particles into SV classes using countercurrents of varying speeds. A portion of the particulate samples from the sediment trap was introduced into the custom-built polycarbonate elutriator and separated into 5 fractions with SVs of >500, 150-500, 50-150, 15-50, <15 m d^{-1}. After the swimmers are removed using the tweezers under microscope, each sample was filtrated onto pre-combusted GF/F filter and stored frozen. The organic carbon content in samples will be determined on shore, which derive the settling velocity spectra of the trapped particles. The carbon and nitrogen isotope abundances are also determined.

(3) Preliminary result

We present the photomicrographs of sinking particle from 85-95m depth of station K2 (Fig. 1). The overview image (top) of all particles before SV fractionation shows that they consist of various materials (fecal pellets, detritus etc.). The below images give the representatives of particle in each SV fraction, which reveals that foraminifera shells and larger fecal pellets were common in the fast-sinking fractions (>500, 150-500 m d^{-1}). On the other hand, smaller fecal pellets and detritus were observed in the slow-sinking fraction (15-50 m d^{-1}).

(4) Data archive

The experimental data sets from this study will be submitted to JAMSTEC Data Integration and Analyses Group (DIAG).

(5) References

Armstrong et al. (2002), Deep-Sea Res. II, 49, 219-236.
Armstrong et al. (2009), Deep-Sea Res. II, 56, 1470-1478.
Berelson, (2001), Oceanography, 14, 59-67.
Buesseler et al. (2007), Science, 316, 567-570.
Peterson et al. (2005), Limnol. Oceanogr.: Methods, 3, 520-532.
Trull et al. (2008), Deep-Sea Res. II, 55, 1684-1695.

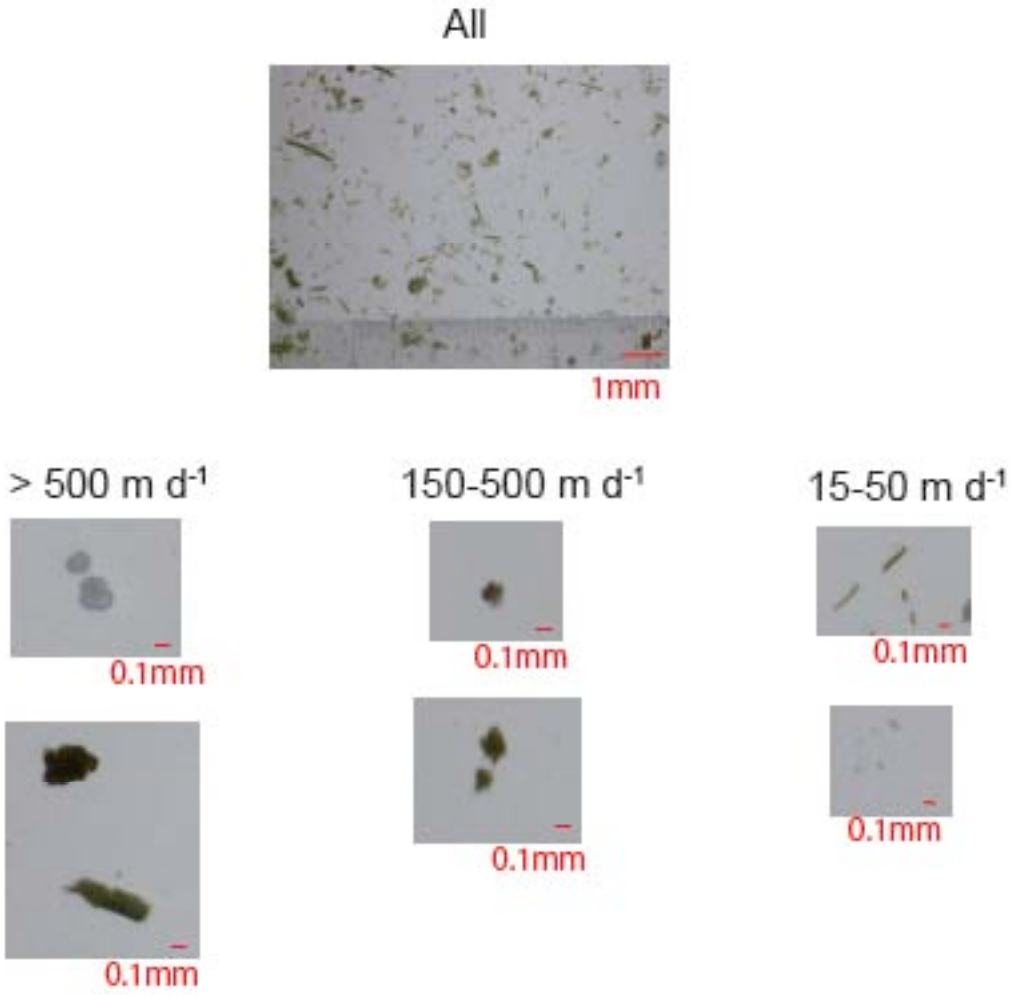

Figure 1. Photomicrographs of sinking particle from 85-95m depth of station K2.

3.8 Zooplankton
3.8.1 Community structure and ecological roles

Minoru KITAMURA **(JAMSTEC, BioGeos)**
Toru KOBARI **(Kagoshima Univ.)**
Keisuke UNNO **(Kagoshima Univ.)**
Kei ISAMI **(Kagoshima Univ.)**

(1) Objective

Subarctic western North Pacific is known to be a region with high biological draw down of atmospheric CO_2 due to extensive diatom bloom in spring. Time-series biogeochemical observations conducted at the Station K2 have revealed high annual material transportation efficiency to the deep compared to the other time-series sites set in the subtropical regions.

Zooplankton dominated in this regions are large copepods, which mainly feed on diatoms, and supposed to help enhancing Biological Carbon Pump (BCP) function, by repackaging diatoms through the fecal pellet production. However, the reported zooplankton fecal pellet flux to the deep were smaller than expected from the production in the surface layer, suggesting consumption and biological breakdown occurred in surface and mesopelagic layers. In particular, biological processes in the mesopelagic layer are largely unknown.

Besides the fecal pellet production, “active transport” of carbon by ontogenetic migrating copepods, e.g. *Neocalanus* spp. recently was reported large, even equivalent to amount of carbon flux estimated based on the sediment trap experiments. Other copepods, *Metridia* spp. perform extensive diel vertical migration, and could transport large amount of surface carbon to the several hundred meters deep through respiration. Detailed information of timing and biomass of vertical migration of these copepods should be investigated.

With these background, goal of these research is to investigate roles of zooplankton in vertical material transport in the western subarctic North Pacific. We deployed two types of plankton nets to investigate species and size composition of zooplankton from the surface to the greater deep. We also conducted same samplings at a new time-series station, S1, for comparison to K2 ecosystem.

(2) Materials and methods

Mesozooplankton and micronekton samplings (IONESS Sampling)

For collection of stratified sample sets, multiple opening/closing plankton net system, IONESS, was used. This is a rectangular frame trawl with nine nets. Area of the net mouth is 1.5 m^2 when the net frame is towed at 45° in angle, and mesh pore size is 0.33-mm. Researcher can open and close nets at discretion depths and can real time monitor net status. Volume of filtering water of each net is estimated using area of net mouth, towing distance, and filtering efficiency. The area of net mouth is calibrated from frame angle during tow, the towing distance is calculated from revolutions of flow-meter, and the filtering efficiency is 96% which was directory measured. The net system is towed obliquely. Ship speed during net tow was about 2 knot, speeds of wire out and reeling were 0.1-0.7 m/s and 0.1-0.3 m/s, respectively.

Total seven tows (three at K2, four at S1) of IONESS were done. The stratified sampling layers at stations K2 and S1 were as follows; 0-50, 50-100, 100-150, 150-200, 200-300, 300-500, 500-750, and 750-1000m. To understand diel vertical migration of mesozooplankton and micronekton, the stratified samplings were conducted during both day and night. Towing data such as date, time, position, filtering volume are summarized in Table

3.8.1-1.

Collected zooplankton samples were divided using a sample splitter on board. Purpose of the sample dividing, fixation of each subsample are also summarized (Table 3.8.1-2).

NORPAC net sampling

A twin-type NORPAC net with fine mesh (100 mm) and flow meters was used. The net was vertically towed 0-50 m and 0-150 m at the Station K2 and S1 (Table 3.8.1-3) at night. Zooplankton collected were preserved in the 5% buffered formalin seawater for the later analysis.

Vertical distribution of nano- and microzooplankton

Two series of seawater samples were collected at Stations K2 and S1. Each series comprises eight waters which collected using bucket and Niskin bottles at different depths. These depths corresponded to nominal specific optical depths approximately 100, 50, 25, 10, 5, 2.5, 1 and 0.5% light intensity relative to the surface irradiance as determined from the optical profiles obtained by ‘‘Free-Fall Sensor’’. Additionally, midwater samples were also collected at 200, 400 and 800 m in depth in both the stations.

Seawater samples were immediately treated with the final concentration of 1% glutaraldehyde and were kept at 4°C until filtering. Each seawater sample were filtered through 1μm pore size Nuclepore fitter, pre-stained by irgalan black, at the low vacuum of 15 cmHg, and were double-stained using DAPI (4’6-diamidino-2-phenylindole dihydrochloride) and proflavine (3-6-diamidino-acridine hemisulfate). Just before the finish of filtering, DAPI was added to sample in filtering funnel for the staining DNA. After the DAPI staining, proflavine was also added for the staining of flagella. Both the staining time is five minute. The working solution of DAPI (10 μg/ml) and proflavine (0.033%) were pre-filtered through 0.45 μm pore size of non-pyrogenic Durapore membrane filter (Millipore, Millex-GX). After the filtering, sample filters put on a slide-glass with one drop of immersion oil, and covered with micro cover glass. All preparations were stored in the deep freezer (-80°C) until the observation.

Above mentioned water samples are for analysis of nanozooplankton. Because filtering volume is little (up to 400 ml), these samples are not appropriate for microzooplankton analysis such as tintiniids whose abundance is low. So, additional seawater samples for this taxon were collected in the same depths, same time. Collected water samples were immediately fixed in 1% acid Lugol’s solution.

Sampling data such as depths or filtering volume are summarized in Table 3.8.1-4.

Table 3.8.1-1. Summary of IONESS samplings.

MR10-01 IONESS Samplings

including filtering efficiency, 96%, in calculations of filtering volume of water

Stn.	Tow ID	Local Time		Position		Sampling layer (upper, m) and filtering vol. (lower, m^3)									Remarks
			in out	in out		Net No. 0	1	2	3	4	5	6	7	8	
K2	I101029A	2010.10.29	11:00 13:52	46° 54.24' N 159° 55.82' E 46° 50.16' N 159° 51.78' E		0~1020~1000	1000~750 2066.0	750~500 3005.8	500~300 2153.6	300~200 1184.2	200~150 766.2	150~100 694.5	100~50 642.1	50~0 571.1	
	I101029B	2010.10.29	21:00 23:40	46° 55.71' N 159° 54.38' E 46° 57.44' N 159° 49.82' E		0~1026~997	997~750 1419.3	750~500 1497.6	500~300 1145.3	300~200 636.9	200~150 262.9	150~100 701.3	100~50 698.2	50~0 641.3	
	I101101A	2010.11.1	10:58 13:50	46° 49.40' N 159° 54.22' E 46° 55.25' N 159° 53.61' E		0~1033~1000	1000~750 2468.4	750~500 3146.4	500~300 2781.6	300~200 1366.0	200~150 908.5	150~100 865.2	100~50 847.8	50~0 721.0	
S1	I101108A	2010.11.8	11:09 14:04	30° 01.60' N 145° 03.04' E 30° 04.94' N 145° 08.64' E		0~1038~1000	1000~750 2915.9	750~500 2653.2	500~300 2012.4	300~200 1342.8	200~150 690.8	150~100 854.7	100~50 955.6	50~0 1065.1	
	I101110A	2010.11.10	21:01 0:04	29° 59.84' N 145° 01.38' E 30° 01.78' N 144° 55.43' E		0~1054~1000	1000~750 2436.6	750~500 2655.6	500~300 1611.9	300~200 928.8	200~150 752.5	150~100 524.6	100~50 322.8	50~0 345.5	#1
	I101111A	2010.11.11	21:07 0:01	29° 59.79' N 144° 59.04' E 30° 02.15' N 144° 54.02' E		0~1055~1000	1000~750 2278.2	750~500 2583.9	500~300 2310.0	300~200 1284.5	200~150 909.1	150~100 -	100~50 232.6	50~0 249.3	#2
	I101112A	2010.11.12	11:05 14:02	30° 07.93' N 145° 04.51' E 30° 02.40' N 145° 03.26' E		0~1048~1000	1000~750 3116.8	750~500 3108.1	500~300 2195.0	300~200 1543.2	200~150 884.0	150~100 1109.6	100~50 652.4	50~0 552.8	

#1: No.7 net did not completely close, some 50-0m zooplankton were included in this net sample

#2: No sample was collected from the 6th net because the net was entangled in a frame

Table 3.8.1-2. Division of each sample

Stn.	Tow ID	Division	Fixation	Strage	Pourpose
K2	I101029A, I101029B, I101101A	1/2	5% Folmaline	JAMSTEC	community structure analysis
		1/4	5% Folmaline	Kagoshima Univ.	community structure analysis
		1/8	5% Folmaline	JAMSTEC	biomass composition in higher taxa level
		1/16	-30°C Frozen	JAMSTEC	dry mass measurement
		1/16	-30°C Frozen	JAMSTEC	archives
S1	I101108A, I101110A	1/2	5% Folmaline	JAMSTEC	community structure analysis
		1/4	5% Folmaline	Kagoshima Univ.	community structure analysis
		1/8	5% Folmaline	Kagoshima Univ.	biomass composition in higher taxa level
		1/8	-30°C Frozen	JAMSTEC	dry mass measurement
	I101111A, I101112A	1/4	5% Folmaline	JAMSTEC	community structure analysis
		1/4	5% Folmaline	Kagoshima Univ.	community structure analysis
		1/4	5% Folmaline	JAMSTEC	dry mass measurement
		1/4	-30°C Frozen	JAMSTEC	archives

Table 3.8.1-3. Summary of NORPAC samplings

flow-meter No.: yellow net; 3332, green net; 1997
Rewind speed: 1.0 m / sec

Stn.	Date	Local Time	Position		Sampling Layer	Wire out	Wire angle	Flow-meter revolution	
			Lat.	Long.	(m)	(m)	(°)	yellow net	green net
K2	2010 Oct. 27	19:55	46° 49.33' N	160° 00.64' E	50-0	50	0	633	642
		20:10			150-0	150	0	1653	1768
S1	2010 Nov. 9	19:05	29° 59.99' N	145° 00.00' E	50-0	50	0	531	544
		19:18			150-0	150	0	1402	1523

Table 3.8.1-4. Summary of water samplings for nano- and microzooplankton abundance

* local ship time # Kitamura, ## Kagoshima Univ.

Stn.	Date*	CTD		Depth	Irradiance	Nanozooplankton samplings #			Microzoo ##	Remarks
		Time*	Cast ID	(m)	(%)	Sample No.	Filtering vol. (ml)	Funnel No.	Sample vol. (ml)	
K2 (006)	2010 Oct. 26	4:00	K2 cast 3 (PP)	55	0.5	K2, 1	280	1	1000	
				45	1	K2, 2	290	2	1000	
				35	2.5	K2, 3	250	3	1000	
				30	5	K2, 4	270	4	1000	
				20	10	K2, 5	205	1	1000	
				10	25	K2, 6	270	2	1000	
				5	50	K2, 7	275	3	1000	
				0	100	K2, S	305	4	1000	Bucket
	2010 Oct. 27	8:00	K2 cast 6 (PE)	200	<0.5	K2, 200	500	1	-	
				400	<0.5	K2, 400	500	2	-	
				800	<0.5	K2, 800	500	3	-	
S1 (011)	2010 Nov. 8	9:00	S1 cast 5 (PE)	200	<0.5	S1, 200	500	1	-	
				400	<0.5	S1, 400	500	2	-	
				800	<0.5	S1, 800	500	3	-	
	2010 Nov. 10	4:00	S1 cast 10 (PP2)	110	0.5	S1-1	310	1	1000	
				95	1	S1-2	355	2	1000	
				80	2.5	S1-3	240	3	1000	
				65	5	S1-4	295	4	1000	
				55	10	S1-5	250	1	1000	
				35	25	S1-6	445	2	1000	
				10	50	S1-7	295	3	1000	
				0	100	S1-S	435	4	1000	Bucket

(3) Future plans and sample archives

Community structure and ecological role of mesozooplankton

Subsamples are stored at JAMSTEC or Kagoshima Univ. We will analyze as follows; (1) vertical distribution of zooplankton carbon mass, (2) vertical distribution of biomass in higher taxa revel (copepods, euphausiids, etc.) and taxa composition based on the carbon weight, (3) vertical distribution, composition, biomass, and diel vertical migration for each species of dominant taxa such as copepods, euphausiids and chaetognaths, (4) estimation of carbon transport through diel or ontogenetic migration.

Environmental (T, S) and net status (net number, towing distance, etc.) data were recorded during each IONESS tow. All data is under Kitamura and Kobari.

Vertical distribution of microzooplankton

Sample analysis is consigned to Marine Biological Research Institute of Japan Co. LTD., Shinagawa, Tokyo.

3.8.2 Grazing pressure of microzooplankton

Minoru KITAMURA (JAMSTEC, BioGeos)
Toru KOBARI (Kagoshima Univ.)
Keisuke UNNO (Kagoshima Univ.)
Kei ISAMI (Kagoshima Univ.)

(1) Objective

To understand material export from surface to deep ocean, not only estimations of primary productivity or vertical flux but also evaluation of grazing impacts at surface is needed. Grazing by larger organisms might bring about efficient vertical carbon transport through repacking phytoplankton into fecal pellets or active carbon transport by diel and ontogenetic migrator. On the other hand, grazing by smaller organisms might have small or negative impact to vertical export. Identification of influential grazers and quantitative estimation of their grazing rates are essential to discuss the carbon cycle in the ocean. Recently, large grazing pressure of not only the crustacean plankton but also microzooplankton has been recognized in the several area. The grazing pressure by the micro organisms maybe important in the northwestern north Pacific in winter because large calanoid copepods migrate to midwater. Based on this background, we estimated grazing rate of them.

(2) Materials and methods

Six dilution incubation experiments were done through the cruise (Table 3.8.2-1). For each experiment 40 l of water were collected from Niskin bottle or bucket. Water was pre-screened through 200 μm mesh to exclude larger zooplankton. Dilution series were prepared with 25, 50, 75, and 100% of natural seawater. Filtered water was obtained by direct gravity flow through a compact cartridge filter (ADVANTEC, MCS-020-D10SR). Incubation of the dilute water was done in transparent polycarbonate bottle. Duplicate or triplicate bottle were prepared. Incubation lasted for 24 h in a tank with continuous flow of surface seawater under natural light conditions. All the water samplings, filtering, and incubate items were soaked in 10% HCl and rinsed Milli-Q water between each use on board. Nutrient was added in the incubation bottles. To measure initial and final chl.*a* concentration, experiment water were filtered onto GF/F filter and extracted 6 ml DMF at –20°C until measurement. Chl. *a* were measured fluorometrically (Welshmeyer method) with a Turner Design fluorometer. Phytoplankton cell numbers were also counted using flowcytometry.

Apparent phytoplankton growth rate (d^{-1}) were calculated using following equation:

$$\text{Apparent growth rate} = (1/t)\ln(P_t/P_0)$$

where t is incubation time (day), P_t and P_0 are final and initial chlorophyll a concentration or cell number, respectively. When the apparent phytoplankton growth rate is plotted as a function of dilution factor, the y-intercept and negative slope of the approximate line means true phytoplankton growth (k; d^{-1}) and grazing coefficient of microzooplankton (g: d^{-1}), respectively. According to Verity et al. (1993) and Zhang et al. (2006), microzooplankton grazing pressure on primary production (P_p; %) is calculated as the following equation:

$$P_p = (e^{kt} - e^{(k-g)t}) / (e^{kt}-1)*100$$

Through the three incubation experiments, we tried to estimate true growth rate of phytoplankton, grazing rate of microzooplankton and grazing pressure of microzooplankton on primary production. Incubation states are summarized in Table 3.8.2-1.

References

Verity, P.G., D.K. Stoecker, M.E. Sieracki & J.R. Nelson. 1996. Grazing, growth and mortality of microzooplankton during the 1989 North Atlantic spring bloom at 47°N, 18°W. Deep-Sea Res., 40: 1793-1814.

Zhang, W., H. Li, T. Xiao, J. Zhang, C. Li & S. Sun. 2006. Impact of microzooplankton and

copepods on the growth of phytoplankton in the Yellow Sea and East China Sea. Hydrobiologia, 553: 357-366.

Table 3.8.2-1. Dilution experiments, sampling and incubation conditions.

Station	Date	Exp. ID.	Water sampling						Incubation					Remarks
			Depth m	Irradiance %	Temp. °C	Chl.*a* µg/l	CTD cast No.	Niskin Type	Start (LST)	End (LST)	Temp. °C	Irradiance %	Added nutrients	
K2	2010 Oct. 26-27	K2-a	5	50	8.7	0.58	K2 cast 3 (PP)	Normal	6:30	6:30	8.8-9.2	50	A	
K2	2010 Oct. 29-30	K2-b	5	50	8.5	0.65	K2 cast 9 (PP)	Normal	6:10	6:10	8.6-8.9	50	A	
S1	2010 Nov. 6-7	S1-a	0	100	25.3	0.10	Bucket		18:50	18:50	25.5-26.2	100	B	
S1	2010 Nov. 8-9	S1-b	96	<1	19	0.29	S1 cast 4 (PP)	Normal	6:00	6:15	19	2.5	B	water was sampled from Chl.*a* max. depth
S1	2010 Nov. 9-10	S1-c	0	100	25.3	0.12	Bucket		10:40	10:40	25.2-26.1	100	B	
S1	2010 Nov. 9-10	S1-d	90	1	19.2	0.26	S1 cast 8 (particle)	Clean	20:30	19:30	19	2.5	B	water was sampled from just below the Chl.*a* max. (84m)

Added nutrients
Pattern A in the stn.K2: $NaNO_3$; 0.5uM, Na_2HPO_4; 0.03uM
Pattern B in the stn.S1: $NaNO_3$; 10nM, Na_2HPO_4; 20nM

(3) Preliminary results

All measurements of Chl. *a* and count of phytoplankton cells numbers using flowcytometry were finished on board. Preliminary results of the first experiment in the station K2 are shown in the Figures 3.8.2-1 and 3.8.2-2, the latter figure suggested that grazing pressure on smallest eukaryote by microzooplankton was the most highest.

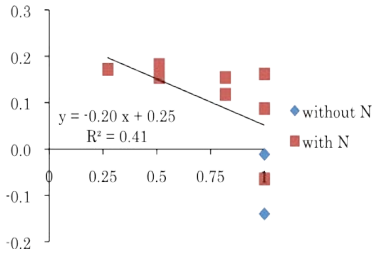

Fig.3.8.2-1. Correlation between apparent growth rates of phytoplankton community and dilution factors estimated from Chl. *a* measurements in the first dilution experiment in K2. Slope of the regression equation means grazing rate of the microzooplakton community. 'N' means added nutrients.

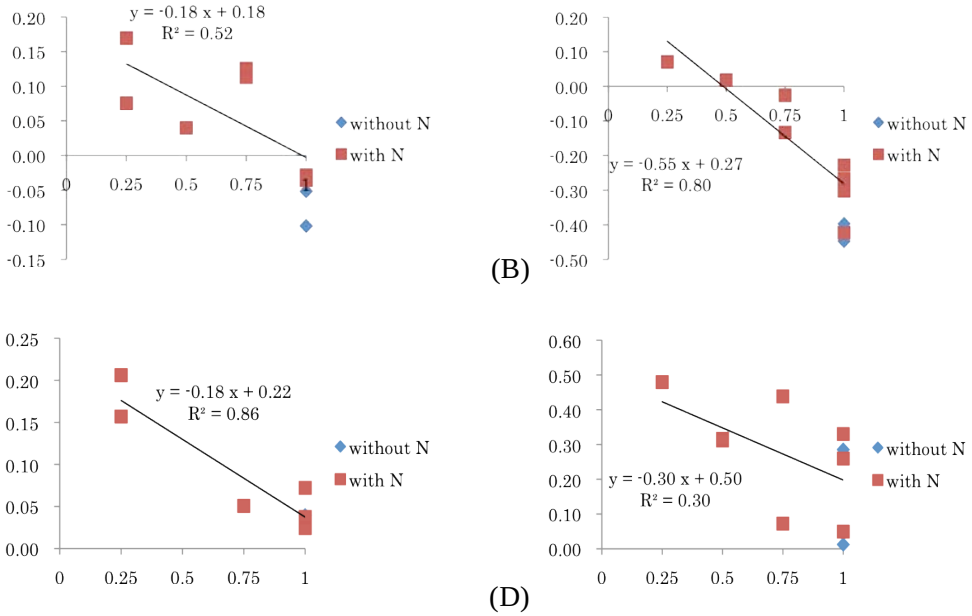

Fig. 3.8.2-2. Correlations between apparent growth rates of synecococcus and dilution factors (A), small eukaryote and dilution factors (B), medium eukaryote and dilution factors (C), large eukaryote and dilution factors (D). All estimated from based on the phytoplankton cell numbers counted using flowcytometry in the first dilution experiment in K2.

3.9 Effects of zooplankton on sinking carbon flux

Toru KOBARI (Kagoshima University)
Keisuke UNNO (Kagoshima University)

3.9.1 Active carbon flux

(1) Objective

It has been long accepted that sinking particles are major pathway of vertical carbon flux into the ocean interior and support mesopelagic carbon demand (Fowler and Knauer, 1986; Zhang and Dam, 1997; Aristegui et al., 2002). In the past decade, a number of studies have also shown that diel vertical migrants significantly contribute to carbon flux by consuming POC in surface waters and respiring and excreting the metabolized POC at depth. This "active carbon flux" is equivalent to 3–127%, of the sinking POC flux in tropical to subarctic waters (Al-Mutairi and Landry, 2001; Dam et al., 1995; Longhurst et al., 1990; Le Borgne and Rodier, 1997; Steinberg et al., 2000, 2008; Zhang and Dam, 1997). Thus, we should evaluate how mesozooplankton community transports carbon to mesopelagic depth as active carbon flux.
In the present study, we compare mesozooplankton abundance and community structure between day and night at K2 and S1 in Northwestern Pacific Ocean to estimate active carbon flux.

(2) Methods

Samplings were carried out during the RV Mirai cruise (MR10-06) from 18 October to 16 November 2010 at K2 and S1 in the Northwestern Pacific Ocean. Mesozooplankton were collected from 200 m to sea surface using Twin North Pacific Standard net (Motoda 1957: diameter 45 cm, mesh size 0.1 mm) at a speed of 1 m sec^{-1}. One sample was preserved in borax-buffered 5% formaldehyde for microscopic identification. Another sample was immediately anesthetized with soda water. Sample was frozen in liquid nitrogen after blotting adhering seawater on paper towels and stored at -80^{o}C for measurement of gut pigments.

(3) Preliminary results

During the cruise, 7 samples for microscopic indentification and 7 samples for gut pigments were collected (Table). In the land laboratory, major taxa and predominant copepods will be identified under a stereo dissecting microscope from fixed samples. For frozen samples, gut pigments of the predominant copepods will be measured by fluorometer.

(4) Reference

Al-Mutairi, H., Landry, M.R. (2001). Active export of carbon and nitrogen at Station ALOHA by diel migrant zooplankton. Deep-Sea Research II, 48, 2083–2103.
Arıstegui, J., Duarte, C.M., Agustı, S., Doval, M., A´ lvarez-Salgado, X.A., Hansell,

D.A. (2002). Dissolved organic carbon support of respiration in the dark ocean. Science, 298, 1967.

Dam, H.G., Roman, M.R., Youngbluth, M.J. (1995). Downward export of respiratory carbon and dissolved inorganic nitrogen by diel-migrant mesozooplankton at the JGOFS Bermuda time-series station. Deep-Sea Research I, 42, 1187–1197.

Fowler, S.W. Knauer, G.A. (1986). Role of large particles in the transport of elements and organic compounds through the oceanic water column. Progress in Oceanography. 16, 147–194.

Le Borgne, R., Rodier, M. (1997). Net zooplankton and the biological pump: a comparison between oligotrophic and mesotrophic equatorial Pacific. Deep-Sea Research II, 44, 2003–2023.

Longhurst, A.R., Bedo, A.W., Harrison, W.G., Head, E.J.H., Sameoto, D.D. (1990). Vertical flux of respiratory carbon by oceanic diel migrant biota. Deep-Sea Research, 37, 685–694.

Motoda, S., (1957). North Pacific standard net. Information Bulletin of Planktology in Japan, 4, 13-15.

Steinberg, D.K., Carlson, C.A., Bates, N.R., Goldthwait, S.A., Madin, L.P., Michaels, A.F. (2000). Zooplankton vertical migration and the active transport of dissolved organic and inorganic carbon in the Sargasso Sea. Deep-Sea Research I, 47, 137–158.

Steinberg, D.K., Cope, J.S., Wilson, S.E., Kobari, T. (2008). A comparison of mesopelagic mesozooplankton community structure in the subtropical and subarctic North Pacific Ocean. Deep-Sea Research II, 55, 1615– 1635.

Zhang, X., Dam, H.G. (1997). Downward export of carbon by diel migrant mesozooplankton in the central equatorial Pacific. Deep-Sea Research II, 44, 2191–2202.

3.9.2 Production and consumption of fecal pellets

(1) Objective

Fecal pellets are changed by zooplankton ingestion (coprophagy), fragmentation via sloppy feeding or swimming activity (coprorhexy) and loosening of membrane (coprochaly) during sinking (Paffenhöfer and Strickland, 1970; Lampitt et al., 1990; Noji et al., 1991). These processes largely affect transfer efficiency of POC flux (Wilson et al., 2008). It has been believed that fecal pellets are declined by bacterial decomposition (Honjo and Roman, 1978; Arístegui et al., 2002) and/or coprophagy/coprorhexy of small copepods such as cyclopoids and poecilostomatoids for last two decades (González and Smetacek, 1994; Suzuki et al., 2003; Svensen and Nejstgraard, 2003; Huskin et al., 2004; Poulsen and Kiørboe, 2006). In recent years, however, these copepods showed minor contributions to coprophagy/coprorhexy from the field observations (Iversen and Poulsen, 2007) and laboratory experiments (Reigstad et al., 2005), and heterotrophic microbes consume fecal pellets (Poulsen and Iversen, 2008). Thus, we should re-consider how fecal pellets are declined or changed during sinking from surface to mesopelagic depths.

In the present study, we carried out on-board experiments to evaluate how heterotrophic microbes and copepods affect fecal pellets at K2 and S1 in Northwestern Pacific Ocean.

(2) Methods

Samplings were carried out during the RV Mirai cruise from January to February 2010 at K2 and S1 in the Northwestern Pacific Ocean. Live copepods were collected in the water column above 200 m using North Pacific Standard net (Motoda 1957: diameter 45 cm, mesh size 0.1 mm) at a speed of 0.5 m sec^{-1}.

We carried out on-board experiments to evaluate effects of heterotrophic microbes and copepods on fecal pellets at both stations. Live copepods were indentified under stereomicroscope and transferred into chambers (20-mL glass bottle with GF/F filtered seawater) and placed at ambient temperature under dark condition. Fecal pellets were gently collected from incubation bottle from *Artemia salina*. Following the methods of Poulsen and Iversen (2008), bottle incubations were done.

(3) Preliminary results

During the cruise, we carried out twice on-board experiments at K2 and S1, respectively. Each sample will be brought back to the land laboratory for microscopic analysis on number, shape and volume for fecal pellets.

(4) Reference

Aristegui, J., Duarte, C.M., Agusti, S., Doval, M., Alvarez-Salgado, X.A., Hansell, D.A. (2002). Dissolved organic carbon support of respiration in the dark ocean. Science, 298, 1967-1967.

González, H. E., Smetacek, V. (1994). The possible role of the cyclopoid copepod

Oithona in retarding vertical flux of zooplankton fecal material. Marine Ecology Progress Series, 113, 233-246.

Honjo, S., Roman, M. R. (1978). Marine copepod fecal pellets: production, preservation and sedimentation. Journal of Marine Research, 36, 45-57.

Huskin, I., Viesca, L., Anado´ n, R. (2004). Particle flux in the Subtropical Atlantic near the Azores: influence of mesozooplankton. Journal of Plankton Research, 26, 403-415.

Iversen, M. H., Poulsen, M. R. (2007). Coprorhexy, coprophagy, and coprochaly in the copepods *Calanus helgolandicus, Pseudocalanus elongates*, and *Oithona similis*. Marine Ecology Progress Series, 350, 79-89.

Lampitt, R.S., Noji, T.T., von Bodungen, B. (1990). What happens to zooplankton faecal pellets? Implications for material flux. Marine Biology, 104, 15-23.

Motoda, S., (1957). North Pacific standard net. Information Bulletin of Planktology in Japan, 4, 13-15.

Noji, T. T., Estep, K. W., MacIntyre, F., Norrbin, F. (1991). Image analysis of faecal material grazed upon by three species of copepods: evidence for coprohexy, coprophagy, and coprochaly. Journal of the Marine Biological Association of the United Kingdom, 71, 465-480.

Paffenhöfer, G.-A ., Strickland, J. D. H. (1970). A note on the feeding of *Calanus helgolandicus* on detritus. Marine Biology, 5, 97-99.

Poulsen, L. K., Kiørboe, T. (2006). Vertical flux and degradation rates of copepod fecal pellets in a zooplankton community dominated by small copepods. Marine Ecology Progress Series, 323, 195-204.

Poulsen, M. R., Iversen, M. H. (2008). Degradation of copepod fecal pellets: key role of protozooplankton. Marine Ecology Progress Series, 367, 1-13.

Reigstad, M., Riser, C. W., Svensen, C. (2005). Fate of copepod faecal pellets and the role of *Oithona* spp. Marine Ecology Progress Series, 304, 265-270.

Suzuki, H., Sasaki, H., Fukuchi, M. (2003). Loss processes of sinking fecal pellets of zooplankton in the mesopelagic layers of the Antarctic marginal ice zone. Journal of Oceanography, 59, 809-818.

Svensen, C., Nejstgaard, J. C. (2003). Is sedimentation of copepod faecal pellets determined by cyclopoids? Evidence from enclosed ecosystems. Journal of Plankton Research, 25, 917-926.

Wilson, S. E., Steinberg, D. K., Buesseler, K. O. (2008). Changes in fecal pellet characteristics with depth as indicators of zooplankton repackaging of particles in the mesopelagic zone of the subtropical and subarctic North Pacific Ocean. Deep-Sea Research II, 55, 1636-1647.

3.10 Biological study for phytoplankton and zooplankton

Katsunori KIMOTO (JAMSTEC RIGC)
Atsushi KURASAWA (JAMSTEC BioGeos, Tohoku University)

3.10.1 Planktonic foraminifera

(1) Objective

Planktic foraminifers produce calcium carbonate test and contribute to the carbon cycle. Planktic foraminifers show wide distributions in the surface water. Recent molecular biological studies revealed the high genetic variations within many planktic foraminifera species. These intra-specific genetic variations considered be the indications of the cryptic speciation and their ecologies could be different among these cryptic species. Moreover, morphological variations which correspond to the genetic populations is confirmed on several species. The water mass structure is considered as one of the factors which affect the distribution of the genetic populations. However, the genetic variability of the planktic foraminifers is not fully understood. In this study, we collected living planktic foraminifer in order to reveal the genetic populations of the planktic foraminifera in the North Pacific Subpolar gyre and the Subtropical gyre.

(2) Methods

Living planktic foraminifera samples were collected by filtration of surface seawater and vertical towing of a NORPAC net. Surface seawater taken from onboard seawater tap was filtered using filtration apparatus (100 μm opening). The filtering apparatus was connected to seawater supply tap and placed in a bucket. Surface seawater filtrations were carried out for 17 times during navigation (Table 1). The NORPAC net towing was conducted at station K2 and S1. A closing NORPAC net (63 μm opening) was used in order to obtain depth-stratified samples. The sampling depths of the NORPAC net tows are summarized in Table 2. A CTD logger (Star-Oddi Ltd., DST-CTD) was attached to the NORPAC net to obtain the depths, temperature and salinity profiles of the water column during towing. Data recording interval of the logger was set to 1 or 2 seconds. Obtained NORPAC net samples were divided using sample separation apparatus and the half volume of the sample were used for DNA analysis.

The divided samples were stored at 4 ºC and living plankic foraminifer individuals were picked under a stereomicroscope. Picked specimens were cleaned in filtered seawater with fine brushes. Specimens were air dried on the faunal slides and stored at -80 ºC.

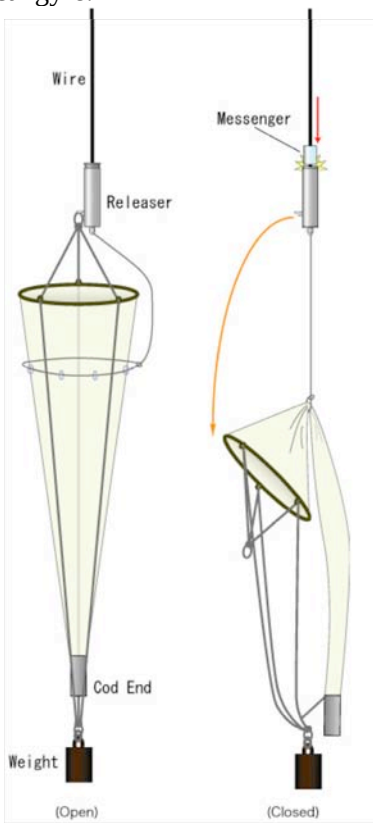

Fig.1 Schematic illustration of closing NORPAC net. Plankton net is open during towing (left), and closed at the top of the sampling depth range by deploying a messenger (right).

Table1. Summary of surface seawater filtration sampling

Sample No.	Region	Start Latitude	Longitude	Date	End Latitude	Longitude	Date
SW01	Bering Sea	54° 20.23' N	168° 19.83' W	19 Oct 4:47 UTC	54° 23.39' N	168° 51.8' W	19 Oct 6:58 UTC
SW02	Bering Sea	55° 14.19' N	173° 13.63' W	19 Oct 22:54 UTC	55° 18.04' N	173° 34.86' W	20 Oct 0:59 UTC
SW03	Bering Sea	55° 42.07' N	176° 15.69' W	20 Oct 9:13 UTC	55° 47.01' N	176° 50.78' W	20 Oct 11:01 UTC
SW04	Bering Sea	56° 8.31' N	179° 7.466' W	20 Oct 20:50 UTC	56° 8.85' N	179° 7.81' W	20 Oct 22:22 UTC
SW05	Bering Sea	55° 22.14' N	173° 23.06' E	22 Oct 0:11 UTC	55° 10.05' N	173° 6.57' E	22 Oct 1:26 UTC
SW06	Bering Sea	53° 46.61' N	171° 15.18' E	22 Oct 10:36 UTC	53° 35.08' N	170° 59.97' E	22 Oct 11:47 UTC
SW07	North Pacific	52° 24.02' N	169° 9.79' E	23 Oct 1:13 UTC	52° 14' N	168° 59.92' E	23 Oct 3:25 UTC
SW08	North Pacific	51° 21.23' N	168° 10.13' E	23 Oct 7:50 UTC	50° 56.05' N	167° 40.88' E	23 Oct 9:58 UTC
SW09	North Pacific	49° 23.85' N	163° 50.32' E	24 Oct 2:18 UTC	49° 14.8' N	163° 36.36' E	24 Oct 4:19 UTC
SW10	North Pacific	44° 22.31' N	156° 24.43' E	2 Nov 2:39 UTC	44° 2.43' N	155° 54.19' E	2 Nov 4:44 UTC
SW11	North Pacific	41° 59.92' N	152° 7.145' E	3 Nov 5:09 UTC	41° 49.66' N	151° 58.73' E	3 Nov 7:07 UTC
SW12	North Pacific	39° 48.73' N	149° 11.23' E	3 Nov 23:54 UTC	39° 27.45' N	148° 29.4' E	4 Nov 2:54 UTC
SW13	North Pacific	37° 59.85' N	146° 29.44' E	4 Nov 12:24 UTC	37° 49.84' N	146° 27.94' E	4 Nov 14:14 UTC
SW14	North Pacific	35° 26.7' N	145° 33.28' E	5 Nov 1:08 UTC	34° 22.12' N	145° 12.12' E	5 Nov 5:46 UTC
SW15	North Pacific	30° 4.4' N	144° 58.02' E	6 Nov 3:25 UTC	29° 59.28' N	144° 59.46' E	7 Nov 7:50 UTC
SW16	North Pacific	33° 34.63' N	144° 2.25' E	12 Nov 22:16 UTC	34° 17.65' N	143° 50.24' E	13 Nov 1:52 UTC
SW17	North Pacific	38° 31.14' N	142° 38.35' E	14 Nov 0:05 UTC	38° 54.83' N	142° 31.69' E	14 Nov 2:09 UTC

Table 2. Summary of NORPAC net tows

Station	Latitude	Longitude	Depth (m)	Date	Time
K2	46° 51.64' N	160° 2.62' E	0-20	26 Oct	8:50 JST
K2	46° 51.64' N	160° 2.62' E	20-50	26 Oct	9:00 JST
K2	46° 51.64' N	160° 2.62' E	50-100	26 Oct	9:20 JST
K2	46° 51.64' N	160° 2.62' E	100-150	26 Oct	9:33 JST
K2	46° 51.64' N	160° 2.62' E	150-200	26 Oct	9:49 JST
K2	46° 51.64' N	160° 2.62' E	0-5	26 Oct	10:06 JST
K2	46° 51.64' N	160° 2.62' E	200-300	26 Oct	10:13 JST
K2	46° 51.32' N	159° 57.19' E	700-1000	27 Oct	11:49 JST
K2	46° 51.32' N	159° 57.19' E	500-700	27 Oct	12:56 JST
K2	46° 51.32' N	159° 57.19' E	300-500	27 Oct	13:44 JST
K2	46° 51.32' N	159° 57.19' E	0-50	27 Oct	14:30 JST
K2	46° 51.32' N	159° 57.19' E	50-100	27 Oct	14:39 JST
S1	30° 0.10' N	144° 59.93' E	0-20	6 Nov	17:17 JST
S1	30° 0.10' N	144° 59.93' E	20-50	6 Nov	17:24 JST
S1	30° 0.10' N	144° 59.93' E	50-100	6 Nov	17:34 JST
S1	30° 0.10' N	144° 59.93' E	100-150	6 Nov	17:46 JST
S1	30° 0.10' N	144° 59.93' E	150-200	6 Nov	18:01 JST
S1	30° 0.10' N	144° 59.93' E	200-300	6 Nov	18:20 JST
S1	30° 0.10' N	144° 59.93' E	0-100	6 Nov	18:44 JST
S1	30° 0.10' N	144° 59.98' E	300-500	8 Nov	14:08 JST
S1	30° 0.10' N	144° 59.98' E	500-700	8 Nov	14:48 JST
S1	30° 0.20' N	145° 0.00' E	0-20	10 Nov	16:57 JST
S1	30° 0.20 N	145° 0.00' E	20-50	10 Nov	17:04 JST
S1	30° 0.20 N	145° 0.00' E	50-100	10 Nov	17:14 JST
S1	30° 0.20 N	145° 0.00' E	100-150	10 Nov	17:25 JST
S1	30° 0.20 N	145° 0.00' E	150-200	10 Nov	17:52 JST
S1	30° 0.20 N	145° 0.00' E	200-300	10 Nov	18:10 JST
S1	30° 0.20 N	145° 0.00' E	700-1000	11 Nov	13:29 JST
S1	30° 0.20 N	145° 0.00' E	0-300	11 Nov	14:25 JST

(3) Preliminary result

Species identifications under stereomicroscope show that planktic foraminifer species at K2 consist of subpolar species while species at S1 is consist of subtropical species. Samples collected at the Bering Sea and Subpolar Gyre (including station K2) contained *Globigerina bulloides, Neogloboquadrina pachyderma, Turborotalita quinqueloba, Globigerinita glutinata*. Planktic foraminifera species observed in the samples collected in the Subtropical Gyre region include *Globigerinoides ruber, Globigerinoides sacculifer, Globigerinoides conlobatus, Orbulina universa, Hastigerina pelagica, Globorotalia truncatulinoides, Globorotalia menardii.* The number of individuals collected at S1 was very few compared to the samples collected at K2.

(4) Data archive

The planktic foraminifer samples are stored at JAMSTEC. Molecular phylogenetic analyses and morphological observations will be conducted.

3.10.2 Shell-bearing phytoplankton studies in the western North Pacific

(1) Objectives

Shell-beared phytoplanktons (Diatoms, Silicoflagellates, and Coccolithophorids) are main primary producer of the ocean, therefore it is important to know their seasonal distribution, interactions, and transgressions of assemblages. Furthermore, hard skeletons of phytoplankton remains in the deep sea sediments and it provide useful information for paleoceanographic changes of sea surface water conditions. In this study, we collected water samples from the Bering Sea, K2 and S1 to investigate vertical distributions and ecological features of each phytoplankton.

(2) Methods

Seawater samples were obtained from upper 200 m water depths at all hydrocast stations by CTD/Niskin systems of 12L bottle capacity. The locations that were collected seawater were listed in Table 3.

For coccolithophorid separations, maximally 10 litter seawaters were filtered using 0.8 μm membrane filter (ADVANTEC MFS, Inc., JAPAN) immediately after collection. For diatoms and silicoflagellates separations, maximally 5 litter seawaters were also filtered using 0.45 um membrane filter.

(3) Future works

Collected samples were analyzed assemblages, diversities and spacial distributions for each taxon at onshore laboratory. These data will be compared with the sediment trap datasets that are moored at St. S1 and K2, same locations with water sampling points in this time. That should be provided the important information of seasonal and spacial variability of phytoplankton related with oceanographic changes in the western north Pacific.

Table 3. Summary of seawater sampling for phytoplankton

Station	Latitude		Longitude		Depth (m)	Date	Time	
St. 002	56° 8'	N	179° 7'	E	200	2010.10.20	23:00	UTC
	56° 8'	N	179° 7'	E	150	2010.10.20	23:00	UTC
	56° 8'	N	179° 7'	E	100	2010.10.20	23:00	UTC
	56° 8'	N	179° 7'	E	75	2010.10.20	23:00	UTC
	56° 8'	N	179° 7'	E	50	2010.10.20	23:00	UTC
	56° 8'	N	179° 7'	E	30	2010.10.20	23:00	UTC
	56° 8'	N	179° 7'	E	10	2010.10.20	23:00	UTC
St. 004	52° 24'	N	169° 10'	E	200	2010.10.23	2:28	UTC
	52° 24'	N	169° 10'	E	150	2010.10.23	2:28	UTC
	52° 24'	N	169° 10'	E	100	2010.10.23	2:28	UTC
	52° 24'	N	169° 10'	E	75	2010.10.23	2:28	UTC
	52° 24'	N	169° 10'	E	50	2010.10.23	2:28	UTC
	52° 24'	N	169° 10'	E	30	2010.10.23	2:28	UTC
	52° 24'	N	169° 10'	E	10	2010.10.23	2:28	UTC
St. 005	49° 24'	N	163° 50'	E	200	2010.10.24	3:28	UTC
	49° 24'	N	163° 50'	E	150	2010.10.24	3:28	UTC
	49° 24'	N	163° 50'	E	100	2010.10.24	3:28	UTC
	49° 24'	N	163° 50'	E	75	2010.10.24	3:28	UTC
	49° 24'	N	163° 50'	E	50	2010.10.24	3:28	UTC
	49° 24'	N	163° 50'	E	30	2010.10.24	3:28	UTC
	49° 24'	N	163° 50'	E	10	2010.10.24	3:28	UTC
St. 006 (K2)	47° 00'	N	160° 00'	E	200	2010.10.25	6:20	UTC
	47° 00'	N	160° 00'	E	150	2010.10.25	6:20	UTC
	47° 00'	N	160° 00'	E	100	2010.10.25	6:20	UTC
	47° 00'	N	160° 00'	E	75	2010.10.25	6:20	UTC
	47° 00'	N	160° 00'	E	50	2010.10.25	6:20	UTC
	47° 00'	N	160° 00'	E	30	2010.10.25	6:20	UTC
	47° 00'	N	160° 00'	E	10	2010.10.25	6:20	UTC
St. 009	38° 00'	N	146° 24'	E	200	2010.11.4	12:56	UTC
	38° 00'	N	146° 24'	E	150	2010.11.4	12:56	UTC
	38° 00'	N	146° 24'	E	100	2010.11.4	12:56	UTC
	38° 00'	N	146° 24'	E	75	2010.11.4	12:56	UTC
	38° 00'	N	146° 24'	E	50	2010.11.4	12:56	UTC
	38° 00'	N	146° 24'	E	30	2010.11.4	12:56	UTC
	38° 00'	N	146° 24'	E	10	2010.11.4	12:56	UTC
St. 010	34° 00'	N	145° 05'	E	200	2010.11.5	9:14	UTC
	34° 00'	N	145° 05'	E	150	2010.11.5	9:14	UTC
	34° 00'	N	145° 05'	E	100	2010.11.5	9:14	UTC
	34° 00'	N	145° 05'	E	75	2010.11.5	9:14	UTC
	34° 00'	N	145° 05'	E	50	2010.11.5	9:14	UTC
	34° 00'	N	145° 05'	E	30	2010.11.5	9:14	UTC
	34° 00'	N	145° 05'	E	10	2010.11.5	9:14	UTC
St. 011 (S1)	30° 00'	N	145° 00'	E	200	2010.11.9	10:28	UTC
	30° 00'	N	145° 00'	E	150	2010.11.9	10:28	UTC
	30° 00'	N	145° 00'	E	100	2010.11.9	10:28	UTC
	30° 00'	N	145° 00'	E	75	2010.11.9	10:28	UTC
	30° 00'	N	145° 00'	E	50	2010.11.9	10:28	UTC
	30° 00'	N	145° 00'	E	30	2010.11.9	10:28	UTC
	30° 00'	N	145° 00'	E	10	2010.11.9	10:28	UTC

3.11 Community structures and metabolic activities of microbes

Toshi NAGATA
(Atmosphere and Ocean Research Institute, The University of Tokyo : AORI)
Kazuhiro KOGURE (AORI)
Koji HAMASAKI (AORI)
Hiroshi OGAWA (AORI)
Hideki FUKUDA (AORI)
Yuya TADA (AORI)
Mario UCHIMIYA (AORI)

(1) Objective

A significant fraction of dissolved and particulate organic matter produced in the euphotic layer of oceanic environments is delivered to meso- and bathypelatic layers, where substantial transformation and decomposition of organic matter proceeds due to the actions of diverse microbes thriving in these layers. Statio-temporal variations in organic matter transformation and decomposition in the ocean's interior largely affect patterns in carbon cycling in the global ocean. Thus elucidating diversity, activities and distribution patterns of microbes in deep oceanic waters is fundamentally important in order to better understand major controls of oceanic material cycling in the ocean.

The objective of this study is to determine seasonal variability of microbial diversity and activities during the time-series observation of vertical fluxes at the two distinctive oceanic stations located in the subarctic and subtropical western North Pacific. We investigated i) full-depth profiles of prokaryotic activity and abundance and related biogeochemical parameters including dissolved organic carbon and nitrogen concentrations (potential resources of prokaryotes), and the abundances of nanoflagellates and viruses (potential predators of prokaryotes), ii) community structures of Bacteria and Archaea and iii) sinking velocity and physic-chemical properties of suspended particles in the mixing layer.

(2) Method

Seawater samples were collected from predetermined depths of two or three CTD casts, i.e. the Bacteria cast and the Routine cast, conducted at Stations K2 and S1 (see the meta-data sheet for details). Sinking particles were collected by drifting traps to determine fluxes of sinking POC/PON, their weight and microbial community structures (see the meta-data sheet for details).

i) Full-depth profiles of prokaryotic activity and abundance and related biogeochemical parameters

a) Prokaryotic abundance: Flow cytometry
b) Prokaryotic production: ^{3}H-leucine incorporation
c) Virus abundance: Flow cytometry
d) Nanoflagellate abundance: Direct counting under the epifluorescent microscopy
e) DOC/DON: Concentrations of dissolved organic carbon and total dissolved nitrogen were determined by the high temperature catalytic oxidation (HTCO) method. The concentration of dissolved organic nitrogen was calculated by subtracting the concentration of dissolved inorganic nitrogen (determined by Auto-analyzer) from that of total dissolved nitrogen.

ii) Relationship between community structures of Bacteria and Archaea and their metabolic activities

a) Bacterial community structures: PCR-fingerprinting/cloning method after extracting DNA from particles collected on 0.22 μm-pore-size filters (Sterivex).

b) Abundance of bacteria: Direct counting by the fluorescent microscopy after filtering fixed seawater with 0.2 and 3 μm pore-size polycarbonate filters, respectively.

c) Activities of bacteria: Bromodeoxyuridine-incorporating methods

d) Bacterial phylotype abundance and productivity: Direct counting by the fluorescent microscopy with the use of CARD-FISH and BrdU immunocytochemistry-FISH

iii) Sinking velocity and physic-chemical properties of suspended particles

a) Concentrations of particulate organic carbon and nitrogen: Determined using an elemental analyzer for samples collected on GF/F filters.

b) Weight of suspended solid: Determined by weighing samples collected on pre-weighted GF/F filter.

c) Particle size distribution of suspended particles in upper layer (0-200 m): Determined by an *in situ* particle sizing instrument, LISST-100 (Sequoia Scientific Inc., USA).

d) Settling velocity of suspended particles: Determined from time course changes of particle abundance in a settling chamber attached to LISST-100X (Sequoia Scientific Inc., USA).

(3) Data archived

All results will be submitted to Data Management Office, JAMSTEC after analysis and validation and be opened to public via the web site.

3.12 Dissolved Organic Carbon

Masahide WAKITA (Mutsu Institute for Oceanography, JAMSTEC)

(1) Objective

Fluctuations in the concentration of dissolved organic carbon (DOC) in seawater have a potentially great impact on the carbon cycle in the marine system, because DOC is a major global carbon reservoir. A change by < 10% in the size of the oceanic DOC pool, estimated to be ~ 700 GtC, would be comparable to the annual primary productivity in the whole ocean. In fact, it was generally concluded that the bulk DOC in oceanic water, especially in the deep ocean, is quite inert based upon ^{14}C-age measurements. Nevertheless, it is widely observed that in the ocean DOC accumulates in surface waters at levels above the more constant concentration in deep water, suggesting the presence of DOC associated with biological production in the surface ocean. This study presents the distribution of DOC during autumn in the northwestern North Pacific Ocean.

(2) Sampling

Seawater samples were collected at stations K2 (Cast 1, 6, 7 and 9) and S1 (Cast 2, and 10) and brought the total to ~130. Δ^{14}C of DOC and DIC are also sampled to estimate the ^{14}C-age of DOC at station K2 (Cast 6 and 7). Seawater from each Niskin bottle was transferred into 60 ml High Density Polyethylene bottle (HDPE) (for DOC) or 1000 ml Duran glass bottle (forΔ^{14}C of DOC) rinsed with same water three times. Water taken from the surface to 250 m is filtered using precombusted (450°C) GF/F inline filters as they are being collected from the Niskin bottle. At depths > 250 m, the samples are collected without filtration. After collection, samples are frozen upright and preserved at ~ -20 ℃ cold until analysis in our land laboratory. Before use, all glassware was muffled at 550 ℃ for 5 hrs.

(3) Analysis

Prior to analysis, samples are returned to room temperature and acidified to pH < 2 with concentrated hydrochloric acid. DOC analysis was basically made with a high-temperature catalytic oxidation (HTCO) system improved a commercial unit, the Shimadzu TOC-V (Shimadzu Co.). In this system, the non-dispersive infrared was used for carbon dioxide produced from DOC during the HTCO process (temperature: 680 ℃, catalyst: 0.5% Pt-Al_2O_3).

(4) Preliminary result

The distributions of DOC will be determined as soon as possible after this cruise.

(5) Data Archive

All data will be submitted to JAMSTEC Data Management Office (DMO) within 2 years.

3.13 Chlorofluorocarbons

Masahide WAKITA (JAMSTEC MIO)
Ken'ichi SASAKI (JAMSTEC MIO)

(1) Objective

Chlorofluorocarbons (CFCs) are chemically and biologically stable gases that have been synthesized at 1930's or later. The atmospheric CFCs can slightly dissolve in sea surface water by air-sea gas exchange and then are spread into the ocean interior. Three chemical species of CFCs, CFC-11 (CCl_3F), CFC-12 (CCl_2F_2), and CFC-113 ($C_2Cl_3F_3$), can be used as transient chemical tracers for the ocean circulation on timescale of several decades. We measured concentrations of these compounds in seawater.

(2) Apparatus

Dissolved CFCs are measured by an electron capture detector (ECD) – gas chromatograph attached with a purging & trapping system.

Table 3-14-1 Instruments

Gas Chromatograph:	GC-14B (Shimadzu Ltd.)
Detector:	ECD-14 (Shimadzu Ltd)
Analytical Column:	
Pre-column:	Silica Plot capillary column [i.d.: 0.53mm, length: 8 m, film thickness: 0.25μm]
Main column:	Connected two capillary columns (Pola Bond-Q [i.d.: 0.53mm, length: 9 m, film thickness: 6.0μm] followed by Silica Plot [i. d.: 0.53mm, length: 14 m, film thickness: 0.25μm])
Purging & trapping:	Developed in JAMSTEC. Cold trap columns are 1/16" SUS tubing packed with Porapak T.

(3) Procedures

3-1 Sampling

Seawater sub-samples for CFC measurements were collected from 12 litter Niskin bottles to 300 ml glass bottles at stations K2 (Cast 1) and S1 (Cast 2) and brought the total to ~80. The bottles were filled by nitrogen gas before sampling. Three times of the bottle volumes of seawater sample were overflowed. The bottles filled by seawater sample were kept in water bathes controlled at 5°C until analysis in our land-based laboratory. The CFCs concentrations were determined as soon as possible after this cruise.

In order to confirm CFC concentrations of standard gases and their stabilities, CFC mixing ratios in air were also analyzed. Air samples were collected into a 200ml glass cylinder at outside of our laboratory.

3-2 Analysis

The analytical system is modified from the original design of Bullister and Weiss (1988). Constant volume of sample water (50ml) is taken into a sample loop. The sample is send into

stripping chamber and dissolved CFCs are de-gassed by N_2 gas purging for 8 minutes. The gas sample is dried by magnesium perchlorate desiccant and concentrated on a trap column cooled down to -50 °C. Stripping efficiencies of CFCs are confirmed by re-stripping of surface layer samples and more than 99.5 % of dissolved CFCs are extracted on the first purge. Following purging & trapping, the trap column is isolated and electrically heated to 140 °C. CFCs are desorbing by electrically heating the trap column, and lead into the pre-column. CFCs are roughly separated from other compounds in the pre-column and are sent to main analytical column. And then the pre-column is switched to another line and flushed by counter flow of pure nitrogen gas. CFCs sent into main column are separated further and detected by an electron capture detector (ECD). Nitrogen gases used in this system was filtered by gas purifier tube packed Molecular Sieve 13X (MS-13X).

Table 3-14-2 Analytical conditions of dissolved CFCs in seawater.

Temperature	
Analytical Column:	95 °C
Detector (ECD):	240°C
Trap column:	-50 °C (at adsorbing) & 140 °C (at desorbing)
Mass flow rate of nitrogen gas (99.99995%)	
Carrier gas:	15 ml/min
Detector make-up gas:	22 ml/min
Back flush gas:	20 ml/min
Sample purge gas:	130 ml/min
Standard gas (Japan Fine Products co. ltd.)	
Base gas:	Nitrogen
CFC-11:	300 ppt (v/v)
CFC-12:	160 ppt (v/v)
CFC-113:	30 ppt (v/v)

(4) Preliminary result

The distributions of CFCs will be determined as soon as possible after this cruise. The standard gases used in this analysis will be calibrated with respect to SIO scale standard gases and then the data will be corrected.

(5) Data archive

All data will be submitted to JAMSTEC Data Management office (DMO) and under its control.

(6) Reference

Bullister, J.L and Weiss R.F. 1988. Determination of CCl_3F and CCl_2F_2 in seawater and air. Deep Sea Research, 35, 839-853.

3.14 Estimation of primary productivity by measurements of oxygen isotopes, N_2 and noble gases

Osamu ABE (Nagoya University)

(1) Introduction

$\Delta^{17}O$ of dissolved O_2, which is defined approximately as $\delta^{17}O - 0.5\delta^{18}O$ and controlled by primary productivity and gas transfer between atmosphere and water, can be regarded as a conservative component at the subsurface (hypolimnion) water. This means that it may be used to reconstruct past changes of productivity when the water was at the surface. In this study, I aim to clarify inter-annual variation of primary productivity at the subduction area of north Pacific intermediate water (NPIW) by measuring $\Delta^{17}O$ of subsurface water of NPIW. In order to achieve this purpose, vertical water sampling was conducted between Station K2 and S1, dissolved O_2 concentration and isotopic composition will be determined along with measurements for N_2 and noble gases concentrations.

(2) Sampling

For MR10-06 cruise, vertical water sampling was conducted from 6 stations including Station K2, S1 four stations between these locations (one of them was station KNOT). Additionally, 4 other samplings were conducted between Dutch Harbor and Station K2, in order to measure $\Delta^{17}O$ profile at Bering Sea. As a result, samples were collected from total 10 locations. At Station 2 (Bering Sea), K2 and S1, water samples were collected from surface to bottom, whereas samples were collected until 1000m for other locations.

Vacuum sampling flasks, each of which has a volume of 300mL, were used for sampling. About 150mL of water was introduced to it directly from CTD water bottles. These flasks were kept at room temperature on board and brought back to laboratory on land.

(3) Measurements

Most of all dissolved gas components in sampling flasks will be collected using a vacuum line. Then O_2 gas will be purified using molecular sieve packed column and measured by isotope ratio mass spectrometer (IRMS) for $\Delta^{17}O$. For the determination of N_2 and noble gases concentrations, collected gases from flasks will be directly injected to IRMS, and N_2/O_2 or Ar/O_2 ratios will be determined. These gas concentrations will be calculated by these results of gas ratios and dissolved O_2 concentrations those were measured on board.

(4) Expected results

Previous investigations for $\Delta^{17}O$ has been limited to surface mixed layer and used for “present” primary productivity at the surface water. This study will first investigate whether this parameter would be really conserved the surface condition. On that basis, $\Delta^{17}O$ values for NPIW water masses from each location can be regarded as those surface values when water masses were at the surface. Compare to surface $\Delta^{17}O$, subsurface $\Delta^{17}O$ values would be controlled not only by primary productivity and gas transfer between atmosphere and water, but also by the amount of isopycnal and diapycnal mixing. With regard to gas exchanges between air-water, and stratified water masses could be quantified by measuring degrees of super-saturation for nitrogen and/or noble gases.

3.15 Argo Float

Toshio SUGA (JAMSTEC/RIGC)
Mizue HIRANO (JAMSTEC/RIGC)
Shigeki HOSODA (JAMSTEC/RIGC)
Kanako SATO (JAMSTEC/RIGC)
Hiroki USHIROMURA (MWJ)

(1) Objective

The objective of deployment is to clarify the structure and temporal/spatial variability of water masses in the North Pacific such as North Pacific Subtropical Mode Water and its formation mechanism. To achieve the objective, profiling floats are launched to measure vertical profiles of temperature and salinity automatically every five days. As the vertical resolution of the profiles is very fine, the structure and variability of the water mass can be displayed well. Therefore, the profile data from the floats will enable us to understand the variability and the formation mechanism of the water mass.

(2) Methods (Description of instruments deployed)

We launched one APEX float manufactured by Webb Research Ltd. The float equips one SBE41 CTD sensor manufactured by Sea-Bird Electronics Inc to measure temperature, salinity and pressure from surface to 2000 dbar. The float usually drifts at a depth of 1500 dbar (called the parking depth), then it dives to a depth of 2000 dbar. During the ascent to the sea surface with increasing its volume in order to change its buoyancy, the float measures sea water temperature, salinity, and pressure. To send the measured data to the Argo data center via the ARGOS transmitting system in real time, the float stays at the sea surface for enough time, approximately 10 hours. Finally the float returns to the parking depth with decreasing volume. The cycle of the float moving repeats each 10 days for 3 or 4 years. The status of the float and the launch is shown in Table 1.

Table 1 Specification of launched float

Float Type	APEX floats manufactured by Webb Research Ltd.
CTD sensor	SBE41 manufactured by Sea-Bird Electronics Inc.
Cycle	5 days (approximately 10 hours at the sea surface)
ARGOS transmit interval	30 sec
Target Parking Pressure	1500 dbar
Sampling layers	115

	(2000,1950,1900,1850,1800,1750,1700,1650,1600,1550,1500,1450,1400,1350,1300,1250,1200,1150,1100,1050,1000,980,960,940,920,900,880,860,840,820,800,780,760,740,720,700,680,660,640,620,600,580,560,540,520,500,490,480,470,460,450,440,430,420,410,400,390,380,370,360,350,340,330,320,310,300,290,280,270,260,250,240,230,220,210,200,195,190,185,180,175,170,165,160,155,150,145,140,135,130,125,120,115,110,105,100,95,90,85,80,75,70,65,60,55,50,45,40,35,30,25,20,15,10,4 or surf, dbar)

(3) Preliminary result

The Float S/N, ARGOS ID, launched date/time, launched position observation cycle of the float is summarized in Table.2. The data will be measured automatically each observation cycle and can be obtained via internet promptly and freely.

Table 2 Launching area and date/time

Float S/N	ARGOS ID	Date and Time of Reset (UTC)	Date and Time of Launch(UTC)	Location of Launch	Observation Cycle
4226	86564	2010 / 11/12 03: 50	2010 / 11/12 04:25	30-02.27 [N] 145-03.09[E]	5days

(4) Data archive

The real-time data are provided to meteorological organizations, research institutes, and universities via Global Data Assembly Center (GDAC: http://www.usgodae.org/argo/argo.html, http://www.coriolis.eu.org/) and Global Telecommunication System (GTS), and utilized for analysis and forecasts of the ocean conditions and the climates.

3.16 Optical measurement of marine snow

Makio HONDA (JAMSTEC RIGC)

(1) Objective

Aggregated sinking particles, namely “marine show”, play an important role in transporting atmospheric CO_2 to the ocean interior. The study of marine snow has been traditionally conducted by collecting these with “sediment trap” and by chemical and biological analysis in laboratory. On the other hand, in situ qualitative observations of marine snow such as measurement of turbidity and light attenuation have also been conducted. Bishop et al. (2009) tried to estimate abundance and flux of particulate organic carbon (POC) by using the “carbon explorer”, that is “ARGO float” type optical method. Recently application of visual plankton recorder (VPR) to marine snow observation (Lindsay et al., 2008) has been examined. In addition, in situ laser raman spectrometry (LR) has been also examined (Brewer et al., 2004) in order to know chemical composition of seawater and sea-floor sediment (see appendix). In order to conduct the research and development of optical measurement of marine snow, I have started to evaluate VPR and LR.

(2) Method

In this cruise, I was not able to bring VPR and portable laser raman spectrometry (PLRS, see appendix) onboard. I collected seawater samples at various depths of stations K2 and S1 for LR method.

	K2	S1
Sampling date	October 26 (LST) , 2010	November 8 (LST) , 2010
Cast #	6	5
Sampling depth (m)	5, 20, 50, 100, 150, 200, 300, 500, 800, 1000 (10 layers)	5, 20, 50, 100, 150, 200, 300, 400, 500, 800, 1000 (11 layers)
Sampling volume (ml)	200 (50ml x 4)	200 (50ml x 4)

Seawater samples were freezed until seawater samples are used for research and development of LR in land laboratory.

Visual Plankton Recorder

Image analysis of marine snow

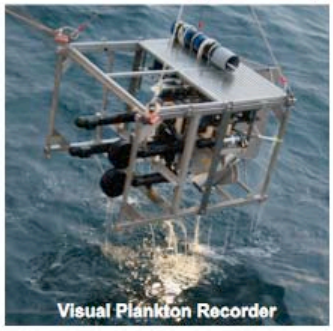

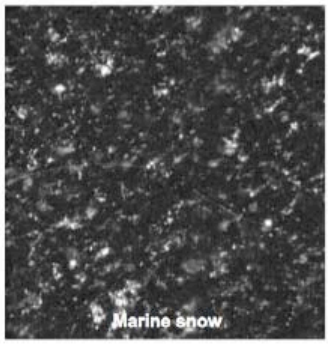

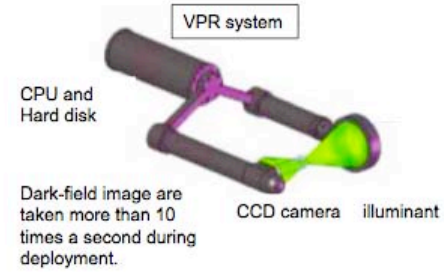

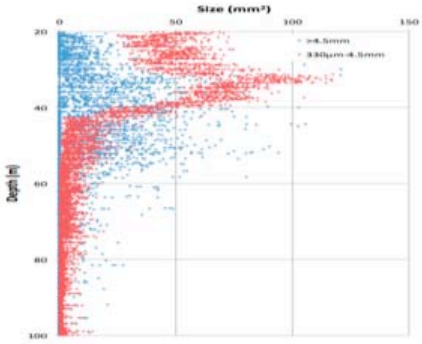

Vertical distribution of particulate materials

Laser Raman Spectrometry

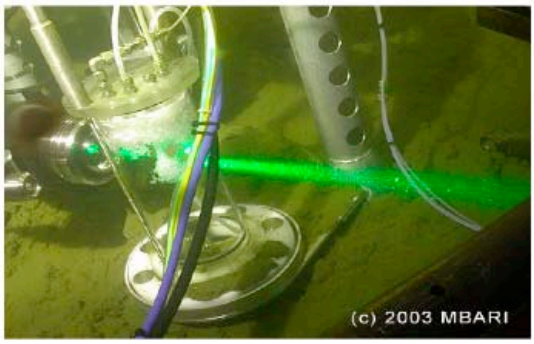

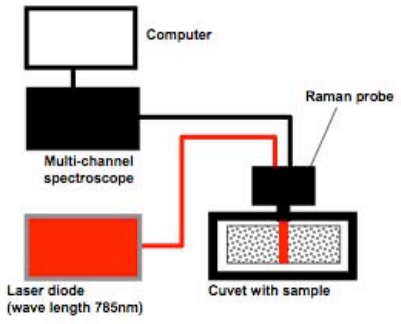

Conceptual diagram of PLRS

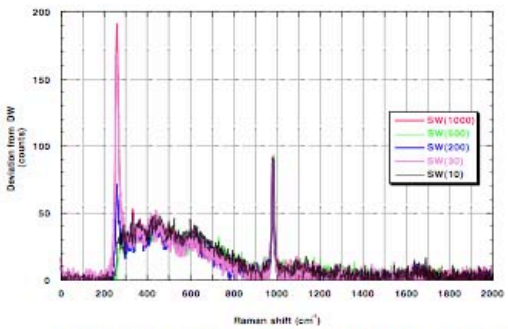

Raman shift of seawater collected from 10 m to 1000m

4. Geophysical observation

4.1 Swath Bathymetry

Takeshi MATSUMOTO (University of the Ryukyus) : Principal Investigator (not on-board)
Masao NAKANISHI (Chiba University) : Principal Investigator（not on-board）
Katsuhisa MAENO (Global Ocean Development Inc.: GODI)
Kazuho YOSHIDA (GODI)
Wataru TOKUNAGA (Mirai Crew)

(1) Introduction

R/V MIRAI is equipped with a Multi narrow Beam Echo Sounding system (MBES), SEABEAM 2112.004 (SeaBeam Instruments Inc.). The main objective of MBES is collecting continuous bathymetric data along ship's track to make a contribution to geological and geophysical investigations and global datasets. We carried out bathymetric survey throughout the MR10-06 cruise

(2) Data Acquisition

The "SEABEAM 2100" on R/V MIRAI was used for bathymetry mapping during the MR10-06 cruise from 18 October to 16 November 2010.

To get accurate sound velocity of water column for ray-path correction of acoustic multibeam, we used Surface Sound Velocimeter (SSV) data to get the sea surface (6.2m) sound velocity, and the deeper depth sound velocity profiles were calculated by temperature and salinity profiles from CTD and XCTD data by the equation in Del Grosso (1974) during the cruise.

Table 4.1-1 shows system configuration and performance of SEABEAM 2112.004 system.

Table 4.1-1 System configuration and performance

SEABEAM 2112.004 (12 kHz system)	
Frequency:	12 kHz
Transmit beam width:	2 degree
Transmit power:	20 kW
Transmit pulse length:	3 to 20 msec.
Depth range:	100 to 11,000 m
Beam spacing:	1 degree athwart ship
Swath width:	150 degree (max) 120 degree to 4,500 m 100 degree to 6,000 m 90 degree to 11,000 m
Depth accuracy:	Within < 0.5% of depth or +/-1m, whichever is greater, over the entire swath. (Nadir beam has greater accuracy; typically within < 0.2% of depth or +/-1m, whichever is greater)

(3) Preliminary Results

The results will be published after primary processing.

(4) Data Archives

Bathymetric data obtained during this cruise will be submitted to the Data Management Group (DMG) in JAMSTEC, and will be archived there.

4.2 Sea surface gravity

Takeshi MATSUMOTO (University of the Ryukyus) : Principal Investigator (not on-board)
Masao NAKANISHI (Chiba University) : Principal Investigator（not on-board）
Katsuhisa MAENO (Global Ocean Development Inc.: GODI)
Kazuho YOSHIDA (GODI)
Wataru TOKUNAGA (Mirai Crew):

(1) Introduction

The local gravity is an important parameter in geophysics and geodesy. We collected gravity data at the sea surface.

(2) Parameters

Relative Gravity [CU: Counter Unit]
[mGal] = (coef1: 0.9946) * [CU]

(3) Data Acquisition

We measured relative gravity using LaCoste and Romberg air-sea gravity meter S-116 (Micro-g LaCoste, LLC) during the MR10-06 cruise from 18 October 2010 to 16 November 2010.

To convert the relative gravity to absolute one, we measured gravity, using portable gravity meter (Scintrex gravity meter CG-3M), at Sekinehama as the reference points.

(4) Preliminary Results

Absolute gravity shown in Tabel 4.2-1

Table 4.2-1

No.	Date	U.T.C.	Port	Absolute Gravity [mGal]	Sea Level [cm]	Draft [cm]	Gravity at Sensor *[1] [mGal]	L&R *[2] Gravity [mGal]
#1	18 Aug.	02:56	Sekinehama	980371.95	248	644	980372.77	12669.81
#2	16 Nov.	05:22	Sekinehama	980371.92	252	620	980372.74	12654.66

*[1]: Gravity at Sensor = Absolute Gravity + Sea Level*0.3086/100 + (Draft-530)/100*0.0431
*[2]: LaCoste and Romberg air-sea gravity meter S-116

(5) Data Archives

Surface gravity data obtained during this cruise will be submitted to the Data Management Group (DMG) in JAMSTEC, and will be archived there

4.3 Sea Surface three-component magnetic field

Takeshi MATSUMOTO (University of the Ryukyus) : Principal Investigator (not on-board)
Masao NAKANISHI (Chiba University) : Principal Investigator（not on-board）
Katsuhisa MAENO (Global Ocean Development Inc.: GODI)
Kazuho YOSHIDA (GODI)
Wataru TOKUNAGA (Mirai Crew):

(2) Introduction

Measurements of magnetic force on the sea are required for the geophysical investigations of marine magnetic anomaly caused by magnetization in upper crustal structure. We measured geomagnetic field using a three-component magnetometer during the MR10-06 cruise from 18 October 2010 to 16 November 2010.

(3) Principle of ship-board geomagnetic vector measurement

The relation between a magnetic-field vector observed on-board, **H**ob, (in the ship's fixed coordinate system) and the geomagnetic field vector, **F**, (in the Earth's fixed coordinate system) is expressed as:

$$\mathbf{H}ob = \mathbf{A}\,\mathbf{R}\,\mathbf{P}\,\mathbf{Y}\,\mathbf{F} + \mathbf{H}p \qquad (a)$$

where **R**, **R** and **Y** are the matrices of rotation due to roll, pitch and heading of a ship, respectively. $\underset{\sim}{\mathbf{A}}$ is a 3 x 3 matrix which represents magnetic susceptibility of the ship, and **H**p is a magnetic field vector produced by a permanent magnetic moment of the ship's body. Rearrangement of Eq. (a) makes

$$\mathbf{B}\,\mathbf{H}ob + \mathbf{H}bp = \mathbf{R}\,\mathbf{P}\,\mathbf{Y}\,\mathbf{F} \qquad (b)$$

where $\mathbf{B} = \mathbf{A}^{-1}$, and $\mathbf{H}bp = -\mathbf{B}\,\mathbf{H}p$. The magnetic field, **F**, can be obtained by measuring **R**, **P**, **Y** and **H**ob, if **B** and **H**bp are known. Twelve constants in **B** and **H**bp can be determined by measuring variation of **H**ob with **R**, **P** and **Y** at a place where the geomagnetic field, **F**, is known.

(4) Instruments on *R/V MIRAI*

A shipboard three-component magnetometer system (Tierra Technica SFG1214) is equipped on-board *R/V MIRAI*. Three-axes flux-gate sensors with ring-cored coils are fixed on the fore mast. Outputs of the sensors are digitized by a 20-bit A/D converter (1 nT/LSB), and sampled at 8 times per second. Ship's heading, pitch, and roll are measured utilizing a ring-laser gyro installed for controlling attitude of a Doppler radar. Ship's position (GPS) and speed data are taken from LAN every second.

(5) Data Archives

Magnetic force data obtained during this cruise will be submitted to the Data Management Group (DMG) in JAMSTEC, and will be archived there.

(6) Remarks

1) For calibration of the ship's magnetic effect, we made a "Figure eight" turn (a pair of clockwise and anti-clockwise rotation). The periods were follows;

i) 08:00 - 08:23 UTC 31 Oct. 2010 around at 47-01N, 160-03E
ii) 09:00 - 09:24 UTC 11 Nov. 2010 around at 30-00N, 145-00E

2) The following periods, data were invalid due to the serial communication trouble.
09:58UTC 03 Nov. 2010 - 00:52UTC 04 Nov. 2010
13:06UTC 06 Nov. 2010 - 05:00UTC 07 Nov. 2010
17:08UTC 12 Nov. 2010 - 01:32UTC 13 Nov. 2010

3) The following periods, data acquisition was stopped due to the maintenance.
00:52UTC 04 Nov. 2010 - 00:58UTC 04 Nov. 2010
05:00UTC 07 Nov. 2010 - 05:54UTC 07 Nov. 2010
01:32UTC 13 Nov. 2010 - 02:11UTC 13 Nov. 2010

4) The following periods, time stamp and navigation data (longitude, latitude, depth, ship speed and gyro) were not updated due to network trouble.
13:08UTC 08 Nov. 2010 - 13:40UTC 08 Nov. 2010

5 Satellite Image Acquisition (MCSST from NOAA/HRPT)

Makio HONDA (JAMSTEC): Principal Investigator
Katsuhisa MAENO (Global Ocean Development Inc.: GODI)
Kazuho YOSHIDA (GODI)
Wataru YOKUNAGA (Mirai Crew)

(1) Objectives

It is our objectives to collect data of sea surface temperature in a high spatial resolution mode from the Advance Very High Resolution Radiometer (AVHRR) on the NOAA polar orbiting satellites and to build a time and depth resolved primary productivity model.

(2) Method

We receive the down link High Resolution Picture Transmission (HRPT) signal from NOAA satellites. We processed the HRPT signal with the in-flight calibration and computed the sea surface temperature by the Multi-Channel Sea Surface Temperature (MCSST) method. A daily composite map of MCSST data is processed for each day on the R/V MIRAI for the area, where the R/V MIRAI located.

We received and processed NOAA data throughout MR10-06 cruise from 18 October 2010 to 16 November 2010.

The sea surface temperature data will be applied for the time and depth resolved primary productivity model to determine a temperature field for the model.

(3) Preliminary results

Fig.5-1 showed MCSST composite image during this cruise from 20 January 2010 to 24 February 2010 at the Northern-west Pacific Ocean.

(4) Data archives

The raw data obtained during this cruise will be submitted to the Data Management Group (DMG) in JAMSTEC, and will be archived there.

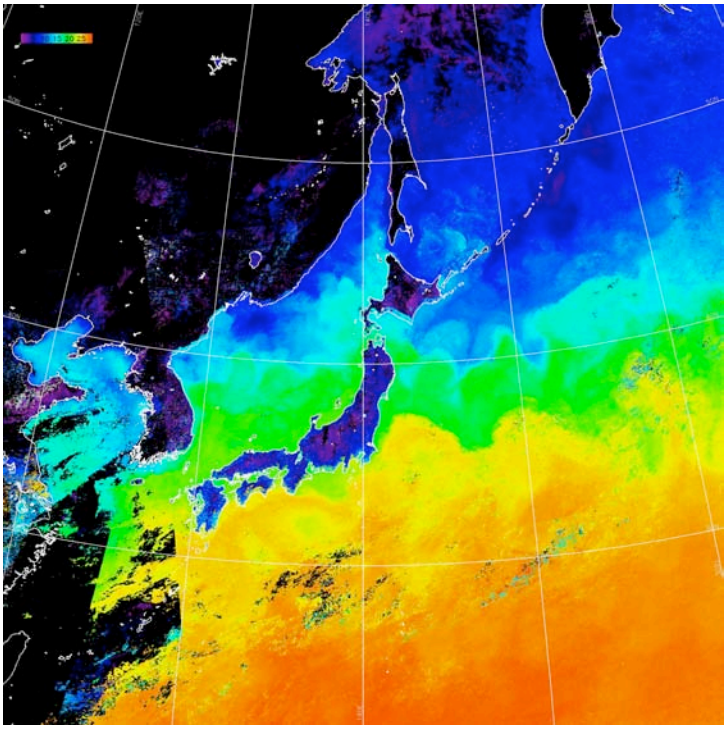

Fig.5-1 MCSST composite image at Northern-west Pacific Ocean.
from 18 October to 15 November 2010